Synthesis of non-natural amino acids as covalent inhibitors for protein-protein interactions

A thesis submitted in fulfilment of the

requirements for the degree of

Master of Science

Of

University of KwaZulu-Natal

College of Agriculture, Engineering and Science

School of Chemistry and Physics

by

Siphamandla Austen Dladla

February 2023

Declaration of Originality

The experimental work described in this thesis was carried out by me in the School of Chemistry and Physics, College of Agriculture, Engineering and Science, University of KwaZulu-Natal, Pietermaritzburg Campus, under the supervision of Dr. Siphamandla Sithebe and Prof. Clinton G. L. Veale.

I declare that I am the sole author of this thesis, and no part of this thesis has been published or submitted for publication.

I certify that, to the best of my knowledge, my thesis does not infringe upon anyone's copyright nor violate any proprietary rights and that any ideas, techniques, or any other material from the work of other people included in my thesis, published or otherwise, are fully acknowledged in accordance with the standard referencing practices.

[redacted]

Signed …… Siphamandla Austen Dladla (Candidate)

I hereby certify that the above statement is correct

[redacted]

Signed……Dr. Siphamandla Sithebe (Supervisor)

[redacted]

Signed…… Prof. Clinton G. L. Veale (Co-supervisor)

Abstract

There is still a need to develop new cancer therapies for troubling cancers. Hence, a resurging interest in compounds that engage their target through covalent interactions. Lysine's amine can be engaged covalently with a weak electrophile (SO_2F) extending the potential of covalent inhibitors. Herein, we were prompted to investigate the synthesis of non-natural amino acids, modified to include weakly electrophilic warheads, which could potentially target specific lysine residues.

Three new non-natural amino acids were successfully synthesized, methyl (*S*)-2-((*tert*-butoxycarbonyl)amino)-3-(4-((fluorosulfonyl)oxy)phenyl)propanoate, **3.5**, methyl (*S*)-2-((*tert*-butoxycarbonyl)amino)-2-(4-((fluorosulfonyl)oxy)phenyl)acetate, **3.9**, and methyl (*S*)-2-((tert-butoxycarbonyl)phenyl)propanoate, **3.35**, in 85%, 89%, and 63.7% yield, respectively. Our study explored the synthetic pathway of a three-step procedure toward the target compounds, with the initial esterification of the carboxylic acid group, followed by the *N*-Boc protection of the amine group. Finally, the key sulfonation of the *N*-Boc protected amino methyl ester, where for **3.5** and **3.9**, was performed through *ex-situ* generation of sulfuryl fluoride, which was installed following the substitution of the hydrogen on the hydroxyl group by SO_2F. For **3.35**, it was achieved through a palladium-catalyzed system and an *in-situ* fluorine introduction, where *para* iodine was substituted by the SO_2 generated from DABSO.

Under physiological conditions, compound **3.5** was assessed for possible interaction through its electrophilic warhead, with nucleophilic *N*-Boc-lysine side chain. The LCMS and NMR buffered assays were conducted, and in both these studies, the characteristics of a possible binding happening can be observed, hence an adduct N^2-(*tert*-butoxycarbonyl)-N^6-((4-((*S*)-2-

((*tert*-butoxycarbonyl)amino)-3-methoxy-3-oxopropyl)phenoxy)sulfonyl)-*L*-lysine **3.5a** formation.

Table of Contents

List of Figures

List of Schemes

List of Tables

List of Abbreviations

Å	Angstrom
AcOH	Acetic acid
Aldh2	Aldehyde dehydrogenase 2 family member
aq.	Aqueous
Boc	*Tert*-butyl dicarbonate
Boc_2O	Di-*tert*-butyl dicarbonate
br	Broad
^{13}C NMR	Carbon-13 Nuclear magnetic resonance
calcd	Calculated
conc.	Concentrated
δ	Chemical Shift
Cys797	Cysteine-797
C93	Cysteine-93
Da	Dalton
DABSO	1,4-Diazabicyclo[2.2.2]octane bis(sulfur dioxide)
°C	Degrees Celsius
DCM	Dichloromethane
Dpyd	Dihydropyrimidine dehydrogenase deficiency

d	Doublet
dd	Doublet of doublets
DMF	*N*,*N*-dimethyl formamide
DMSO	Dimethyl sulfoxide
Et_2O	Diethyl ether
EtOAc	Ethyl acetate
et al	Et alia
FAM96B	Family with sequency similarity 96 member B
FDA	Food and drug administration
Gstt1	Glutathione S-transferase theta 1
HAB and BF	Hillcrest Advice Bureau and Bursary Fund
h	Hour
Hz	Hertz
Hsp90	Heat shock protein 90
HOP	Hsp70-Hsp90 organizing protein
IR	Infra-red spectroscopy
KEAP1	Kelch-like ECH-associated protein 1
K497	Lysine 497
Lys89	Lysine-89

m/z	Mass to charge ratio
MeOH	Methanol
MHz	Megahertz
Mp	Melting point
mg	Milligram
mL	Millilitre
mmol	Millimole
m	Multiplet
NMR	Nuclear magnetic resonance
NFSI	*N*-fluorobenzenesulfonimide
NR0B1	Nuclear receptor subfamily 0 group B member 1
Nrf2	Nuclear factor erythroid 2-related factor 2
ppm	Parts per million
%	Percentage
PPI	Protein-protein interactions
R_f	Retention factor
r.t	Room temperature
sat.	Saturated
Ser-529	Serine-529

Ser-516	Serine-516
s	Singlet
SDI	1,1'Sulfonyldiimidazole
J	Spin-spin coupling constant
TFA	Trifluoroacetic acid
t	Triplet
TEA/Et_3N	Triethylamine
TLC	Thin layer chromatography
µL	Microlitre
cm^{-1}	Wavenumber
WHO	World health organization

“Opportunity is missed by most people because it is dressed in overalls and looks like work.”

-Thomas A. Edison-

In the memory of my father: Musawenkosi W. Dladla, who passed away during the course of this degree.

Acknowledgements

First and foremost, I would like to thank the Lord Almighty for blessing me with good health and well-being which was necessary to complete this work.

I would like to thank my two supervisors Dr. Siphamandla Sithebe and Prof. Clinton Veale for proper guidance, advice, patience, and constant encouragement throughout this project. I greatly benefitted from their supervision and unique set of skills during the research and writing this thesis.

Additionally, I would like to thank Dr. Annie Braine, Ms. Abigail Milne, Mrs. Tanya Harvey, and the rest of the HAB and BF team for proofreading this work and supporting me continuously.

My thanks also go out to Dr. Shivani Naidoo for holding my hand at the beginning of this project and providing support during difficult times, and Dr. Shantal Maharaj who, when things were unclear regarding the biochemistry aspect of this work, was always willing to guide me.

I gratefully thank Mr. Graig Grimmer and Mrs. Caryl Janse van Rensburg, who run the samples for analysis. Their office doors were always open should there be anything I did not understand about the spectrum. Their immense knowledge is fruitful.

I would also like to thank all my fellow research colleagues, especially in Warren lab, and the medicinal chemistry research group, the support we gave to each other has encouraged me to continue to the end with this work.

My sincere love and appreciation must go to my mother Thobile Dladla and her sibling (Skhumbuzo, Busi, Gah, Scelo, Nobuhle, Samke, and Mpume), my brothers (Lungelo Ndlela, Bradley, Lungelo, Sibonelo, and Wonder), and the rest of my family and friends.

Finally, the financial support through Prof. Veale from the grant he obtained from Future Leaders – African Independent Research (FLAIR) Fellowships.

Chapter One

Introduction and literature review

1.1 General overview of covalent inhibitors

The term "covalent inhibitor" refers to small molecules that by design are intended to bind covalently to targets in a specific amino acid residue and temporarily or permanently inactivate them. There is generally a two-step process involved in covalent inhibition.[1] The first is reversible inhibition which occurs when an inhibitor associates with an enzyme, allowing its chemical warhead to interact with the enzyme's reactive amino acid residue. During the second step, covalent bonds are formed between the two reactive entities on the enzyme and inhibitor (**Scheme 1.1**).[2] It is important to note that reversible inhibitors do not require the second step as covalent inhibitors do. It is possible for a covalently conjugated inhibitor to undergo further chemical transformations to get released from its target enzyme after a certain period. Furthermore, it can permanently bind to the target, effectively locking the enzyme in an inactive mode.[3]

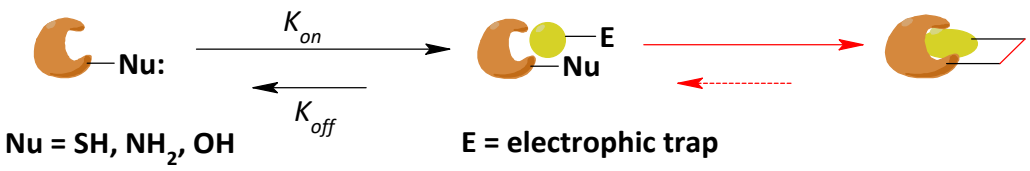

Scheme 1.1: Illustration of binary complex formation (selectivity) and covalent reaction (secondary selectivity filter; terminal inhibition).

1.2 Historic background of covalent inhibitors

The earliest covalent inhibitor was introduced by Bayer who began manufacturing aspirin in the late 19th century as a painkiller and anti-inflammatory drug. Small molecules were used as covalent inhibitors to target enzymes that are critical for cell function[4] and these are molecules with a molecular weight less than 900 Da and approximately 90% of pharmaceutical drugs are small molecules such as aspirin, and antihistamines to name but a few.[5] Since the beginning of the 20th century, aspirin has been on the market, but its mechanism of action was not resolved until the 1970s when Roth *et al.* identified that aspirin selectively acetylates Ser-529 and Ser-516 on cyclooxygenase-1 (COX-1) and cyclooxygenase-2 (COX-2) respectively, thus disrupting prostaglandin biosynthesis, resulting in an anti-inflammatory effect (**Scheme 1.2**). [6, 7]

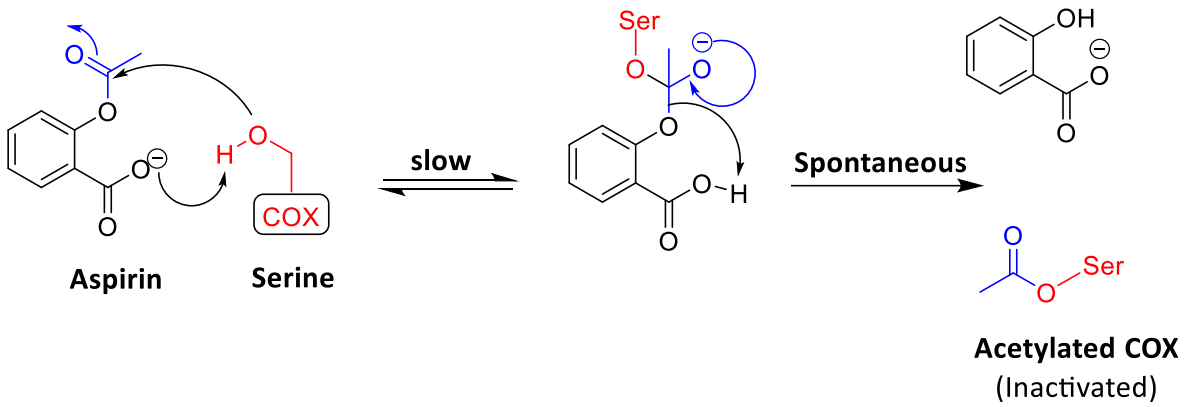

Scheme 1.2: The mechanism of action involving covalent modification of aspirin by serine residue.

Among early covalent drugs, penicillin is another drug that was discovered in 1928, and it acts as a covalent inhibitor.[8] It is noteworthy that penicillin was found as an antibiotic serendipitously and can be considered one of the most important discoveries in the history

of drugs. It is used to treat infections caused by bacteria such as *Streptococcus pneumoniae* which causes pneumonia, *Streptococcus pyogenes* which causes strep throat, and *Neisseria gonorrhoeae* which causes gonorrhoea to name but a few.[9] There have been a number of penicillin analogues approved for human use to date and they all have a similar mechanism of action to that of penicillin and β-lactam as the chemical warhead. According to the World Health Organization (WHO) report on surveillance of antibiotic consumption, these are the most frequently used class of antibiotics.[10, 11] Antibiotics of this class possess a reactive four-membered β-lactam ring (**1.1**), which is fundamental to their bactericidal properties.[12] Penicillins (**1.2**), cephalosporins (**1.3**), and carbapenems (**1.4**) are the distinct subclasses that result when β-lactam rings are fused with heterocycles, whose resultant ring strain prevents the resonance stabilization normally associated with amides, thus rendering them susceptible to electrophilic attach. Furthermore, they are functionalized in several critical positions, to facilitate target interaction (**Figure 1.1**).

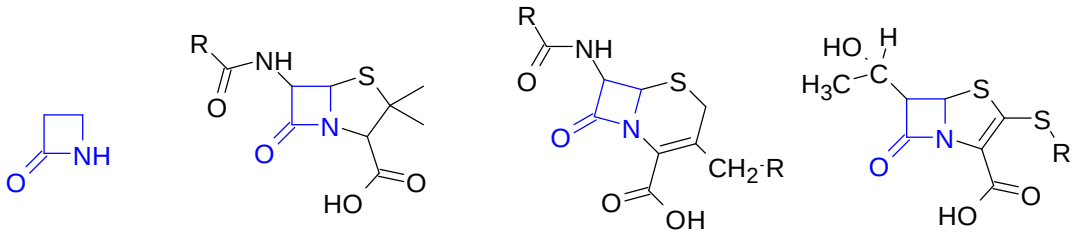

1.1 β-lactam **1.2 Penicillin** **1. 3 Cephalosporin** **1. 4 Carbapenem**

Figure 1.1: The chemical structure of the β-lactam ring (**1.1**), alongside with its antibiotic subclasses (**1.2** – **1.4**).

This β-lactam reacts with an active site serine residue in D-Alanyl-D-Alanine transpeptidase, which functions in bacterial cell wall biosynthesis, inactivating it, causing disruption of bacterial cell wall biosynthesis and, as a result, bacterial cell lysis (**Scheme 1.3**).[13]

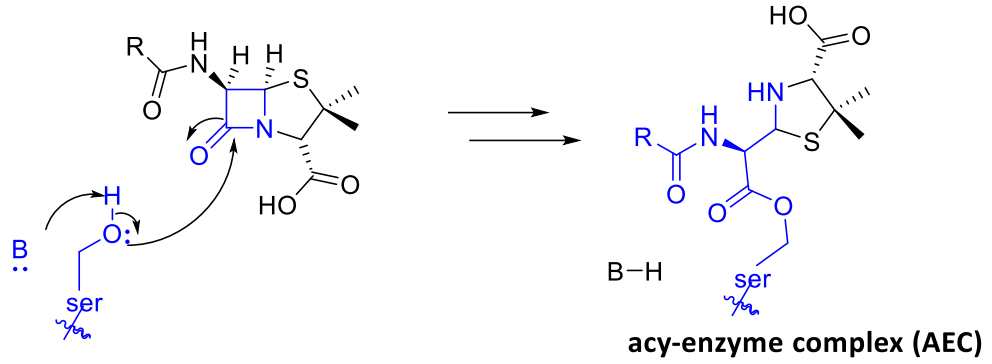

Scheme 1.3: The mechanism of action of β-lactam with an active site serine in D-alanyl-D-alanine transpeptidase

Other than aspirins and penicillins as covalent inhibitors, there are other covalent inhibitors that have been developed into several successful drugs (**Figure 1.2**). These include *Cephalosporin C* (**1.5**), an inhibitor of DD-transpeptidase, *Omeprazole* (**1.6**) and *Lansoprazole* (**1.7**), the inhibitors of H^+K^+ ATPase, *Fosfomycin* (**1.8**), an inhibitor of MurA, *Clopidogrel* (**1.9**), a $P2Y_{12}$ receptor inhibitor, *Afatinib* (**1.10**), an inhibitor of EGFR and erbB-2, *Ibrutinib* (**1.11**), and *Acalabrutinib* (**1.12**), an inhibitor of BTK and *SML-8-73-1* (**1.13**) and *ARS-853* (**1.14**) the inhibitors of KRAS G12C. These examples mentioned have encouraged medicinal chemists to consider this strategy when the biochemical mechanism supports such an approach.[1, 4, 14]

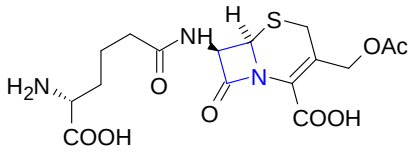

1.5 ***Cephalosporin C***

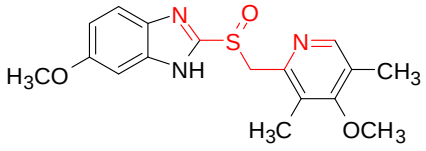

1.6 ***Omeprazole***

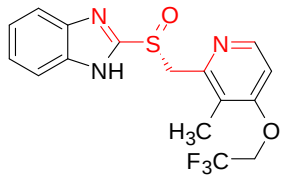

1.7 ***Lansoprazole***

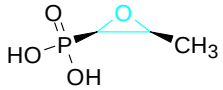

1.8 ***Fosfomycin***

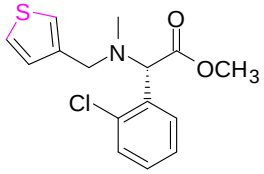

1.9 ***Clopidogrel***

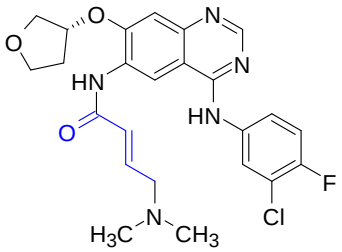

1.10 ***Afatinib***

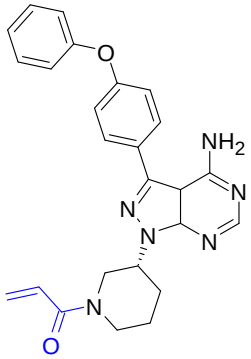

1.11 ***Ibrutinib***

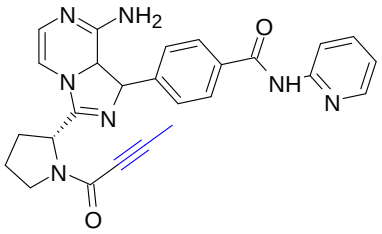

1.12 ***Acalabrutinib***

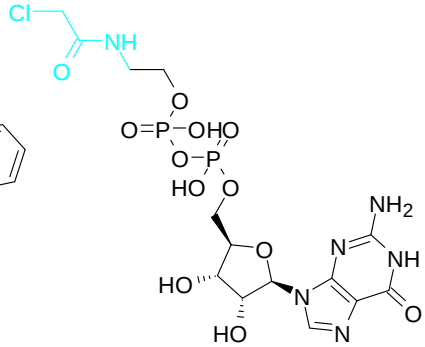

1.13 ***SML-8-73-1***

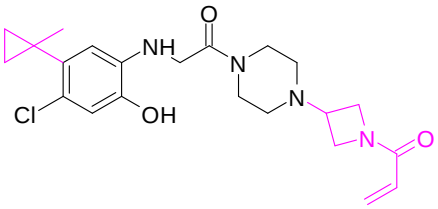

1.14 ***ARS-853***

Figure 1.2: (**1.5**-**1.14**) are the covalent inhibitors that have led to successful drugs since the 1890s.

1.3 General overview: Discovering a covalent inhibitor

George Santayana once said, "Those who do not remember the past are condemned to repeat it". As with other aspects of human endeavour, this observation is relevant to drug discovery as well.[15] In recent years, computer-assisted data exploration has gained momentum in the area of drug discovery.[16] Pipeline diagrams are often represented as chevrons in the drug development process, and the identification and validation of one or more biological targets is the first step in the drug discovery process, several other important steps follows (**Figure 1.3**).[17] Consequently, covalent drugs require some special considerations.

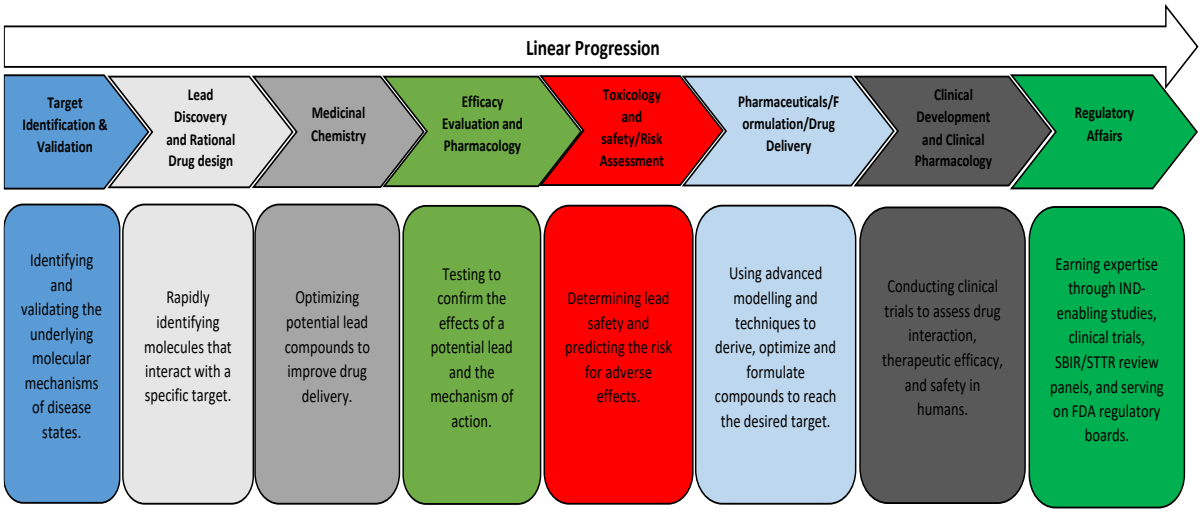

Figure 1.3: A classical representation of the overall process of a covalent drug discovery paradigm.

As with any drugs, there are always advantages and limitations. And there have been concerns that human health may be negatively affected by covalent inhibition. For instance, the cellular metabolites of acetaminophen are hepatotoxic.[18] In acetaminophen metabolism, the drug is oxidized by cytochrome P450 into the highly reactive *N*-acetyl-*p*-benzoquinone imine (NAPQI) that covalently modifies glutathione (GSH) or cysteine residues in proteins.[14]

In patients, non-specific covalent drug-protein adducts may cause unwanted immunogenic responses.

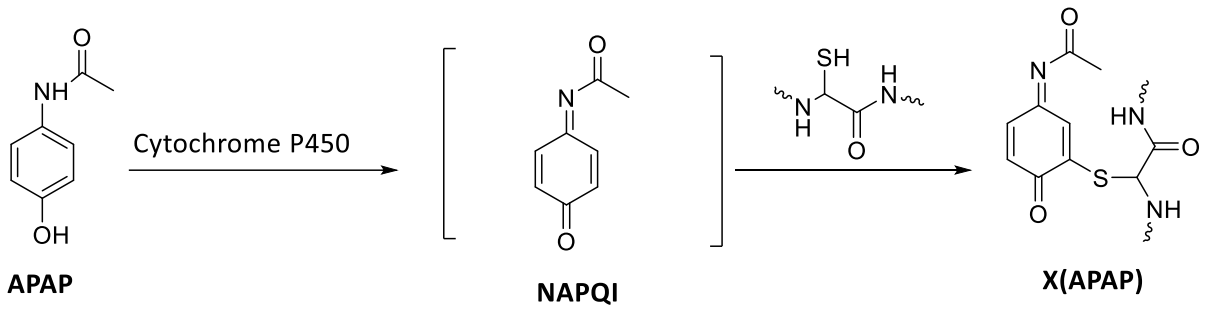

Scheme 1.4: The oxidation of acetaminophen to its toxic intermediate quinone imine metabolites and the covalent modification of the glutathione.

Against all these drawbacks, there has been a resurgence of interest in covalent drugs in the pharmaceutical industry, furthermore with natural products being covalent inhibitors.[4] The advantages of covalent inhibitors include having a high affinity for their target and a longer duration of action than reversible inhibitors. In addition, these inhibitors have pharmacodynamic properties that outlast measurable inhibitor concentration in the plasma, which means undesirable pharmacokinetic properties can sometimes be tolerated.[3] Accordingly, covalent inhibitors can be used as therapeutics if the reactivity of the warhead can be controlled.[3]

1.4 The electrophilic "warheads" in designing covalent inhibitor

In the design of covalent inhibitors, an electrophilic moiety that forms a covalent bond between a nucleophilic amino acid and the inhibitor is employed. These functional groups are often termed "warheads", and they are electrophilic.[19] When designing covalent drug molecules, they are crucial, for selectivity to be obtained, and it may be of utility to consider binding as it occurs in the two distinct steps to avoid toxicity. In comparison with traditional

non-covalent inhibitors, they have exceptional pharmaceutical attributes such as ability to validate pharmacological specificity, high potency, and prolonged pharmacodynamics.[4, 20]

A traditional reversible drug first binds to the target *via* non-covalent bonds, and for this, it depends on the overall structure of the binding site. The drug must then form a covalent bond with a specific nucleophilic residue in the target. The non-covalent binding must be optimized through the overall compound structure design. The second part, on the other hand, is optimized by careful selection of the covalent warhead to ensure appropriate reactivity and orientation within the active site.[21] When held in the correct orientation by the recognition motif, the warhead should have enough reactivity to form a covalent bond with the active site residue but not enough reactivity to react with residues in other proteins. In designing covalent inhibitors, it is essential to choose a warhead designed specifically for the target amino acid side chain.[21]

1.4.1 Cysteine-reactive electrophilic warheads in covalent modification

In proteins, cysteine is a highly nucleophilic amino acid residue with multiple biochemical functions. Despite the low abundance of cysteine in nature, it has an electron-rich thiol group that exhibits high reactivity and has a number of roles, including metal binding, redox catalysis, and allostery.[22] By far, cysteine residues are mostly targeted by covalent inhibitors due to their high nucleophilicity (**Figure 1.4**).

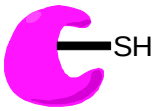

Cysteine

Figure 1.4: A cartoon depiction of a highly nucleophilic cysteine

Among the most popular electrophiles for cysteine residues include epoxides,[23] sulfonate-ester (SE),[24] Michael acceptors, (including acrylates, acrylamides, haloacetamides, cyanoacrylates, and vinyl-sulfonamides).[25, 26] and α-halocarbonyl compounds.[27]

In recent years, FDA-approved drugs have contained acrylamide moiety, which reacts with a specific cysteine residue near the active site of the tyrosine kinase family, making them the frontline treatment for some cancer types. Some of the FDA drugs examples include *afatinib* (2013) (**1.10**), *ibrutinib* (2013) (**1.11**), *osimertinib* (2015) (**1.15**), and *neratinib* (2017) (**1.16**).[28-34]

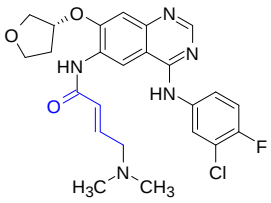

1.10 *Afatinib* (2013)

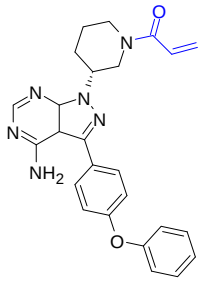

1.11 *Ibrutinib* (2013)

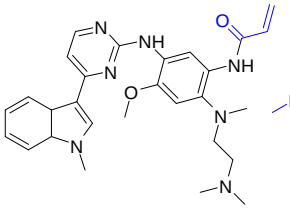

1.15 *Osimertinib* (2015)

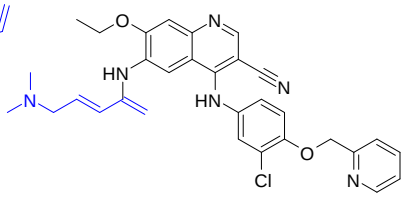

1.16 *Neratinib* (2017)

Afatinib (**1.10**) and *Osimertinib* (**1.15**), were designed to covalently bind to Cys797 in the epidermal growth factor receptor (EGFR). The EGFR is a transmembrane tyrosine kinase involved in activating cell proliferation pathways. Certain cancers, such as non-small cell lung cancer (NSCLC), are known to be driven by mutations that maintain EGFR in an active state.[35] Inhibition of EGFR tyrosine kinase activity is a valid treatment for patients with NSCLC caused by EGFR activating mutations.

Weerapana *et al*. developed a proteomics approach that used isotopic tandem orthogonal proteolysis-activity-based protein profiling (isoTOPABPP) to quantify the intrinsic reactivity of cysteine residues. Breast cancer cells were examined for the presence of hyperreactive

cysteine sites, such as the residue C93 in the uncharacterized/ unidentified protein FAM96B, using iodoacetamide-alkyne (**1.17**).[36]

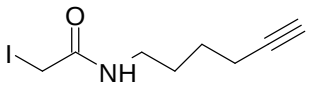

1.17 Iodoacetamide (IA)-alkyne

In a screen of thousands of human proteins, the same team mentioned above used cysteine-reactive small-molecule fragments to identify 700 cysteines in both druggable and non-druggable proteins. Using fragment-based covalent ligand discovery, it is possible to uncover unknown functions of proteins using ligandable proteins and small molecules. This group identified druggable proteins expressed in KEAP1-mutant NSCLC cells using chemical proteomics in 2017 (It's the same reference as of the one in the next line). NR0B1 is a druggable transcriptional regulator that plays a critical role in lung cancers that are Nrf2-dependent.[37]

An innovative chemoproteomic platform was developed by Sprandlin *et al.,* to characterize metabolic enzymes that are predominant in breast cancer cells.[38] This new target inhibits the progression of triple-negative breast cancer (TNBC) by inhibiting glutathione *S*-transferase Pi 1 (GSTP1). Using the same method, nimbolide-alkyne (**1.18**) interacts with an E3 ubiquitin ligase RNF114, and nimbolide recruits RNF114 to recognize substrates.[38]

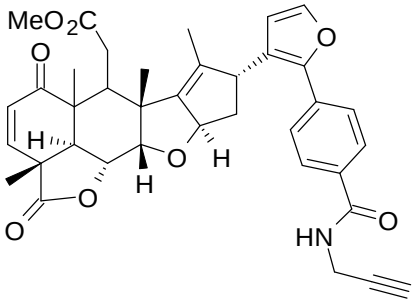

1.18 Nimbolide-alkyne

Yu *et al.* reported a 4-substituted cyclopentenone (**1.19**) for fast and cysteine-specific modification of proteins. This method provides rapid kinetics and a stable product. Additionally, this alteration has almost no impact on the structure or conformation or the biological function of proteins.[39]

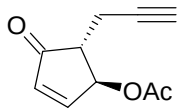

1.19 4-substituted cyclopentanone

Likewise, vinyl sulfones undergo Michael addition with thiols and are often used to inhibit viral and parasite cysteine proteases,[40, 41] such as the main protease (M^{pro}) of severe acute respiratory syndrome coronavirus 2 (SARS-CoV-2) (**1.20**).[42]

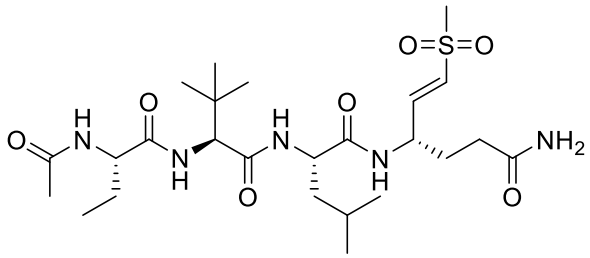

1.20 SARS-CoV-2 Protease

This follows after in December 2019, an acute respiratory disease of an anonymous origin unfolded in Wuhan, Hubei province, China.[43, 44] The initial patient's symptoms resembled the flu and included fever, coughing, and myalgia, but they also had a propensity to progress to potentially deadly dyspnea and acute respiratory distress syndrome.[44]

1.4.2 Lysine-reactive electrophilic warheads in covalent modification

Lysine is one of the amino acids with the greatest potential for covalent modification owing to its large natural abundance (5.9% of human proteins) and inherent nucleophilicity.[45] Importantly, the protein surface has several functional lysine residues that are exposed, which

presents an excellent chance for covalent bioconjugation. However, selective modification of lysine residues *in situ* still presents a significant difficulty due to moderate nucleophilicity compared to the strong nucleophilicity of cysteine. Another obstacle is that the selective modification of functional lysine residues is affected by the significant quantity of non-functional lysines and *N*-terminal lysine residues. The nucleophilic addition of an ε-amine lysine is the typical bioconjugation technique. The ε-amine of lysine is a harder nucleophile than that of cysteine, so should react more readily with harder electrophiles.[46] Aldehydes have been frequently employed to modify residues in proteins, particularly in proteomics.[47, 48] But since the aldimine formation is easily reversed in aqueous conditions, reduction using metal hydrides[49] or transfer hydrogen[50] is often utilized to trap the modified lysine as an amine.

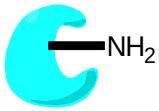

Lysine

Figure 1.5: A cartoon illustration of a lysine residue with its ε-amine group.

Originally, natural products were the only source of lysine targeting covalent inhibitors. Manoalide (**1.21**), a sesterterpenoid antibiotic, was first isolated in 1977 from *Luffariella* variabilis sponge in Palau and possessed good *in vitro* activity against *Streptomyces pyogenes* and *Staphylococcus aureus*.[51] The mechanism of action associated with it was suggested to be the irreversible inhibition of phospholipase A_2 (PLA_2) by covalently binding to Lys6 and Lys79, as confirmed by one-point mutation and structure activity relationships, through bis-imine formation with the lysine residues *via* the two masked aldehydes lactols (**Scheme 1.5**)[52-55]

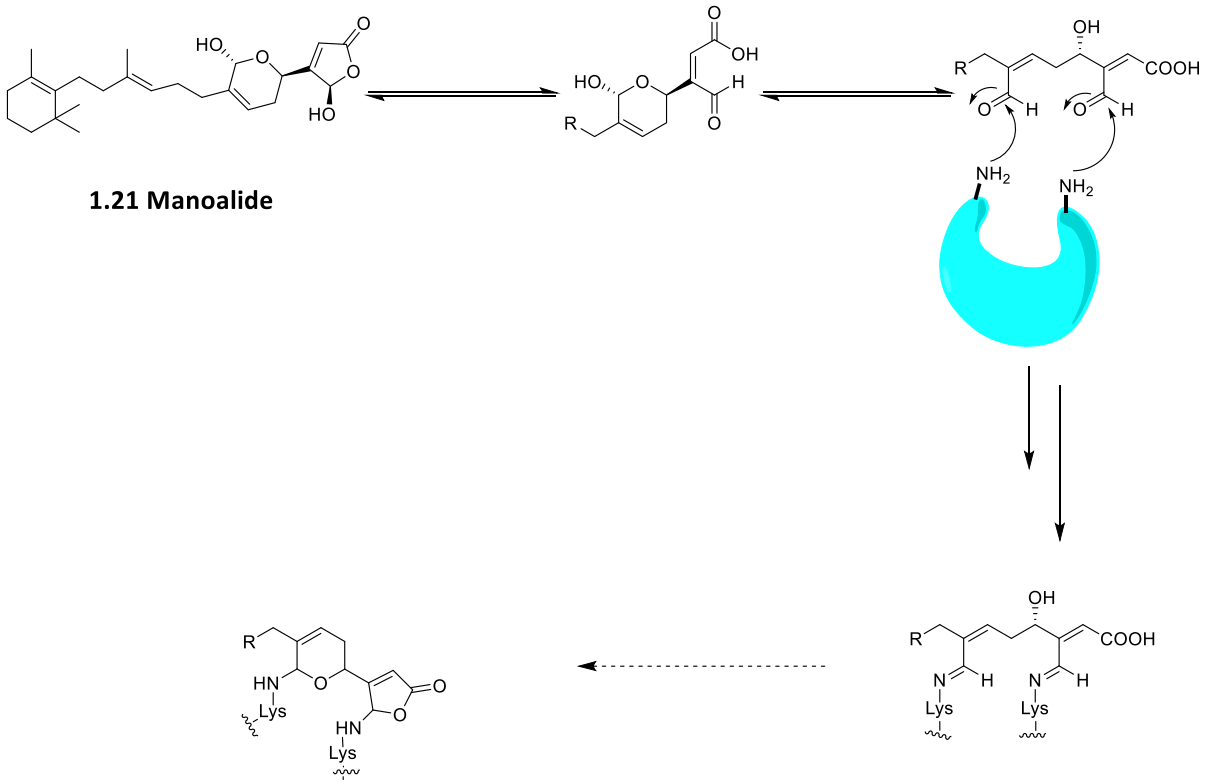

Scheme 1.5: The mechanism of an irreversible inhibitor of PLA_2 by manoalide (**1.21**) forming the hydrolytically stable cyclized bis-hemiaminal.

Numerous electrophilic warheads have been designed to increase the toolbox for selective modification of lysine, such as 2-acetylphenylboronic acids compounds,[56] dichlorotriazines,[57, 58] active esters,[59] sulfur (VI)-based reagents including α,β-unsaturated systems.[60-64] and sulfonyl fluoride compounds.[65, 66]

An investigation by Ward *et al.* demonstrated the use of an alkyne-functionalized *N*-hydroxysuccinimide ester (**1.22**) to map ligand-susceptible hotspots in the proteome. The reagents are capable of profiling a wide range of amino acid residues, including tyrosine, cysteine, and threonine, as well as lysine.[59] The selectivity of specific lysines on Gstt1, Dpyd, and Aldh2 was investigated using fragment-based NHS ester ligands. It is important to note that each of these proteins contains its own active lysine site, such as K71, K497, and K211,

which could be druggable. In these instances, NHS-esters have been proven to be a desirable available reactive site for covalent ligand discovery.[59]

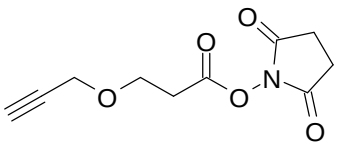

1.22 Alkyne-functionalized N-hydroxysuccinimide ester

In a study conducted by Hacker *et al.* an electrophilic group called sulfotetrafluorophenyl (STP) ester (**1.23**) was developed as a warhead targeting lysine.[45] Over 9,000 lysines in human cell proteins could be detected using the alkyne-containing probe coupled with the isoTOPABPP platform. This method identified 100 reactive lysine residues at the functional sites of proteins. An allosteric mechanism was discovered to inhibit enzymes by lysine-reactive fragment electrophiles, and to inhibit protein-protein interactions in transcriptional regulatory complexes. As a result, they gained a deeper knowledge of functional and ligandable lysines in the proteome and expanded the list of druggable proteins for fundamental and translational studies.

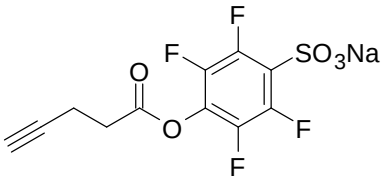

1.23 Sulfotetrafluorophenyl (STP) ester

In Anscombe *et al*. study, a previously known sulfonamide moiety (**1.24**) was replaced in a reversible inhibitor of cancer target cyclin-dependent kinase 2 (CDK2) with a vinyl sulfone warhead, which is located near two non-catalytic lysines in the active site.[60] The resultant molecule, NU6300 acted as an irreversible covalent inhibitor by reacting with Lys89 and has

been shown to be effective in cells, however the potency is weak due to a slow reaction rate between NU6300 and CDK2.[67]

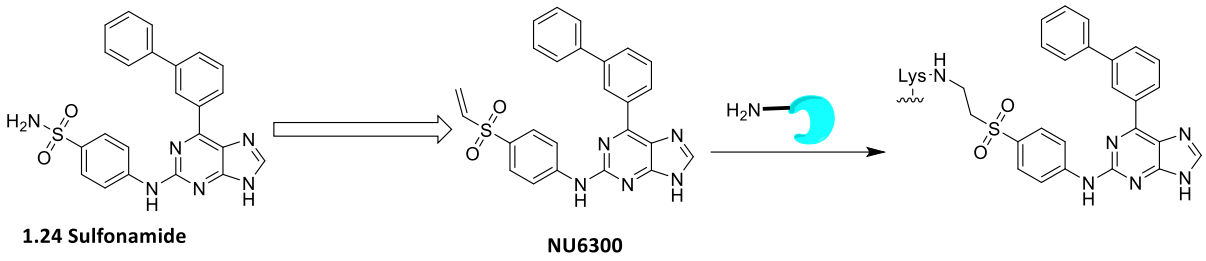

Scheme 1.6: The inception of vinyl-sulfone in place of the sulfonamide in **1.24** which resulted in covalent reaction of NU6300 with Lys89 of CDK2.

Baker *et al.* conducted a study showing the sulfonyl fluoride (-SO_2F) group as a re-emerging promising warhead for the covalent modification of proteins.[68-71] Since then, there has been a continuous development of the irreversible protein binders containing sulfonyl fluorides that are potentially selective and covalent modifiers because of their low reactivity.[72] There are several reasons for the espousal of the (-SO_2F)-based warheads, which include but not limited to, their capability to covalently modify a range of nucleophilic amino acids under physiological conditions, including; lysine,[65] tyrosine,[73] proline,[74] cysteine,[75, 76] histidine,[77, 78] catalytic serine,[79, 80] and threonine[81] and the biological benign nature of the fluoride leaving group.

Pal *et al.* designed a chemical analogue of 5'-benzoyl-substituted adenosine, 5'-*p*-fluorosufonylbenzoyl adenosine (FSBA **1.25**), to study glutamate dehydrogenase's binding site (**Scheme 1.7**).[82] A lysine residue with a *pKa* that reacts readily with the sulfur of the aromatic sulfonyl fluoride moiety, which is a hard electrophile, though its hydrolysis is stable.[83] After FSBA **1.25** was discovered, it was used to study the kinase protein family, as

adenosine has modest affinity but low selectivity for most members of this family. The covalent bond formation with the catalytic lysine is made possible by the 5'-hydroxyl moiety of adenosine, which hints towards a solvent channel vector that is extremely conserved.

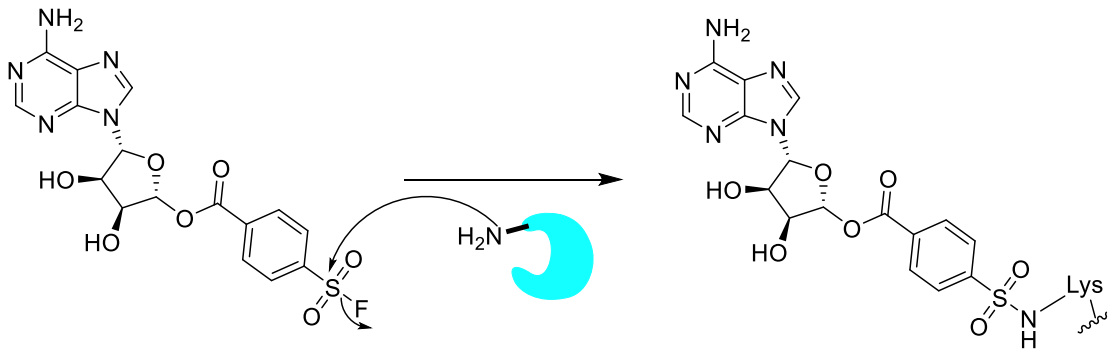

1.25 5'-*p*-fluorosulfonylbenzoyl adenosine

Scheme 1.7: The mechanism of covalent bond formation between the active site lysine and the sulfonyl fluorides of FSBA.

In a study by Li *et al.*, sulfur–fluoride exchange (SuFEx) platforms were developed from SOF_4-derived iminosulfoxy difluoride (**1.26**).[84] In aqueous solution, these groups react with phenols and primary amines, enabling modification of DNA tagged with amines and phenols. Interestingly, only lysine residues were modified, even with very high probe concentrations when labelling proteins with bovine serum albumin (BSA). Using the biocompatible SuFEx ligation for bioconjugation can be beneficial.[85, 86]

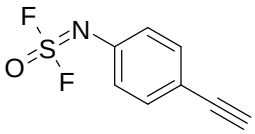

1.26 Iminosulfoxy difluoride

Cuesta *et al*. recently discovered lysine-targeting covalent inhibitors of the eukaryotic translation initiation factor 4E (eIF4E) (**1.27**) and heat shock protein 90 (Hsp90) (**1.28**). [87] The

eIF4E binds m7GTP cap structures at the 5′-end of mRNAs to promote translation of proteins involved in cancer cell growth. The group also indicates that it is notoriously difficult to inhibit eIF4E, and most reported inhibitors are negatively charged guanine analogues with negligible cell permeability. A covalent targeting strategy was envisioned as a solution to these challenges. A covalent docking approach based on lysine was developed since cysteines are not present near the eIF4E cap-binding site. A "make-on-demand" virtual library was utilized to use covalent docking to determine the target of arylsulfonylfluorides on eIF4E's noncatalytic lysine (Lys162). [87, 88]

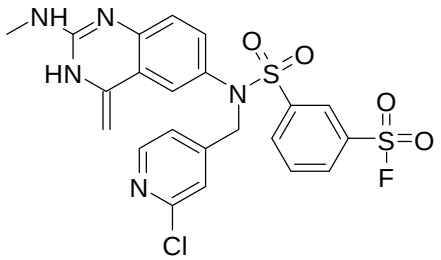

1.27 eIF4E Inhibitor

In another study, Cuesta *et al*., utilized an alternative strategy to increase the binding affinity of lysine targeted covalent Hsp90 inhibitors, independently of their intrinsic electrophilicity or reversible interaction (K_i).[87] An arylsulfonyl fluoride is orientated toward Lys58 on the Hsp90's surface by a chiral, conformationally constrained linker, which allows rapid and enantioselective reaction with the ligand. They discovered that the best covalent Hsp90 inhibitor, arylsulfonyl fluoride (**1.28**), to spanning the 10 Å distance between the purine noncovalent recognition element and the sulfonyl-fluoride, which upon binding to Hsp90, the (S)-methylpiperidine of **1.28** as nucleophilically attacked by Lys58.[87]

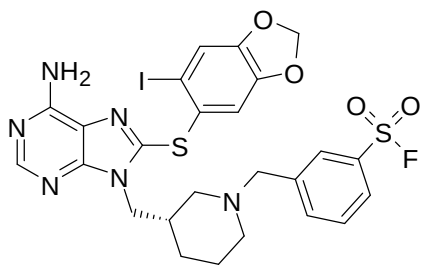

1.28 Hsp90 Inhibitor

On the other hand, the arylfluorosulfates (**1.29**) were first reported in the 1930s by Lange *et al.*[89] however, as a result of the lack of robust synthetic methods for their preparation, this functional group was only briefly discussed, and its use as a warhead for covalent modification of proteins was not explored until 2015 by Baranczak *et al.*[90]

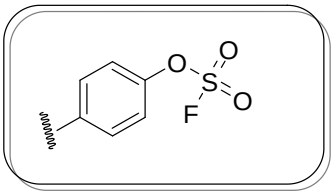

1.29 Arylfluorosulfonate

Using fluorosulfates for covalent protein modification for the first time, Kelly *et al.* replaced the sulfonyl fluoride-based warheads in previously reported fluorogenic transthyretin (TTR) probes with fluorosulfates.[65] The arylfluorosulfates **1.30** and **1.31** reacted slowly and did not reach full conversion when exposed to the targeted transthyretin ε-amino group with a higher *pKa*, and due to their lower reactivity.

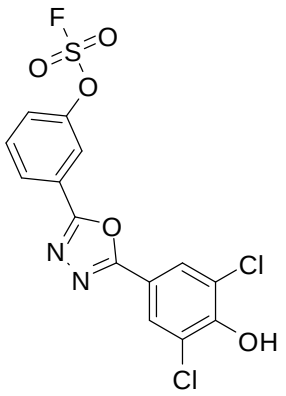

1.30

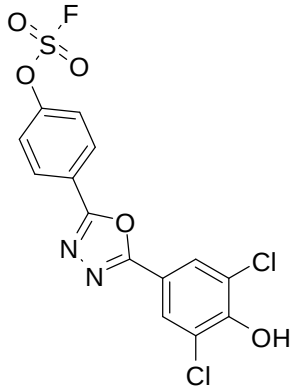

1.31

In view of the fact that fluorosulfate-based warheads have such low and narrow intrinsic reactivity, off-target nucleophiles are rarely covalently labelled in a cellular context, making them largely inactive towards human proteomes unless rigorous conditions are met, such as the presence of basic residues that decrease the *pKa* of the targeted nucleophilic residue and/or facilitate the departure of the fluoride ion. It is therefore possible to use rational targeting of intrinsically reactive Tyr, Lys, or even Ser and His residues in drug discovery when the protein of interest displays a fluorosulfate favoured protein microenvironment, especially when a high-affinity, reversible ligand is on hand and can be modified.[91]

Liu *et al.* have discovered that three arylfluorosulfates (**1.32b**, **1.33b**, and **1.34b**) have better anticancer cell proliferation properties than their phenol (**1.32a**, **1.33a**, and **1.34a**) precursors.[92] Among the previously mentioned three compounds, fluorosulfate derivatives of fulvestrant (**1.33b**) exhibits substantially increased activity in reducing expression of the estrogen receptor (ER) in the MCF7 breast cancer cell line. The fluorosulfate derivative of a drug called Combretastatin A4 (**1.34b**) extert a 70-fold more in potency in drug-resistant colon cancer cells HT-29. In this study, the method of SuFEx chemistry for the conversion of phenolic compounds to respective arylfluorosulfates derivatives *in situ* in 96-well plates was utilized

and this approach is compatible with the synthesis and screening to efficiently evaluate the biological activities of the *in situ* generated aryl fluorosulfates derivatives.[92]

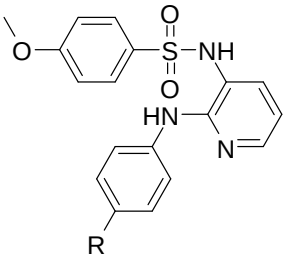

1.32a: R = OH
1.32b: R = OSO_2F

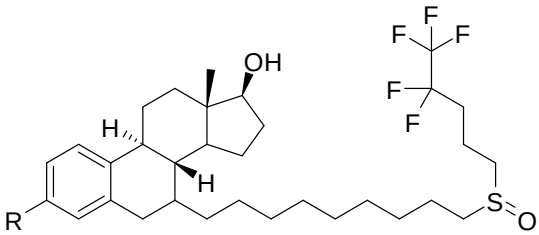

1.33a: R = OH
1.33b: R = OSO_2F

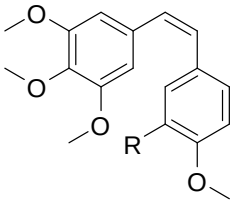

1.34a: R = OH
1.34b: R = OSO_2F

Baggio *et al*. discovered X-linked inhibitor of apoptosis protein (XIAP) **1.35** covalent binder based on aryl fluorosulfate that targets Lys311 in the BIR3 domain.[93] These aryl sulfonyl fluoride-based agents, in particular, can inhibit protein-protein interactions (PPIs) by targeting a poorly nucleophilic lysine on the protein surface.

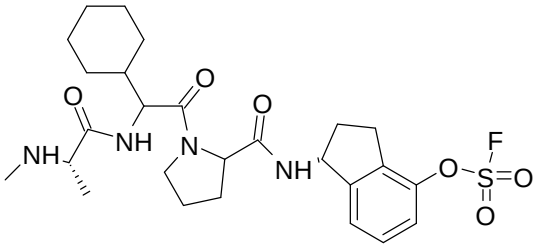

1.35 XIAP Inhibitor

1.5 Hsp90-HOP Inhibition

In tumour biology, heat shock protein 90 (Hsp90) promotes the stabilization and activity of oncogenic 'client' proteins.[94] Hsp90 plays an essential role in chaperoning cancer, as demonstrated by a landmark 1994 study linking **1.36**, benzoquinone geldanamycin, a natural product with antitumor activity, with Hsp90-dependent degradation of the viral oncoprotein v-SRC.[95] This was the first study demonstrating that Hsp90 inhibitors can be used to target cancer cells, and the subsequent study of the ATPase-dependent biochemistry involved in the interactions between chaperones and clients with this inhibitor.[96, 97]

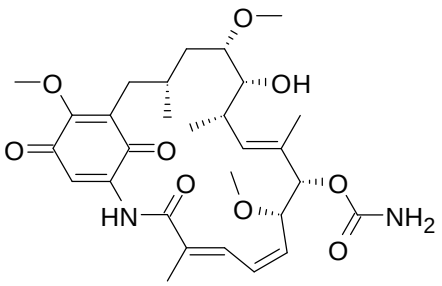

1.36 Geldanamycin

Numerous clinical and pre-clinical drug discovery programs in academic laboratories and the pharmaceutical industry have focused on the Hsp90 molecular chaperone.[98-100] Hsp90 is a multifunctional hub that requires numerous accessory or regulatory cochaperone proteins to function effectively. [101] In a variety of ways, these cochaperone proteins interact with Hsp90 and its complexes. Most of these cochaperones share a common tetratricopeptide repeat (TPR) domain that binds to a distinct MEEVD sequence at the *C*-terminus of Hsp90.[102] One of the best studied co-chaperone Hsp70-Hsp90 Organizing Protein (HOP) is a monomer protein consisting of three TPR domains, namely TPR1, TPR2A and TPR2B, which partake in the protein-protein interactions (PPIs) with Hsp70 and Hsp90, thereby mediating the transfer of client proteins. Inhibition of the PPI between HOP and Hsp90 will result in the disruption of

this pro-oncogenic assembly, potentially leading to cell death. The PPI between Hsp90 and HOP, is mediated by an acid rich MEEVD motif at the *C*-terminus of Hsp90 interact with a lysine rich central groove on the TPR2A domain, known as carboxylate clamp (**Figure 1.6**).[103-105] According to the Cancer Genome Atlas, the co-chaperone HOP is mutated or overexpressed in the cancers which disproportionately affect Southern Africa (breast, esophageal, colorectal, prostate, and cervical cancer). This, therefore, represents an ideal target to develop new cancer therapies for these troubling cancers. The HOP forms a specific interaction with Heat Shock Protein 90, which facilitates the correct folding of proteins, under conditions of cellular stress. This function is particularly important in the cancer cell environment which is characterized by mutated proteins and high growth rates of cancer cells.[106, 107] Therefore, disruption of this PPI, would result in simultaneous degradation of client proteins leading to tumor death and is considered a promising target for cancer drug discovery.

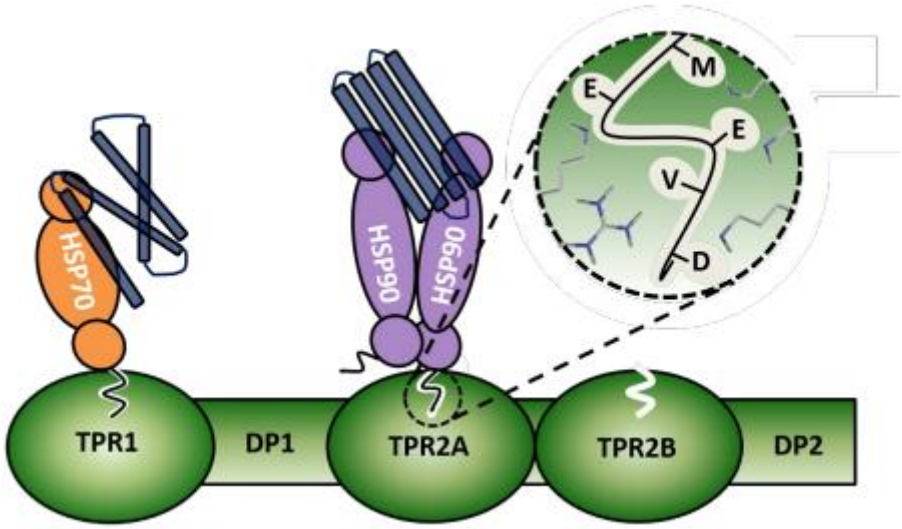

Figure 1.6: The structural representative of Hsp70-HOP-Hsp90 ternary chaperone complex.[105]

1.6 Aim and objectives of the thesis

From the examples discussed above, it is evident that electrophilic warheads are a critical part of many medicinally important compounds, displaying a wide variety of positive impact on improving human health, especially in the fight against cancer.

The aim of this work is to develop electrophilic warheads that are lysine-targeting covalent inhibitors.

The objectives of this research are to:

- Synthesize non-natural amino acids by incorporating sulfonyl-fluorides moieties as electrophilic warheads onto a series of amino acids.
- Characterize each compound using ^{1}H NMR, ^{13}C NMR, ^{19}F NMR, HRMS, and FTIR.

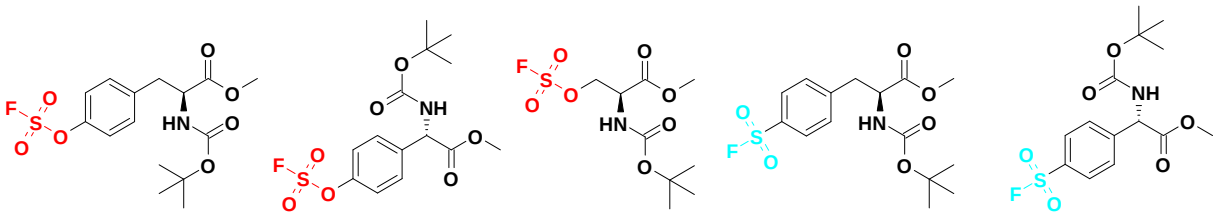

Figure 1.7: Chemical structure representative of the desired electrophilic warheads.

Chapter Two

Review of the Fluorosulfates and Sulfonyl fluoride Synthetic Methods

2.1 Introduction

Years back, sulfonyl fluorides drew an increased attention due to their unique properties and wide application range. In chemical biology and drug discovery, sulfonyl fluorides have been used as covalent probes and inhibitors,[72] and as one of Sulfur Fluorine Exchange (SuFEx) clickable moieties, aryl fluorosulfates (Ar-OSO_2F) have the unique property of being relatively unreactive toward hydrolysis, reduction, nucleophilic substitution, and thermolysis, while only reacting at the sulfur centre when appropriate conditions are met. As selectively addressable scaffolds, they are particularly useful in chemical biology and drug discovery for a wide range of targets.[90, 108]

2.2 Synthesis of arylfluorosulfates (Ar-OSO_2F)

In 1901, Moissan first reported sulfuryl fluoride (SO_2F_2) gas synthesis[109] and Dow Chemical developed it as the pest control agent Vikane in the 1950s.[110] A colourless, odourless gas, SO_2F_2 is 3.5 times heavier than air at normal temperatures and pressures. Gaseous SO_2F_2 has been widely used as a fumigant for more than five decades[111] and recently, it has gained considerable attention in organic synthesis as a reagent.

The reaction between phenols and SO_2F_2 gas reaches its highest point for aromatic compounds, as the aryloxy-fluorosulfate derivatives produced are highly stable. Specifically, aliphatic amines and phenols undergo selective modification by SO_2F_2, whereas aromatic amines, carboxylates, and aliphatic alcohols remain unreactive.

The first arylfluorosulfates were synthesized by pyrolysis in 1930 by Lange and Muller.[112] Later, Coffman and Cramer made substituted phenol fluorosulfates using pyridine and $ClSO_2F$.[113] Both methods, however, had disadvantages due to the high cost of the starting materials, the risky reaction conditions, and the low yields. A simple method for making arylfluorosulfate derivatives from cheap and abundant phenols and SO_2F_2 gas was reported by Firth[114] and other researchers[115] in the 1970s. Chen *et al.* reported in 2014 a more advanced and efficient synthetic method for producing arylfluorosulfates (**2.2**) from phenol derivatives (**2.1**) using gaseous SO_2F_2 in the presence of a base (**Scheme 2.1**).[83, 116]

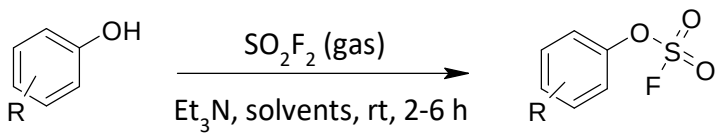

2.1 **2.2** 54% -100%

R = Me, OMe, CF_3, COOEt, Cl, CN, CHO, etc.

Solvents = CH_2Cl_2 or CH_2Cl_2/H_2O

Scheme 2.1: Preparation of arylfluorosulfate derivatives from phenols treated with gaseous SO_2F_2.

In 2016, Chen *et al*. synthesized the Fmoc-Y(OSO_2F)-OH amino acid (**2.4**) that is used on protein ligation, the compound was synthesized from Fmoc-protected tyrosine (**2.3**) in a biphasic solvent system (saturated aqueous borax buffer/CH_2Cl_2) by reacting it with SO_2F_2 (**Scheme 2.2**).[117]

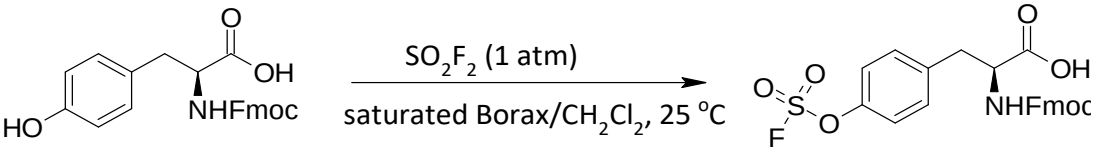

2.3 **2.4** 96%

Scheme 2.2: Preparation of Fmoc-fluorosulfated tyrosine **2.4**.

In 2017, Ren *et al.* synthesized 2-(diphenylphosphanyl) phenyl fluorosulfate (**2.7**). As a result of a Pd-catalysed coupling reaction of diphenylphosphine and 2-iodophenol (**2.5**), 2-(diphenyl)phosphanylphenol (**2.6**) was produced in , which then reacted with SO_2F_2 gas to yield 2-(diphenylphosphanyl)phenyl fluorosulfate (**2.7**) in 97% yield (**Scheme 2.3**).[118]

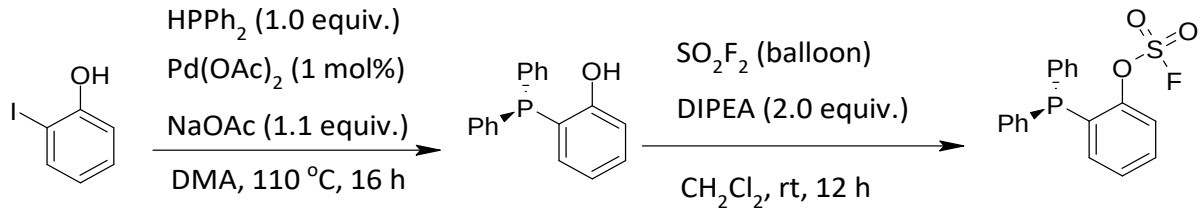

2.5 **2.6** 76% **2.7** 97%

Scheme 2.3: Synthesis of 2-(diphenylphosphanyl)phenyl fluorosulfate.

According to Wu *et al.,* the Sulfur Fluorine Exchange (SuFEx) method can be successfully used for late-stage functionalization of phenolic anticancer drugs by converting them *in situ* into arylfluorosulfonates (**Scheme 2.4**).[92] Three (**1.32b**, **1.33b**, and **1.34b**) mentioned before, *in situ* generated arylfluorosulfonates exhibits stronger anticancer cell proliferation activity than their phenolic precursors.

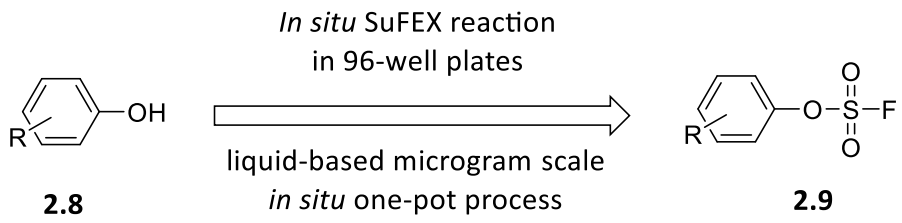

Scheme 2.4: SuFEx click chemistry late-drug functionalized.

Veryser *et al.* came up with another practical transformation of phenols to aryl fluorosulfates in 2017, developing it by *ex situ* generation of SO_2F_2 by means of a dual-chamber reactor.[119] In this method, 1,1'-sulfonyldiimidazole was used as a precursor to generate nearly stoichiometric amounts of SO_2F_2 gas through a dual-chamber reactor (**Scheme 2.5**). The compounds were successfully synthesized, a series of phenols and hydroxylated heteroarenes were also flourosulfated in promising yields.

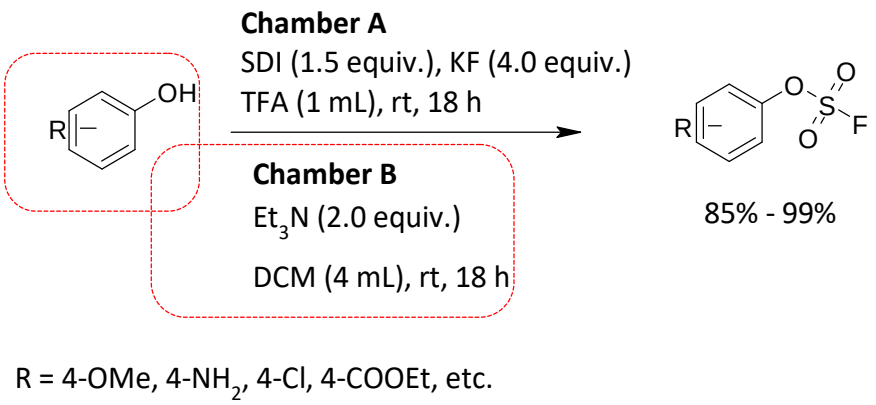

Scheme 2.5: Synthesis of aryl fluorosulfates through *ex situ* generation of sulfuryl fluoride in a two-chamber reactor, with red boxes indicating Chamber B.

2.3 Synthesis of aryl sulfonyl fluorides (Ar-SO_2F)

In 1931, Davies and Dick reported pioneering work on the nucleophilic fluorination of the corresponding sulfonyl chlorides in the presence of a fluoride source to produce arenesulfonyl

fluorides.[120, 121] The corresponding sulfonyl fluorides were readily prepared by boiling aromatic or aliphatic sulfonyl chlorides with aqueous potassium fluoride solutions.

Bianchi *et al.*, developed a method for producing sulfonyl fluorides with KF and 18-crown-6 in dry acetonitrile in 1977 (**Scheme 2.6**).[122]

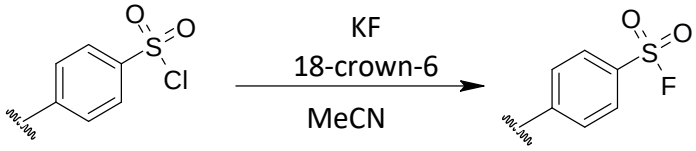

Scheme 2.6: Bianchi's synthesis of sulfonyl fluorides *via* F-Cl exchange.

Although this method may have advantages, side reactions may occur, and alkyl sulfonyl fluorides may be hydrolysed under these conditions.[122, 123] Dong *et al*. developed an improved method using potassium bifluoride as an alternative fluoride source to address this challenge (**Scheme 2.7**).[83] A high yield of sulfonyl fluorides can be produced using this method, from alkyl and aryl sulfonyl chlorides. At the water/organic interface, solvation and hydrogen bonds may play an important role in increasing fluorine's nucleophilicity toward fluorine-chlorine exchange.

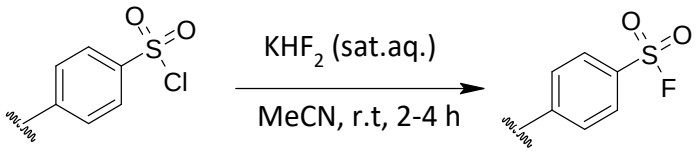

Scheme 2.7: Dong's method of synthesis of aryl sulfonyl fluorides *via* F-Cl exchange.

Insofar as sulfonyl chlorides have poor accessibility and highly sensitive reactivity, alternative methods for synthesizing sulfonyl fluorides have been developed using a range of starting materials. Several aromatic sulfur compounds have been demonstrated to be precursors to

sulfonyl fluorides, including thiols,[124] disulfides,[125] sulfonic acid,[126] sodium sulfonates,[127, 128] sulfinates,[129] sulfonic hydrazides,[130] and sulfonamides[131] (**Scheme 2.8**).

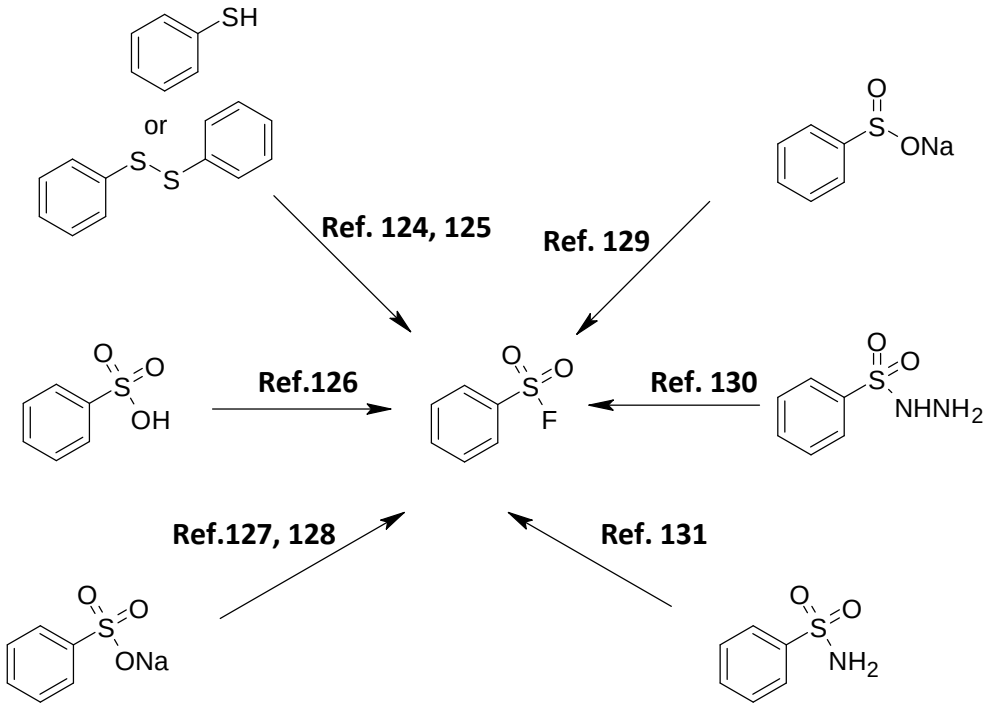

Scheme 2.8: Synthetic path of sulfonyl fluorides from various aromatic sulfur compounds.

Wright and Hallstrom developed an efficient method for synthesizing heterocyclic sulfonyl fluorides compounds in 2006.[124] An oxidative chlorination step is carried out using aqueous sodium hypochlorite to form sulfonyl chlorides *in situ*, followed by a fluoride-chloride exchange step to form the desired sulfonyl fluoride compound. In this reaction, readily available reagents are used, and chlorine gas is not used. This methodology, however, demonstrated only heteroaromatic thiols (**Scheme 2.9**).

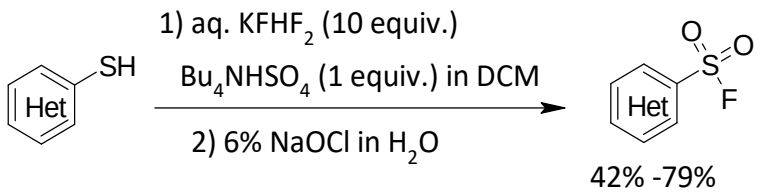

Scheme 2.9: Synthetic approach for the heterocyclic sulfonyl fluorides from thiols.

In 2019, Laudadio *et al*. reported an efficient electrochemical oxidative approach for obtaining sulfonyl fluorides from widely available thiols and disulfides using KF as a cheap fluorine source.[132] As the protocol is mild, it does not require any additional oxidants or catalysts, and it can be applied to any substrate, including alkyl, aryl, heteroaryl, benzyl, or heteroaryl thiols or disulfides (**Scheme 2.10**).

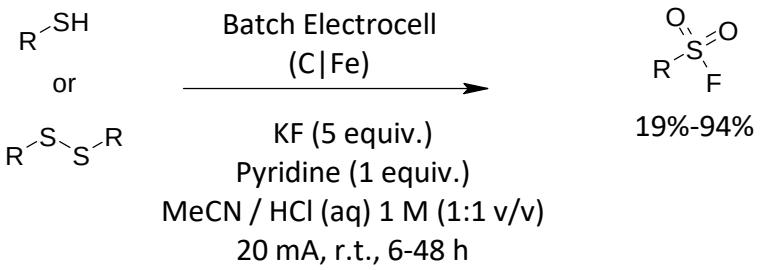

Scheme 2.10: Preparation approach of sulfonyl fluorides from thiols or disulfides using excess KF as oxidant.

Besides using (hetero) aromatic sulfur compounds, a more diverse set of starting materials have also been explored for the synthesis of sulfonyl fluorides. In 2017, Davies *et al*. were the first to report the synthesis of sulfonyl fluorides from heteroaryl bromides.[133] This was the first method to use non-sulfur compounds as a starting point. The two-step, one-pot procedure involved the initial palladium-catalysed sulfonylation of aryl bromides using DABSO as a source of SO_2 to generate an ammonium sulfinate intermediate, followed by *in situ*

electrophilic fluorination of the sulfinate intermediate with NFSI (*N*-fluorobenzenesulfonimide). In moderate to good yields, a variety of aryl and heteroaryl sulfonyl fluorides were obtainable. Notably, this tactic worked well to introduce the fluorosulfonyl moiety late into pharmaceutical intermediates. Additionally, by applying successive DABSO and NFSI treatments to a series of aryl, benzyl, and alkyl Grignard reagents, the relating sulfonyl fluorides can also be produced (**Scheme 2.11**).[133]

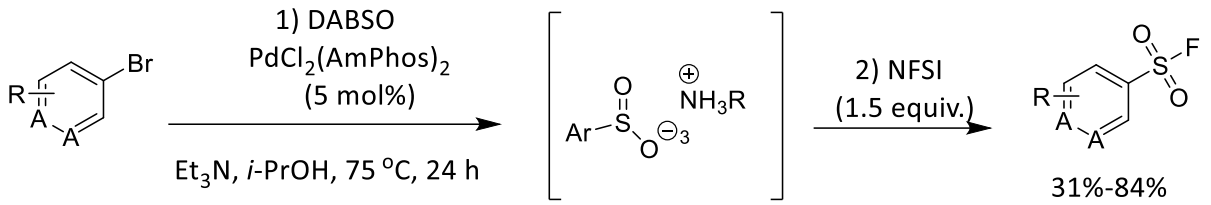

Scheme 2.11: Pd-catalysed synthesis of sulfonyl fluorides from aryl bromides.

A similar strategy was soon developed by Ball *et al*. to produce aryl sulfonyl fluorides from aryl iodides catalysed by $Pd(OAc)_2$ with Selectfluor as the fluorine source (**Scheme 2.12**).[134]

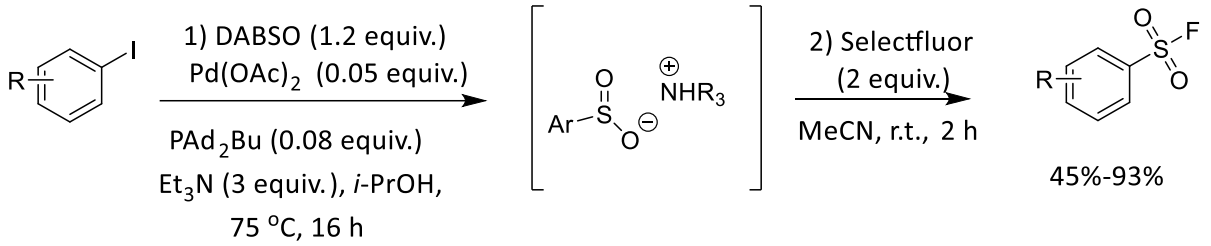

Scheme 2.12: Pd-catalysed synthesis of sulfonyl fluorides from aryl iodides.

A one-pot fluorosulfonylation reaction using Grignard reagents and sulfuryl fluoride (SO_2F_2) was reported by Lee *et al*. icon 2019.[135] At room temperature, a series of aryl, alkyl, and heteroaryl Grignard reagents were converted to desired sulfonyl fluorides in a sulfuryl

fluoride solution. The substrate scope, on the other hand, was relatively limited and inefficient for strongly electron-withdrawing substituted phenyl derivatives (**Scheme 2.13**).

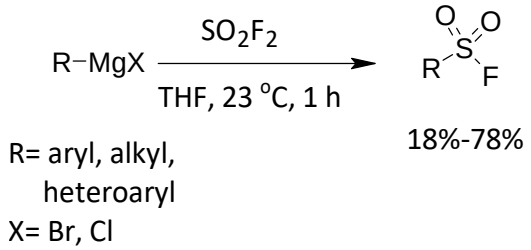

Scheme 2.13: Synthesis of sulfonyl fluorides from Grignard reagents using sulfuryl fluoride.

Chapter Three

Synthesis of non-natural amino acids incorporated with sulfonyl fluorides and fluorosulfates

3.1 Introduction

A series of commercially available natural amino acids were modified into non-naturally analogues by adding weakly electrophilic sulfonyl fluoride moiety to generate lysine targeting covalent inhibitors. Recent work in our lab revealed that a series of tetrazole-containing non-canonical amino acid penta-peptides can bind to the critical lysine in the TPR2A domain of HOP and disrupt the formation of protein-protein interactions between HOP and Hsp90,[105] which gave birth to this work. As a result, we develop non-natural amino acids by incorporating covalent warheads that can potentially target lysine, in the surface of TPR2A of HOP.

3.2 Results and discussion

3.2.1 *Ex-situ* generation of fluorosulfates

One literature procedure for fluorosulfonation was adapted from Chapter two, substituting the hydrogen of the hydroxyl functional group of *L*-tyrosine (**3.1**) with OSO_2F (**3.2**, **Scheme 3.1**). The procedure taken directly from that of Veryser *et al.,*[119] used specific two chamber reactor as reported (**Scheme 2.13**), however, in the initial absence of the two chamber reactor, we used a system of two separate 100 mL round bottom flasks, where flask A acted as chamber A, and flask B, acted as Chamber B. The gas was generated after the precusor SDI and KF were added in flask A, and TFA injected into flask A, the gas was transferred from flask A to flask B using a syringe, until no more gas was produced. The reaction was allowed to run

for 18 hours as stipulated. However, no product was obtained, which we attributed to the low solubility of tyrosine in dichloromethane, due to its zwitterionic effect.[136, 137]

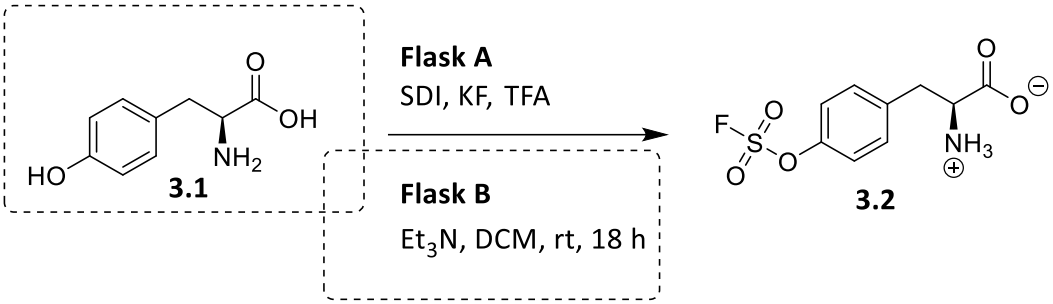

Scheme 3.1: SO_2F insertion in a natural *L*-tyrosine, with highlighted indicating flask B.

To improve the solubility in dichloromethane, as well as preventing unwanted side reactions between the SO_2F group and the amine,[138] we proceeded to protect the polar acid and amine groups. Esterification of compound **3.1** under Fischer conditions proceeded smoothly (**Scheme 3.2**), and the product was found to be a shiny white soft powder, at a yield of 90%.

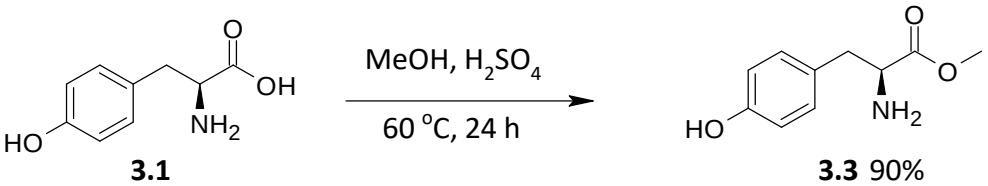

Scheme 3.2: Esterification of *L*-tyrosine.

The ^{1}H NMR spectrum (**Figure 3.1**) of compound **3.3** revealed a characteristic of *O*-methyl chemical shift at δ 3.57 ppm integrating for 3 protons, confirming that the esterification occurred and there are no traces of a starting materials.

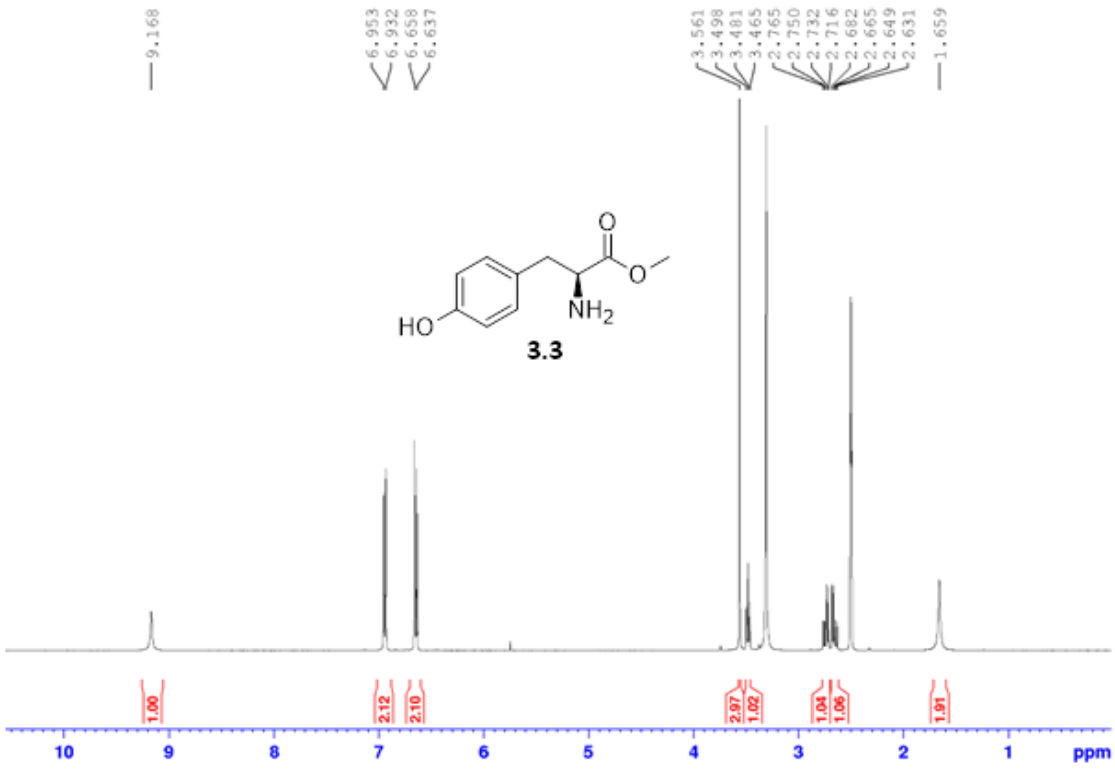

Figure 3.1: ^{1}H NMR spectrum (400 MHz, DMSO-d_6) for compound **3.3**.

Similarly, the amine group was protected, using di-*tert*-butyl dicarbonate in the presence of sodium bicarbonate and water/acetone as a solvent system (**Scheme 3.3**). Compound **3.3** was then Boc protected, the product was obtained in yields of 70%, as a colourless oil.

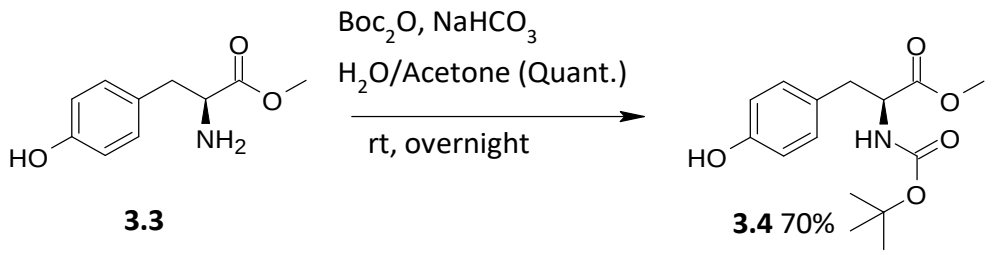

Scheme 3.3: Reaction scheme of a Boc protection of an amine group in compound **3.3**.

The structure of the product **3.4** was confirmed with ^{1}H NMR spectrum (**Figure 3.2**), and it showed a singlet resonating at δ 1.35 ppm, integrating for 9 protons, assigned to Boc.

Additionally, a doublet resonating at δ 7.03 ppm, integrating for 1 proton was assigned to the newly formed carbamate N-H signal, likely to be coupling to a proton of a carbon where the N-H is bonded.

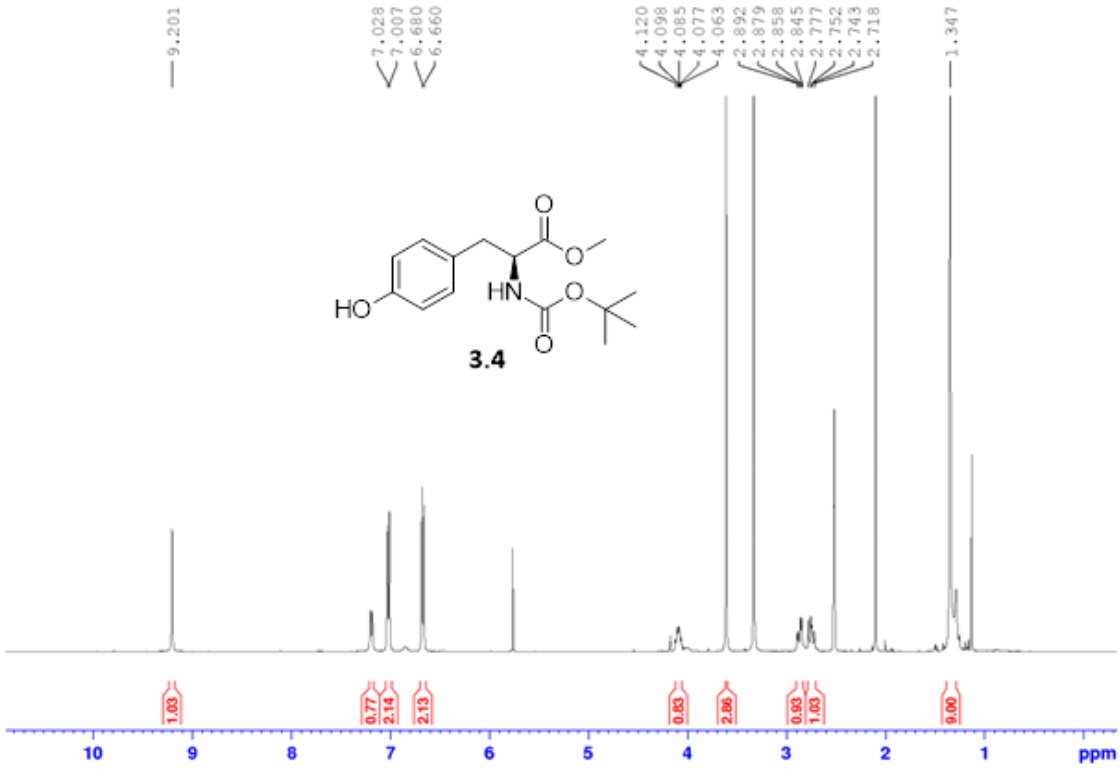

Figure 3.2: ^{1}H NMR spectrum (400 MHz, DMSO-d_6) for compound **3.4**.

With the Boc protected *L*-tyrosine in hand, we once again attempted the sulfonation using two flasks as depicted in **Scheme 3.1** above, unfortunately this method was not successful. When the sample was analysed using ^{19}F NMR spectroscopy, a fluorine signal was not visible. The ^{1}H NMR spectrum (**Figure 3.3**) for the crude product **3.5**, closely resembled the starting material, including the OH signal at δ 9.19 ppm.

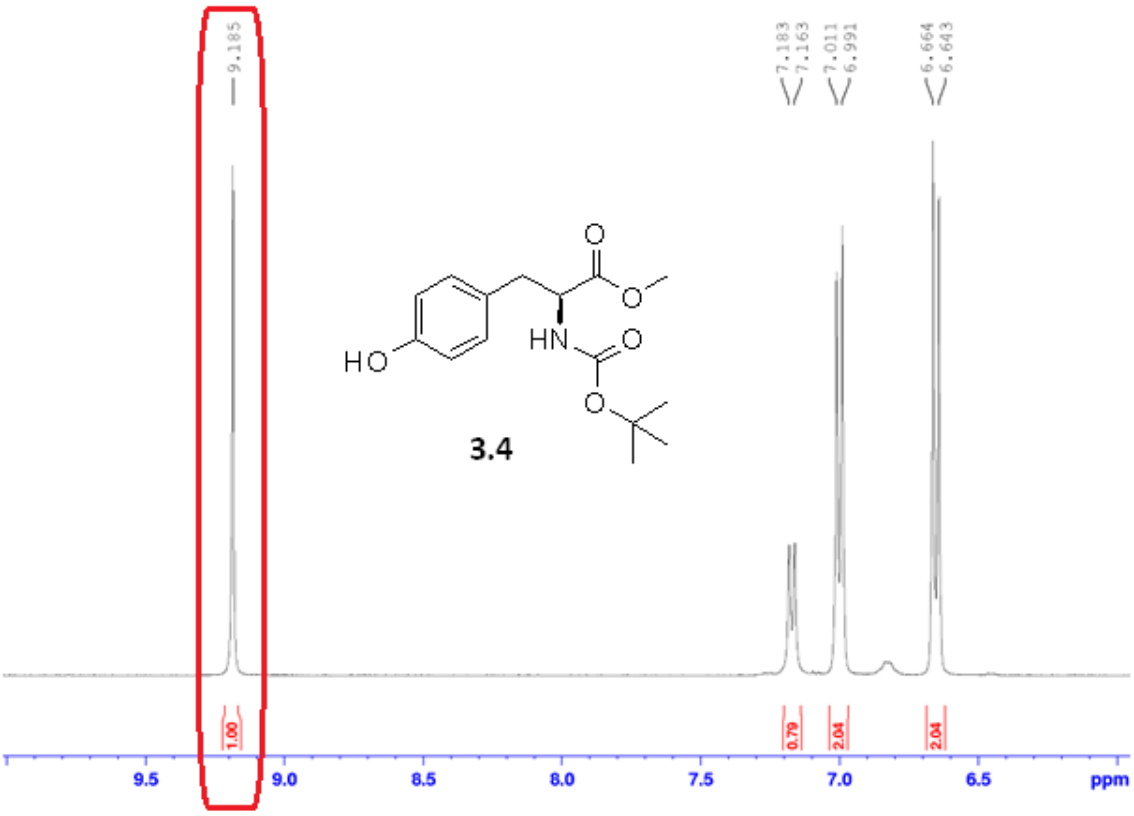

Figure 3.3: Downfield region (δ 6.5 – δ 9.5) ^{1}H NMR spectrum (400 MHz, DMSO-d_6) of **3.4**.

From the ^{1}H NMR above (**Figure 3.3**), it was deduced that the reaction did not work and 3.4 was recovered. For if it was successful, the highlighted singlet resonating at δ 9.19 would be absent and compound 3.5 would be formed.

To circumvent the challenges faced, a dual-chamber reactor glass was purchased (**Figure 3.4**).

Figure 3.4: Dual-chamber reactor, chamber A (left), contains the SO_2F_2 gas, and it is in motion to chamber B (right), where there is a **3.4**, in DCM and triethylamine.

Compound **3.5** was obtained following chamber A (left) being filled with 1,1'-sulfonyldiimidazole (SDI), and potassium fluoride (KF), and chamber B (right) charged with **3.4**, triethylamine and dichloromethane. Lastly, trifluoroacetic acid (TFA) injected through the septum in chamber A (left), and immediate gas forms, flowing from chamber A (left) to chamber B (right). The crude product was then purified by column chromatography on silica (EtOAc: MeOH, 8:2). The product **3.5** was successfully produced in an 85% yield. The ^{19}F NMR was used to confirm the presence of a fluorine atom on the compound, and the signal

appeared as a singlet resonating at δ -73.48 ppm, confirming a successful sulfonation and the presence of only one fluorine on the compound (**Figure 3.5**).

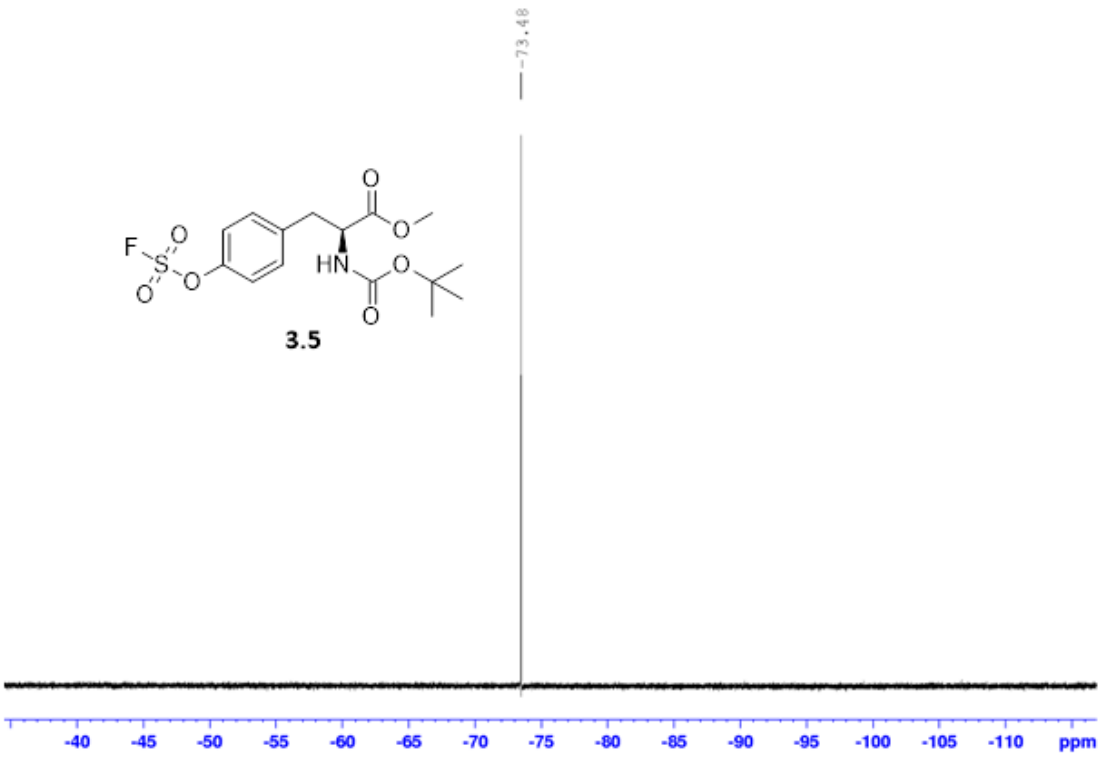

Figure 3.5: ^{19}F NMR spectrum (376 MHz, DMSO-d_6) for compound **3.5**.

Further confirmation of the structure was done using a HRMS (ESI), and in the HRMS spectrum (**Figure 3.6**) a sodium adduct of the molecular ion was observed at *m/z* 400.0848, corresponding to a molecular formular $C_{15}H_{20}NO_7SF$ (calcd for $C_{15}H_{20}NO_7SFNa$, 400.0842).

Elemental Composition Report **Page 1**

Single Mass Analysis
Tolerance = 5.0 PPM / DBE: min = -1.5, max = 500.0
Element prediction: Off
Number of isotope peaks used for i-FIT = 3

Monoisotopic Mass, Even Electron Ions
138 formula(e) evaluated with 1 results within limits (all results (up to 1000) for each mass)
Elements Used:
C: 15-20 H: 20-25 N: 0-5 O: 5-10 S: 0-1 F: 0-1 Na: 0-1

sd_01_088 52 (1.791) Cm (1:58) TOF MS ES+ 5.43e+005

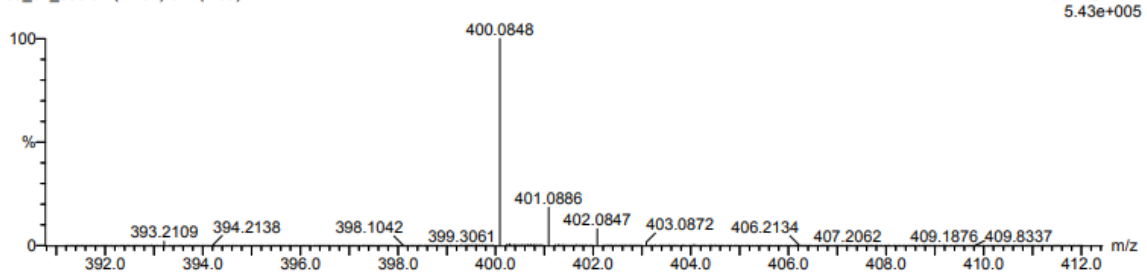

Minimum:				-1.5			
Maximum:		5.0	5.0	500.0			
Mass	Calc. Mass	mDa	PPM	DBE	i-FIT	i-FIT (Norm)	Formula
400.0848	400.0842	0.6	1.5	5.5	703.4	0.0	C15 H20 N O7 S F Na

Figure 3.6: The HRMS spectrum of compound **3.5**.

In addition to the characterization done for compound **3.5**, the ^{1}H NMR analysis was also done to verify the substitution of the hydrogen in the hydroxyl group of the starting material. **Table 3.1** below outlines the ^{1}H NMR of **3.5**, and it validates that the disappearance of the hydrogen of the hydroxyl group. The analysis was based on the likely coupling constants of the protons in the aromatic ring where the OH was in the *para* position, and the other hydrogens being in *ortho* and *meta* position, $^{a}J_{H\text{-}H}$ and $^{b}J_{H\text{-}H}$ coupling (8.7 and 8.6 Hz) respectively.

Table 3.1: ^{1}H NMR analysis of product **3.5** eluted as fluffy light brown needle-like solid (400 MHz, DMSO-d_6).

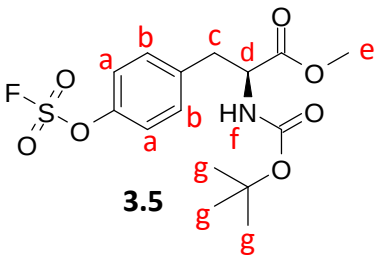

3.5

δ (ppm)	Integral	Multiplicity	*J* (Hz)	Assignments
7.52	2	Doublet	8.7	H-a
7.46	2	Doublet	8.7	H-b
7.34	1	Doublet	8.4	H-f
4.29 – 4.23	1	Multiplet	NA[1]	H-d
3.64	3	Singlet	NA[1]	H-e
3.11	1	Doublet of doublet	13.8, 4.8	H-c
2.92	1	Doublet of doublet	13.8, 4.8	H-c
1.32	9	Singlet	NA[1]	H-g

1) Not Applicable

We then proceeded to include 4-hydoxyl-*L*-phenylglycine (**3.6**) and apply the same procedure as above (**Scheme 3.4**).

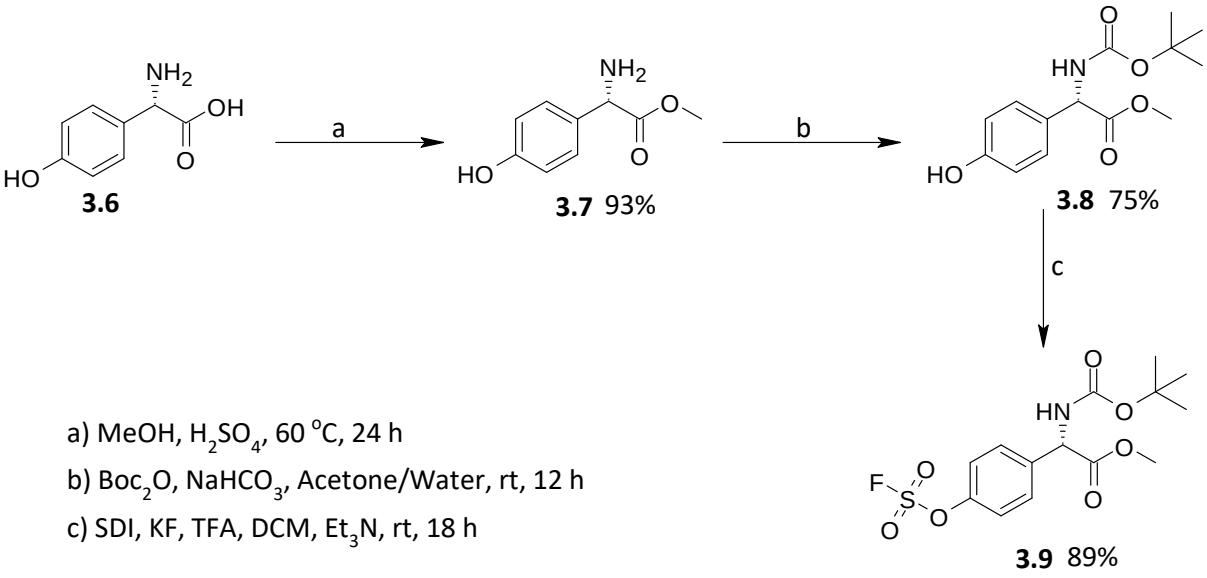

Scheme 3.4: Three steps synthesis of compound **3.9**.

3.2.1.1 Characterisation of compounds 3.6 – 3.9

To illustrate successful formation of our target compound, the characterisation needed to be monitored for the last two steps, the Boc protection and sulfonation. Compound **3.7** was obtained a soft powder solid, in 93% yield. The ^{13}C NMR spectrum (**Figure 3.7**) of compound **3.7** is shown. Here we observed a chemical shift at δ 52.1 ppm, which correlates to a CH_3 group bonded to oxygen to form an ester functional group.

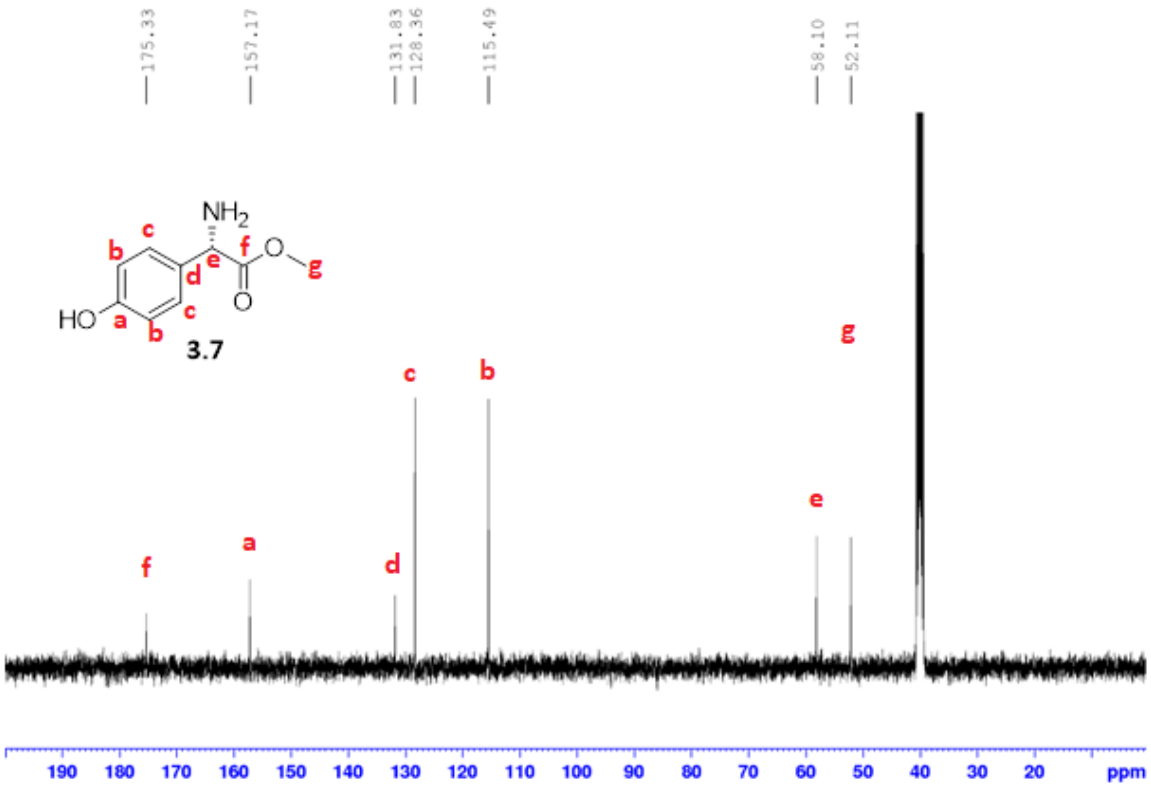

Figure 3.7: ^{13}C NMR spectrum (100 MHz, DMSO-d_6) for compound **3.7**.

The protection step was performed using the same general technique as indicated (**Scheme 3.4)** step b. The product **3.8** was obtained as a clear sticky oil at a yield of 75%. The ^{13}C NMR spectrum (**Figure 3.8**) of the product revealed the characteristics of the Boc-protecting group, with the chemical shift at δ 28.6 ppm representing the three methyl groups, chemical shift at δ 78.9 ppm representing the carbon connecting the three methyl groups mentioned, making it a *tert*-butyl, and the chemical shift at δ 172.3 ppm being the carbonyl of the carbamate.

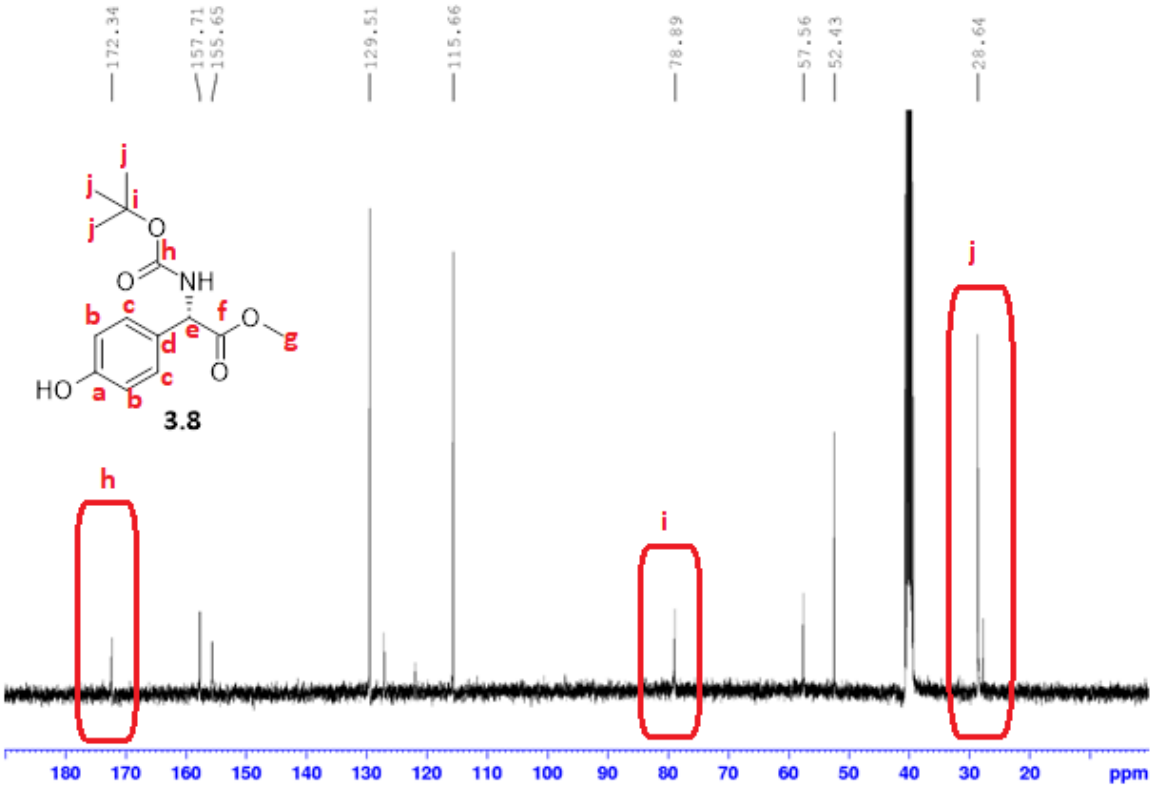

Figure 3.8: The highlighted (h, i, and j) in the ^{13}C NMR (100 MHz, DMSO-d_6) are the peaks of interest indicating the presence of carbamate in compound **3.8**.

Finally, the fluorosulfation of **3.8** was carried out using the SDI precursor of sulfuryl fluoride, and the successful conversion of phenol derivative of **3.8** to aryl fluorosulfate was observed. This transformation had a very good yield of 89%, with the presence of light orange needle-like solid as the product **3.9**. The ^{19}F NMR spectrum (**Figure 3.9**) displayed a singlet resonating at the chemical shift δ –73.5 ppm, of which was in concurrence with what was expected, as there should be only one fluorine signal.

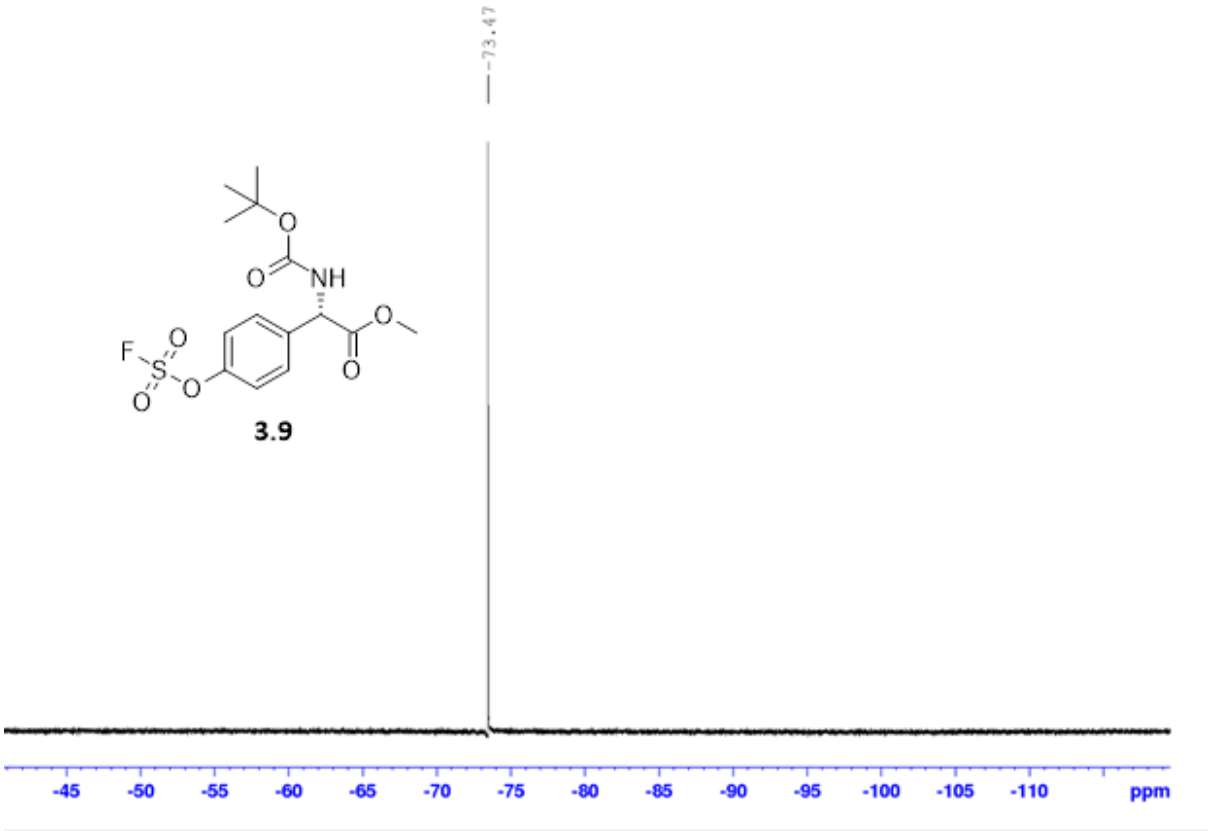

Figure 3.9: The ^{19}F NMR (376 MHz, DMSO-d_6) of compound **3.9**.

The HRMS spectrum (**Figure 3.10**) verified the structure of compound **3.9**, with a sodium adduct being present at *m/z* 386.0692, corresponding to a molecular formular of $C_{14}H_{18}NO_7SF$ (calcd for $C_{14}H_{18}NO_7SFNa$, 386.0686).

Elemental Composition Report **Page 1**

Single Mass Analysis
Tolerance = 5.0 PPM / DBE: min = -1.5, max = 500.0
Element prediction: Off
Number of isotope peaks used for i-FIT = 3

Monoisotopic Mass, Even Electron Ions
62 formula(e) evaluated with 1 results within limits (all results (up to 1000) for each mass)
Elements Used:
C: 10-15 H: 15-20 N: 0-5 O: 5-10 S: 0-1 F: 0-1 Na: 1-1

sd_01_065 89 (1.500) Cm (1:118)
TOF MS ES+

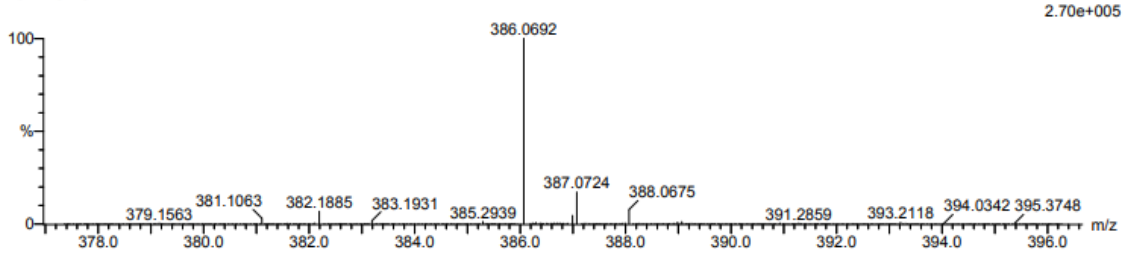

Minimum:				-1.5			
Maximum:		5.0	5.0	500.0			
Mass	Calc. Mass	mDa	PPM	DBE	i-FIT	i-FIT (Norm)	Formula
386.0692	386.0686	0.6	1.6	5.5	639.8	0.0	C14 H18 N O7 S F Na

Figure 3.10: The HRMS spectrum of compound **3.9**.

3.2.1.2 Fluorosulfation of aliphatic amino acids

We then expanded the scope of this study to aliphatic amino acids, to afford an array of fluorosulfonated amino acids.

At the outset, the attempt was to follow the same procedure as the one used on the aromatic amino acids, using the sequence of the three steps process *vide supra*. At the esterification step, several attempts using serine **3.10**, dissolved in methanolic solution, concentrated H_2SO_4, at a 60 °C refluxing, were not successful, as only small amount of crude product obtained (**Scheme 3.5**), and the ^{1}H NMR contained unidentifiable peaks (**Figure 3.11**).

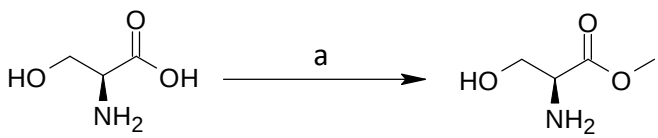

3.10 **3.11** 5%

a) MeOH, H_2SO_4, 60 ^oC, 24 h

Scheme 3.5: Esterification of compound **3.10**.

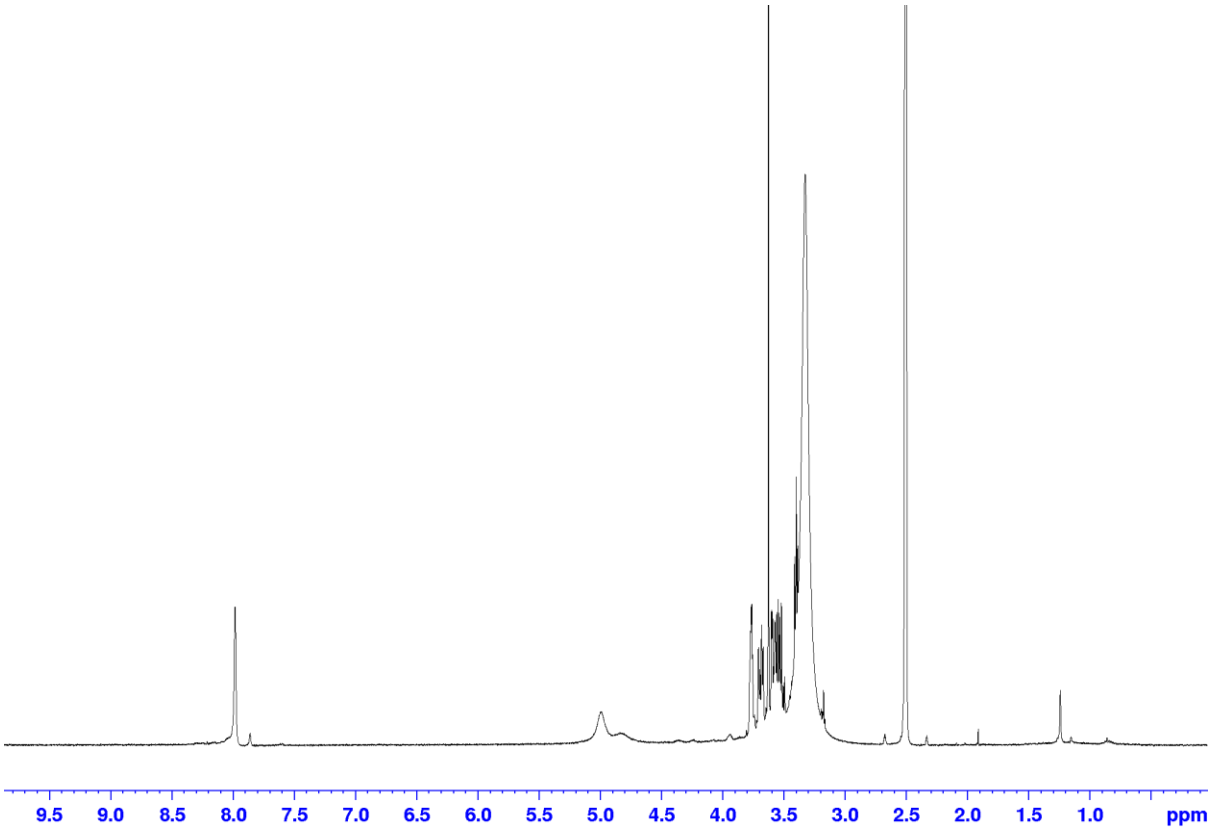

Figure 3.11: The ^1H NMR (400 MHz, DMSO-d_6) of compound **3.11**.

The method that has proven to be working according to literature was when thionyl chloride is used, where the amino acids/ carboxylic acid compounds are dissolved in methanolic solution, under ice-cooling, and thionyl chloride added dropwise for 10 min.[139, 140] However,

due to scarcity of thionyl chloride in the market during the pandemic lock down (2019 to late 2022), this method was not used.

We were therefore compelled to consider other esterification methods, such as the one using methanol/TMSCl, as it has shown to be an expedient transformation system for the preparation of amino acid methyl esters of numerous carboxylic acids.[141, 142]

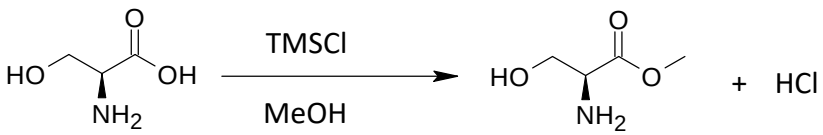

3.10 **3.11** 10%

Scheme 3.6: Transformation of compound **3.10** to methyl ester.

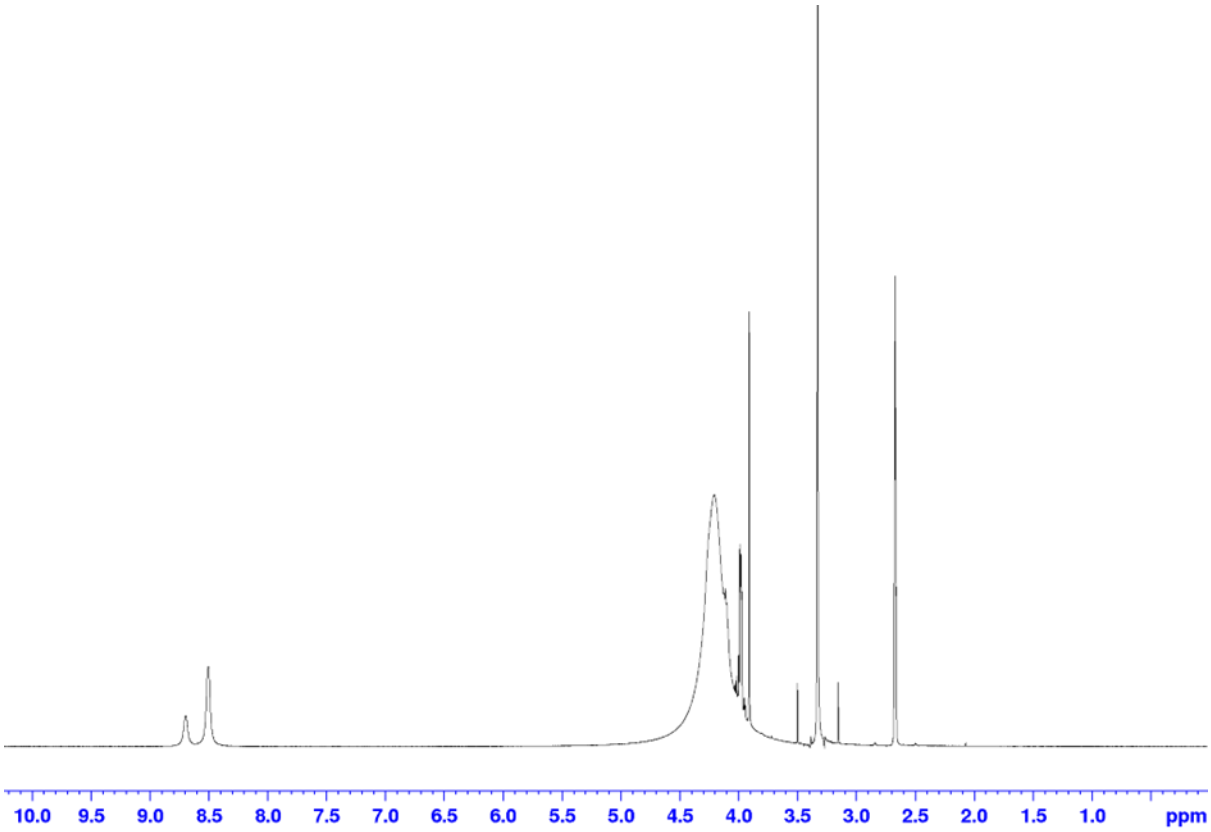

Figure 3.12: The ^{1}H NMR (400 MHz, DMSO-d_6) of compound **3.11**.

The method (**Scheme 3.6**) appeared to have worked, however, the issue encountered was with the purification of the crude product **3.11**, as the crude product was not ultra-violet active. The ^{1}H NMR spectrum (**Figure 3.12**) of the crude compound **3.11** was obtained, however, significant signals were unidentifiable, as the product was impure.

Another attempt was the esterification of *L*-serine using a reagent of an ion-exhange resins, the amberlyst-15 (**Scheme 3.7**),[143] this method had 0% in yield, and the mixture was inseparable with the catalyst.

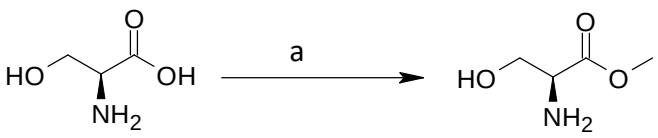

3.10 **3.11** 0%

a) Amberlyst-15, MeOH, rt, 12 h

Scheme 3.7: Amberlyst-15 catalysed esterification.

Without giving up, the last attempt, was when we Boc-protected an amino acid before esterification. An *N*-Boc protected amino acid was transformed to ethyl esters (**Scheme 3.8**).[144, 145] This method gave 86% & 93% in yields.

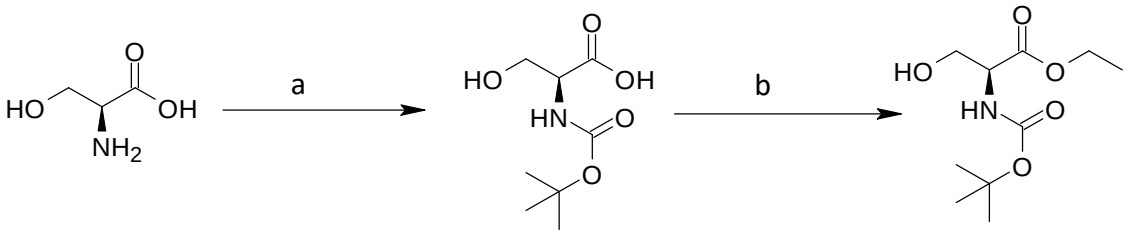

3.10 **3.12** 86% **3.13** 93%

a) Boc_2O, Acetone/Water, rt, 12 h
b) C_2H_5I, DMF, 0 ^{o}C- rt, 12 h

Scheme 3.8: Reaction pathway of an *N*-Boc amino acid ester of compound **3.13**.

The physical property of compound **3.12** were initially a colourless oil, upon drying, it started to solidify to white crystalline structure. The ^{1}H NMR had characteristics of Boc with a singlet signal at a δ 1.40 ppm integrating for 9 protons, and the signal of carbamate N-H where, a doublet was observed at chemical shift δ 6.68 ppm integrating for 1 proton. The hydroxyl signal masked by water signal at 3.33 ppm. (**Figure 3.13**).

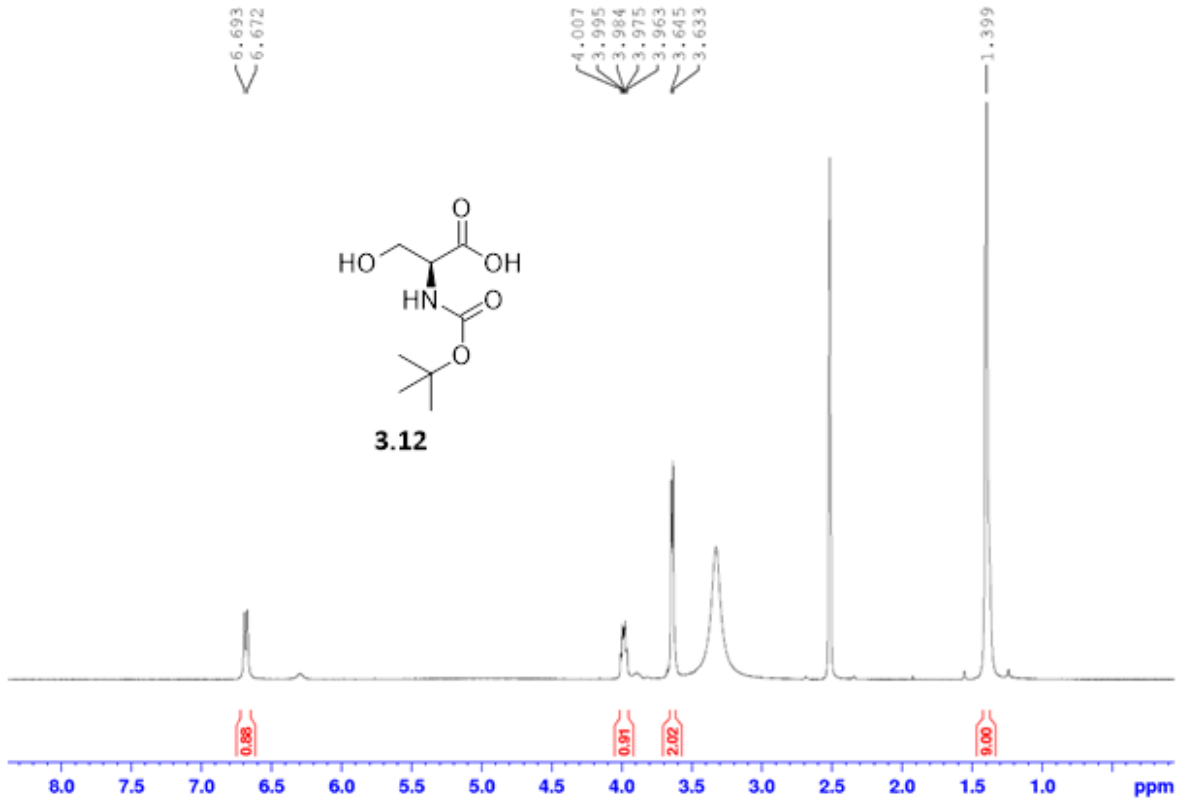

Figure 3.13: The ^{1}H NMR spectrum (400 MHz, DMSO-d_6) of compound **3.12**.

The HRMS spectrum (**Figure 3.14**) confirmed the structure of compound **3.12** with sodium adduct being present at *m/z* 228.0850, corresponding to a molecular formular of $C_8H_{15}NO_5$ (calcd for $C_8H_{15}NO_5Na$, 228.0848).

Elemental Composition Report **Page 1**

Single Mass Analysis
Tolerance = 5.0 PPM / DBE: min = -1.5, max = 500.0
Element prediction: Off
Number of isotope peaks used for i-FIT = 3

Monoisotopic Mass, Even Electron Ions
17 formula(e) evaluated with 1 results within limits (all results (up to 1000) for each mass)
Elements Used:
C: 5-10 H: 15-20 N: 0-5 O: 0-5 Na: 1-1

boc serine 2 (0.034) Cm (1:61) TOF MS ES+ 4.28e+005

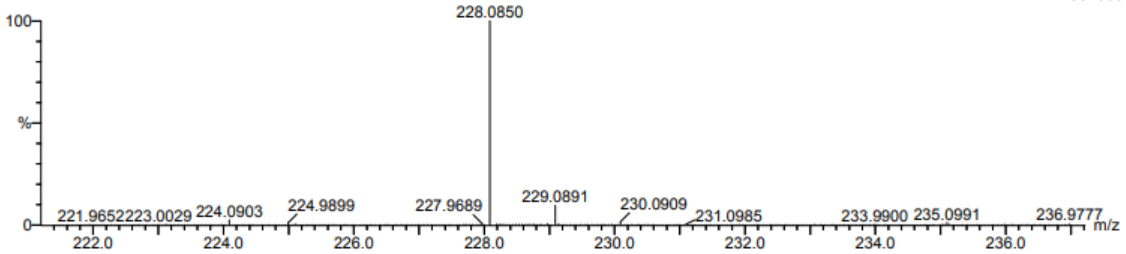

Minimum:				-1.5			
Maximum:		5.0	5.0	500.0			
Mass	Calc. Mass	mDa	PPM	DBE	i-FIT	i-FIT (Norm)	Formula
228.0850	228.0848	0.2	0.9	1.5	661.6	0.0	C8 H15 N O5 Na

Figure 3.14: The HRMS of compound **3.12**.

Compound **3.13** was obtained as an amber yellow oil at 93% in yield following several attempts, this was the depiction prior to the removal of the solvent under *vacuo*, (**Figure 3.15**).

Figure 3.15: Compound **3.13** as crude prior to roto evaporation of the solvent (DMF).

The ^{1}H NMR spectroscopy was used to characterise the product obtained for compound **3.13**, and a triplet signal at chemical shift δ 1.21 ppm and a multiplet signal at a chemical shift δ 4.11 ppm confirmed the presence of an ethoxy group, and next to it, a singlet could still be spotted at a chemical shift δ 1.41 ppm, and it was that of a carbamate, meaning that Boc was still intact, the highlighted region in (**Figure 3.16**).

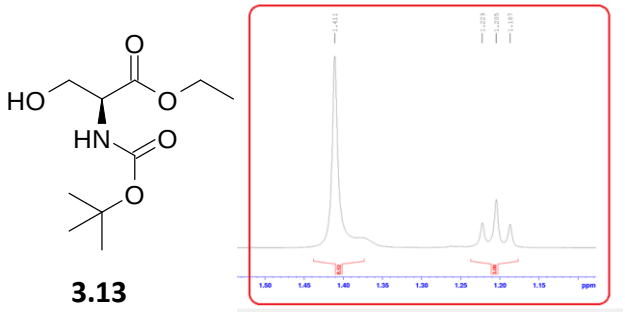

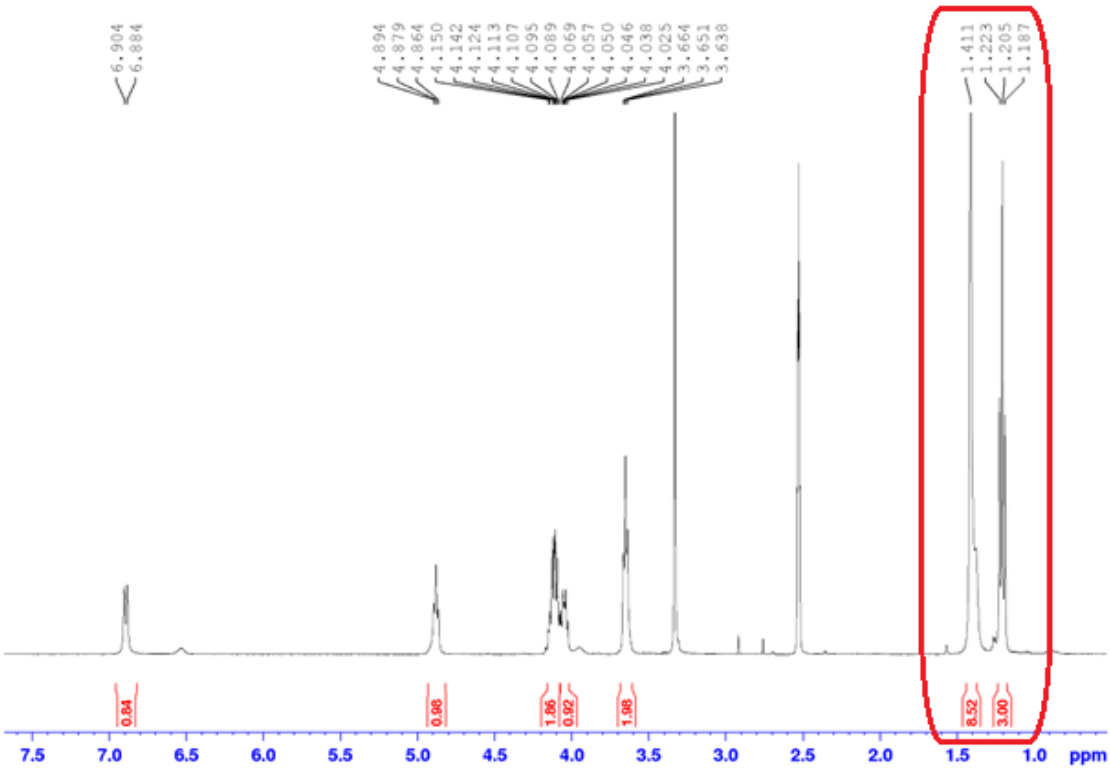

Figure 3.16: The chemical shift δ 0.88 — 1.97 of the ^{1}H NMR spectrum (400 MHz, DMSO-d_6) acquired from the crude product after ethylation of compound **3.12**.

In light of our success with protecting both the amine and carboxylic acid group, we attempted the two-chamber reactor protocol for the installation of the SO_2F group on compound **3.13**. Generating the sulfuryl fluoride gas that would flow from chamber A to chamber B, as previously stipulated. The ^{19}F signal was noted on the spectrum, however it was possibly be of the traces of fluorine in the reaction mixture, the particular reason for this

was that the ^{1}H NMR was not in agreement with this observation, as the hydrogen signal associated with hydroxyl group was not supposed to be visible, should the sulfonation have occurred successfully. And the product was not detectable on the HRMS due to possible overlap of the product with adducts and impurities, hence unable to confirm the structure of the compound.

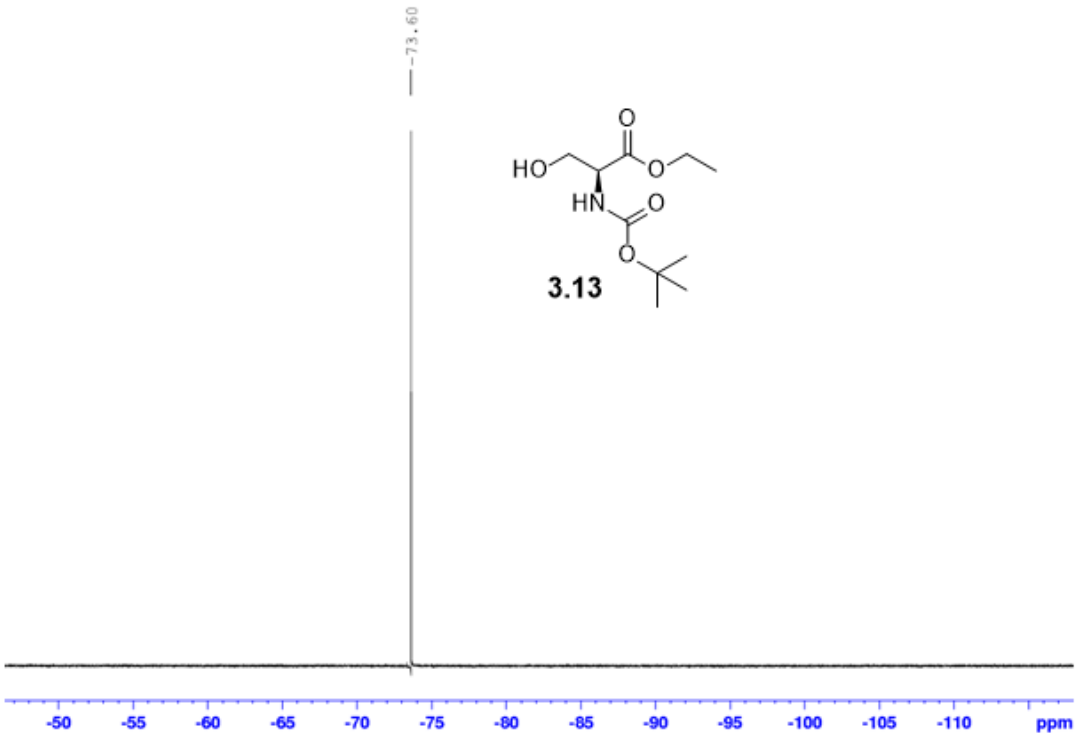

Figure 3.17: The detected traces of ^{19}F NMR (376 MHz, DMSO-d_6) on the string material **3.13**.

The red highlighted triplet (**Figure 3.18**), indicates the integration of the proton that was supposed to be absent, should the reaction have been successful. This meant that the substitution of a hydrogen in the hydroxyl group by sulfur was not a success.

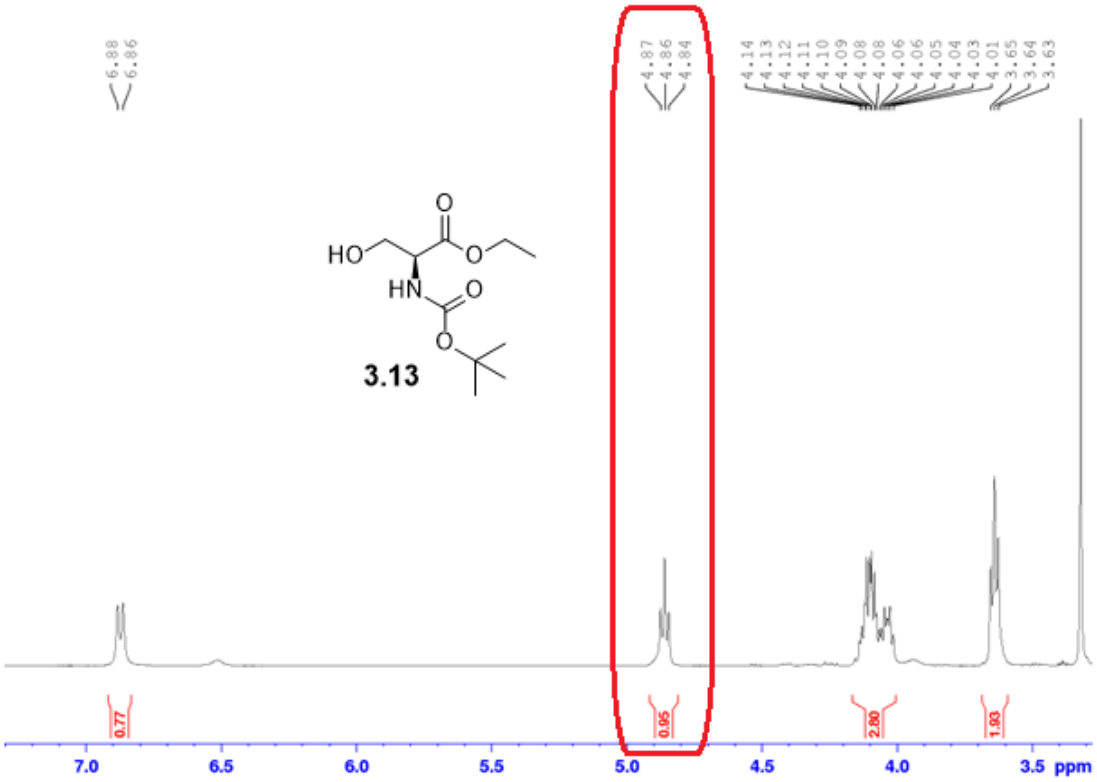

Figure 3.18: ^{1}H NMR (400 MHz, DMSO-d_6) breakdown of brown oil product **3.13**.

The predicament did not put halt in attempting other starting materials, however, at this instance, homoserine **3.15** was used, following the same protocol designed when working with aliphatic amino acids, in terms of protecting the groups of interest (**Scheme 3.9**).

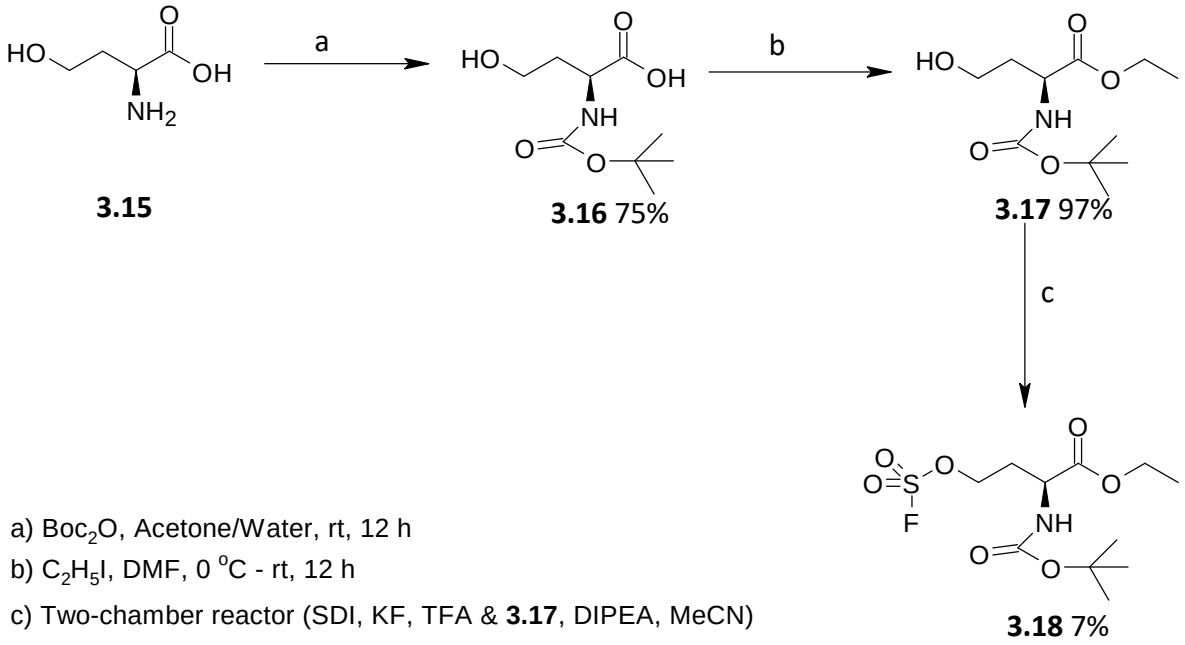

a) Boc_2O, Acetone/Water, rt, 12 h
b) C_2H_5I, DMF, 0 ^oC - rt, 12 h
c) Two-chamber reactor (SDI, KF, TFA & **3.17**, DIPEA, MeCN)

Scheme 3.9: Three steps synthetic pathway towards **3.18**.

The ^{13}C NMR spectrum (**Figure 3.19**) revealed signals at a chemical shift δ 28.5 ppm, δ 79.3 ppm, and δ 155.7 ppm, all these signals showed the characteristics of the presence of the carbamate group on compound **3.16**, the three methyl groups, carbon connecting these methyl groups and carbonyl group, respectively.

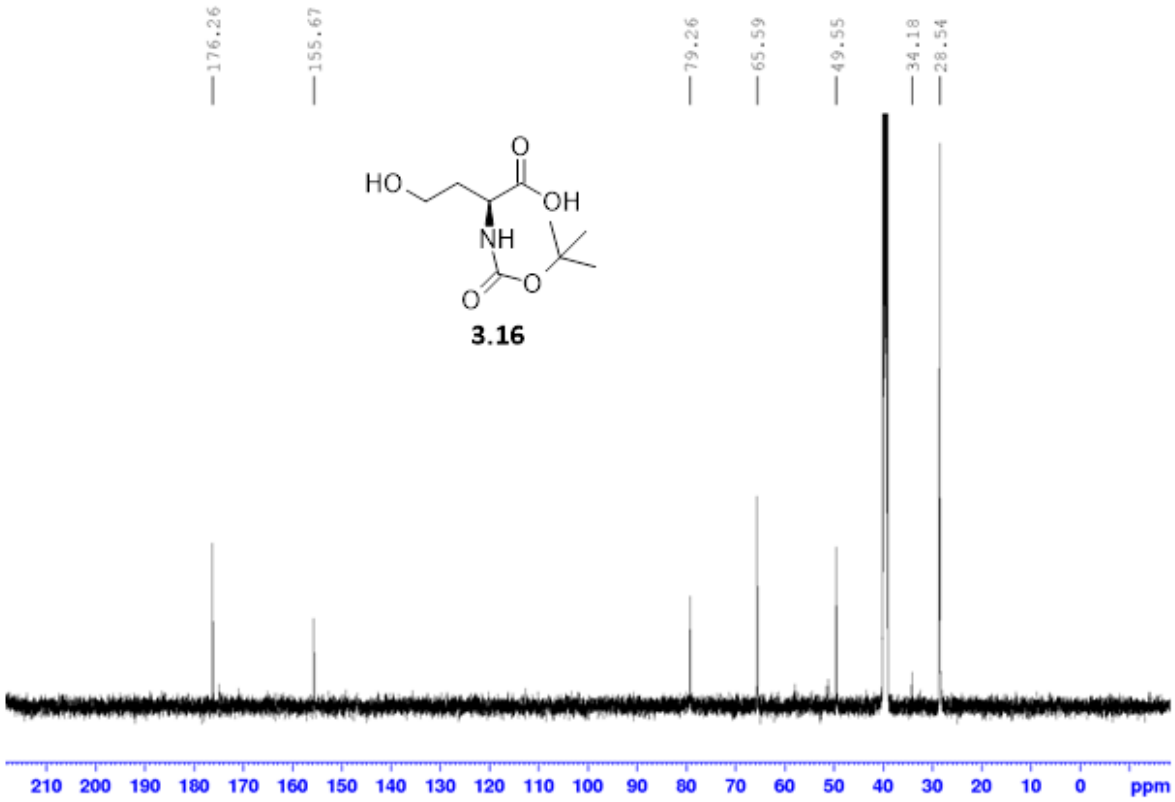

Figure 3.19: The ^{13}C NMR spectrum (100 MHz, DMSO-d_6) of compound **3.16**.

The crude product for compound **3.17** was confirmed with the ^{13}C NMR spectroscopy, the spectrum (**Figure 3.20**) showed the presence of the signals for CH_3 and CH_2 of the ethoxy at chemical shift δ 14.0 ppm and δ 61.3 ppm, respectively.

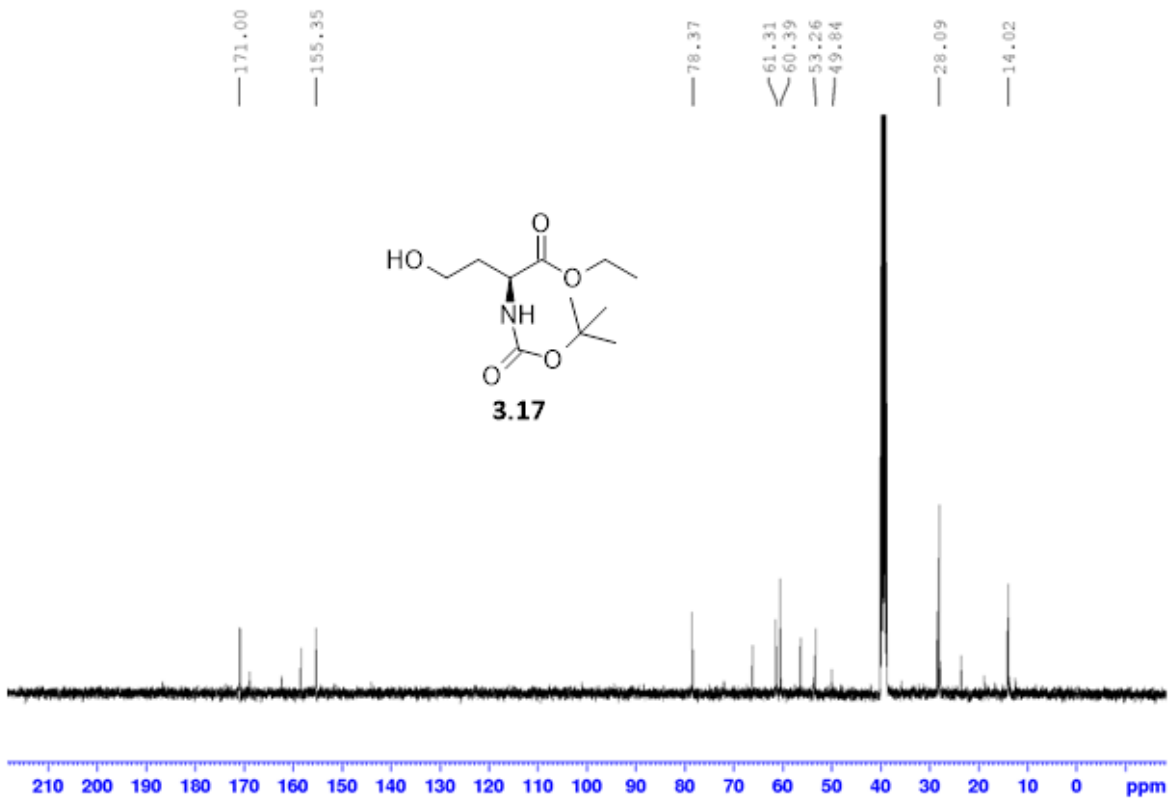

Figure 3.20: The ^{13}C NMR spectrum (100 MHz, DMSO-d_6) of the crude product of compound **3.17**.

Compound **3.18** was found in an insignificant yield of 7% as a brown oil, and the signals of interest were unidentifiable. The ^{1}H NMR spectrum (**Figure 3.21**) was obtained for compound **3.18**.

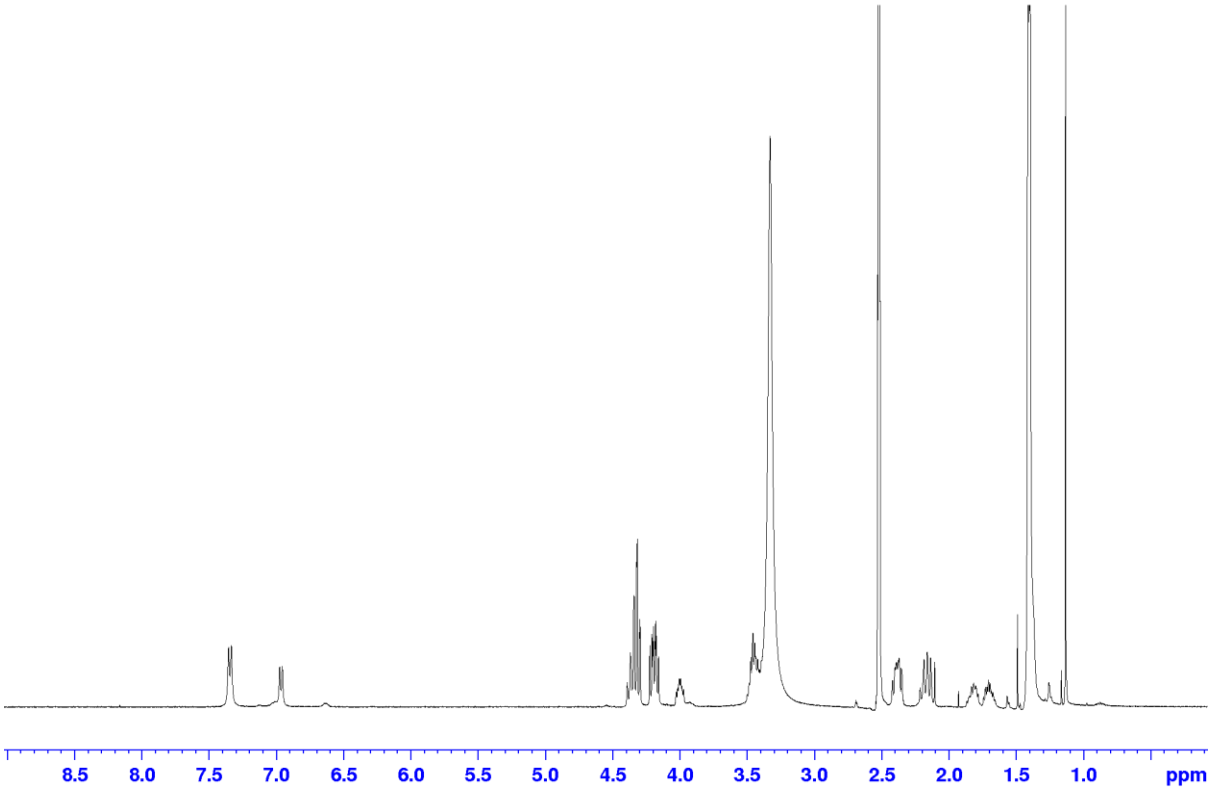

Figure 3.21: The ^{1}H NMR spectrum (400 MHz, DMSO-d_6) of compound **3.18**.

This then led to a necessity of the perusal of Veryser's work, on which it was noted that the aliphatic compounds were only tolerated, as it was only the aromatic hydroxyl groups that reacted with sulfuryl fluoride,[119] and this was concurring with what was observed by Dong's group.[83] We inferred that this was rather a sacrosanct information that should be famed.

3.2.2 One-pot synthesis of sulfonyl fluoride

Davies *et al.,*[133] developed a method of synthesising sulfonyl fluorides from heteroaryl bromides. It was a two-step, one-pot procedure involving an initial palladium-catalysed sulfonylation of aryl bromides using 1,4-diazabicyclo[2.2.2]octane bis(sulfur dioxide) (DABSO)

as a source of SO_2 to make ammonium sulfinate intermediate, which reacted with *N*-fluorobenzenesulfonimide (NFSI).

This literature method was adopted, however, in this work, the halogen was chlorine and fluorine and for all these aryl halogen compounds, a three-steps process was implemented, of which entailed the esterification, Boc protection, and sulfonylation. The initial attempt was with 4-chloro-*L*-phenylalanine **3.19**, transforming it from it to **3.22**, *via* a three-steps process (**Scheme 3.10**). Each transformation was noted and characterised.

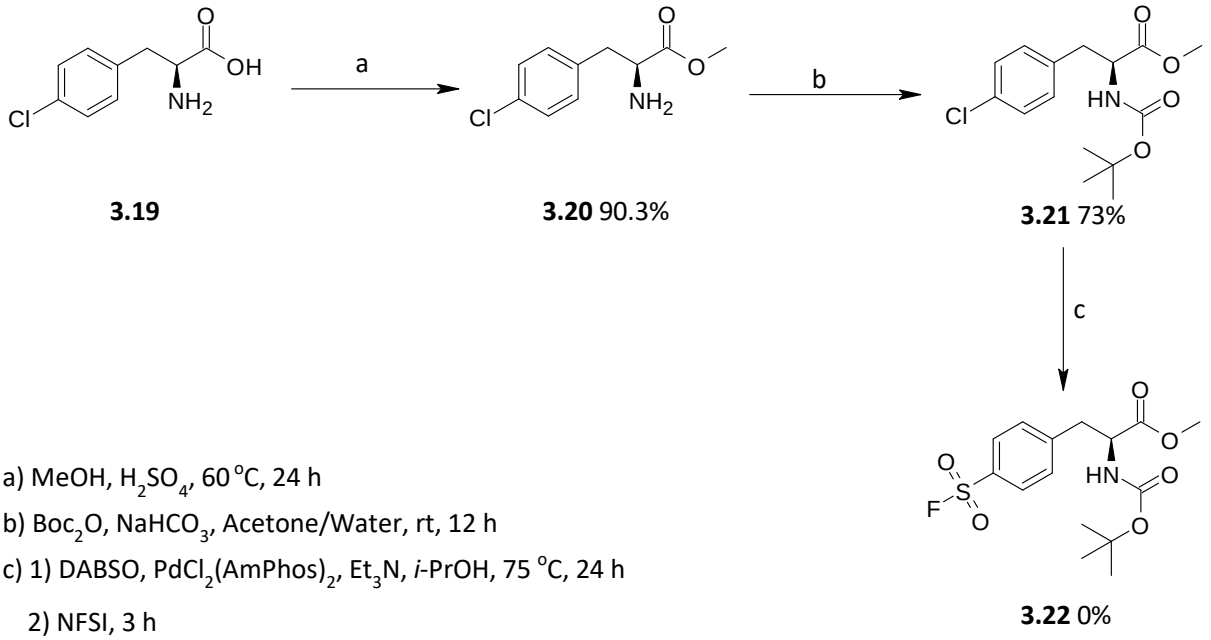

Scheme 3.10: The synthetic pathway for the sulfonylation of compound **3.22**.

The structures were confirmed by NMR spectroscopy and HRMS. The product and the intermediate compounds (**3.20** & **3.21**) were observed, however, compound **3.22** was 0% in yield. This three steps process to **3.22** was repeated numerous times, but the results were without significant improvement. Compound **3.20** was obtained as a light viscous clear liquid at 90.3% yield (**Scheme 3.10**). Without any purification, **3.20** was Boc protected giving clear

oil **3.21**, in 73% yield. The ^{1}H NMR spectrum for this transition, esterification and Boc protection was obtained (**Figure 3.22**), the highlighted are the signals of interest, the red coloured signal was assigned to the three methyl groups of the carbamate, integrating for 9 protons, and the blue highlighted signal was assigned to a methoxy integrating for 3 protons.

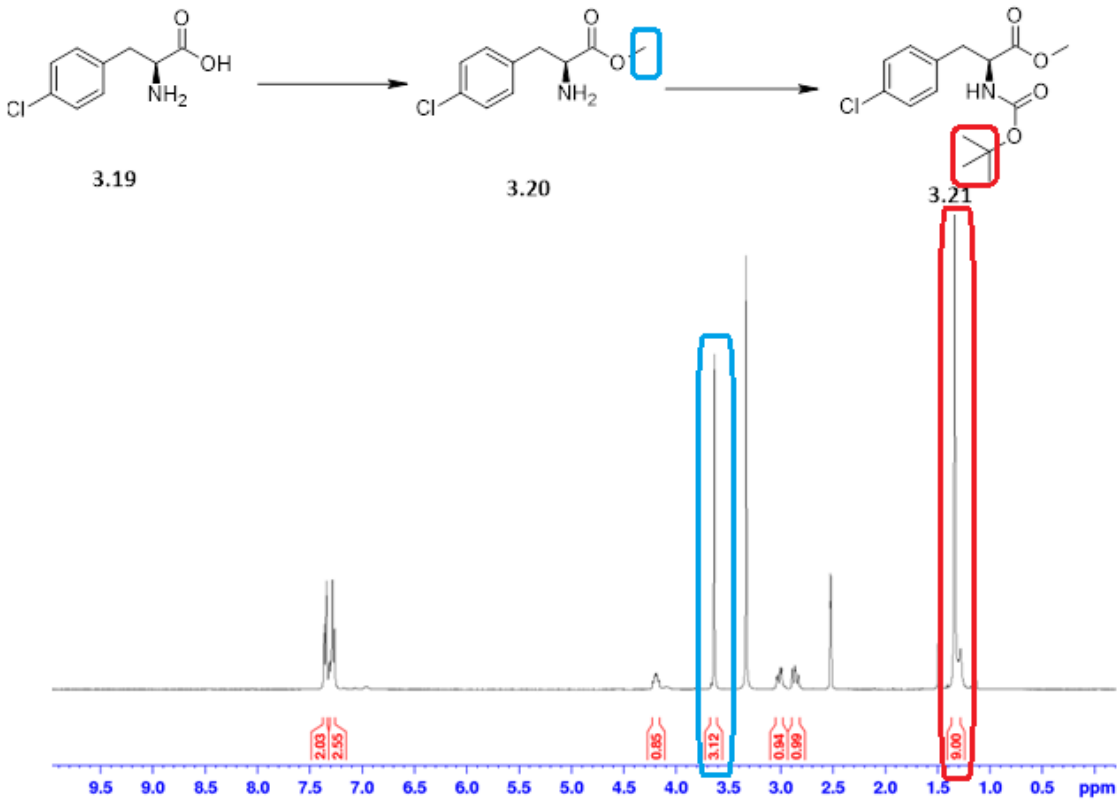

Figure 3.22: The ^{1}H NMR spectrum (500 MHz, DMSO-d_6) of the conversion of **3.19** to Boc protected product **3.21**.

With the sulfonylation of compound **3.20** unsuccessful, we attempted the three-step process using compound **3.23**. Compound **3.24** was obtained as alight-yellow viscous liquid, in 92% yield, and compound **3.25** was obtained as a light-yellow oil, in 75% yield, (**Scheme 3.11**). Sulfonylation of compound **3.25** yielded 0% of expected compound **3.26**.

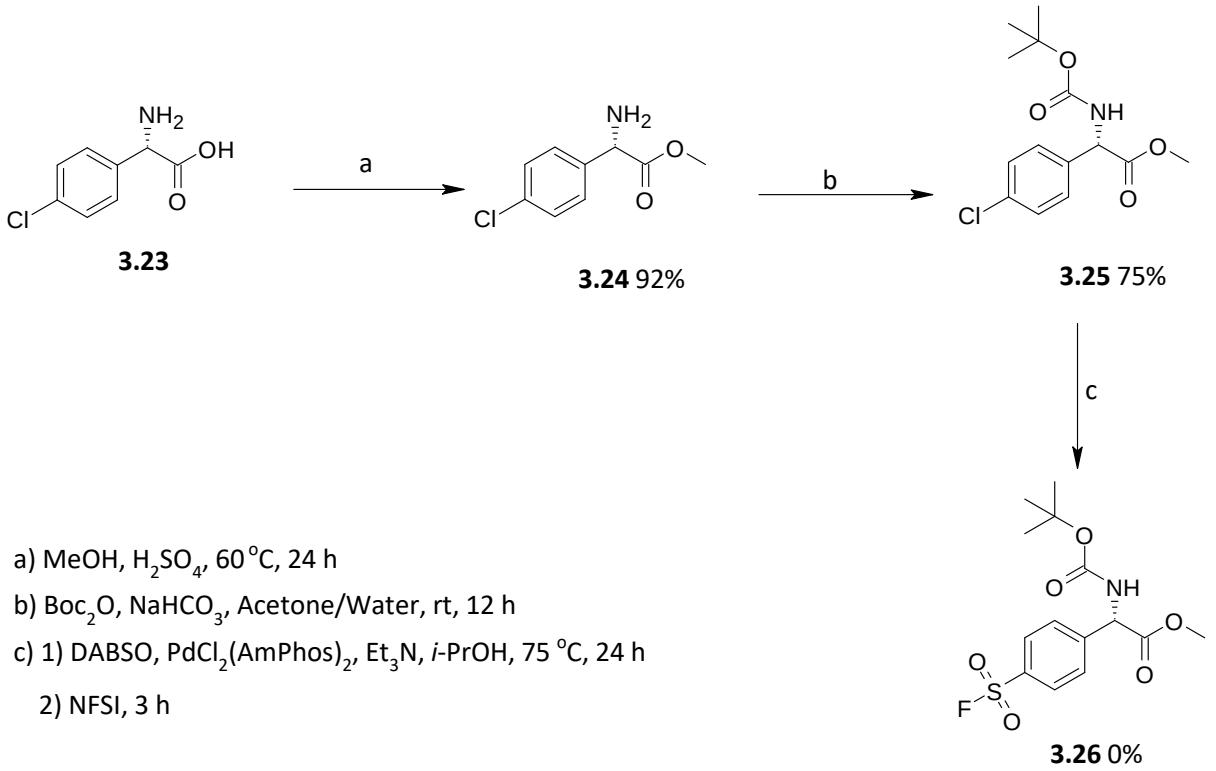

a) MeOH, H_2SO_4, 60 °C, 24 h
b) Boc_2O, $NaHCO_3$, Acetone/Water, rt, 12 h
c) 1) DABSO, $PdCl_2(AmPhos)_2$, Et_3N, *i*-PrOH, 75 °C, 24 h
2) NFSI, 3 h

Scheme 3.11: Pathway demonstration from compound **3.23** to compound **3.26**.

The ^{1}H NMR spectrum (**Figure 3.23**) of compound **3.24** showed the characteristic singlet of methoxy at a chemical shift δ 3.61 ppm, integrating for 3 protons. This indeed confirmed the success of esterification with no traces of starting material.

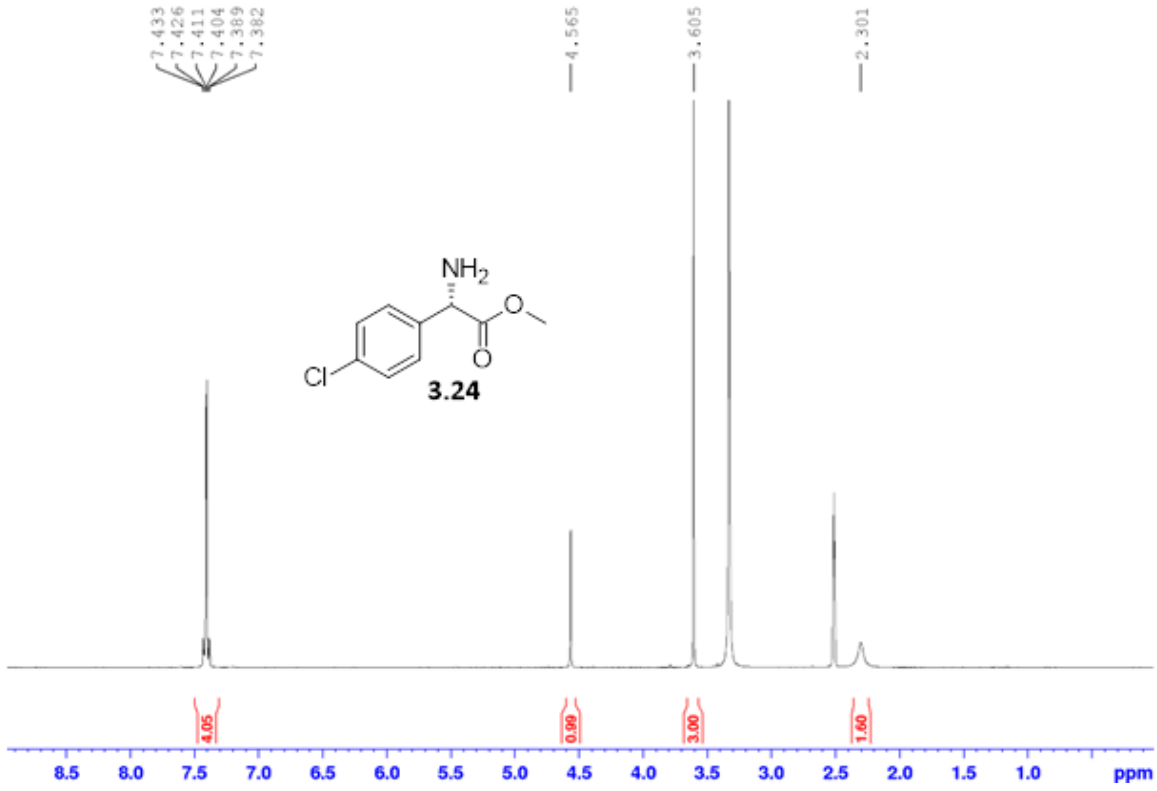

Figure 3.23: ^{1}H NMR spectrum (500 MHz, DMSO-d_6) for compound **3.24**.

The amine group was successfully Boc-protected, **3.25**, as evident the HRMS (negative ion mode) (**Figure 3.24**) that detected ions of *N*-Boc protected 4-chloro-*L*-phenylaglycine, the experimental mass of 298.0845 $C_{14}H_{17}NO_4Cl$ and the calculated mass of 298.0846 $[M-H]^-$.

Elemental Composition Report **Page 1**

Single Mass Analysis
Tolerance = 5.0 PPM / DBE: min = -1.5, max = 500.0
Element prediction: Off
Number of isotope peaks used for i-FIT = 3

Monoisotopic Mass, Even Electron Ions
15 formula(e) evaluated with 1 results within limits (all results (up to 1000) for each mass)
Elements Used:
C: 10-15 H: 15-20 N: 0-5 O: 0-5 Cl: 1-1
sd-087 59 (1.956) Cm (1:61)

TOF MS ES-
5.34e+004

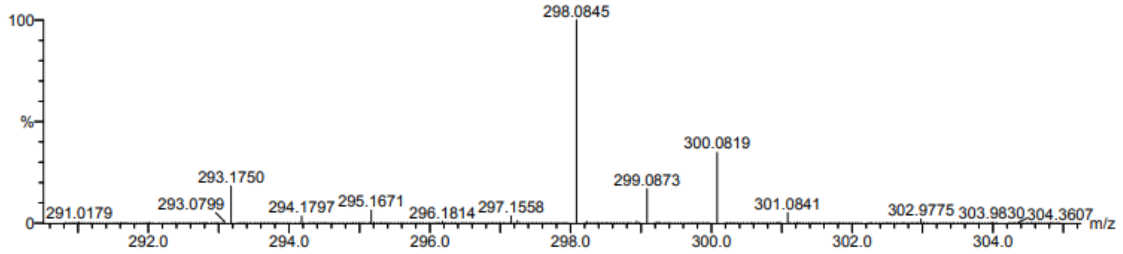

Minimum:				-1.5			
Maximum:		5.0	5.0	500.0			
Mass	Calc. Mass	mDa	PPM	DBE	i-FIT	i-FIT (Norm)	Formula
298.0845	298.0846	-0.1	-0.3	6.5	415.4	0.0	C14 H17 N O4 Cl

Figure 3.24: The affirmation of the success in conversion of the NH_2 to *N*-Boc protected compound **3.25**.

Last attempt was with *p*-fluoro-*L*-phenylalanine **3.27**, where its esterification was a success as anticipated **3.28** as a clear liquid, and Boc protection was achieved as a clear oil **3.29**, however, **3.30**, the sulfonylation was not a success.

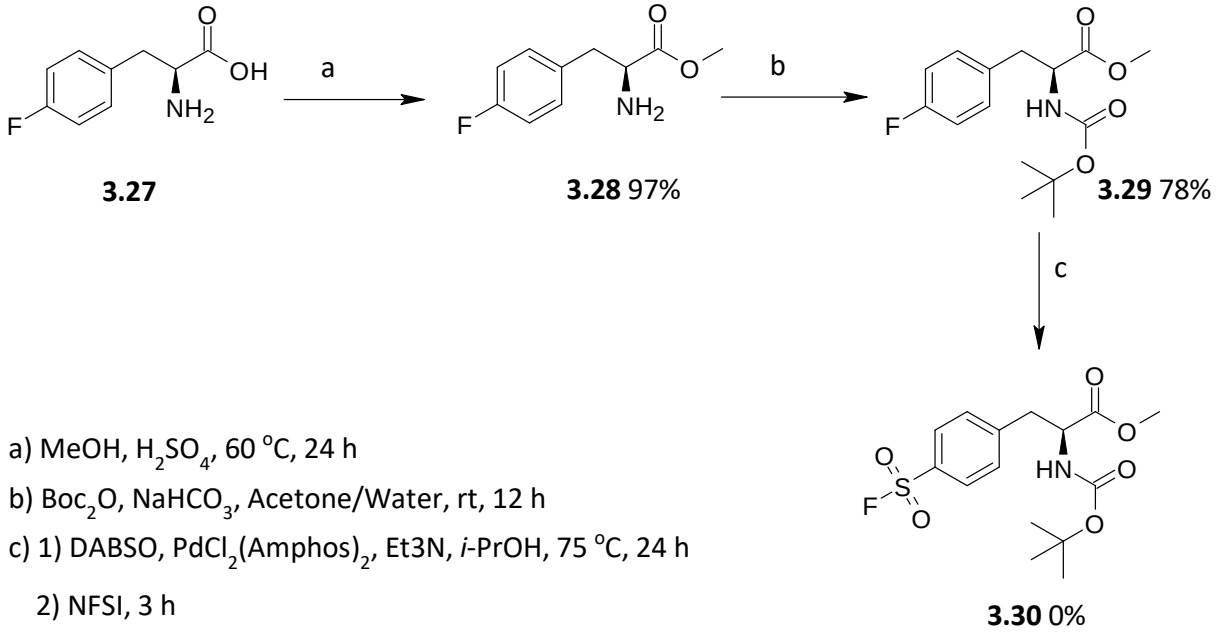

Scheme 3.12: Ternary steps mechanism towards obtaining compound **3.30**.

This then raised numerous questions in terms of the chemistry of carbon-halogen bond. The halogen-atoms are among the most electronegative atoms of the periodic table of elements. It is worth noting that going from fluorine to iodine on the periodic table, the electronegativity becomes less,[146] with 3.98, 3.26, 2.96, 2.66 for F, Cl, Br, and I respectively. Owing to the greater electronegativities of halogen-atoms compared to carbon, carbon-halogen bonds are polarised, with certain bond lengths.[147, 148] The key parameter to take into account when predicting the reactivity of such bonds, is the longitudinal polarisability, α. The value increases from Cl to I, transcribing an easier deformation of the electron cloud by an external field. This therefore translates into the increased reactivity of carbon-iodine bonds compared to carbon-bromine and carbon-chlorine bonds in organic chemistry. [149]

It was then for these reasons and information stipulated that there was a need to synthesise *p*-iodo-*L*-phenylalanine **3.32** from *L*-phenylalanine **3.31**, using the method previously described by Lei *et al.,* where the I_2 and $NaIO_3$ were added to a solution mixture of *L*-phenylalanine in HOAc and concentrated H_2SO_4.[150] The mixture was heated at 70 °C and stirred vigorously for 20 hours and $NaIO_4$ was added. The reaction mixture was then complete when the solution turned orange. HOAc was then diluted with water, and the mixture was washed with Et_2O and DCM. The aqueous layer was decoloured with activated charcoal, then filtered and neutralized with aqueous concentrated NaOH to get the precipitate of the product **3.32**, which, after chilling, was filtered under vacuum and rinsed with water and ethanol to afford a dry white powder, in 87% yield (**Figure 3.25** & **Figure 3.26**).

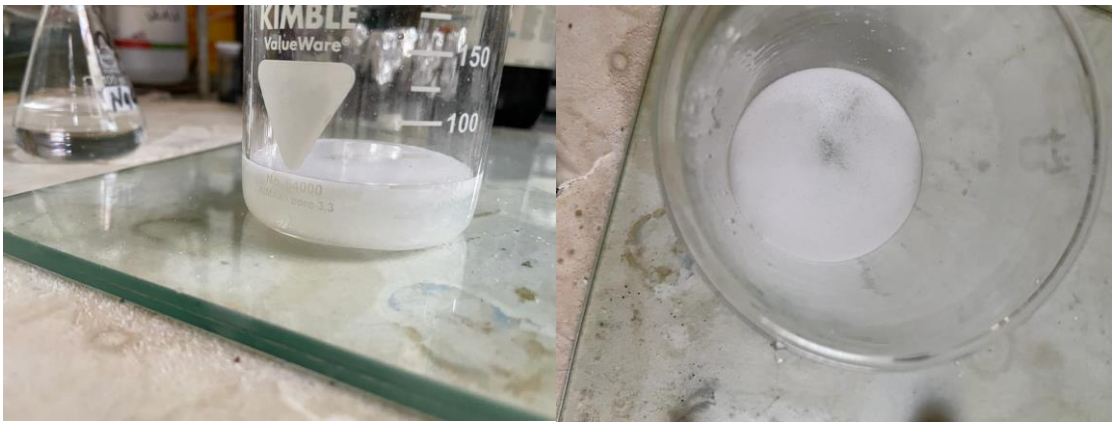

Figure 3.25: The depiction of the formation of the precipitate at pH ~ 7.

Figure 3.26: Dried product of compound **3.32**.

The ^{1}H NMR spectrum was in agreement with what Lei *et al.*, found on their characterisation. Two doublets can be observed at the chemical shift δ 7.63 and δ 7.08 ppm, indicating the absence of the proton at the *para* position (**Figure 3.27**).[150]

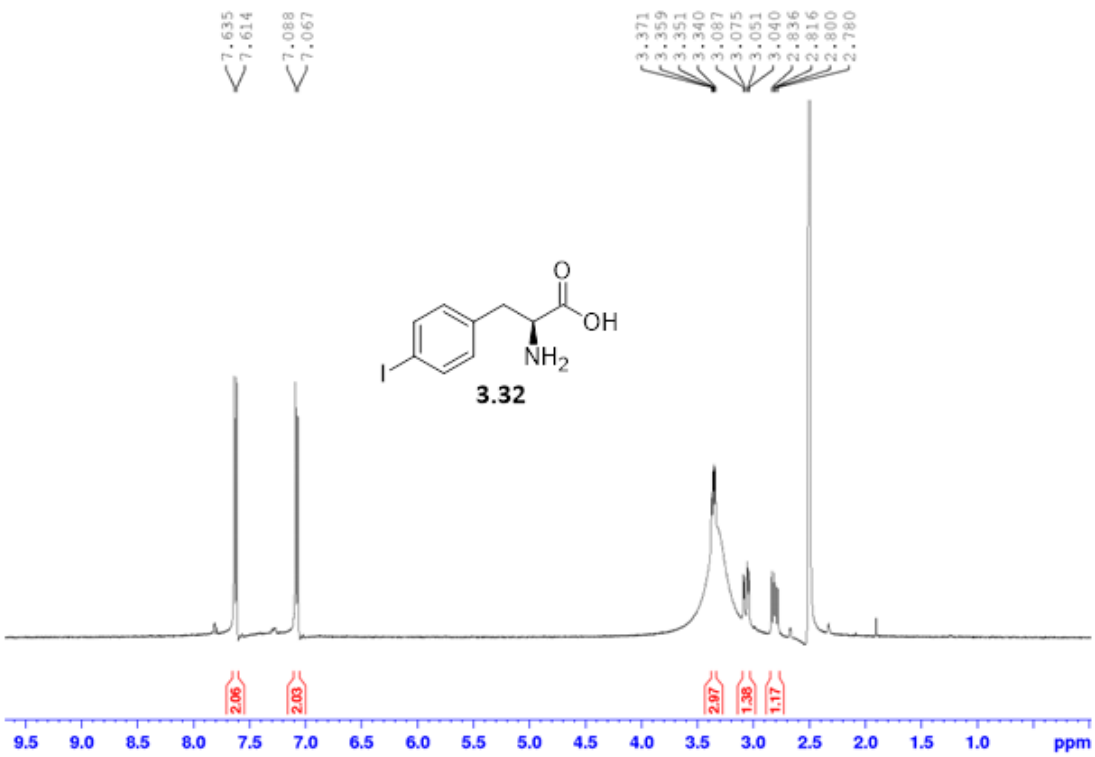

Figure 3.27: ^{1}H NMR spectrum (500 MHz, DMSO-d_6) of compound **3.32**.

To further validate the structure, HRMS (ESI) was used, and in the HRMS spectrum (**Figure 3.28**) a sodium adduct of the molecular ion was observed at *m/z* 313.947, corresponding to a molecular formular $C_9H_{10}NO_2I$ (calcd for $C_9H_{10}NO_2NaI$, 313.9654).

Elemental Composition Report **Page 1**

Single Mass Analysis
Tolerance = 5.0 PPM / DBE: min = -1.5, max = 500.0
Element prediction: Off
Number of isotope peaks used for i-FIT = 3

Monoisotopic Mass, Even Electron Ions
53 formula(e) evaluated with 1 results within limits (all results (up to 1000) for each mass)
Elements Used:
C: 5-10 H: 10-15 N: 0-5 O: 0-5 Na: 1-1 I: 0-1

sd_01_125 2 (0.034) Cm (1:61) TOF MS ES+ 8.65e+005

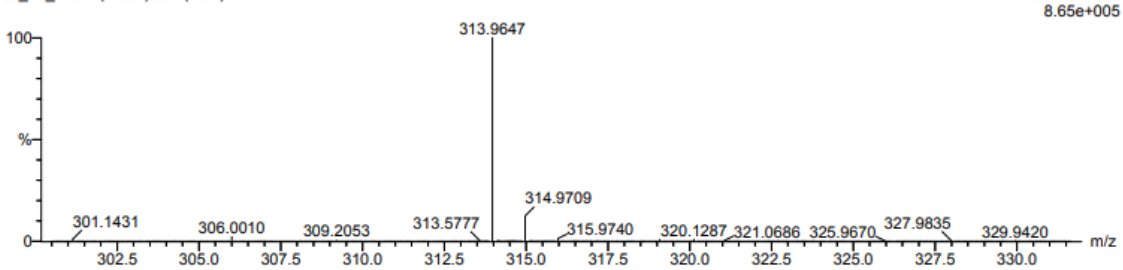

Minimum:				-1.5			
Maximum:		5.0	5.0	500.0			
Mass	Calc. Mass	mDa	PPM	DBE	i-FIT	i-FIT (Norm)	Formula
313.9647	313.9654	-0.7	-2.2	4.5	694.4	0.0	C9 H10 N O2 Na I

Figure 3.28: The HRMS confirming the structure of compound **3.32**.

With compound **3.32** in hand, the three steps process began (**Scheme 3.13**).

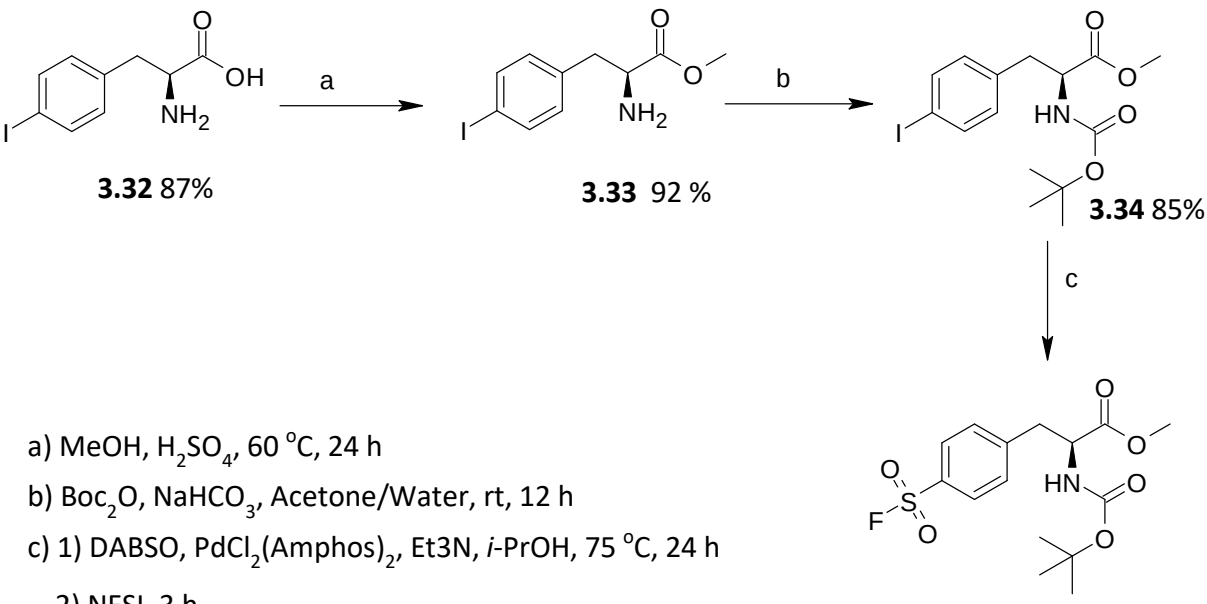

a) MeOH, H_2SO_4, 60 °C, 24 h
b) Boc_2O, $NaHCO_3$, Acetone/Water, rt, 12 h
c) 1) DABSO, $PdCl_2(Amphos)_2$, Et3N, *i*-PrOH, 75 °C, 24 h
2) NFSI, 3 h

Scheme 3.13: Reaction conditions for the transformation of compound **3.32** to compound **3.35**.

The esterification reaction of compound **3.32** with methanol afforded compound **3.33** in a yield of 92% as a clear liquid. The ^{13}C NMR spectrum (**Figure 3.29**), showed the surfacing of a carbon signal **C-2**, at δ 51.9 ppm, this indicated the presence of the methoxy group. And the carbon signal **C-4**, at δ 92.52 ppm, characterized the carbon coupled to iodine, at *para* position.

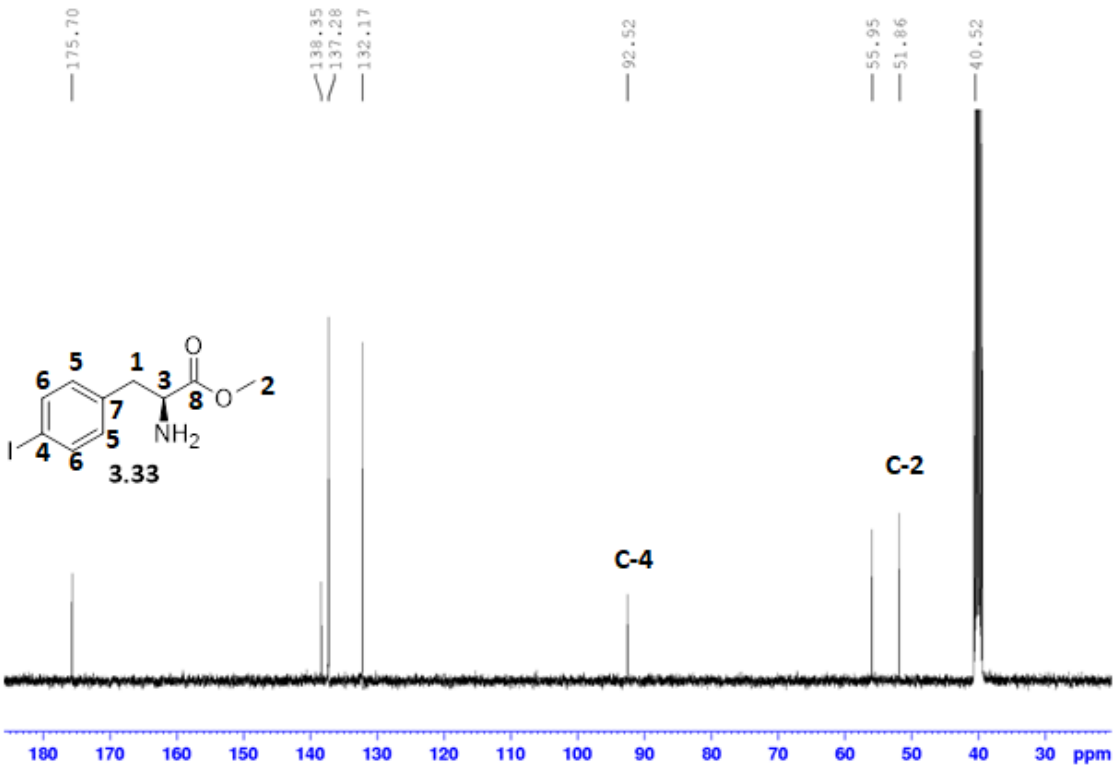

Figure 3.29: The ^{13}C NMR spectrum (125 MHz, DMSO-d_6) of compound **3.33**.

Methyl (*S*)-2-((*tert*-butoxycarbonyl)amino)-3-(4-iodophenyl)propanoate **3.34** was obtained as a clear oil in 85% yield. The ^{1}H NMR spectrum (**Figure 3.30**) was obtained, showing the characteristics of that of a compound that is Boc protected.

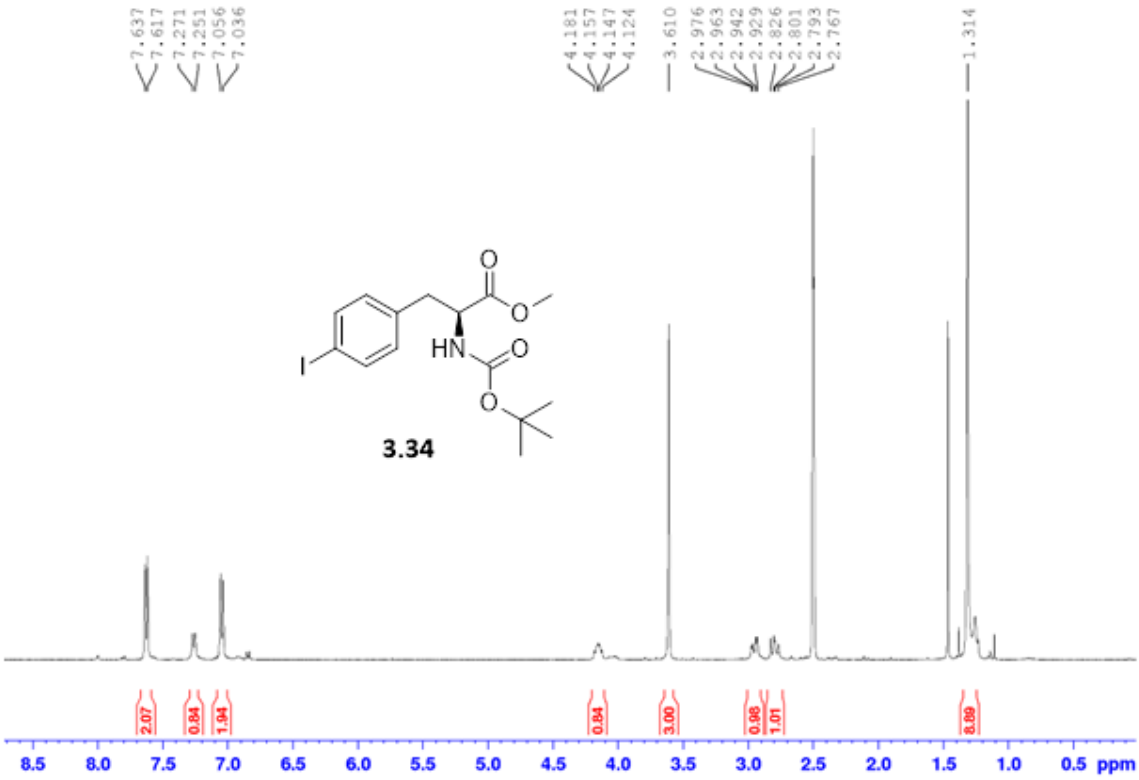

Figure 3.30: ^{1}H NMR spectrum (500 MHz, DMSO-d_6) of compound **3.34**.

Sulfonylation reaction of compound **3.34** afforded methyl (*S*)-2-((*tert*-butoxycarbonyl)amino)-3-(4-(fluorosulfonyl)phenyl)propanoate **3.35** was obtained as a brown oil, in moderate 63.7% yield. The successful synthesis of compound **3.35** was delighting following the struggle encountered in previous attempts. The characterization of the product indeed confirmed its successful synthesis. The ^{1}H NMR spectrum (**Figure 3.31**) shows that aromatic protons have shifted further downfield (δ 8.10 – 7.67 ppm), this is potentially

because of an introduction of an SO_2F group that brings about this effects on the protons as they coupled to sulfur that is directly bonded to two electronegative oxygen and fluorine, as compared to the ^{1}H NMR spectrum (**Figure 3.31**), where the protons in the aromatic ring were only coupled to iodine atom, and their signals were at a chemical shift range of (δ 7.64 & 7.04 ppm).

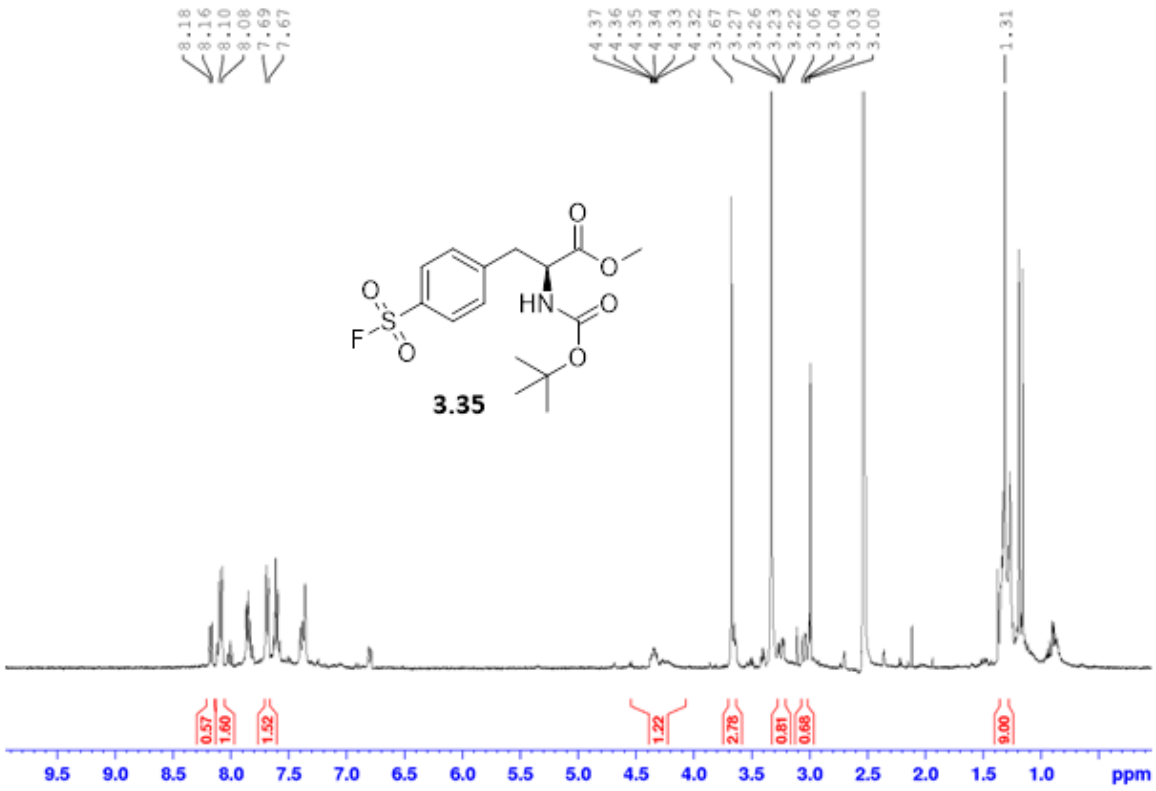

Figure 3.31: The ^{1}H NMR spectrum (500 MHz, DMSO-d_6) of compound **3.35**.

HRMS spectrum (**Figure 3.32**) of the product showed a chlorine adduct of the molecular ion was observed at *m/z* 396.0686, corresponding to a molecular formular $C_{15}H_{20}NO_6SF$ (calcd for $C_{15}H_{20}NO_6SClF$, 396.0684).

Elemental Composition Report **Page 1**

Single Mass Analysis
Tolerance = 5.0 PPM / DBE: min = -1.5, max = 500.0
Element prediction: Off
Number of isotope peaks used for i-FIT = 3

Monoisotopic Mass, Even Electron Ions
121 formula(e) evaluated with 1 results within limits (all results (up to 1000) for each mass)
Elements Used:
C: 10-15 H: 15-20 N: 0-5 O: 5-9 S: 0-1 Cl: 0-1 F: 0-1

sd_01_152 59 (1.989) Cm (1:60) TOF MS ES- 3.47e+005

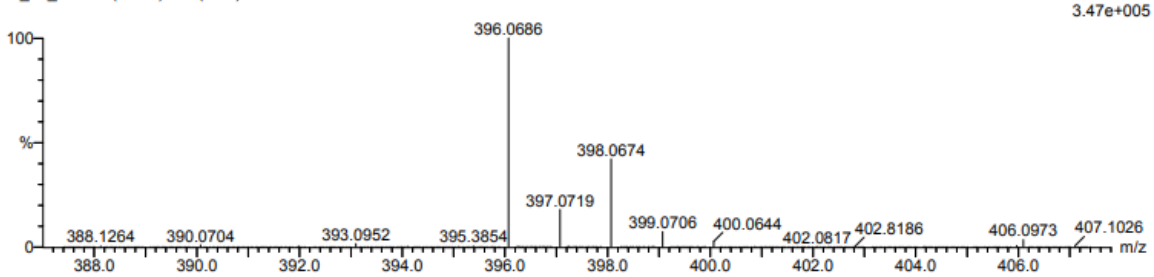

Minimum:				-1.5			
Maximum:		5.0	5.0	500.0			
Mass	Calc. Mass	mDa	PPM	DBE	i-FIT	i-FIT (Norm)	Formula
396.0686	396.0684	0.2	0.5	5.5	498.8	0.0	C15 H20 N O6 S Cl F

Figure 3.32: The HRMS spectrum of compound **3.35**.

3.3 Instrument-based interaction studies

The sulfonyl fluoride amino acid analogues which can be incorporated into active penta-peptides scaffolds can covalently interact with *L*-lysine present in the active site of target, that is the lysine rich TPR2A domain of HOP. In this section, we are looking at mimicking the TPR2A that is lysine rich, with the normal lysine, as it also contains the nucleophilic side chain. The aim is to assess possible interaction between the electrophilic warheads and the nucleophilic side chain of the target compound. These studies were conducted under biological physiological settings. Recognizing the potential sensitivity difference in the electrophile to various analytical techniques, we then developed two distinct detection methods described below. The mass spectrometric detection (Method A) was preferred due to its easy interface with the react-array liquid handling system. However, in certain cases where ionization was inadequate for quantitation, appropriate NMR studies (Method B) were performed to ensure that the studies are in good agreement.

3.3.1 Method A: The LCMS Assay

To better understand the possible interactions between the electrophilic sulfonyl fluoride utilized in covalent inhibitor design and the nucleophilic *L*-lysine side chain, we used *N*-Boc-lysine (2 M) as a model nucleophile and subjected to **3.5** (0.2 M) as an electrophile (**Scheme 3.14**).

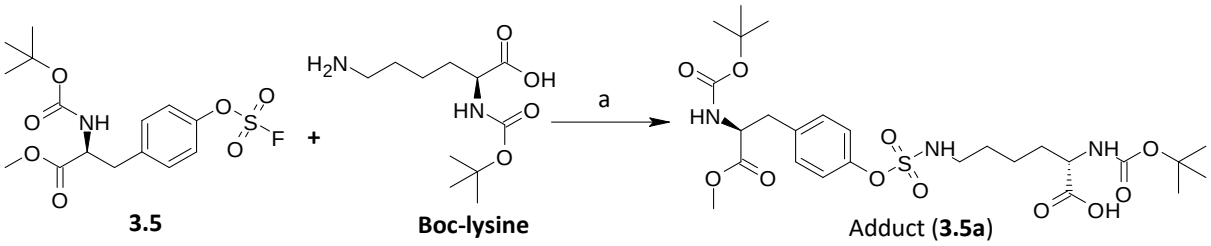

a) Ammonium acetate,
90% ACN,
pH 7.3, 30 °C

Scheme 3.14: Example reaction for compound **3.5** and the standard conditions.

During the study, possible interaction can be noted between the weakly electrophilic warhead and the nucleophilic target compound. The mass of compound **3.5** with a buffer was recorded, and an *m/z* value of 376 with a negative ionization, although this peak is not the base peak (**Figure 3.33**). This molecule does not fragment very much, moreover, it forms a stable fragment during the process of electron bombardment, i.e., *m/z* 422 as base peak.

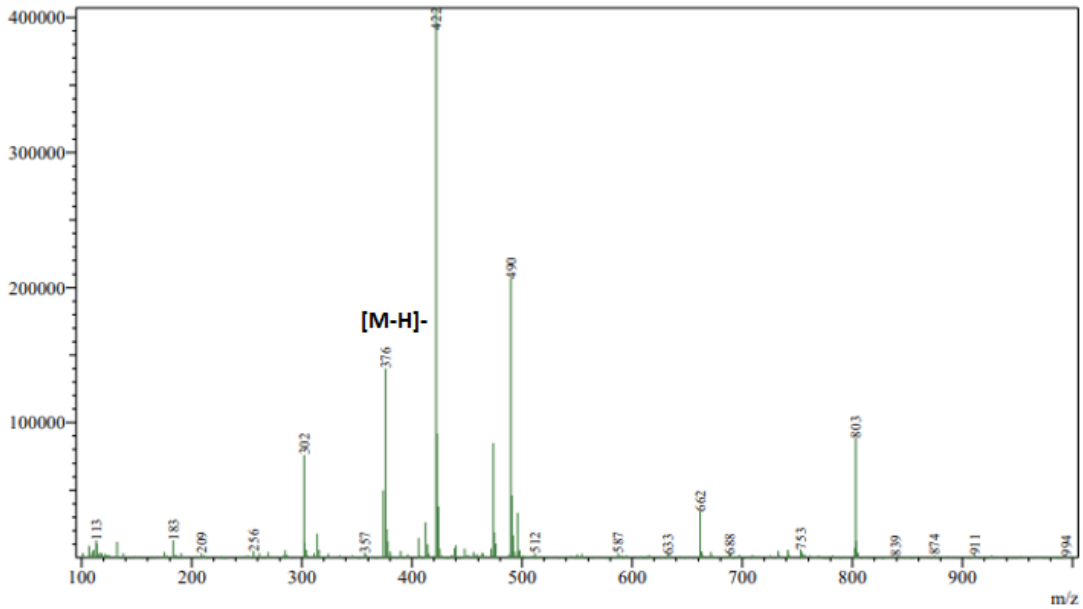

Figure 3.33: The LCMS spectrum of compound **3.5**, prior the interaction studies.

The *N*-Boc-lysine LCMS was also run-in combination with the buffer of interest. It can be observed that the *m/z* value for the nucleophilic *N*-Boc-lysine was 247 with a positive ionization, (**Figure 3.34**).

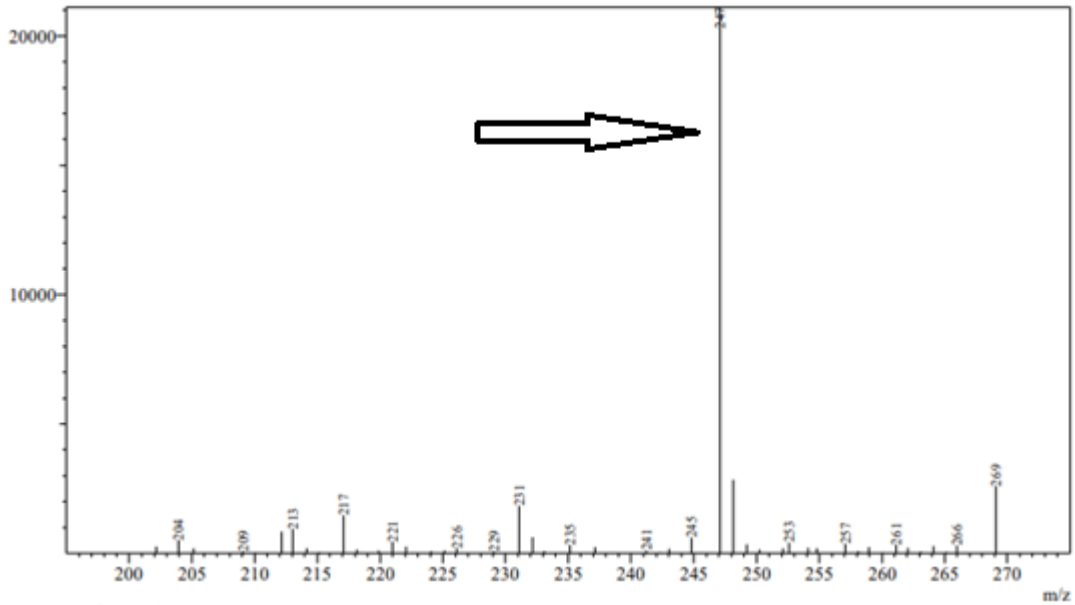

Figure 3.34: *N*-Boc-lysine mixed with ammonium acetate buffer.

With the adduct formation, a potential defluorination can be observed in the base peak fragment, however, the potential interaction of compound **3.5** with *N*-Boc-lysine did fragment, although it had its own ionization of about *m/z* of 15, hence it fragments at *m/z* of 589, meaning there is about m/z 15 ionizing from the m/z 604 (**Figure 3.35**).

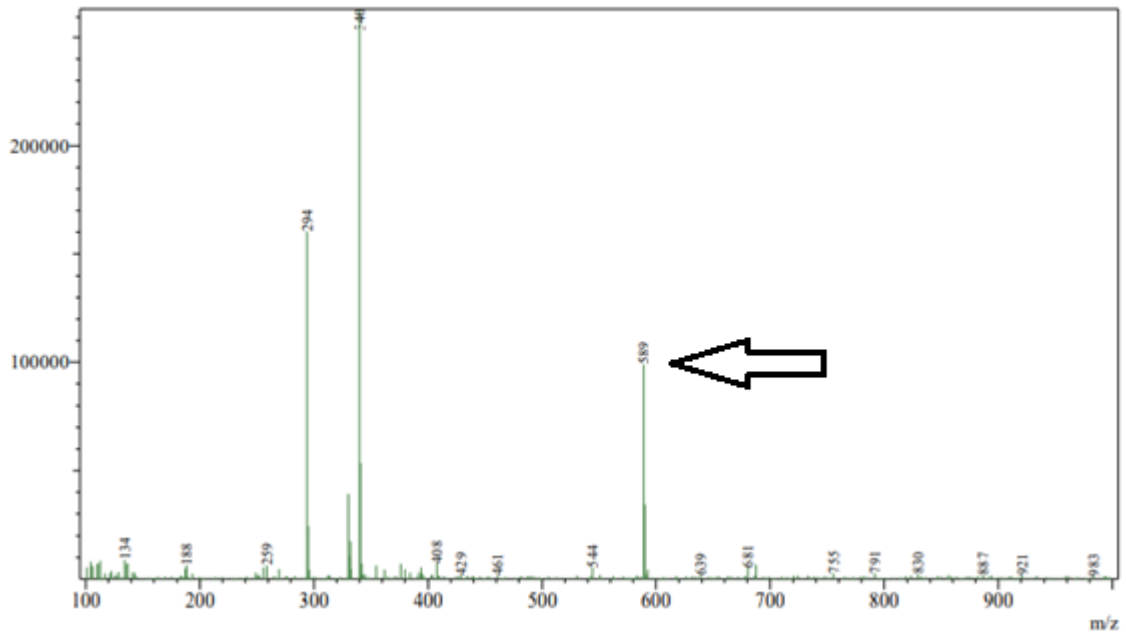

Figure 3.35: Interaction spectrum of compound **3.5** and *N*-Boc-lysine.

3.3.2 Method B: NMR Assay

For further evaluation and assessment purposes on the interactions, the NMR assay was conducted using the ^{1}H NMR and ^{19}F NMR, to observe if there was any significant change on the chemical shifts and integration, that would be adequate evidence to supporting the possible interactions between the electrophilic warheads ($-SO_2F$) and the nucleophilic amine of target compound, *L*-lysine. Each data point was approximately 15 minutes, for 15 scans. In the ^{1}H NMR analysis (**Figure 3.36**), there appeared to be doublet signal showing the characteristics of the methylene (CH_2) that is directly bonded to an amine (NH_2) in *N*-Boc-lysine, and this was the point of interest in ^{1}H NMR. A spectrum shift in this point of interest can be noted, from the 9th spectrum to the 15th spectrum, this signal shift is towards the downfield side, and this is a characteristic of a possible interaction taking place between the *N*-Boc-lysine side chain (NH_2) and the electrophilic warhead ($-SO_2F$) of compound **3.5**. This

shift characterise the transformation of the methylene directly bonded to NH_2 to methylene directly bonded to NH that is bonded to an electronegative group, ($-SO_2$).

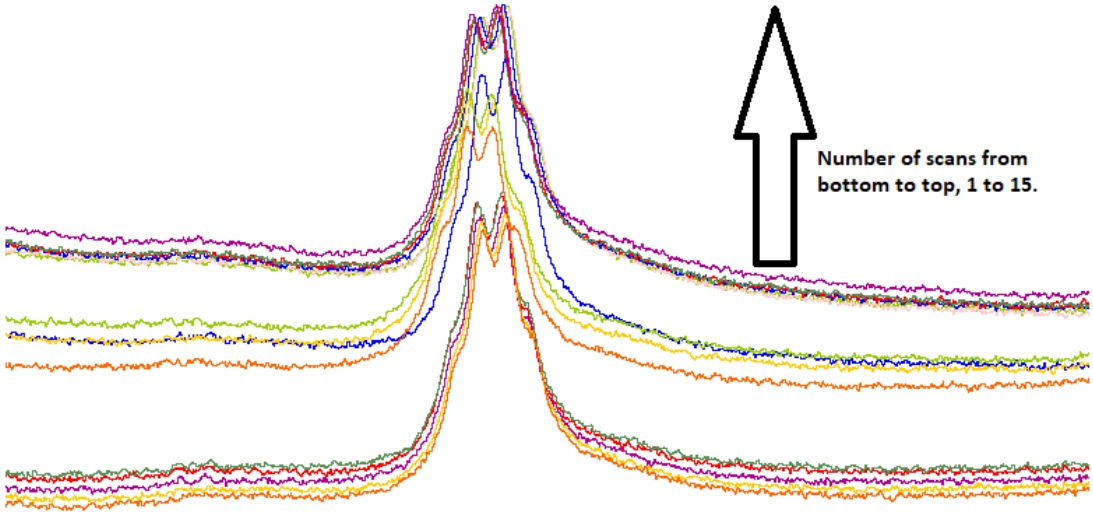

Figure 3.36: The 15 scans ^{1}H NMR spectrum (400 MHz, DMSO-d_6) of interaction assessment.

On a closer look, comparing scan 1, 10, and 15 (**Figure 3.37**), these scans are of the same mixture, however at different times, the signal scan of the first 15 min, is slightly shifted as compared to the 10th fifteen scan, the last 15 minutes of the last signal scan.

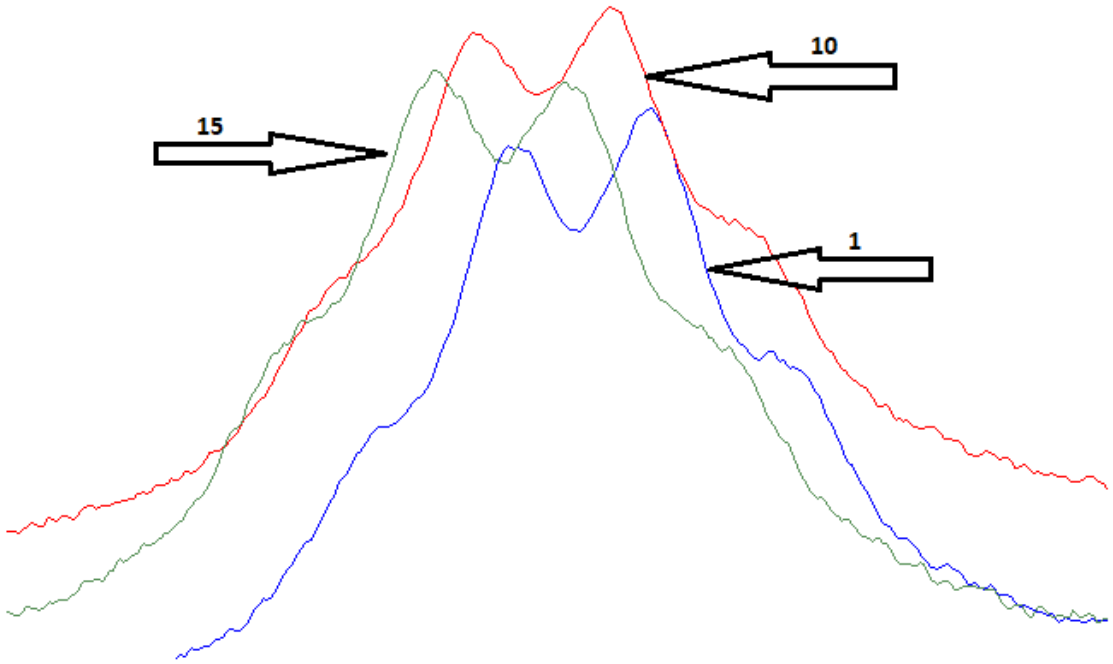

Figure 3.37: The on-zoom spectra comparison of *N*-Boc-lysine and the mixture of *N*-Boc-lysine and compound **3.5**.

For further validation of possible interaction occurring, a ^{19}F NMR for first and the last run was obtained, taking about 4.5 h acquisition time each run, and this was simply because the objective was to focus only on fluorine. In the comparison below (**Figure 3.38**), the fluorine signal can be observed resonating from –73.41 ppm (blue signal) to –120.27 ppm (red signal), this indicated a possible detachment of the fluorine in a form of fluorine ion to hydrogen fluoride in aqueous mixture. Thus, suggesting a possible binding taking place where the amine group of the *N*-Boc-lysine as a nucleophile attacked the electrophilic warhead of compound **3.5**, hence fluorine detached as a leaving group.

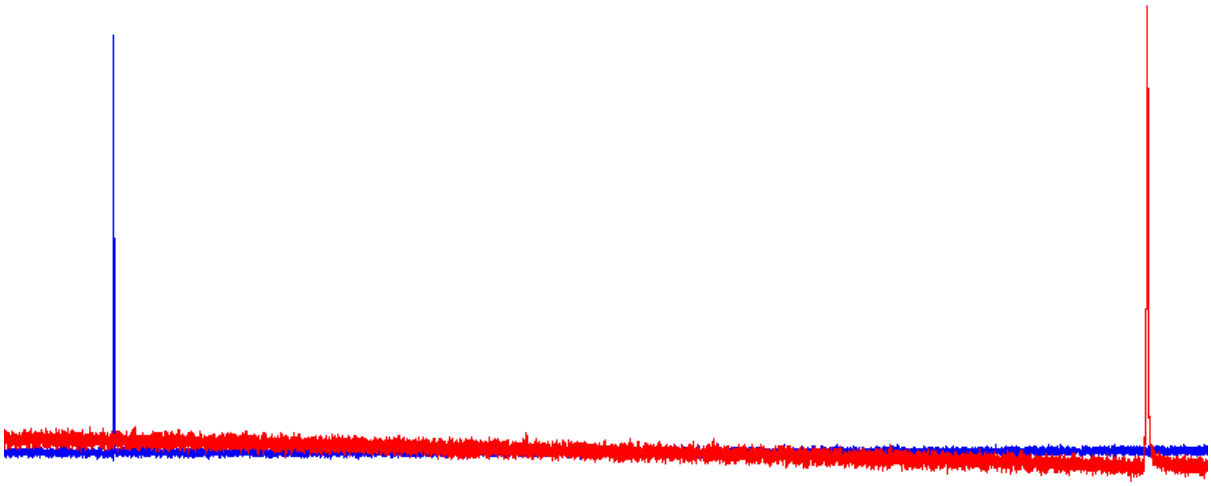

Figure 3.38: The ^{19}F NMR spectra of the interaction assessments, this comparison is of the one species mixture, at different times, and each run of the species took about 4.5 h acquisition time.

3.4 Conclusions

In conclusion, we were able to successfully synthesise our desired compounds in moderate to good yields. We adopted a protocol to synthesise our target compounds following a three-steps process beginning with esterification of amino acids (with excellent yields 90% – 98%), *N*-Boc protection of the amine group (with good yields of 70% – 88%) , and finally the installation of the lysine targeting warhead, the SO_2F, *via* the *ex-situ* generation of sulfuryl fluoride (with good yields of 85% and 89%), and the palladium catalysed and an *in-situ* fluorine insertion (with moderate 63.7% yield). It was interesting to observe the transformation in each step, and the lessons led to the adoption of each step. We further successfully explored potential interactions of methyl (*S*)-2-((*tert*-butoxycarbonyl)amino)-3-(4-((fluorosulfonyl)oxy)phenyl)propanoate, **3.5** with *N*-Boc-lysine using two distinct detection methods, the LCMS (Method A) and the NMR (Method B), mimicking the lysine rich TPR2A of HOP. The characteristics of a potential interaction taking place were observed in both methods developed.

It was however unfortunate that sulfonation of the aliphatic amino acids, ethyl (*tert*-butoxycarbonyl)-*L*-serinate, **3.13**, and ethyl *(tert*-butoxycarbonyl)-*L*-homoserinate, **3.17** did not work as planned. Furthermore, the sulfonation of the aryl *p*-halogen containing amino esters *via* the substitution of chlorine in methyl (S)-2-((tert-butoxycarbonyl)amino)-3-(4-chlorophenyl)propanoate, **3.21**, methyl (S)-2-((tert-butoxycarbonyl)amino)-2-(4-chlorophenyl)acetate, **3.25**, and fluorine in methyl (S)-2-((tert-butoxycarbonyl)amino-3-(4-fluorophenyl)propanoate, **3.29**, was unsuccessful due to their physical properties.

3.5 Future work extending from this study

- This study focused mostly on synthesising non-natural amino acids by installing the lysine targeting warhead, SO_2F. However, in that process, there was a need to protect both carboxyl group and amine group on the amino acids, but that should not interfere with the peptide synthesis process, as it should be done in continuation of this study.
- Following the peptide synthesis on the non-natural amino acids, the biological studies should be done, using the lysine rich TPR2A domain of HOP and interact it with an acid rich MEEVD motif at the *C*-terminus of Hsp90, to see if the inhibition of this protein-protein interaction occurs or not, and how it can be advanced.

Chapter Four

Experimental Section

4.1 General Information

4.1.1 Analytical

Melting points were determined using Kolfer hot-stage melting apparatus and are uncorrected, expressed in degrees Celsius. NMR spectra were acquired using standard pulse sequences on Bruker Avance III 500 (500 MHz for ^{1}H, 125 MHz for ^{13}C, and 470 MHz for ^{19}F) and 400 (400 MHz for ^{1}H, 100 MHz for ^{13}C, and 376 MHz for ^{19}F) spectrometers. Chemical shifts (δ) are reported in units of parts per million (ppm) and are referenced to residual solvent resonances (DMSO-d_6: δ ^{1}H 2.50 and ^{13}C 39.50 ppm, aliphatic methylene carbon masked by solvent).[151] Peak multiplicities are designated as b for broad, s for singlet, d for doublet, t for triplet, q for quartet, and m for multiplet. Coupling constants (*J*) are reported in Hz directly from the NMR spectra. Infrared (IR) spectra were recorded on an Alpha II FTIR spectrometer, samples were placed on a diamond and compressed with infra-red pressure steel and the absorption maxima are expressed in wavenumbers (cm^{-1}). High-resolution mass spectrometry was performed on a Waters Micromass LCT Premier time-of-flight (TOF) spectrometer with an electrospray ionization (ESI) source. Spectra were acquired in both the positive and negative ion modes and were both used for analysis. Liquid chromatography mass spectrometer analysis was performed with the Shimadzu LC system, with Shim-Pack GIST C18-HP in the column (3.5 µm ×4.6 mm × 150 mm), kept at 30 °C. Eluting with 0.1% formic acid in water and acetonitrile (90:10) as the mobile phase. The flow rate was 0.40 mL/min. The LC isocratic program was 0 - 10 min (90% - 10%, ACN: water). The detector used was an LC-2030/2040 photo-diode array (PDA). The detection was set at a wavelength of 200 nm to 400

nm. Metrohm 827 pH meter used to measure the pH level on the buffer solutions. Theoretical molecular weight values were calculated using ChemDraw Professional.

4.1.2 Chromatography

Purifications of products were performed by flash-column chromatography and Column chromatography packed with silica gel (silica gel 60, 0.063-0.0200 mm, 70-230 Mesh ASTM), and for qualitative analysis of products, and reactions, thin layer chromatography (TLC) (TLC silica gel 60 F_{254}, aluminium-backed plates) with detection under long-or short-wavelength (λ) UV radiation (254 and 365 nm, respectively) or staining with *p*-anisaldehyde reagent was used. The stain solution was prepared according to the Reagents MERCK book[152] with some modification, by putting a 250 mL volumetric flask in an ice bath and adding the following reagents, shaking the flask after each addition:

- 1 mL of *p*-anisaldehyde (98%)
- 20 mL of glacial acetic acid
- 170 mL of MeOH
- 4 mL of concentrated sulfuric acid

All the reagents were added to a 250 mL volumetric flask, cooled in an ice bath. After preparation, the solution was stored in a fridge (4 °C).

4.1.3 Materials

All solvents and reagents that were used are commercially available and purchased from Sigma Aldrich or Honeywell and except where stated used without purification. All reactions that included the use of air and/or moisture sensitive reagents were carried out under an inert atmosphere of nitrogen using over-dried glassware and anhydrous solvents.

4.1.4 Synthesis

All reactions requiring anhydrous conditions were conducted in oven-dried apparatus under nitrogen gas. The anhydrous solvents were prepared by standard procedures outlined by Perrin and Armarego [153] as well as Casey, Leornard, Lygo and Procter.[154] All the solvents were stored over 4 Å molecular sieves to hold any possible moisture. All reactions were magnetically stirred, and the organic extracts dried over anhydrous $MgSO_4$.

4.2 Synthetic Procedures and Characterization

4.2.1 The *p*-Iodination Reaction[150]

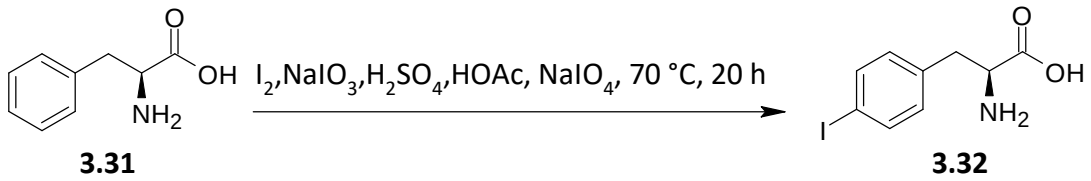

***p*-iodo-*L*-phenylalanine (3.32)**[155]: I_2 (126.9 mg, 1 mmol) and $NaIO_3$ (107 mg, 0.5 mmol) were added to a solution mixture of *L*-phenylalanine (412.9 mg, 2.2 mmol) in HOAc (20 mL) and concentrated H_2SO_4 (1.5 mL). The mixture was heated at 70 °C and stirred vigorously for 20 hours, $NaIO_4$ (2 × 15.76 mg) was added. The reaction mixture was then complete when the solution turned orange. The HOAc mixture was then diluted with 40 mL of water, and the mixture was washed with Et_2O (2 × 30 mL) and DCM (2 × 30 mL). The aqueous layer was decoloured with activated charcoal (30 mg), then filtered and neutralized with aqueous concentrated NaOH to precipitate the crude product, which, after chilling, was filtered under vacuum and rinsed with water 100 mL and then 70 mL of ethanol to afford a dry white powder, with 87% yield. **Mp**: 259 – 260 °C. **IR** (ν_{max} cm^{-1}): 2932, 1582, 1520, 1395, 1318, 854, 799, 515. **^{1}H NMR** (500 MHz, DMSO-d_6): δ 7.63 (d, *J* = 8.2 Hz, 2H), 7.08 (d, *J* = 8.2 Hz, 2H), 3.37 – 3.33 (m, 3H), 3.06 (dd, *J* = 14.3, 4.5 Hz, 1H), 2.80 (dd, *J* = 14.0, 6.2 Hz, 1H). **^{13}C NMR** (125

MHz, DMSO-d_6): δ 170.7, 137.8, 135.1, 132.3, 93.7, 53.4, 35.7 ppm. **HRMS** (ESI) *m/z* 289.9687 (calcd for $C_9H_9NO_2I$ $[M-H]^-$ 289.9678).

4.2.2 General Procedure A: The esterification of aromatic amino acids

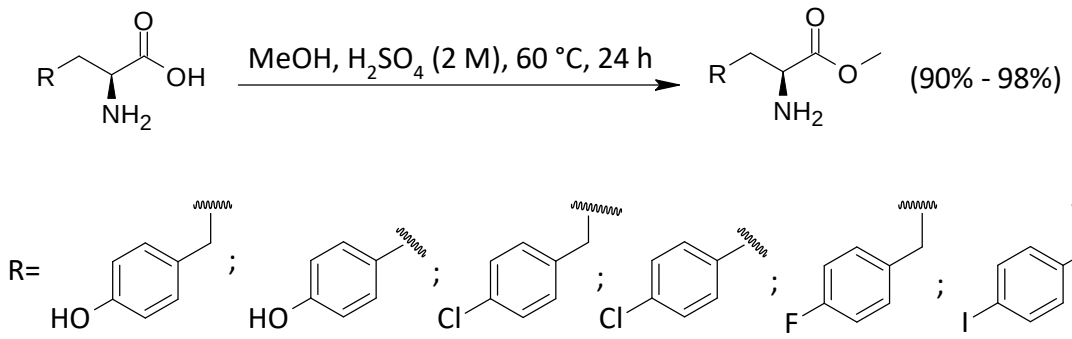

The aromatic amino acid esterification was performed according to the methodology proposed by Laulloo[156] with modifications. Briefly, the corresponding amino acids (1.0 mmol) were dissolved in MeOH (7.0 mL), and the conc. H_2SO_4 (0.7 mL) was added dropwise to a stirring solution. The reaction mixture was heated to 60 °C for 24 h in oil bath while refluxing. Upon completion, the solvent was removed to half of its original volume under reduced pressure, the solution was then neutralized with Na_2CO_3 saturated aqueous solution and extracted with ethyl acetate (3 × 15 mL). Organic phases were combined and washed with brine (2×10 mL), dried over anhydrous $MgSO_4$, filtered, and the filtrate was concentrated under *vacuo* to obtain esterified amino acid compounds in 90-98% yield.

Methyl *L*-tyrosinate (3.3)

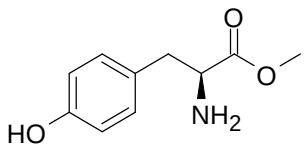

3.3

General Following Procedure A, *L*-tyrosine (181.19 mg, 1 mmol) gave **3.3** as a white shiny powder, at a 90% yield. **Mp:** 138 – 140 °C **IR** (ν_{max} cm^{-1}): 3351, 2924, 2598, 1738, 1594, 1510, 1474, 1258, 1176, 1011, 589, 510. **^{1}H NMR** (400 MHz, DMSO-d_6): δ 9.17 (s, 1H), 6.95 (d, *J* = 8.5 Hz, 2H), 6.66 (d, *J* = 8.5 Hz, 2H), 3.57 (s, 3H), 3.49 (t, *J* = 6.6 Hz, 1H), 2.75 (dd, *J* = 13.4, 6.2 Hz, 1H), 2.67 (dd, *J* = 13.4, 6.2 Hz, 1H), 1.67 (s, 2H). **^{13}C NMR** (100 MHz DMSO-d_6): δ 175.9, 156.3, 130.5, 128.3, 115.4, 56.4, 51.7, 40.5 ppm. **HRMS** (ESI) *m/z* 194.0821 (calcd for $C_{10}H_{12}NO_3$ $[M-H]^-$ 194.0817).

Methyl (*S*)-2-amino-2-(4-hydroxyphenyl)acetate (3.7)

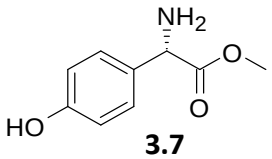

3.7

Following General Procedure A, 4-Hydroxy-*L*-phenylglycine (167.16 mg, 1 mmol) gave **3.7** as a white powder, at 93% yield. **Mp**: 187 – 189 °C. **IR** (ν_{max} cm^{-1}): 3336, 3280, 2942, 2596, 1734, 1584, 1518, 633, 579. **^{1}H NMR** (400 MHz, DMSO-d_6): δ 9.37 (s, 1H), 7.17 (d, *J* = 8.5 Hz, 2H), 6.72 (d, *J* = 8.5 Hz, 2H), 4.42 (s, 1H), 3.60 (s, 3H), 2.41 (s, 2H). **^{13}C NMR** (100 MHz DMSO-d_6): δ 175.3, 157.2, 131.8, 128.4, 115.5, 58.1, 52.1 ppm. **HRMS** (ESI) *m/z* 180.0656 (calcd for $C_9H_{10}NO_3$ $[M-H]^-$ 180.0661).

Methyl (S)-2-amino-3-(4-chlorophenyl)propanoate (3.20)

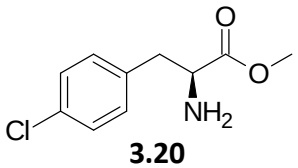

3.20

Following General Procedure A, 4-chloro-*L*-phenylalanine (199.63 mg, 1 mmol) gave **3.20** as a light viscous clear liquid, at 90.3% yield. **IR** (ν_{max} cm^{-1}): 3046, 2953, 1734, 1670, 1440, 673, 521. **^{1}H NMR** (500 MHz, DMSO-d_6): δ 7.33 (d, *J* = 8.4 Hz, 2H), 7.21 (d, *J* = 8.4 Hz, 2H), 3.59 (s, 3H), 3.57 – 3.55 (m, 1H), 2.87 (dd, *J* = 13.4, 6.1 Hz, 1H), 2.77 (dd, *J* = 13.4, 6.1 Hz, 1H), 1.79 (br s, 2H). **^{13}C NMR** (125 MHz, DMSO-d_6): δ 175.6, 137.4, 131.4, 128.4, 55.9, 51.8, 40.3 ppm. **HRMS** (ESI) *m/z* 236.0450 (calcd for $C_{10}H_{12}NO_2ClNa$ $[M+Na]^+$ 236.0454).

Methyl (*S*)-2-amino-2-(4-chlorophenyl)acetate (3.24)

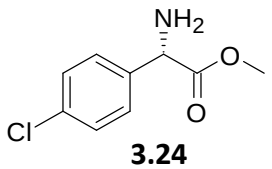

3.24

Following General Procedure A, 4-chloro-*L*-phenylglycine (185.61 mg, 1 mmol) gave **3.24** as alight-yellow viscous liquid, at 92% yield. **IR** (ν_{max} cm^{-1}): 3185, 2915, 1737, 1660, 1580, 1407, 760, 622. **^{1}H NMR** (500 MHz, DMSO-d_6): δ 7.43 – 7.38 (m, 4H), 4.57 (s, 1H), 3.61 (*s*, 3H), 2.30 (br s, 2H). **^{13}C NMR** (125 MHz, DMSO-d_6): δ 174.5, 140.4, 132.5, 129.2, 128.7, 58.0, 52.3 ppm. **HRMS** (ESI) *m/z* 222.0301 (calcd for $C_9H_{10}NO_2NaCl$ $[M+Na]^+$ 222.0298).

Methyl (*S*)-2-amino-3-(4-fluorophenyl)propanoate (3.28)

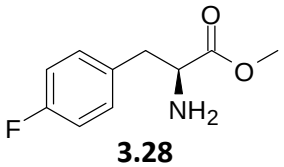

3.28

Following General Procedure A, *p*-fluoro-*L*-phenylalanine (183.10 mg, 1 mmol) gave **3.28** as a clear liquid, at a yield of 97%. **IR** (ν_{max} cm^{-1}): 3048, 1732, 1665, 1505, 1220, 785, 527. **^{1}H NMR** (500 MHz, DMSO-d_6): δ 7.22 – 7.19 (m, 2H), 7.10 – 7.06 (m, 2H), 3.57 (s, 3H), 3.54 – 3.52 (m,

1H), 2.85 (dd, *J* = 13.4, 6.1 Hz, 1H), 2.76 (dd, *J* = 13.4, 7.3 Hz, 1H), 1.75 (s, 2H). **^{13}C NMR** (125 MHz, DMSO-d_6): δ 175.8, 162.6, 160.2, 134.6, 131.5, 131.4, 115.3, 115.1, 56.2, 51.8 ppm. **HRMS** (ESI) *m/z* 220.0750 (calcd for $C_{10}H_{12}NO_2FNa$ $[M+Na]^+$ 220.0750).

Methyl (*S*)-2-amino-3-(4-iodophenyl)propanoate (3.33)

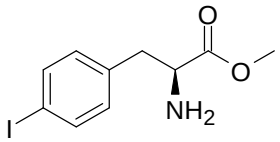

3.33

Following General Procedure A, *p*-iodo-*L*-phenylalanine (291.10 mg, 1 mmol) gave **3.33** as a light-yellow liquid, at 92% yield. **IR** (ν_{max} cm^{-1}): 3371, 2948, 1731, 1666, 1483, 1436, 798, 518. **^{1}H NMR** (500 MHz, DMSO-d_6): δ 7.62 (d, *J* = 8.3 Hz, 2H), 7.01 (d, *J* = 8.3 Hz, 2H), 3.58 (s, 3H), 3.55 – 3.52 (m, 1H), 2.82 (dd, *J* = 13.5, 6.2 Hz, 1H), 2.72 (dd, *J* = 13.2, 5.9 Hz, 1H), 1.79 (s, 2H). **^{13}C NMR** (125 MHz, DMSO-d_6): δ 175.7, 138.4, 137.3, 132.2, 92.5, 56.0, 51.9, 40.5 ppm. **HRMS** (ESI) *m/z* 305.9986 (calcd for $C_{10}H_{13}NO_2I$ $[M+H]^+$ 305.9991).

4.2.3 General Procedure B: The general procedure for preparation of *N*-Boc amino acids[157, 158]

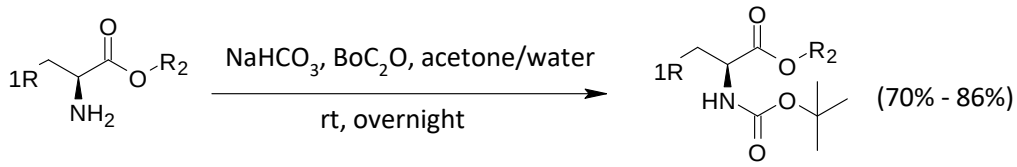

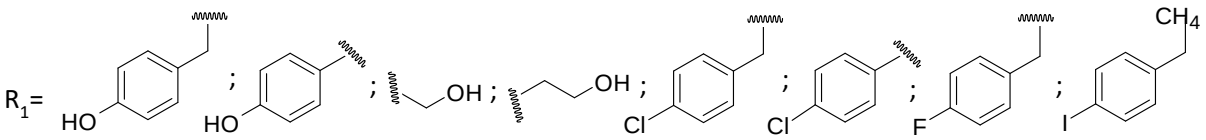

R_2= CH_3; H

To a solution of an amino acid (1 mmol) in a mixture of acetone/water (1:1 v/v 20 mL), solid $NaHCO_3$ (1 mmol), and di-tert-butyl decarbonate (Boc_2O, 1.5 mmol) were added consecutively and the obtained reaction mixture was stirred with magnetic stirrer bar overnight at room temperature. Then, the reaction mixture solvent was removed under reduced pressure to half of its original volume and the aq. solution was acidified to pH 2 by adding 1M HCl and subsequently extracted with DCM (3 × 20 mL). The combined organic layers were dried over anhydrous $MgSO_4$, filtered and the filtrate was concentrated in *vacuo* to obtain *N*-Boc-amino acid.

Methyl (*tert*-butoxycarbonyl)-*L*-tyrosinate (3.4)

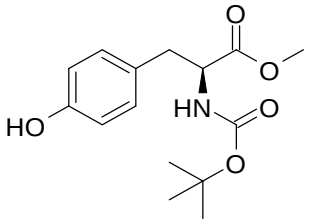

3.4

Following General Procedure B, Methyl-*L*-tyrosinate (195.22 mg, 1 mmol) gave **3.4** as colourless oil, at 70% yield. **IR** (ν_{max} cm^{-1}): 3381, 2969, 1682, 1606, 1515, 1445, 1362, 1259, 1157, 755, 534. **^{1}H NMR** (400 MHz, DMSO-d_6): δ 9.19 (s, 1H), 7.17 (d, *J* = 7.7 Hz, 1H), 7.00 (d, *J* = 8.5 Hz, 2H), 6.65 (d, *J* = 8.4 Hz, 2H), 4.10 – 4.05 (m, 1H), 3.59 (s, 3H), 2.85 (dd, *J* = 13.8, 5.4 Hz, 1H), 2.73 (dd, *J* = 13.7, 3.9 Hz, 1H), 1.32 (s, 9H). **^{13}C NMR** (100 MHz, DMSO-d_6): δ 173.2, 156.4, 155.9, 130.4, 128.0, 115.5, 78.7, 56.0, 52.1, 36.2, 28.6 ppm. **HRMS** (ESI) *m/z* 294.1340 (calcd for $C_{15}H_{20}NO_5$ $[M-H]^-$ 294.1341).

Methyl (*S*)-2-((*tert*-butoxycarbonyl)amino)-2-(4-hydroxyphenyl)aceatate (3.8)

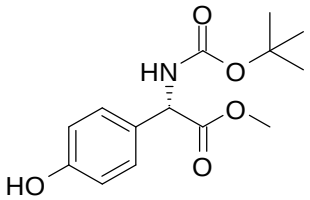

3.8

Following General Procedure B, methyl (*S*)-2-amino-2-(4-hydroxyphenyl)acetate (181.19 mg, 1 mmol) gave **3.8** as a colourless sticky oil, at 75% yield. **IR** (ν_{max} cm^{-1}): 3426, 3661, 2927, 1728, 1666, 1503, 1157, 664, 515. **^{1}H NMR** (400 MHz, DMSO-d_6): δ 9.49 (s, 1H), 7.59 (d, *J* = 7.5 Hz, 1H), 7.19 (d, *J* = 8.6 Hz, 2H), 6.73 (d, *J* = 8.5 Hz, 2H), 5.08 (d, *J* = 7.7 Hz, 1H), 3.62 (s, 3H), 1.41 (s, 9H). **^{13}C NMR** (100 MHz, DMSO-d_6): δ 172.3, 157.7, 129.5, 127.1, 115.7, 78.9, 57.6, 52.4, 28.6 ppm. **HRMS** (ESI) *m/z* 304.1158 (calcd for $C_{14}H_{19}NO_5Na$ $[M+Na]^+$ 304.1161).

(*Tert*-butoxycarbonyl)-*L*-serine (3.12)

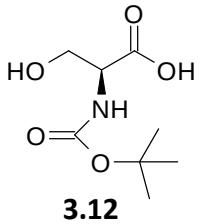

3.12

Following General Procedure B, *L*-serine (mg, 1 mmol) gave **3.12** as sugar-like structures white solids, at 86% yield. **Mp**: 83 – 85 °C (dec.) **IR** (ν_{max} cm^{-1}): 3413, 3368, 2976, 2932, 1749, 1658, 1519. **^{1}H NMR** (400 MHz, DMSO-d_6): δ 6.68 (*d*, *J* = 8.2 Hz, 1H), 4.00-3.96 (*m*, 1H), 3.63 (*d*, *J* = 4.6 Hz, 2H), 1.39 (*s*, 9H). **^{13}C NMR** (100 MHz, DMSO-d_6): δ 172.8, 155.8, 78.6, 61.9, 56.6, 28.6 ppm. **HRMS** (ESI) *m/z* 228.0850 (calcd for $C_8H_{15}NO_5Na$ $[M+Na]^+$ 228.0848).

(*Tert*-butoxycarbonyl)-*L*-homoserine (3.16)

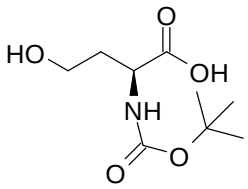

3.16

Following General Procedure B, *L*-homoserine (119.12 mg, 1 mmol) gave **3.16** as white stone-like sugar structure, at 75% yield. **Mp**:139 – 142 °C. **IR** (ν_{max} cm^{-1}): 3352, 2977, 2928, 1770, 1521, 1365. **^{1}H NMR** (400 MHz, DMSO-d_6): δ 7.34 (d, *J* = 8.7 Hz, 1H), 4.40 – 4.31 (m, 2H), 4.23 – 4.17 (m, 1H), 2.42 – 2.36 (m, 1H), 2.22 – 2.11 (m, 1H), 1.41 (s, 9H). **^{13}C NMR** (100 MHz, DMSO-d_6):δ 176.3, 155.7, 79.3, 65.6, 49.6, 34.2, 28.5 ppm. **HRMS** (ESI) *m/z* 218.1030 (calcd for $C_9H_{16}NO_5$ $[M-H]^-$ 218.1028).

Methyl (*S*)-2-((*tert*-butoxycarbonyl)amino)-3-(4-chlorophenyl)propanoate (3.21)

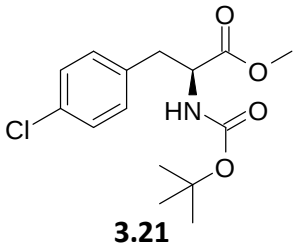

3.21

Following General Procedure B, methyl (S)-2-amino-3-(4-chlorophenyl)propanoate (213.66 mg, 1 mmol) gave **3.21** as a clear oil, at a yield of 73%. **IR** (ν_{max} cm^{-1}): 3351, 2983, 1730, 1676, 1354, 1285, 1161, 725, 611. **^{1}H NMR** (500 MHz, DMSO-d_6): δ 7.35 (d, *J* = 8.3 Hz, 2H), 7.31 – 7.26 (m, 3H), 4.22 - 4.16 (m, 1H), 3.64 (s, 3H), 3.01 (dd, *J* = 13.7, 4.9 Hz, 1H), 2.85 (dd, *J* = 13.7, 4.9 Hz, 1H), 1.32 (s, 9H). **^{13}C NMR (**125 MHz, DMSO-d_6): δ 172.8, 155.8, 137.0, 131.6, 131.4, 128.5, 78.7, 55.3, 52.2, 36.0, 28.5 ppm. **HRMS** (ESI) *m/z* 335.0976 (calcd for $C_{15}H_{20}NO_4NaCl$ $[M+Na]^+$ 336.0979).

Methyl (*S*)-2-((*tert*-butoxycarbonyl)amino)-2-(4-chlorophenyl)acetate (3.25)

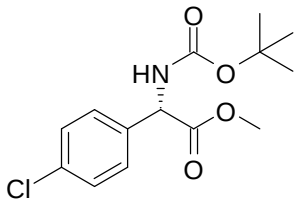

3.25

Following General Procedure B, methyl (*S*)-2-amino-2-(4-chlorophenyl)acetate (199.63 mg, 1 mmol) gave **3.25** as a light-yellow oil, at 75% yield. **IR** (ν_{max} cm^{-1}): 3406, 3369, 2978, 2950, 1740, 1694, 1511, 1490, 1316, 1217, 784, 505. **^{1}H NMR** (500 MHz, DMSO-d_6): δ 7.83 (d, *J* = 7.8, 1H), 7.43 (s, 4H), 5.27 (d, *J* = 8.06, 1H), 3.64 (s, 3H), 1.49 (s, 1H), 1.40 (s, 9H). **^{13}C NMR** (125 MHz, DMSO-d_6): δ 171.5, 133.2, 130.2, 128.9, 79.1, 57.3, 52.7, 28.6 ppm. **HRMS** (ESI) *m/z* 298.0845 (calcd for $C_{14}H_{17}NO_4Cl$ $[M-H]^-$ 298.0846).

Methyl (*S*)-2-((*tert*-butoxycarbonyl)amino)-3-(4-fluorophenyl)propanoate (3.29)

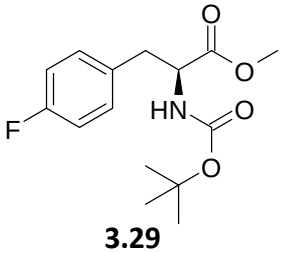

3.29

Following General Procedure B, methyl (*S*)-2-amino-3-(4-fluorophenyl)propanoate (197.21 mg, 1 mmol) gave **3.29** as a clear oil, at 78 % yield. **IR** (ν_{max} cm^{-1}): 3348, 3070, 2973, 1743, 1703, 1603, 1509, 1440, 1366, 759, 695. **^{1}H NMR** (500 MHz, DMSO-d_6): δ 7.28 – 7.24 (m, 3H), 7.11 – 7.07 (m, 2H), 4.19 -4.13 (m, 1H), 3.61 (s, 3H), 2.98 (dd, *J* = 13.8, 5.0 Hz, 1H), 2.83 (dd, *J* = 13.6, 3.5 Hz, 1H), 1.31 (s, 9H). **^{13}C NMR** (125 MHz, DMSO-d_6): δ 172.9, 160.3, 155.8, 131.5,

131.4, 115.4, 78.8, 55.6, 52.2, 36.1, 28.6 ppm. **HRMS** (ESI) *m/z* 320.1266 (calcd for $C_{15}H_{20}NO_4FNa$ $[M+Na]^+$ 320.1274).

Methyl (*S*)-2-((*tert*-butoxycarbonyl)amino)-3-(4-iodophenyl)propanoate (3.34)

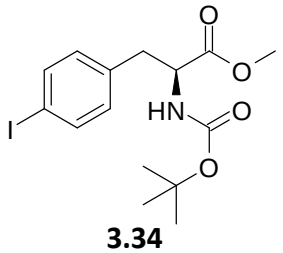

3.34

Following General Procedure B, methyl (*S*)-2-amino-3-(4-iodophenyl)propanoate (305.12 mg, 1 mmol) gave **3.34** as a clear oil, at a yield of 85%. **IR** (ν_{max} cm^{-1}): 3346, 2957, 2931, 1735, 1685, 1522, 1437, 1365, 1157, 654, 547. **^{1}H NMR** (500 MHz, DMSO-d_6): δ 7.63 (d, *J* = 7.1 Hz, 2H), 7.26 (d, *J* = 8.0 Hz, 1H), 7.05 (d, *J* = 8.0 Hz, 2H), 4.18 – 4.12 (m, 1H), 3.61 (s, 3H), 2.96 (dd, *J* = 13.6, 4.9 Hz, 1H), 2.80 (dd, *J* = 13.6, 3.2 Hz, 1H), 1.31 (s, 9H). **^{13}C NMR** (125 MHz, DMSO-d_6): δ 172.8, 155.8, 137.9, 137.4, 132.0, 92.7, 78.8, 55.3, 52.3, 36.4, 28.5 ppm. **HRMS** (ESI) *m/z* 428.0337 (calcd for $C_{15}H_{20}NO_4NaI$ $[M+Na]^+$ 428.0335).

4.2.3 General procedure C: The S_N2 *O*-Alkylation of amino acid[144, 145]

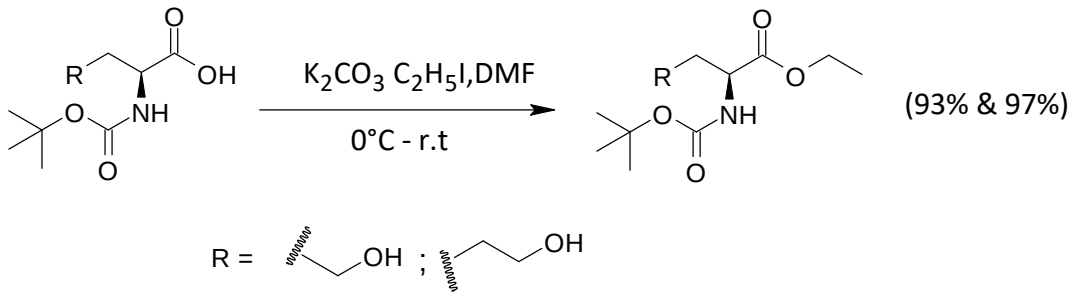

This method was used with modification. To a cold solution of an *N*-Boc protected aliphatic amino acid in DMF (8.75 mL), K_2CO_3 (1 mmol) is added, and the reaction mixture is stirred at

0 °C 10 minutes. Ethyl iodide is added to the mixture, and stirred for further 30 min at 0 °C. The mixture is then warmed to room temperature overnight. The solvent is removed under reduced pressure. Remaining residue dissolved in (5 × 30 mL) ice cold water, extracted with EtOAc (5 × 20 mL). Organic layer washed with sat. NaCl-solution (2 × 20 mL). Dried the mixture over $MgSO_4$ and filter. The solvent then removed to obtain pale amber oil.

Ethyl (*tert*-butoxycarbonyl)-*L*-serinate (3.13)

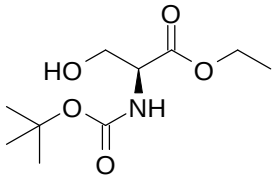

3.13

Following General Procedure C, (*tert*-butoxycarbonyl)-*L*-serine (205.21 mg, 1 mmol) gave **3.13** as an amber yellow oil, at a yield of 93%. **IR** (ν_{max} cm $^{-1}$): 3656, 3348, 3033, 1780, 1731, 1522,1352, 1149, 1050. **^{1}H NMR** (400 MHz, DMSO-d_6): δ 6.89 (d, *J* = 8.0 Hz, 1H), 4.88 (t, *J* = 6.1 Hz, 1H), 4.15 – 4.09 (m, 2H), 4.05 — 4.03 (m, 1H) 3.66 — 3.64 (m, 2H), 1.41 (s, 9H), 1.21 (t, J = 7.1 Hz, 3H). **^{13}C NMR** (100 MHz, DMSO-d_6): δ 171.4, 155.9, 80.0, 61.7, 61.0, 56.7, 28.5, 14.5 ppm.

Ethyl (*tert*-butoxycarbonyl)-*L*-homoserinate (3.17)

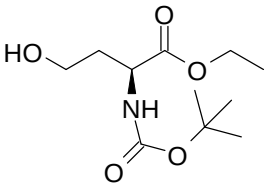

3.17

Following General Procedure C, (*tert*-butoxycarbonyl)-*L*-homoserine (219.24 mg, 1 mmol) gave **3.17** as a yellow oil, at 97% yield. **IR** (ν_{max} cm^{-1}): 3350, 2922, 1770, 1728, 1678, 1521, 1454, 1155, 1003. **^{1}H NMR** (400 MHz, DMSO-d_6): δ 6.88 (d, *J* = 8.0 Hz, 1H),4.87 – 4.84 (m, 1H), 4.20 – 4.15 (m, 1H), 4.13 – 4.00 (m, 3H), 3.63 (t, *J* = 5.4 Hz, 2H), 1.39 (s, 9H), 1.20 – 1.17 (m, 3H). **^{13}C NMR** (100 MHz, DMSO-d_6): δ 171.0, 155.4, 78.4, 61.3, 60.4, 53.3, 49.8, 28.1, 14.0 ppm.

4.2.4 General Procedure D: Ex-situ generation of sulfuryl fluoride in a two-chamber reactor[119]

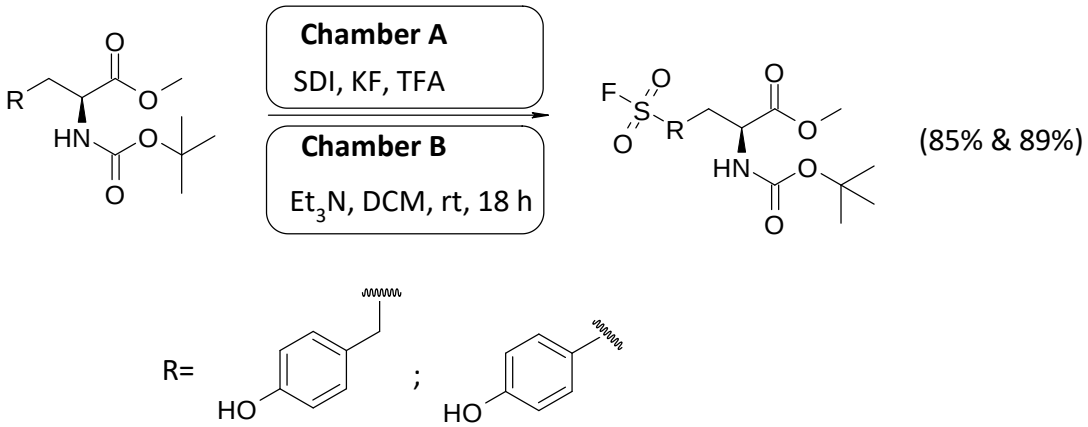

In Chamber A of an oven-dried dual-chamber reactor, the SDI (297 mg, 1.5 mmol) and KF (232 mg, 4.0 mmol) was filled. Then, chamber B was filled with respective amino acid (1,0 mmol), (Et_3N, 279 µl), and DCM (4 mL). Lastly, TFA (1 mL) was added by insertion through the septum in chamber A and an immediate gas formation was observed. 18 Hours later of stirring at room temperature, one of the caps was carefully opened to free the residual pressure. The reaction mixture in chamber B, was stirred for 15 min extra in order to remove sulfuryl fluoride. In chamber B, the contents were transferred to a 100 mL round-bottomed flask. The fractions from Chamber B were added to the same flask after being rinsed five times with 2 mL of dichloromethane. Using rotary evaporation, the solvent was removed from the flask

after adding 200 mg of silica gel. Silica gel column chromatography was used to purify the crude product.

Methyl (*S*)-2-((*tert*-butoxycarbonyl)amino)-3-(4-((fluorosulfonyl)oxy)phenyl)propanoate (3.5)

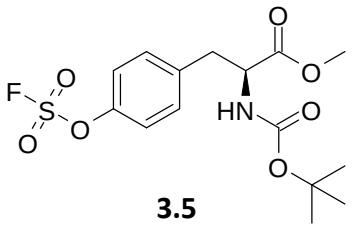

3.5

Following General Procedure D, methyl (*tert*-butoxycabonyl)-L-tyrosinate (295.34 mg, 1 mmol) gave **3.5** that its crude product was purified by solid-flash column chromatography silica gel (ethyl acetate/methanol, 8/2) and it was dried to fluffy light brown needle-like structure solid, at a yield of 85%. **R_f =** 0.87 (ethyl acetate/methanol, 8/2) **Mp**: 83 – 85 °C. **IR** (ν_{max} cm^{-1}): 3335, 2940, 1735, 1678, 1516, 1437, 1226, 1147,918, 787, 548. **^{1}H NMR** (400 MHz, DMSO-d_6): δ 7.52 (d, *J* = 8.6, 2H), 7.46 (d, *J* = 8.7, 2H), 7.34 (d, *J* = 8.4, 1H), 4.29-4.23 (m, 1H), 3.64 (s, 3H), 3.11 (dd, *J* = 13.8, 4.8 Hz, 1H), 2.92 (dd, *J* = 13.6, 3.0 Hz, 1H), 1.32 (s, 9H). **^{13}C NMR** (100 MHz, DMSO-d_6): δ 172.69, 155.80, 148.86, 139.52, 131.94, 121.14, 78.80, 55.14, 52.31, 36.19, 28.51. **^{19}F NMR** (376 MHz, DMSO-d_6): δ –73.48 ppm. **HRMS** (ESI) *m/z* 400.0848 (calcd for $C_{15}H_{20}NO_7SFNa$ $[M+Na]^+$ 400.0842).

Methyl (S)-2-((tert-butoxycarbonyl)amino)-2-(4-((fluorosulfonyl)oxy)phenyl)acetate (3.9)

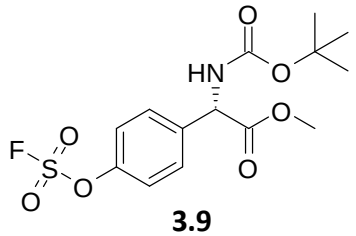

3.9

Following General Procedure D, Methyl (*S*)-2-((*tert*-butoxycarbonyl)amino)-2-(4-hydroxyphenyl)aceatate (281.31 mg, 1 mmol) gave **3.9** that it crude was purified by solid-flash column chromatography silica gel (ethyl acetate/methanol, 8/2). And it was dried to light brown needles-like solid, at a yield of 89%. **R_f =** 0.76 (ethyl acetate/methanol, 8/2) **Mp**: 102 – 103 °C **IR** (ν_{max} cm^{-1}): 3359, 2924, 1731, 1679, 1517, 1444, 1128, 907, 759, 614. **^{1}H NMR** (400 MHz, DMSO-d_6): δ 7.92 (d, J = 7.8 Hz, 1H), 7.61 (m, 4H), 5.37 (d, *J*=7.8 Hz, 1H), 3.65 (s, 3H), 1.39 (s, 9H). **^{13}C NMR** (100 MHz, DMSO-d_6): δ 171.3, 149.7, 138.5, 130.8, 121.6, 79.3, 57.1, 52.9, 28.6. **^{19}F NMR** (376 MHz, DMSO-d_6): δ –73.47 ppm. **HRMS** (ESI) *m/z* 386.0692 (calcd for $C_{14}H_{18}NO_7SFNa$ $[M+Na]^+$ 386.0686).

4.2.5 One-pot Synthesis of methyl (*S*)-2-((*tert*-butoxycarbonyl)amino)-3-(4-(fluorosulfonyl)phenyl)propanoate[134, 159]

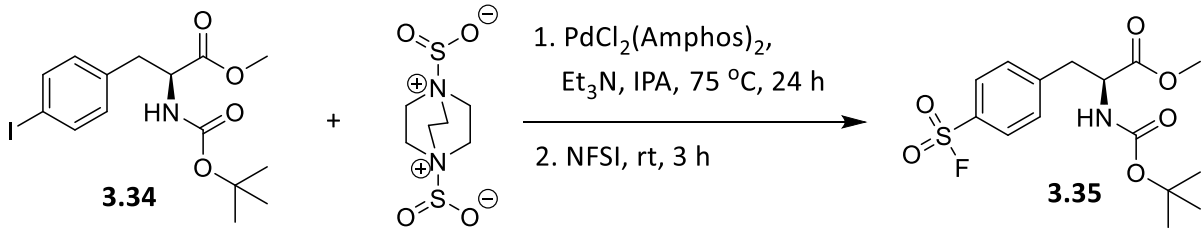

3.34 **3.35**

This method is representative. A glass tube was charged with DABSO (58 mg, 0.24 mmol) followed by $PdCl_2(AmPhos)_2$ (14.2 mg, 0.02 mmol), methyl (*S*)-2-((tert-butoxycarbonyl)amino)-3-(4-iodophenyl)propanoate (0.04 mmol), sealed with a rubber

septum at the top of a condenser and filled with N_2 gas. Anhydrous isopropanol (1.5 mL) and anhydrous triethylamine (167 microlitres, 1.2 mmol) were added sequentially through the septum, and the reaction was stirred under N_2 gas, and heated to 75 °C for 24 hours. Upon completion, the mixture was cooled to room temperature, then the NFSI (189 mg, 0.6 mmol) was added, and the reaction mixture was further stirred for 3 hours at room temperature until completion. The reaction mixture was concentrated using rotary-evaporation, then dissolved in ethyl acetate and filtered through celite. The filtrate was washed with a saturated aqueous solution of sodium thiosulfate and brine, dried with anhydrous magnesium sulfate, filtered, and concentrated in roto-evaporation to leave the crude product, which was purified by column chromatography on silica in (hexane/ethyl acetate, 6/4) solvent system to leave the sulfonyl fluoride amino acid product as a brown oil, at 63.7% yield. **R_f =** 0.67 (hexane/ethyl acetate, 6/4), **IR** (ν_{max} cm $^{-1}$): 3346, 2957, 2931, 1735, 1685, 1522, 1437, 1365, 1289, 1219, 1097, 754, 588. **^{1}H NMR** (500 MHz, DMSO-d_6): δ 8.18 (d, *J* = 7.9 Hz, 1H), 8.09 (d, *J* = 8.3 Hz, 2H), 7.68 (d, *J* = 7.9 Hz, 2H), 4.38 – 4.32 (m, 1H), 3.67 (s, 3H), 3.24 (dd, *J* = 14.3, 5.1 Hz, 1H), 3.06 – 3.00 (m, 1H), 1.31 (s, 9H). **^{13}C NMR** (125 MHz, DMSO-d_6): δ 172.4, 148.0, 137.2, 129.4, 128.8, 128.7, 78.9, 54.7, 52.5, 36.9, 28.5. **^{19}F NMR** (470 MHz, DMSO-d_6): δ – 84.05 ppm. **HRMS** (ESI) *m/z* 396.0686 (calcd for $C_{15}H_{20}NO_6SClF$ $[M+Cl]^-$ 396.0684).

4.2.6 Method A: The LCMS Assay

A 10 Mm ammonium acetate buffer was made by dissolving 15 mg of ammonium acetate in 20 mL of ultra-pure water (UPW). Upon mixed, and the ammonium acetate completely dissolved, the mixture was brought to pH 7.3 by adding few drops of ammonia and the pH was measured using the pH meter. A 10 µL amount of 0.2 M solution of compound **3.5** in methanol was manually transferred to a reaction vial. A 1 mL of an ammonium acetate buffer

pH 7.3 was added to the same reaction vial. The LCMS was obtained. To the same mixture, 10 µL of the Boc-lysine (2 M, MeOH) was added, and the solution mixture was run for LCMS for 15 min for each run. For LCMS spectra see Appendix.

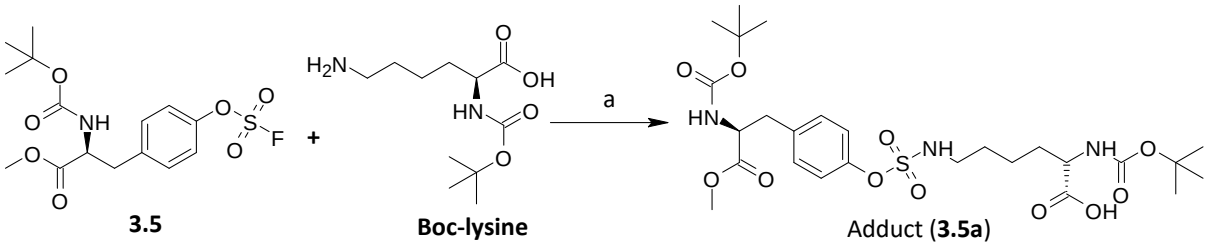

a) MeOH, Ammonium acetate

4.2.7 Method B: The NMR Assay

A phosphate-buffer silane (PBS) tablet was dissolved in 500 mL ultra-pure water (UPW) to make a buffer solution of pH 7.4. To a 0.5 mL of the buffer, (PBS, pH 7.4), 5 µL of compound **3.5** containing a covalent warhead (0.2 M in DMSO-d_6) was added in an NMR tube, and the ^{1}H NMR was obtained. To the same mixture with buffer, 5 µL of *N*-Boc-lysine (2M in DMSO-d_6). This was added to the NMR tube, and the solution was mixed by inverting the tube several times. A ^{1}H NMR was recorded on this mixture, and the acquisition is 15 min for approximately 4 h, of 15 scans, ^{19}F NMR was recorded for 1st and 15th run for 4.5 h each run. For NMR spectra see Appendix.

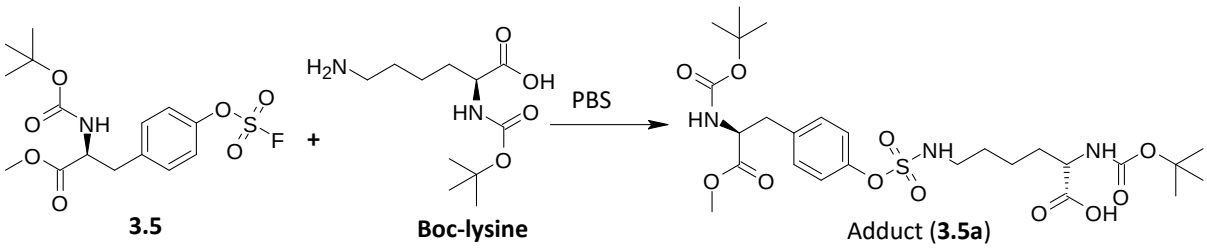

References

1. Baillie, T. A., Targeted Covalent Inhibitors For Drug Design. *Angewandte Chemie International Edition* **2016,** *55* (43), 13408-13421.
2. Lagoutte, R.; Patouret, R.; Winssinger, N., Covalent Inhibitors: An Opportunity for Rational Target Selectivity. *Current Opinion in Chemical Biology* **2017,** *39*, 54-63.
3. Ghosh, A. K.; Samanta, I.; Mondal, A.; Liu, W. R., Covalent Inhibition in Drug Discovery. *ChemMedChem* **2019,** *14* (9), 889-906.
4. Singh, J.; Petter, R. C.; Baillie, T. A.; Whitty, A., The resurgence of covalent drugs. *Nature reviews Drug discovery* **2011,** *10* (4), 307-317.
5. Scaltriti, M.; Dawood, S.; Cortes, J., Molecular Pathways: Targeting Hsp90—Who Benefits and Who Does Not. *Clinical Cancer Research* **2012,** *18* (17), 4508-4513.
6. Roth, G. J.; Stanford, N.; Majerus, P. W., Acetylation of Prostaglandin Synthase by Aspirin. *Proceedings of the National Academy of Sciences* **1975,** *72* (8), 3073-3076.
7. Van Der Ouderaa, F. J.; Buytenhek, M.; Nugteren, D. H.; Van Dorp, D. A., Acetylation of Prostaglandin Endoperoxide Synthetase With Acetylsalicylic Acid. *European Journal of Biochemistry* **1980,** *109* (1), 1-8.
8. Waxman, D. J.; Strominger, J. L., Penicillin-Binding Proteins and the Mechanism of Action of Beta-Lactam Antibiotics. *Annual Review of Biochemistry* **1983,** *52* (1), 825-869.
9. Lobanovska, M.; Pilla, G., Focus: Drug Development: Penicillin's Discovery and Antibiotic Resistance: Lessons For the Future? *The Yale Journal of Biology and Medicine* **2017,** *90* (1), 135.
10. WHO, World Health Organisation report on surveillance of antibiotic consumption: 2016–2018 early implementation. **2018**.
11. Bush, K.; Bradford, P. A., β-Lactams and β-Lactamase Inhibitors: An Overview. *Cold Spring Harbor Perspectives in Medicine* **2016,** *6* (8), a025247.

12. Dougherty, T. J.; Pucci, M. J., *Antibiotic Discovery and Development*. Springer Science & Business Media: 2011.

13. Yocum, R. R.; Rasmussen, J. R.; Strominger, J. L., The Mechanism of Action of Penicillin. Penicillin Acylates the Active Site of Bacillus Stearothermophilus D-Alanine Carboxypeptidase. *Journal of Biological Chemistry* **1980,** *255* (9), 3977-3986.

14. Baillie, T. A., The contributions of Sidney D. Nelson to drug metabolism research. *Drug Metabolism Reviews* **2015,** *47* (1), 4-11.

15. Butler, L. D.; Guzzie-Peck, P.; Hartke, J.; Bogdanffy, M. S.; Will, Y.; Diaz, D.; Mortimer-Cassen, E.; Derzi, M.; Greene, N.; DeGeorge, J. J., Current Nonclinical Testing Paradigms in Support of Safe Clinical Trials: An IQ Consortium DruSafe Perspective. *Regulatory Toxicology and Pharmacology* **2017,** *87*, S1-S15.

16. Ekins, S.; Puhl, A. C.; Zorn, K. M.; Lane, T. R.; Russo, D. P.; Klein, J. J.; Hickey, A. J.; Clark, A. M., Exploiting Machine Learning For End-to-end Drug Discovery and Development. *Nature Materials* **2019,** *18* (5), 435-441.

17. Wagner, J.; Dahlem, A. M.; Hudson, L. D.; Terry, S. F.; Altman, R. B.; Gilliland, C. T.; DeFeo, C.; Austin, C. P., A Dynamic Map For Learning, Communicating, Navigating and Improving Therapeutic Development. *Nature Reviews Drug discovery* **2018,** *17* (2), 150-150.

18. Jollow, D.; Mitchell, J.; Potter, W.; Davis, D.; Gillette, J.; Brodie, B., Acetaminophen-Induced Hepatic Necrosis. II. Role of Covalent Binding *in vivo*. *Journal of Pharmacology and Experimental Therapeutics* **1973,** *187* (1), 195-202.

19. Gehringer, M.; Laufer, S. A., Emerging and Re-emerging Warheads For Targeted Covalent Inhibitors: Applications in Medicinal Chemistry and Chemical Biology. *Journal of Medicinal Chemistry* **2018,** *62* (12), 5673-5724.

20. Benns, H. J.; Wincott, C. J.; Tate, E. W.; Child, M. A., Activity-and Reactivity-Based Proteomics: Recent Technological Advances and Applications in Drug Discovery. *Current Opinion in Chemical Biology* **2021,** *60*, 20-29.

21. Martin, J. S.; MacKenzie, C. J.; Fletcher, D.; Gilbert, I. H., Characterising Covalent Warhead Reactivity. *Bioorganic & Medicinal Chemistry* **2019,** *27* (10), 2066-2074.

22. Visscher, M.; Arkin, M. R.; Dansen, T. B., Covalent Targeting of Acquired Cysteines in Cancer. *Current Opinion in Chemical Biology* **2016,** *30*, 61-67.

23. Greenbaum, D.; Medzihradszky, K. F.; Burlingame, A.; Bogyo, M., Epoxide Electrophiles As Activity-Dependent Cysteine Protease Profiling and Discovery Tools. *Chemistry & Biology* **2000,** *7* (8), 569-581.

24. Pace, N. J.; Pimental, D. R.; Weerapana, E., An Inhibitor of Glutathione S-Transferase Omega 1 that Selectively Targets Apoptotic Cells. *Angewandte Chemie International Edition* **2012,** *51* (33), 8365-8368.

25. Janes, M. R.; Zhang, J.; Li, L.-S.; Hansen, R.; Peters, U.; Guo, X.; Chen, Y.; Babbar, A.; Firdaus, S. J.; Darjania, L., Targeting KRAS Mutant Cancers With a Covalent G12C-Specific Inhibitor. *Cell* **2018,** *172* (3), 578-589.

26. Barf, T.; Covey, T.; Izumi, R.; van de Kar, B.; Gulrajani, M.; van Lith, B.; van Hoek, M.; de Zwart, E.; Mittag, D.; Demont, D., Acalabrutinib (ACP-196): A Covalent Bruton Tyrosine Kinase Inhibitor With A Differentiated Selectivity and *in vivo* Potency Profile. *Journal of Pharmacology and Experimental Therapeutics* **2017,** *363* (2), 240-252.

27. Faleiro, L.; Kobayashi, R.; Fearnhead, H.; Lazebnik, Y., Multiple Species of CPP32 and Mch2 Are the Major Active Caspases Present in Apoptotic Cells. *The EMBO Journal* **1997,** *16* (9), 2271-2281.

28. He, L.; Shao, M.; Wang, T.; Lan, T.; Zhang, C.; Chen, L., Design, Synthesis, and SAR Study of Highly Potent, Selective, Irreversible Covalent JAK3 Inhibitors. *Molecular Diversity* **2018,** *22* (2), 343-358.

29. Allen, C. E.; Curran, P. R.; Brearley, A. S.; Boissel, V.; Sviridenko, L.; Press, N. J.; Stonehouse, J. P.; Armstrong, A., Efficient and Facile Synthesis of Acrylamide Libraries for Protein-Guided Tethering. *Organic Letters* **2015,** *17* (3), 458-460.

30. Brameld, K. A.; Owens, T. D.; Verner, E.; Venetsanakos, E.; Bradshaw, J. M.; Phan, V. T.; Tam, D.; Leung, K.; Shu, J.; LaStant, J., Discovery of the Irreversible Covalent FGFR Inhibitor 8-(3-(4-Acryloylpiperazin-1-yl) propyl)-6-(2, 6-dichloro-3, 5-dimethoxyphenyl)-2-(methylamino) pyrido [2, 3-d] pyrimidin-7 (8 H)-one (PRN1371) For the Treatment of Solid Tumors. *Journal of Medicinal Chemistry* **2017,** *60* (15), 6516–6527.

31. Kwarcinski, F. E.; Steffey, M. E.; Fox, C. C.; Soellner, M. B., Discovery of Bivalent Kinase Inhibitors *via* Enzyme-Templated Fragment Elaboration. *ACS Medicinal Chemistry Letters* **2015,** *6* (8), 898-901.

32. Zhao, Z.; Bourne, P. E., Progress With Covalent Small-Molecule KinaseInhibitors. *Drug Discovery Today* **2018,** *23* (3), 727-735.

33. Flanagan, M. E.; Abramite, J. A.; Anderson, D. P.; Aulabaugh, A.; Dahal, U. P.; Gilbert, A. M.; Li, C.; Montgomery, J.; Oppenheimer, S. R.; Ryder, T., Chemical and Computational Methods For The Characterization of Covalent Reactive Groups For The Prospective Design of Irreversible Inhibitors. *Journal of Medicinal Chemistry* **2014,** *57* (23), 10072-10079.

34. Kathman, S. G.; Xu, Z.; Statsyuk, A. V., A Fragment-Based Method To Discover Irreversible Covalent Inhibitors of Cysteine Proteases. *Journal of Medicinal Chemistry* **2014,** *57* (11), 4969-4974.

35. Sharma, S. V.; Bell, D. W.; Settleman, J.; Haber, D. A., Epidermal Growth Factor Receptor Mutations In Lung Cancer. *Nature Reviews Cancer* **2007,** *7* (3), 169-181.

36. Weerapana, E.; Wang, C.; Simon, G. M.; Richter, F.; Khare, S.; Dillon, M. B.; Bachovchin, D. A.; Mowen, K.; Baker, D.; Cravatt, B. F., Quantitative Reactivity Profiling Predicts Functional Cysteines In Proteomes. *Nature* **2010,** *468* (7325), 790-795.

37. Bar-Peled, L.; Kemper, E. K.; Suciu, R. M.; Vinogradova, E. V.; Backus, K. M.; Horning, B. D.; Paul, T. A.; Ichu, T.-A.; Svensson, R. U.; Olucha, J., Chemical Proteomics Identifies Druggable Vulnerabilities in a Genetically Defined Cancer. *Cell* **2017,** *171* (3), 696-709.

38. Spradlin, J. N.; Hu, X.; Ward, C. C.; Brittain, S. M.; Jones, M. D.; Ou, L.; To, M.; Proudfoot, A.; Ornelas, E.; Woldegiorgis, M., Harnessing the Anti-Cancer Natural Product Nimbolide For Targeted Protein Degradation. *Nature Chemical Biology* **2019,** *15* (7), 747-755.

39. Yu, J.; Yang, X.; Sun, Y.; Yin, Z., Highly Reactive and Tracelessly Cleavable Cysteine-Specific Modification of Proteins *via* 4-Substituted Cyclopentenone. *Angewandte Chemie* **2018,** *130* (36), 11772-11776.

40. Dunny, E.; Doherty, W.; Evans, P.; Malthouse, J. P. G.; Nolan, D.; Knox, A. J., Vinyl Sulfone-Based Peptidomimetics As Anti-Trypanosomal Agents: Design, Synthesis, Biological and Computational Evaluation. *Journal of Medicinal Chemistry* **2013,** *56* (17), 6638-6650.

41. Zhang, H.; Harmon, M.; Radoshitzky, S. R.; Soloveva, V.; Kane, C. D.; Duplantier, A. J.; Ogungbe, I. V., Vinyl Sulfone-Based Inhibitors of Nonstructural Protein 2 Block the Replication of Venezuelan Equine Encephalitis Virus. *ACS Medicinal Chemistry Letters* **2020,** *11* (11), 2139-2145.

42. Rut, W.; Groborz, K.; Zhang, L.; Sun, X.; Zmudzinski, M.; Pawlik, B.; Wang, X.; Jochmans, D.; Neyts, J.; Młynarski, W., SARS-CoV-2 Mpro Inhibitors and Activity-Based Probes For Patient Sample Imaging. *Nature Chemical Biology* **2021,** *17* (2), 222-228.

43. Wang, C.; Horby, P. W.; Hayden, F. G.; Gao, G. F., A Novel Coronavirus Outbreak of Global Health Concern. *The lancet* **2020,** *395* (10223), 470-473.

44. Huang, C.; Wang, Y.; Li, X.; Ren, L.; Zhao, J.; Hu, Y.; Zhang, L.; Fan, G.; Xu, J.; Gu, X., Clinical Features of Patients Infected With 2019 Novel Coronavirus in Wuhan, China. *The Lancet* **2020,** *395* (10223), 497-506.

45. Hacker, S. M.; Backus, K. M.; Lazear, M. R.; Forli, S.; Correia, B. E.; Cravatt, B. F., Global Profiling of Lysine Reactivity and Ligandability in the Human Proteome. *Nature Chemistry* **2017,** *9* (12), 1181-1190.

46. Ho, T.-L., Hard Soft Acids Bases (HSAB) Principle and Organic Chemistry. *Chemical Reviews* **1975,** *75* (1), 1-20.

47. Migneault, I.; Dartiguenave, C.; Bertrand, M. J.; Waldron, K. C., Glutaraldehyde: Behavior In Aqueous Solution, Reaction With Proteins, and Application To Enzyme Crosslinking. *BioTechniques* **2004,** *37* (5), 790-802.

48. Madian, A. G.; Regnier, F. E., Proteomic Identification of Carbonylated Proteins and Their Oxidation Sites. *Journal of Proteome Research* **2010,** *9* (8), 3766-3780.

49. Spears, R. J.; Fascione, M. A., Site-Selective Incorporation and Ligation of Protein Aldehydes. *Organic & Biomolecular Chemistry* **2016,** *14* (32), 7622-7638.

50. McFarland, J. M.; Francis, M. B., Reductive Alkylation of Proteins Using Iridium Catalyzed Transfer Hydrogenation. *Journal of the American Chemical Society* **2005,** *127* (39), 13490-13491.

51. De Silva, E. D.; Scheuer, P. J., Manoalide, An Antibiotic Sesterterpenoid From the Marine Sponge Luffariella Variabilis (Polejaeff). *Tetrahedron Letters* **1980,** *21* (17), 1611-1614.

52. Lombardo, D.; Dennis, E., Cobra Venom Phospholipase A2 Inhibition By Manoalide. A novel Type of Phospholipase Inhibitor. *Journal of Biological Chemistry* **1985,** *260* (12), 7234-7240.

53. Glaser, K. B.; Jacobs, R. S., Inactivation of Bee Venom Phospholipase A2 By Manoalide: A Model Based On the Reactivity of Manoalide with Amino Acids and Peptide Sequences. *Biochemical Pharmacology* **1987,** *36* (13), 2079-2086.

54. Glaser, K. B.; De Carvalho, M.; Jacobs, R. S.; Kernan, M. R.; Faulkner, D., Manoalide: Structure-Activity Studies and Definition of the Pharmacophore For Phospholipase A2 Inactivation. *Molecular Pharmacology* **1989,** *36* (5), 782-788.

55. Bianco, I. D.; Kelley, M. J.; Crowl, R. M.; Dennis, E. A., Identification of Two Specific Lysines Responsible For The Inhibition of Phospholipase A2 By Manoalide. *Biochimica et Biophysica Acta (BBA)-Protein Structure and Molecular Enzymology* **1995,** *1250* (2), 197-203.

56. Cal, P. M.; Vicente, J. B.; Pires, E.; Coelho, A. V.; Veiros, L. s. F.; Cordeiro, C.; Gois, P. M., Iminoboronates: A New Strategy For Reversible Protein Modification. *Journal of the American Chemical Society* **2012,** *134* (24), 10299-10305.

57. Crawford, L.; Weerapana, E., A Tyrosine-Reactive Irreversible Inhibitor For Glutathione S-Transferase Pi (GSTP1). *Molecular Biosystems* **2016,** *12* (6), 1768-1771.

58. Shannon, D. A.; Banerjee, R.; Webster, E. R.; Bak, D. W.; Wang, C.; Weerapana, E., Investigating the Proteome Reactivity and Selectivity of Aryl Halides. *Journal of the American Chemical Society* **2014,** *136* (9), 3330-3333.

59. Ward, C. C.; Kleinman, J. I.; Nomura, D. K., NHS-Esters as Versatile Reactivity-Based Probes For Mapping Proteome-Wide Ligandable Hotspots. *ACS Chemical Biology* **2017,** *12* (6), 1478-1483.

60. Anscombe, E.; Meschini, E.; Mora-Vidal, R.; Martin, M. P.; Staunton, D.; Geitmann, M.; Danielson, U. H.; Stanley, W. A.; Wang, L. Z.; Reuillon, T., Identification and Characterization of An Irreversible Inhibitor of CDK2. *Chemistry & Biology* **2015,** *22* (9), 1159-1164.

61. Pettinger, J.; Le Bihan, Y. V.; Widya, M.; van Montfort, R. L.; Jones, K.; Cheeseman, M. D., An Irreversible Inhibitor of Hsp72 That Unexpectedly Targets Lysine-56. *Angewandte Chemie International Edition* **2017,** *56* (13), 3536-3540.

62. Dalton, S. E.; Campos, S., Covalent Small Molecules As Enabling Platforms For Drug Discovery. *ChemBioChem* **2020,** *21* (8), 1080-1100.

63. Ray, S.; Murkin, A. S., New Electrophiles and Strategies For Mechanism-Based and Targeted Covalent Inhibitor Design. *Biochemistry* **2019,** *58* (52), 5234-5244.

64. Asano, S.; Patterson, J. T.; Gaj, T.; Barbas III, C. F., Site-Selective Labeling of a Lysine Residue in Human Serum Albumin. *Angewandte Chemie International Edition* **2014,** *53* (44), 11783-11786.

65. Grimster, N. P.; Connelly, S.; Baranczak, A.; Dong, J.; Krasnova, L. B.; Sharpless, K. B.; Powers, E. T.; Wilson, I. A.; Kelly, J. W., Aromatic Sulfonyl Fluorides Covalently Kinetically Stabilize Transthyretin To Prevent Amyloidogenesis While Affording A Fluorescent Conjugate. *Journal of the American Chemical Society* **2013,** *135* (15), 5656-5668.

66. Gushwa, N. N.; Kang, S.; Chen, J.; Taunton, J., Selective Targeting of Distinct Ative Site Nucleophiles By Irreversible SRC-Family Kinase Inhibitors. *Journal of the American Chemical Society* **2012,** *134* (50), 20214-20217.

67. Anscombe, E. M., E; Mora-Vidal, R. M., MP Staunton, D Geitmann, M Danielson, UH Stanley, WA ; Wang, L.; Reuillon, T.; Golding, B.; Cano, C.; Newell, D.; Noble, M.; Wedge, S.; Endicott, J.; Griffin, R., Identification and characterization of an irreversible inhibitor of CDK2. *Chemistry & Biology* **2015,** *22* (9), 1159-1164.

68. Baker, B.; Wood, W. F., Irreversible Enzyme Inhibitors. CXXIII. Candidate Irreversible Inhibitors of Guanine Deaminase and Xanthine Oxidase Derived From 9-Phenylguanine Substituted With a Terminal Sulfonyl Fluoride. *Journal of Medicinal Chemistry* **1968,** *11* (4), 650-652.

69. Baker, B.; Lourens, G. J., Irreversible enzyme inhibitors. Cv. 1, 2 differential irreversible inhibition of vertebrate dihydrofolic reductases by derivatives of 4, 6-diamino-1, 2-dihydro-2, 2-dimethyl-1-phenyl-s-triazines substituted with a terminal sulfonyl fluoride3. *Journal of Medicinal Chemistry* **1967,** *10* (6), 1113-1122.

70. Baker, B. R.; Hurlbut, J. A., Irreversible Enzyme Inhibitors. CXIV. Proteolytic Enzymes. 4. Additional Active-Site-Directed Irreversible Inhibitors of Alpha-Chymotrypsin Derived From Phenoxyacetamides Bearing a Terminal Sulfonyl Fluoride. *Journal of Medicinal Chemistry* **1968,** *11* (2), 241-245.

71. Baker, B., Active-site Directed Irreversible Inhibitors of Dihydrofolate Reductase. *Annals of the New York Academy of Sciences* **1971,** *186* (1), 214-226.

72. Narayanan, A.; Jones, L., Sulfonyl Fluorides As Privileged Warheads In Chemical Biology. *Chemical Science* **2015,** *6* (5), 2650-2659.

73. Hett, E. C.; Xu, H.; Geoghegan, K. F.; Gopalsamy, A.; Kyne Jr, R. E.; Menard, C. A.; Narayanan, A.; Parikh, M. D.; Liu, S.; Roberts, L., Rational Targeting of Active-Site Tyrosine Residues Using Sulfonyl Fluoride Probes. *ACS Chemical Biology* **2015,** *10* (4), 1094-1098.

74. Crichlow, G. V.; Lubetsky, J. B.; Leng, L.; Bucala, R.; Lolis, E. J., Structural and Kinetic Analyses of Macrophage Migration Inhibitory Factor Ative Site Iteractions. *Biochemistry* **2009,** *48* (1), 132-139.

75. Annamalai, A. E.; Colman, R., Reaction of The Adenine Nucleotide Analogue 5'-*p*-Fluorosulfonylbenzoyl Adenosine at Distinct Tyrosine and Cysteine Residues of Rabbit Muscle Pyruvate Kinase. *Journal of Biological Chemistry* **1981,** *256* (20), 10276-10283.

76. Oudot, C.; Jault, J. M.; Jaquinod, M.; Negre, D.; Prost, J. F.; Cozzone, A. J.; Cortay, J. C., Inactivation of Isocitrate Dehydrogenase Kinase/Phosphatase By 5'-[*p*-(Fluorosulfonyl benzoyl) Adenosine Is Not Due To the Labeling of the Invariant Lysine Residue Found In The Protein Kinase Family. *European Journal of Biochemistry* **1998,** *258* (2), 579-585.

77. Bullough, D. A.; Allison, W. S., Three Copies of the Beta Subunit Must Be Modified to Achieve Complete Inactivation of the Bovine Mitochondrial F1-ATPase by 5'-*p*-Fluorosulfonylbenzoyl Adenosine. *Journal of Biological Chemistry* **1986,** *261* (13), 5722-5730.

78. Harlow, K.; Switzer, R., Chemical Modification of Salmonella Typhimurium Phosphoribosylpyrophosphate Synthetase with 5'-(*p*-Fluorosulfonylbenzoyl) Adenosine. Identification of An Active Site Histidine. *Journal of Biological Chemistry* **1990,** *265* (10), 5487-5493.

79. Shannon, D. A.; Gu, C.; McLaughlin, C. J.; Kaiser, M.; van der Hoorn, R. A.; Weerapana, E., Sulfonyl Fluoride Analogues As Activity-Based Probes For Serine Proteases. *ChemBioChem* **2012,** *13* (16), 2327-2330.

80. Fahrney, D. E.; Gold, A. M., Sulfonyl Fluorides As Inhibitors of Esterases. I. Rates of Reaction With Acetylcholinesterase, α-Chymotrypsin, and Trypsin. *Journal of the American Chemical Society* **1963,** *85* (7), 997-1000.

81. Dubiella, C.; Cui, H.; Gersch, M.; Brouwer, A. J.; Sieber, S. A.; Krüger, A.; Liskamp, R. M.; Groll, M., Selective Inhibition of the Immunoproteasome By Ligand-Induced Crosslinking of the Active Site. *Angewandte Chemie International Edition* **2014,** *53* (44), 11969-11973.

82. Pal, P. K.; Wechter, W. J.; Colman, R. F., Affinity Labeling of the Inhibitory DPNH Site of Bovine Liver Glutamate Dehydrogenase by 5'-Fluorosulfonylbenzoyl Adenosine. *Journal of Biological Chemistry* **1975,** *250* (20), 8140-8147.

83. Dong, J.; Krasnova, L.; Finn, M.; Sharpless, K. B., Sulfur (VI) Fluoride Exchange (SuFEx): Another Good Reaction For Click Chemistry. *Angewandte Chemie International Edition* **2014,** *53* (36), 9430-9448.

84. Li, S.; Wu, P.; Moses, J. E.; Sharpless, K. B., Multidimensional SuFEx Click Chemistry: Sequential Sulfur (VI) Fluoride Exchange Connections of Diverse Modules Launched from an SOF_4 Hub. *Angewandte Chemie* **2017,** *129* (11), 2949-2954.

85. Liu, F.; Wang, H.; Li, S.; Bare, G. A.; Chen, X.; Wang, C.; Moses, J. E.; Wu, P.; Sharpless, K. B., Biocompatible SuFEx Click Chemistry: Thionyl Tetrafluoride (SOF4)-Derived Connective Hubs For Bioconjugation to DNA and Proteins. *Angewandte Chemie International Edition* **2019,** *58* (24), 8029-8033.

86. Gao, B.; Li, S.; Wu, P.; Moses, J. E.; Sharpless, K. B., SuFEx Chemistry of Thionyl Tetrafluoride (SOF_4) With Organolithium Nucleophiles: Synthesis of Sulfonimidoyl Fluorides, Sulfoximines, Sulfonimidamides, and Sulfonimidates. *Angewandte Chemie* **2018,** *130* (7), 1957-1961.

87. Cuesta, A.; Wan, X.; Burlingame, A. L.; Taunton, J., Ligand Conformational Bias Drives Enantioselective Modification of A Surface-Exposed Lysine On Hsp90. *Journal of the American Chemical Society* **2020,** *142* (7), 3392-3400.

88. Wan, X.; Yang, T.; Cuesta, A.; Pang, X.; Balius, T. E.; Irwin, J. J.; Shoichet, B. K.; Taunton, J., Discovery of Lysine-Targeted eIF4E Inhibitors Through Covalent Docking. *Journal of the American Chemical Society* **2020,** *142* (11), 4960-4964.

89. Lange, W.; Müller, E., Aromatic Fluorosulfates. *Berichte der Deutschen Chemischen Gesellschaft* **1930,** *63*, 2653-2657.

90. Baranczak, A.; Liu, Y.; Connelly, S.; Du, W.-G. H.; Greiner, E. R.; Genereux, J. C.; Wiseman, R. L.; Eisele, Y. S.; Bradbury, N. C.; Dong, J., A fluorogenic aryl fluorosulfate for intraorganellar transthyretin imaging in living cells and in Caenorhabditis elegans. *Journal of the American Chemical Society* **2015,** *137* (23), 7404-7414.

91. Martín-Gago, P.; Olsen, C. A., Arylfluorosulfate-Based Electrophiles For Covalent Protein Labeling: A New Addition To The Arsenal. *Angewandte Chemie International Edition* **2019,** *58* (4), 957-966.

92. Liu, Z.; Li, J.; Li, S.; Li, G.; Sharpless, K. B.; Wu, P., SuFEx Click Chemistry Enabled Late-Stage Drug Functionalization. *Journal of the American Chemical Society* **2018,** *140* (8), 2919-2925.

93. Baggio, C.; Udompholkul, P.; Gambini, L.; Salem, A. F.; Jossart, J.; Perry, J. J. P.; Pellecchia, M., Aryl-Fluorosulfate-Based Lysine Covalent Pan-Inhibitors of Apoptosis Protein (IAP) Antagonists With Cellular Efficacy. *Journal of Medicinal Chemistry* **2019,** *62* (20), 9188-9200.

94. Whitesell, L., and Lindquist, S.L., Hsp90 and Chaperoning of Cancer. *Nature Reviews Cancer* **2005,** *5* (10), 761-772.

95. Whitesell, L., Mimnaugh, E.G., De Costa, B., Myers, C.E., Neckers, L.M., Inhibition of Heat Shock Protein Hsp90-pp60v-src Heteroprotein Complex Formation by Benzoquinone Ansmycins: Essential Role for Stress Proteins In Oncogenic Transformation. *Proceedings of the National Academy of Sciences* **1994,** *91* (18), 8324-8328.

96. Panaretou, B., Prodromou, C., Roe, S.M., O'Brien, R., Ladbury, J.E, Piper, P.W. and Pearl, L.H., ATP-Binding and Hydrolysis Are Essential to the Function of the Hsp90 Molecular Chaperone *in vivo*. *The EMBO Journal* **1998,** *17* (16), 4829-4836.

97. Prodromou, C., Roe, S.M., O'Brien, R., Ladybury, J.E, Piper, P.W., and Pearl, L.H., Identification and Structural Characteriation of the ATP/ADP-Binding Site in the Hsp90 Molecular Charepone. *Cell* **1997,** *90* (1), 65-75.

98. Travers, J., Sharp, S. and Workman, P., Hsp90 Inhibition: Two-Pronged Exploitation of Cancer Dependencies. *Drug Discovery Today* **2012,** *17* (5-6), 242-252.

99. Butler, L. M., Ferraldeschi, R., Armstrong, H.K., Centenera, M.M, and Workman, P., Maximizing the Therapeutic Potential of Hsp90 Inhibitors Therapeutic Potential of Hsp90 Inhibition. *Molecular Cancer Research* **2015,** *13* (11), 1445-1451.

100. Jhaveri, K., Ochiana, S.O., Dunphy, M.P, Gerecitano, J.F., Corbern, A.D., Peter, R.I., Janjigian, Y.Y., Gomes-DaGama, E.M., Koren III, J., Modi, S. and Chiosis, G. , Heat shock protein 90 Inhibition In the Treatment of Cancer: Current Status and Future Directions. *Expert Opinion Investigational Drugs* **2014,** *23* (5), 611-628.

101. Schopf, F. H., Biebl, M.M., and Buchner, J., The Hsp90 Chaperone Machinery. *Nature Reviews Molecular Cell Biology* **2017,** *18* (6), 345-360.

102. Carrello, A., Ingley, E., Minchin, R.F., Tsai, S., and Ratajczak, T., The Common Tetratricopeptide Repeat Acceptor Site for Steroid Receptor-Associated Immunophilins and HOP os located in the dimerization domain of Hsp90. *Journal of Biological Chemistry* **1999,** *274* (5), 2682-2689.

103. Brinker, A., Scheufler, C., Von der Mulbe, F., Fleckenstein, B., Herrmann, C., Jung, G., Moarefi, I., and Hartl, F.U., Ligand Discrimination by TPR domains: Relevance and Selectivity of EEVD-Recognition in Hsp70, HOP, Hsp90 Complexes. *Journal of Biological Chemistry* **2002,** *277* (22), 19265-19275.

104. Kubota, H.; Yamamoto, S.; Itoh, E.; Abe, Y.; Nakamura, A.; Izumi, Y.; Okada, H.; Iida, M.; Nanjo, H.; Itoh, H., Increased Expression of Co-Chaperone HOP with Hsp90 and Hsc70 and Complex Formation In Human Colonic Carcinoma. *Cell Stress and Chaperones* **2010,** *15* (6), 1003-1011.

105. Veale, C. G.; Mateos-Jimenez, M.; Vaaltyn, M. C.; Müller, R.; Makhubu, M. P.; Alhassan, M.; Beatriz, G.; Albericio, F.; Mackay, C. L.; Edkins, A. L., A native mass spectrometry platform identifies HOP inhibitors that modulate the HSP90–HOP protein–protein interaction. *Chemical Communications* **2021,** *57* (83), 10919-10922.

106. Trepel, J.; Mollapour, M.; Giaccone, G.; Neckers, L., Targeting the Dynamic Hsp90 Complex In Cancer. *Nature Reviews Cancer* **2010,** *10* (8), 537-549.

107. Freilich, R.; Arhar, T.; Abrams, J. L.; Gestwicki, J. E., Protein–Protein Interactions in the Molecular Chaperone Network. *Accounts of Chemical Research* **2018,** *51* (4), 940-949.

108. Mortenson, D. E.; Brighty, G. J.; Plate, L.; Bare, G.; Chen, W.; Li, S.; Wang, H.; Cravatt, B. F.; Forli, S.; Powers, E. T., "Inverse drug discovery" strategy to identify proteins that are targeted by latent electrophiles as exemplified by aryl fluorosulfates. *Journal of the American Chemical Society* **2018,** *140* (1), 200-210.

109. Moissan, H.; Lerea, P., Sulphuryl Fluoride. A New Gas. *Comptes Rendus* **1901,** *132* (374).

110. Kenaga, E., Some Biological, Chemical and Physical Properties of Sulfuryl Fluoride As An Insecticidal Fumigant. *Journal of Economic Entomology* **1957,** *50* (1), 1-6.

111. Dow, A., Sulfuryl Fluoride Gas Fumigant. *Indianapolis (US): Dow AgroSciences LLC* **2002**.

112. Lange, W.; Müller, E., Aromatic Fluorosulfates. *Ber. Dtsch. Chem. Ges* **1930,** *63*, 2653-2657.

113. Cramer, R.; Coffman, D., New Synthesis of Aryl Fluorides and Aryl Fluorosulfonates From Oxyfluorides of Sulfur. *The Journal of Organic Chemistry* **1961,** *26* (10), 4164-4165.

114. Firth Jr, W. C., Preparation of Aaromatic Polysulfates and Copoly (Sulfate Carbonates). *Journal of Polymer Science Part B: Polymer Letters* **1972,** *10* (8), 637-641.

115. Falardeau, E. R.; DesMarteau, D. D., Synthesis of Pentafluorophenoxy Derivatives of Sulfur (IV) and-(VI) Fluorides. *Journal of Chemical and Engineering Data* **1976,** *21* (3), 386-387.

116. Dong, J.; Sharpless, K. B.; Kwisnek, L.; Oakdale, J. S.; Fokin, V. V., SuFEx-Based Synthesis of Polysulfates. *Angewandte Chemie* **2014,** *126* (36), 9620-9624.

117. Chen, W.; Dong, J.; Li, S.; Liu, Y.; Wang, Y.; Yoon, L.; Wu, P.; Sharpless, K. B.; Kelly, J. W., Synthesis of Sulfotyrosine-Containing Peptides by Incorporating Fluorosulfated Tyrosine Using an Fmoc-Based Solid-Phase Strategy. *Angewandte Chemie* **2016,** *128* (5), 1867-1870.

118. Ren, G.; Zheng, Q.; Wang, H., Aryl Fluorosulfate Trapped Staudinger Reduction. *Organic Letters* **2017,** *19* (7), 1582-1585.

119. Veryser, C.; Demaerel, J.; Bieliūnas, V.; Gilles, P.; De Borggraeve, W. M., *Ex situ* Generation of Sulfuryl Fluoride For the Synthesis of Aryl Fluorosulfates. *Organic Letters* **2017,** *19* (19), 5244-5247.

120. Davies, W.; Dick, J. H., CCLXXXVI.—Aromatic Sulphonyl Fluorides. A Convenient Method of Preparation. *Journal of the Chemical Society (Resumed)* **1931**, 2104-2109.

121. Davies, W.; Dick, J. H., 57. Aliphatic Sulphonyl Fluorides. *Journal of the Chemical Society (Resumed)* **1932**, 483-486.

122. Bianchi, T. A.; Cate, L. A., Phase Transfer Catalysis. Preparation of Aliphatic and Aromatic Sulfonyl Fluorides. *The Journal of Organic Chemistry* **1977,** *42* (11), 2031-2032.

123. Kim, D.; Jeong, H.; Lim, S.; Sohn, M. K., JA; Chi, D., Facile Nucleophilic Fluorination Reactions Using *Tert*-Alcohols As A Reaction Medium: Significantly Enhanced Reactivity of Alkali Metal Fluorides and Improved Selectivity. *The Journal of Organic Chemistry* **2008,** *73* (3), 957-962.

124. Wright, S. W.; Hallstrom, K. N., A Convenient Preparation of Heteroaryl Sulfonamides and Sulfonyl Fluorides From Heteroaryl Thiols. *The Journal of Organic Chemistry* **2006,** *71* (3), 1080-1084.

125. Kirihara, M.; Naito, S.; Ishizuka, Y.; Hanai, H.; Noguchi, T., Oxidation of Disulfides With Selectfluor™: Concise Syntheses of Thiosulfonates and Sulfonyl Fluorides. *Tetrahedron Letters* **2011,** *52* (24), 3086-3089.

126. Kulka, M., Derivatives of *p*-Chlorobenzenesulfonic Acid. *Journal of the American Chemical Society* **1950,** *72* (3), 1215-1218.

127. Jiang, Y.; Alharbi, N. S.; Sun, B.; Qin, H.-L., Facile One-Pot Synthesis of Sulfonyl Fluorides From Sulfonates or Sulfonic Acids. *RSC Advances* **2019,** *9* (24), 13863-13867.

128. Brouwer, A. J.; Ceylan, T.; van der Linden, T.; Liskamp, R. M., Synthesis of β-Aminoethanesulfonyl Fluorides or 2-Substituted Taurine Sulfonyl Fluorides As Potential Protease Inhibitors. *Tetrahedron Letters* **2009,** *50* (26), 3391-3393.

129. Toulgoat, F.; Langlois, B. R.; Médebielle, M.; Sanchez, J.-Y., An Efficient Preparation of New Sulfonyl Fluorides and Lithium Sulfonates. *The Journal of Organic Chemistry* **2007,** *72* (24), 9046-9052.

130. Tang, L.; Yang, Y.; Wen, L.; Yang, X.; Wang, Z., Catalyst-Free Radical Fluorination of Sulfonyl Hydrazides in Water. *Green Chemistry* **2016,** *18* (5), 1224-1228.

131. Pérez-Palau, M.; Cornella, J., Synthesis of Sulfonyl Fluorides From Sulfonamides. *European Journal of Organic Chemistry* **2020,** *2020* (17), 2497-2500.

132. Laudadio, G.; Bartolomeu, A. d. A.; Verwijlen, L. M.; Cao, Y.; de Oliveira, K. T.; Noël, T., Sulfonyl Fluoride Synthesis Through Electrochemical Oxidative Coupling of Thiols and Potassium Fluoride. *Journal of the American Chemical Society* **2019,** *141* (30), 11832-11836.

133. Davies, A. T.; Curto, J. M.; Bagley, S. W.; Willis, M. C., One-pot palladium-catalyzed synthesis of sulfonyl fluorides from aryl bromides. *Chemical science* **2017,** *8* (2), 1233-1237.

134. Tribby, A. L.; Rodríguez, I.; Shariffudin, S.; Ball, N. D., Pd-catalyzed conversion of aryl iodides to sulfonyl fluorides using SO_2 surrogate DABSO and selectfluor. *The Journal of organic chemistry* **2017,** *82* (4), 2294-2299.

135. Lee, C.; Ball, N. D.; Sammis, G. M., One-Pot Fluorosulfurylation of Grignard Reagents Using Sulfuryl Fluoride. *Chemical Communications* **2019,** *55* (98), 14753-14756.

136. Pradhan, A. A.; Vera, J. H., Effect Of Acids and Bases On The Solubility Of Amino Acids. *Fluid Phase Equilibria* **1998,** *152* (1), 121-132.

137. Carta, R.; Tola, G., Solubilities of *L*-Cystine, *L*-Tyrosine, *L*-Leucine, and Glycine In Aqueous Solutions at Various pHs and NaCl Concentrations. *Journal of Chemical & Engineering Data* **1996,** *41* (3), 414-417.

138. Yang, X.; Beroske, L. P.; Kemmink, J.; Rijkers, D. T.; Liskamp, R. M., Synthesis of Bicyclic Tripeptides Inspired By the ABC-Ring System of Vancomycin Through Ruthenium-Based Cyclization Chemistries. *Tetrahedron Letters* **2017,** *58* (48), 4542-4546.

139. Brenner, v. M.; Huber, W., Herstellung von α-Aminosäureestern durch Alkoholyse der Methylester. *Helvetica Chimica Acta* **1953,** *36* (5), 1109-1115.

140. Hosangadi, B. D.; Dave, R. H., An Efficient General Method For Esterification of Aromatic Carboxylic Acids. *Tetrahedron Letters* **1996,** *37* (35), 6375-6378.

141. Nakao, R.; Oka, K.; Fukumoto, T., A Simple Method For the Esterification of Carboxylic Acids Using Chlorosilanes. *Bulletin of the Chemical Society of Japan* **1981,** *54* (4), 1267-1268.

142. Brook, M. A., A simple procedure for the esterification of carboxylic acids. *Synthesis* **1983**, 201-203.

143. Anand, R. C.; Vimal, A Mild and Convenient Procedure For the Esterification of Amino Acids. *Synthetic Communications* **1998,** *28* (11), 1963-1965.

144. Pavé, G.; Usse-Versluys, S.; Viaud-Massuard, M.-C.; Guillaumet, G., Synthesis of 3-Aminochroman Derivatives By Radical Cyclization. *Organic Letters* **2003,** *5* (23), 4253-4256.

145. Icik, E.; Jolly, A.; Löffler, P.; Agelidis, N.; Bugdayci, B.; Altevogt, L.; Bilitewski, U.; Baro, A.; Laschat, S., Synthesis and Biological Evaluation of a Library of AGE-Related Amino Acid Triazole Crosslinkers. *European Journal of Organic Chemistry* **2020,** *2020* (33), 5368-5379.

146. Tantardini, C.; Oganov, A. R., Thermochemical Electronegativities of The Elements. *Nature Communications* **2021,** *12* (1), 1-9.

147. Patai, S.; More O'Ferrall, R. A., *The Chemistry of the Carbon-Halogen Bond*. Wiley Chichester: 1973.

148. Smith, R. P.; Ree, T.; Magee, J. L.; Eyring, H., The Inductive Effect and Chemical Reactivity. I. General Theory of the Inductive Effect and Application to Electric Dipole Moments of Haloalkanes. *Journal of the American Chemical Society* **1951,** *73* (5), 2263-2268.

149. Reddy, V. P., General Aspects of Organofluorine Compounds. *Organofluorine Compounds in Biology and Medicine* **2015**, 1-27.

150. Lei, H.; Stoakes, M. S.; Schwabacher, A. W.; Herath, K.; Lee, J., Efficient Synthesis of A Phosphinate Bis-Amino Acid and Its Use In The Construction of Amphiphilic Peptides. *The Journal of Organic Chemistry* **1994,** *59* (15), 4206-4210.

151. Gottlieb, H. E.; Kotlyar, V.; Nudelman, A., NMR Chemical Shifts of Common Laboratory Solvents As Trace Impurities. *Journal of Organic Chemistry* **1997,** *62* (21), 7512-7515.

152. Merck, E., *Dyeing Reagents For Thin Layer and Paper Chromatography*. E. Merck: 1980.

153. Perrin, D.; Armarego, W. L., *Purification of Laboratory Chemicals*. Butterworth-Heinemann: 2017.

154. Casey, M.; Leonard, J.; Lygo, B.; Procter, G., Purification and Drying of Solvents. In *Advanced Practical Organic Chemistry*, Springer: 1990; 28-42.

155. Abderhalden, E.; Brossa, G. A., Synthese von Polypeptiden. Derivate des p-Jodphenyl-alanins. *Berichte der Deutschen Chemischen Gesellschaft* **1909,** *42* (3), 3411-3416.

156. Laulloo, S. J., Synthesis of 2, 2-Dithiobisbenzamides Derivatives. *Asian Journal of Chemistry* **2005,** *17* (2), 697.

157. Nicolaou, K.; Boddy, C. N.; Li, H.; Koumbis, A. E.; Hughes, R.; Natarajan, S.; Jain, N. F.; Ramanjulu, J. M.; Bräse, S.; Solomon, M. E., Total Synthesis of Vancomycin—Part 2: Retrosynthetic Analysis, Synthesis Of Amino Acid Building Blocks and Strategy Evaluations. *Chemistry–A European Journal* **1999,** *5* (9), 2602-2621.

158. Green, T. W.; Wuts, P. G., Protective Groups In Organic Synthesis. Wiley, New York: 1999.

159. Davies, A.; Curto, J.; Bagley, S.; Willis, M., One-Pot Palladium-Catalyzed Synthesis of Sulfonyl Fluorides from Aryl Bromides. *Chemical Science* **2017,** *8* (2), 1233-1237.

Appendix A

The ^{1}H, ^{13}C, ^{19}F NMR, HRMS (ESI), LCMS and FTIR Spectroscopic Data

p-iodo-*L*-phenylalanine (4.32)

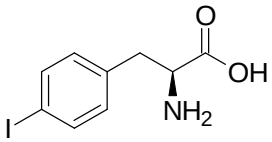

4.32

^{1}H NMR spectrum

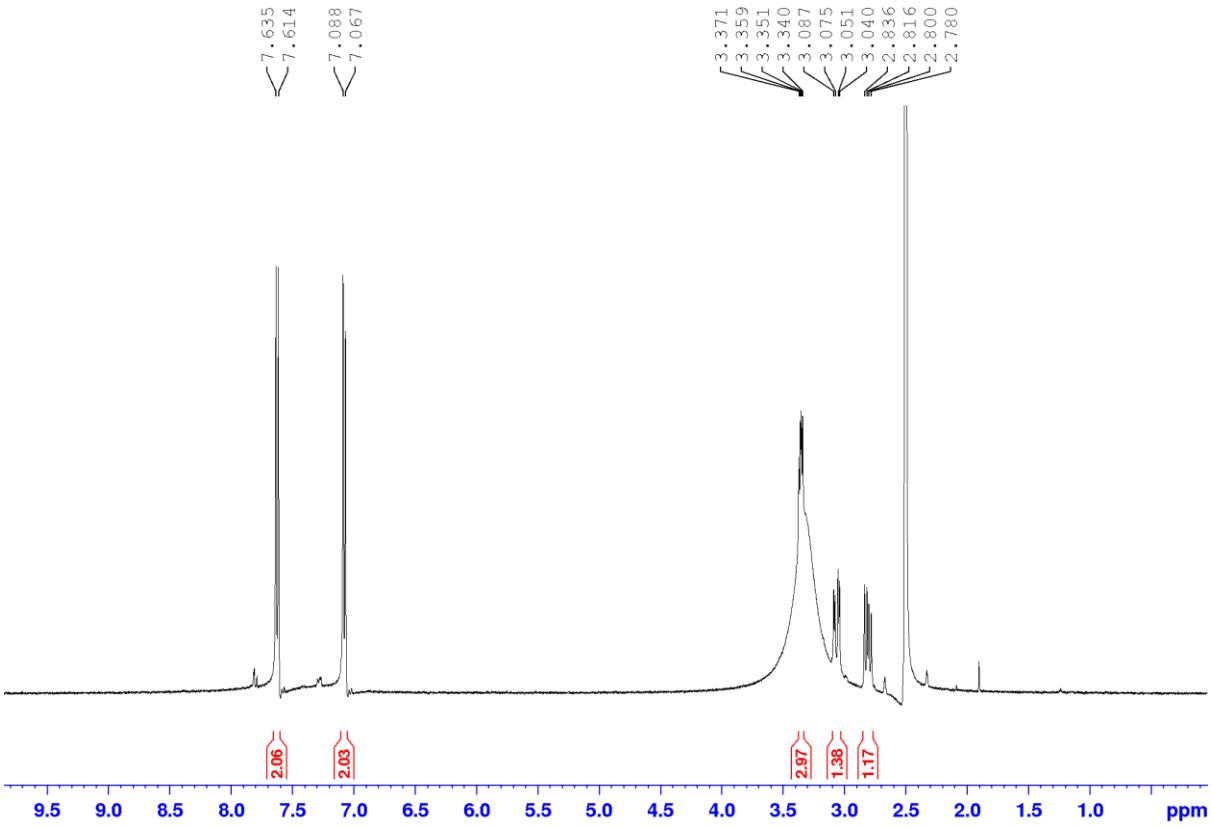

^{13}C NMR spectrum

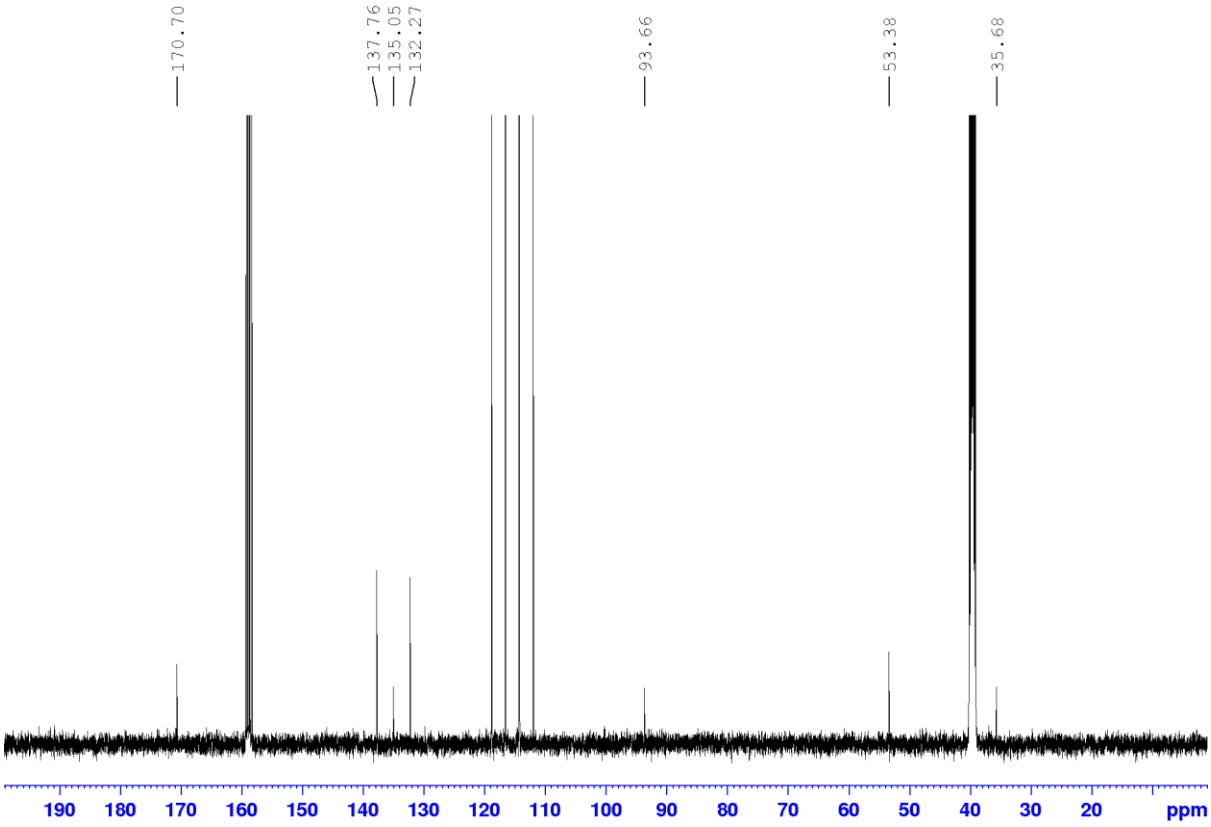

HRMS (ESI) spectrum

Elemental Composition Report **Page 1**

Single Mass Analysis
Tolerance = 5.0 PPM / DBE: min = -1.5, max = 500.0
Element prediction: Off
Number of isotope peaks used for i-FIT = 3

Monoisotopic Mass, Even Electron Ions
50 formula(e) evaluated with 1 results within limits (all results (up to 1000) for each mass)
Elements Used:
C: 5-10 H: 5-10 N: 0-5 O: 0-5 I: 0-1

sd_01_111 35 (1.147) Cm (1:61) TOF MS ES- 2.35e+005

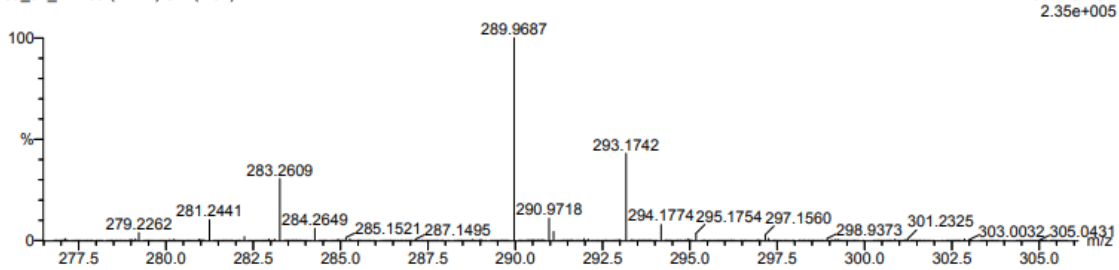

Minimum:				-1.5			
Maximum:		5.0	5.0	500.0			
Mass	Calc. Mass	mDa	PPM	DBE	i-FIT	i-FIT (Norm)	Formula
289.9687	289.9678	0.9	3.1	5.5	435.4	0.0	C9 H9 N O2 I

FTIR spectrum

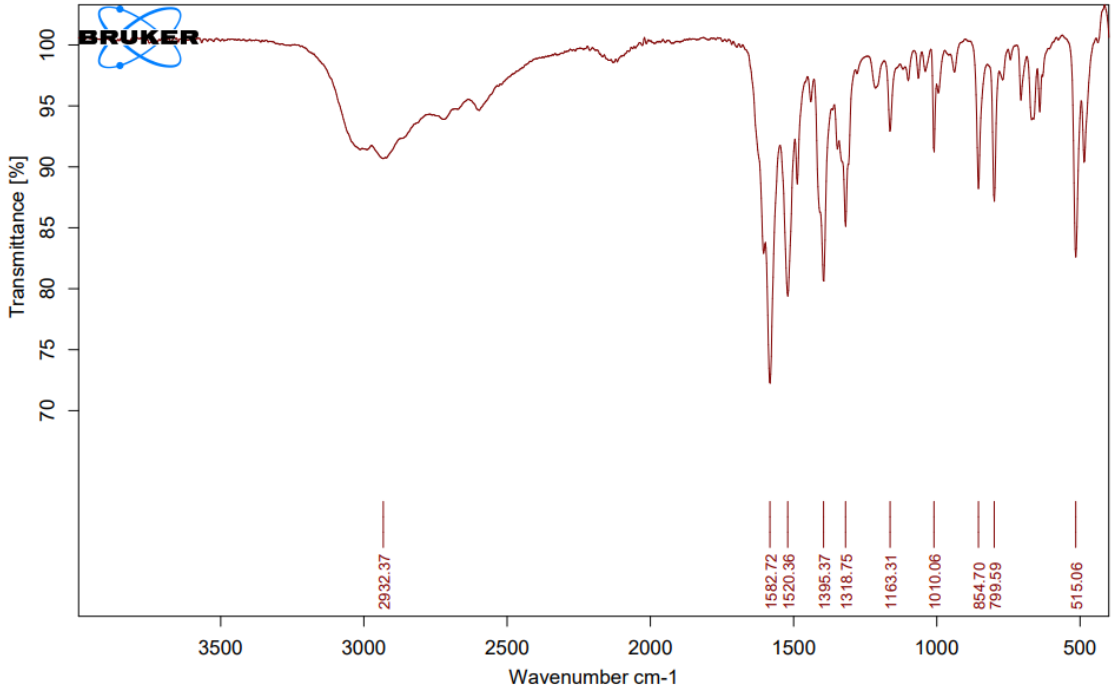

Methyl *L*-tyrosinate (3.3)

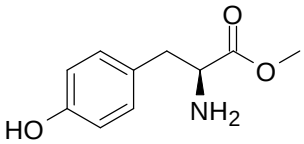

3.3

^{1}H NMR spectrum

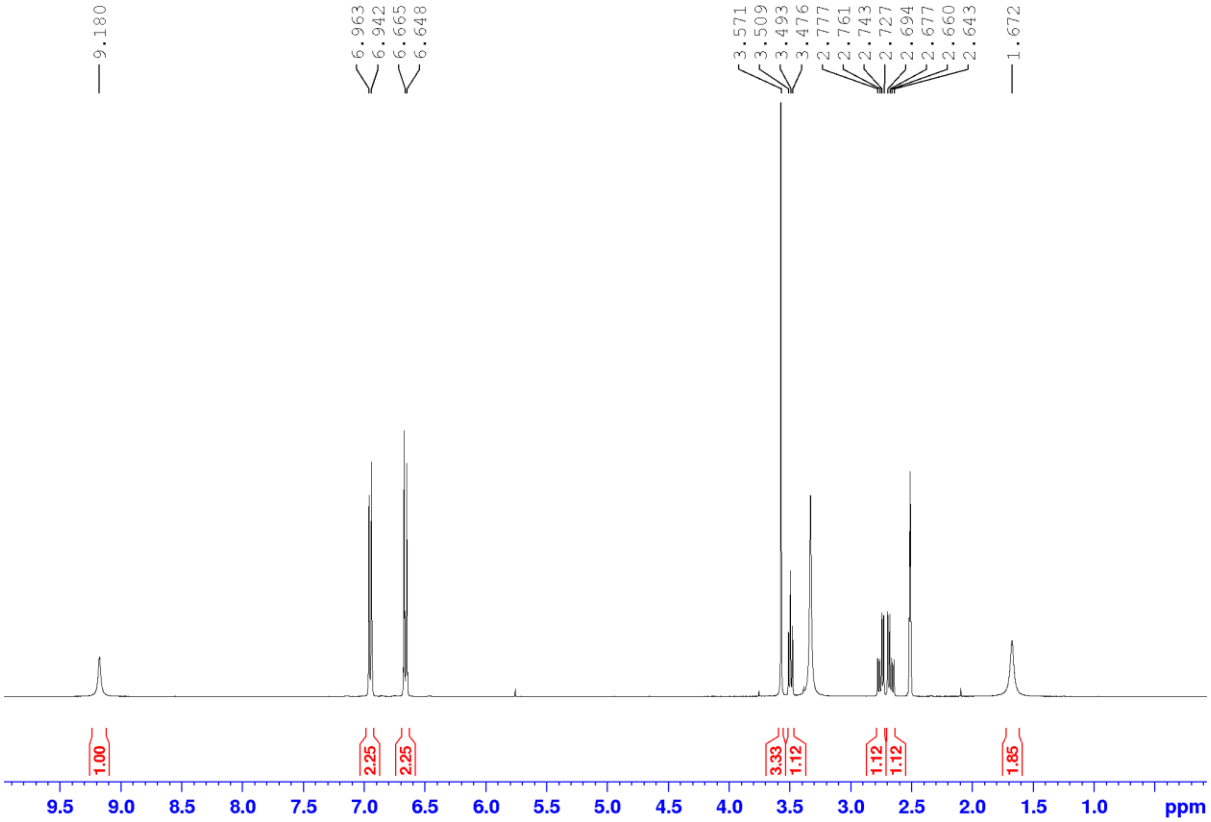

^{13}C NMR spectrum

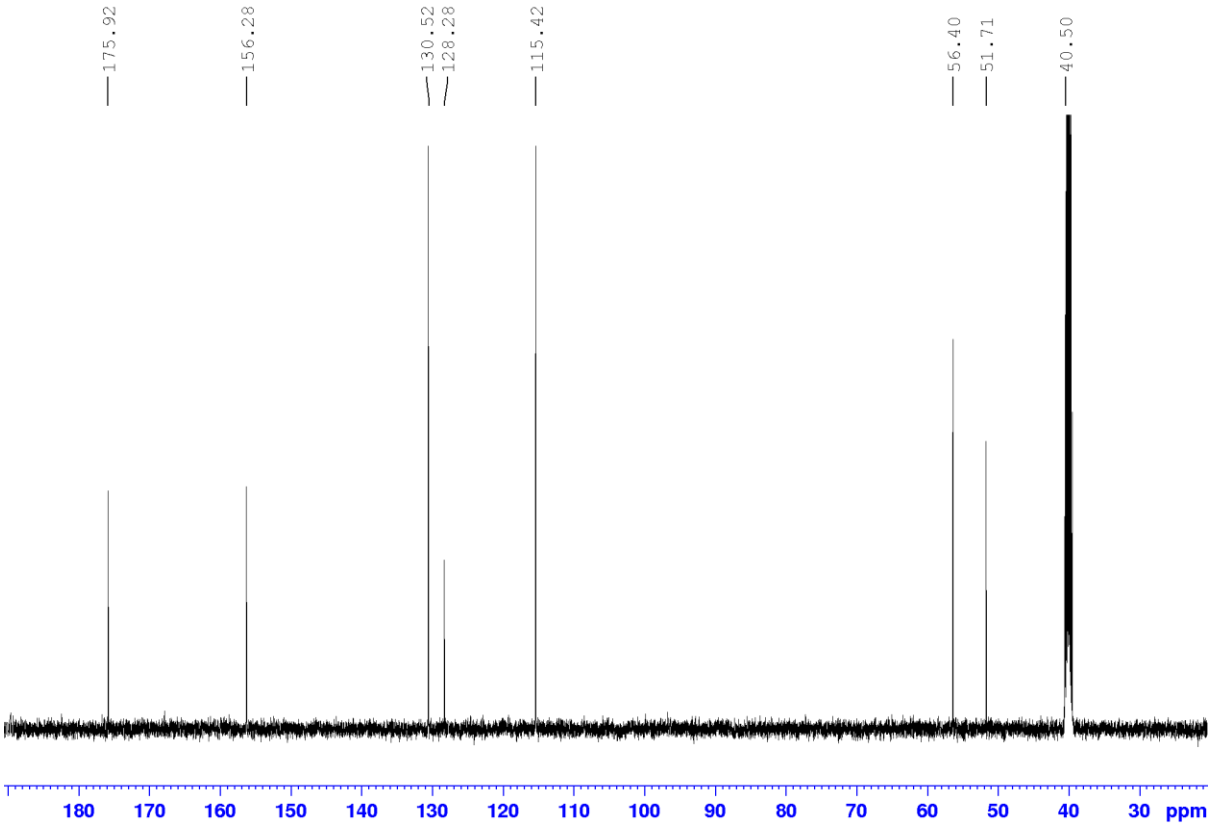

HRMS (ESI) spectrum

Elemental Composition Report **Page 1**

Single Mass Analysis
Tolerance = 5.0 PPM / DBE: min = -1.5, max = 500.0
Element prediction: Off
Number of isotope peaks used for i-FIT = 3

Monoisotopic Mass, Even Electron Ions
18 formula(e) evaluated with 1 results within limits (all results (up to 1000) for each mass)
Elements Used:
C: 5-10 H: 10-15 N: 0-5 O: 0-5
sd_01_038 63 (1.056) Cm (1:119)
TOF MS ES-

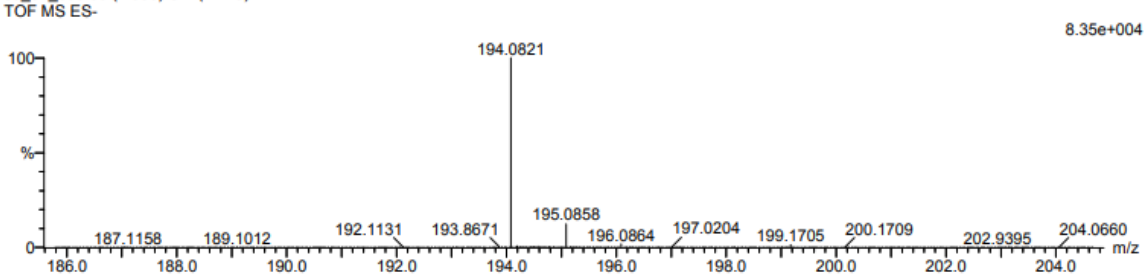

Minimum:				-1.5			
Maximum:		5.0	5.0	500.0			
Mass	Calc. Mass	mDa	PPM	DBE	i-FIT	i-FIT (Norm)	Formula
194.0821	194.0817	0.4	2.1	5.5	536.3	0.0	C10 H12 N O3

FTIR spectrum

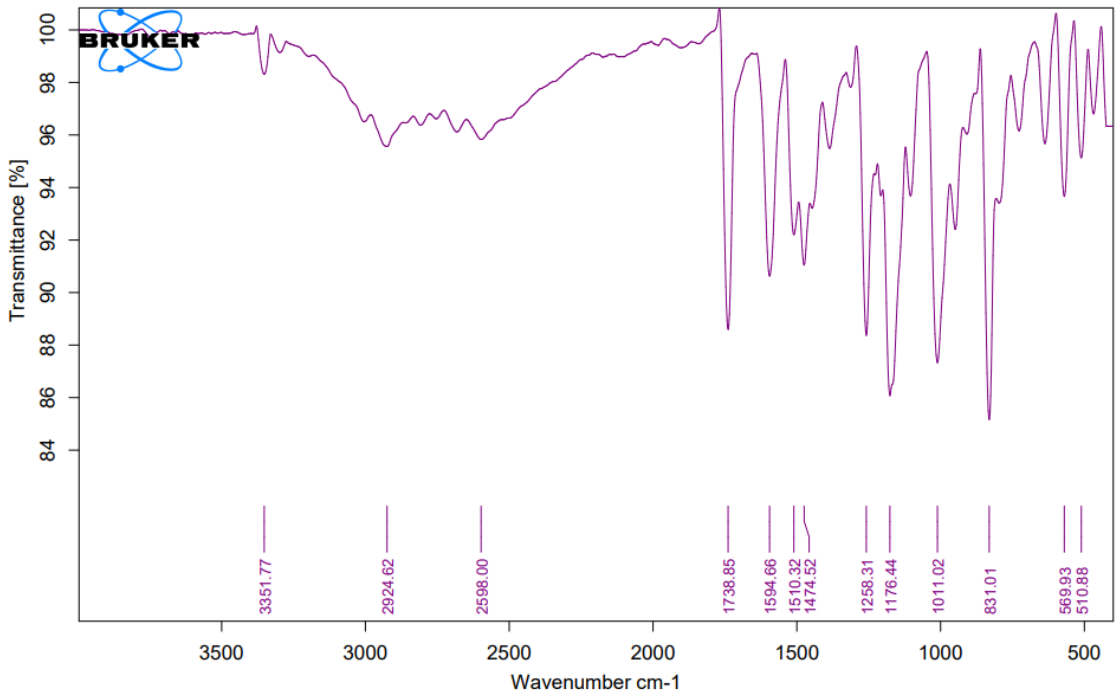

Methyl (*S*)-2-amino-2-(4-hydroxyphenyl)acetate (3.7)

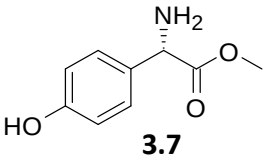

3.7

^{1}H NMR spectrum

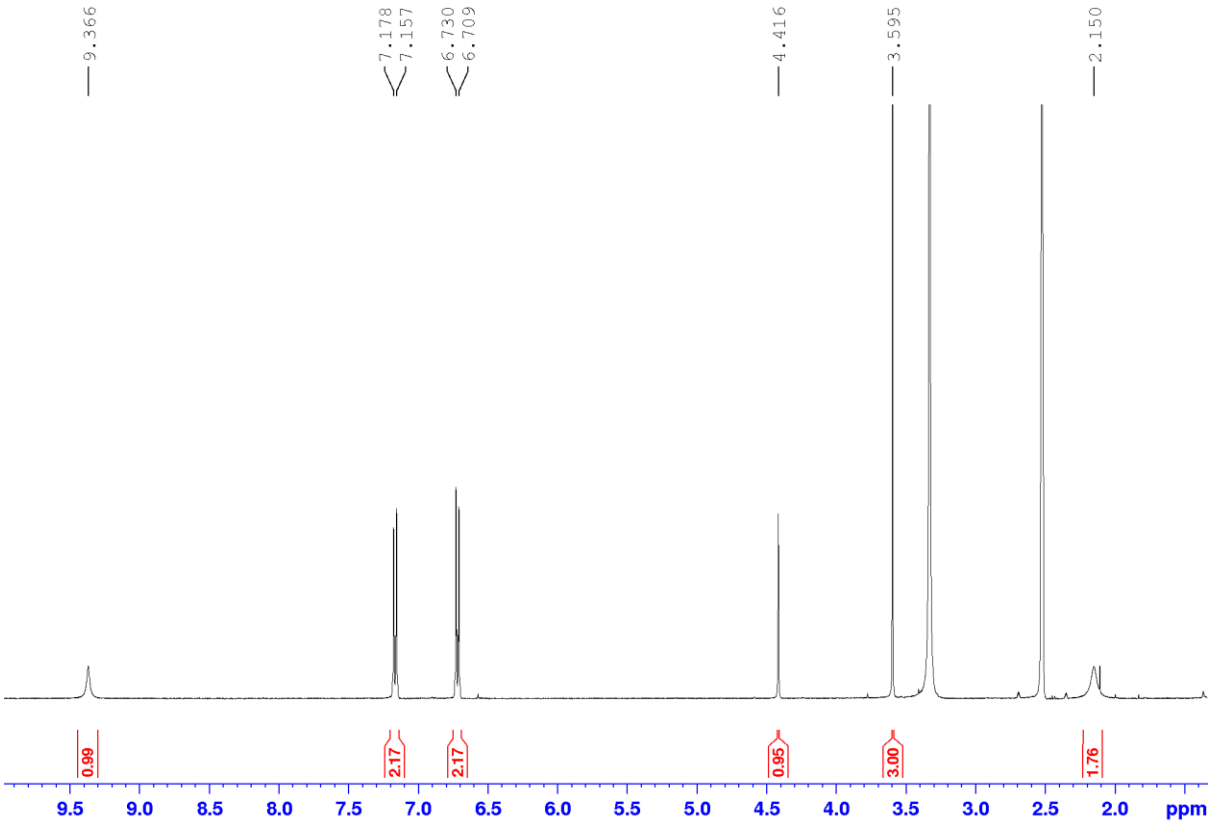

^{13}C NMR spectrum

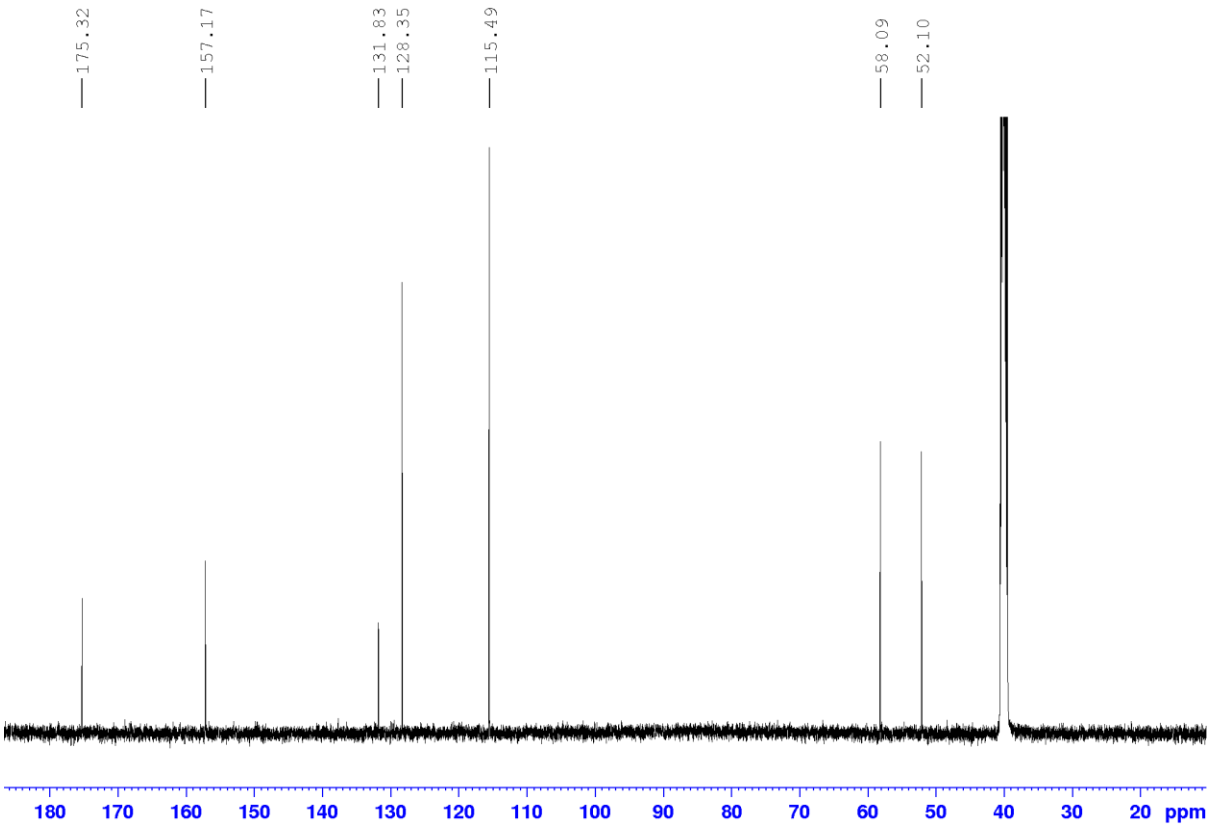

HRMS (ESI) spectrum

Elemental Composition Report **Page 1**

Single Mass Analysis
Tolerance = 5.0 PPM / DBE: min = -1.5, max = 500.0
Element prediction: Off
Number of isotope peaks used for i-FIT = 3

Monoisotopic Mass, Even Electron Ions
18 formula(e) evaluated with 1 results within limits (all results (up to 1000) for each mass)
Elements Used:
C: 5-10 H: 10-15 N: 0-5 O: 0-5
sd-073 30 (0.978) Cm (1:61)

TOF MS ES-
4.30e+004

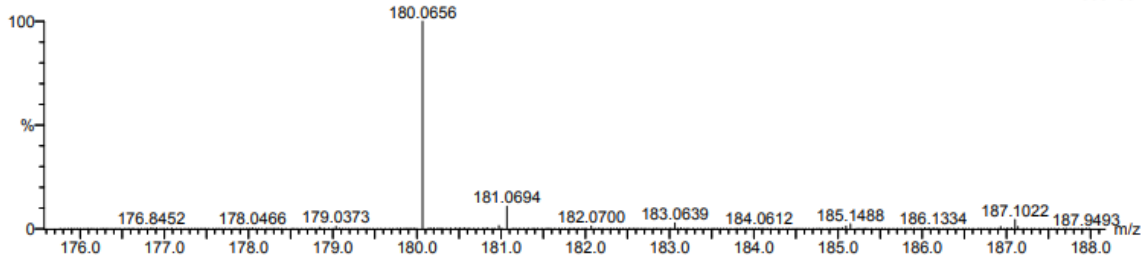

Minimum:				-1.5			
Maximum:		5.0	5.0	500.0			
Mass	Calc. Mass	mDa	PPM	DBE	i-FIT	i-FIT (Norm)	Formula
180.0656	180.0661	-0.5	-2.8	5.5	401.9	0.0	C9 H10 N O3

FTIR spectrum

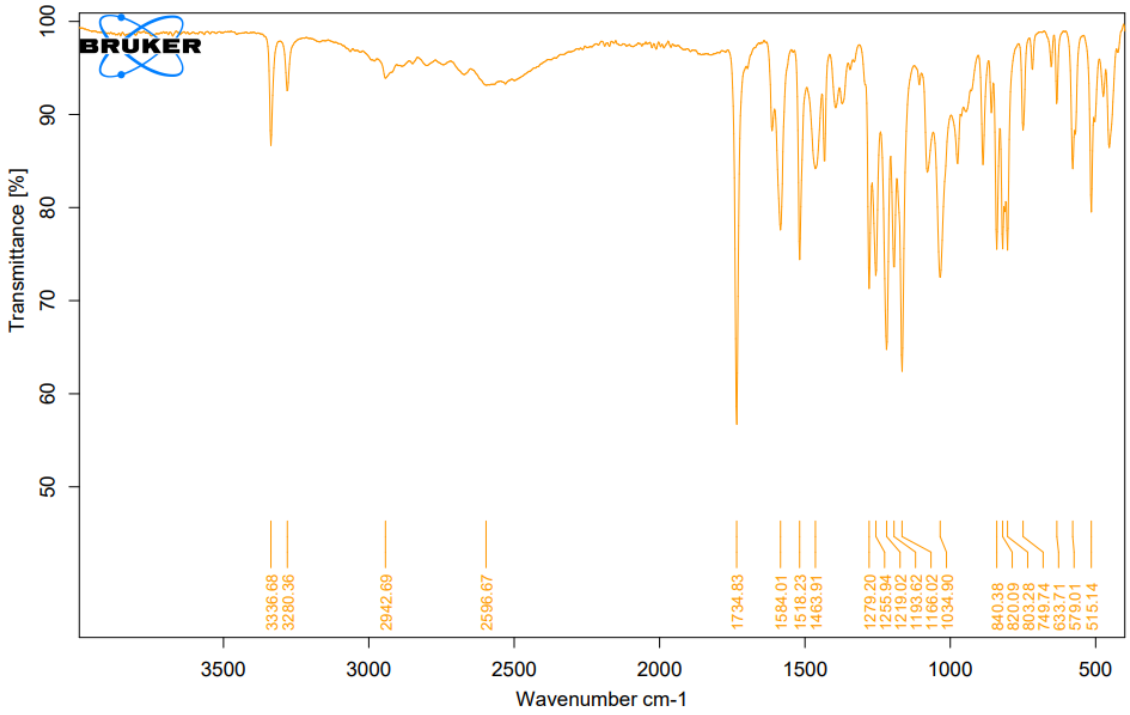

Methyl (S)-2-amino-3-(4-chlorophenyl)propanoate (3.20)

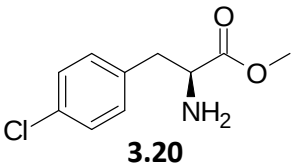

3.20

^{1}H NMR spectrum

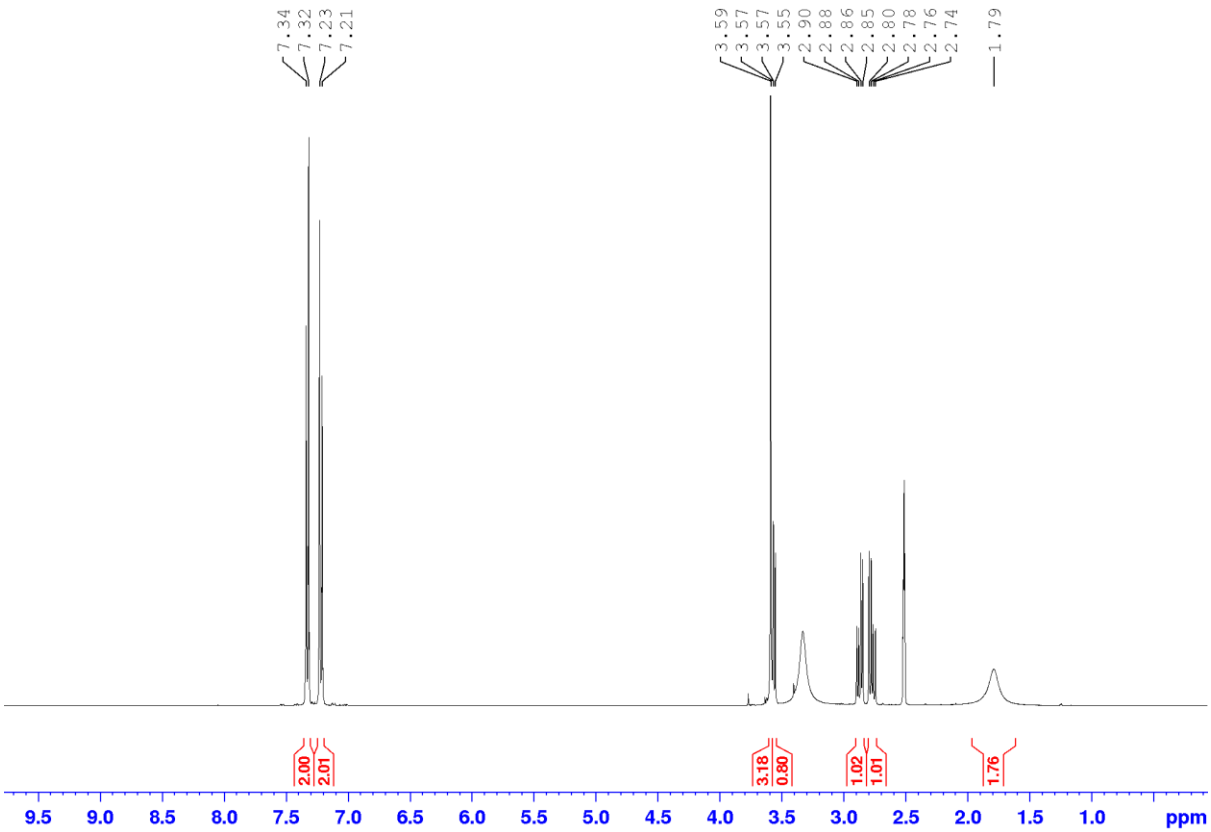

^{13}C NMR spectrum

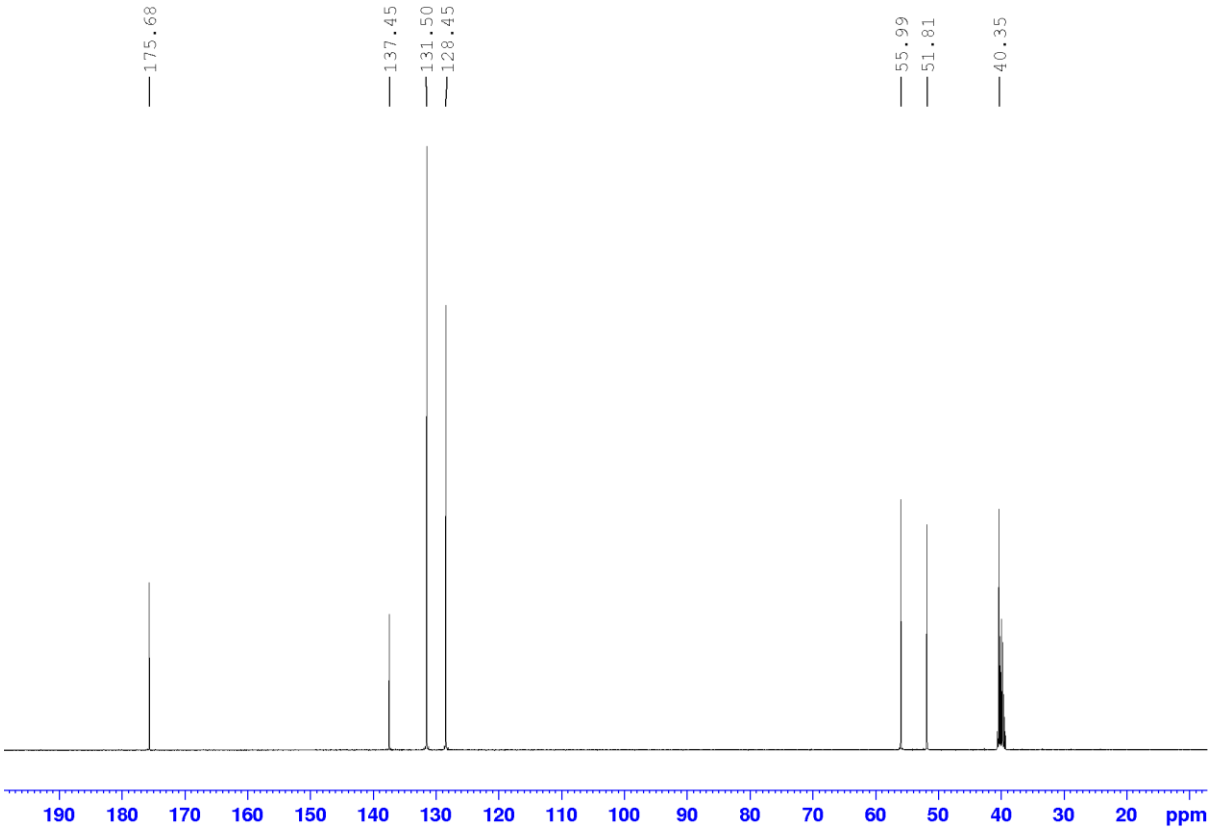

HRMS (ESI) spectrum

Elemental Composition Report **Page 1**

Single Mass Analysis
Tolerance = 5.0 PPM / DBE: min = -1.5, max = 500.0
Element prediction: Off
Number of isotope peaks used for i-FIT = 3

Monoisotopic Mass, Even Electron Ions
46 formula(e) evaluated with 1 results within limits (all results (up to 1000) for each mass)
Elements Used:
C: 10-15 H: 10-15 N: 0-5 O: 0-5 Cl: 0-1 Na: 1-1

sd_01_15 57 (1.888) Cm (1:61) TOF MS ES+ 1.51e+005

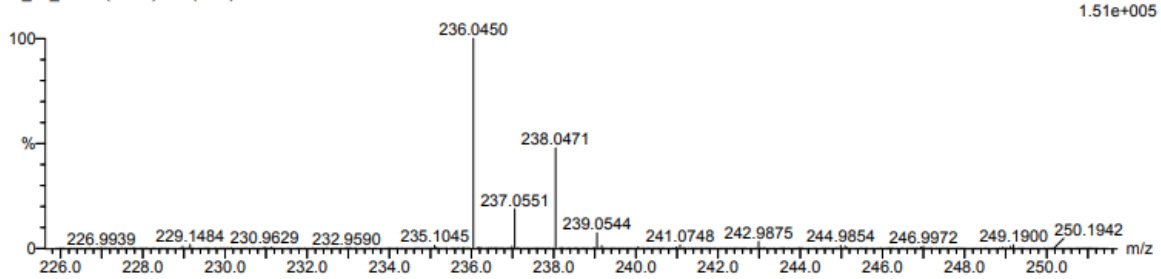

Minimum:				-1.5								
Maximum:		5.0	5.0	500.0								
Mass	Calc. Mass	mDa	PPM	DBE	i-FIT	i-FIT (Norm)	Formula					
236.0450	236.0454	-0.4	-1.7	4.5	627.6	0.0	C10	H12	N	O2	Cl	Na

FTIR spectrum

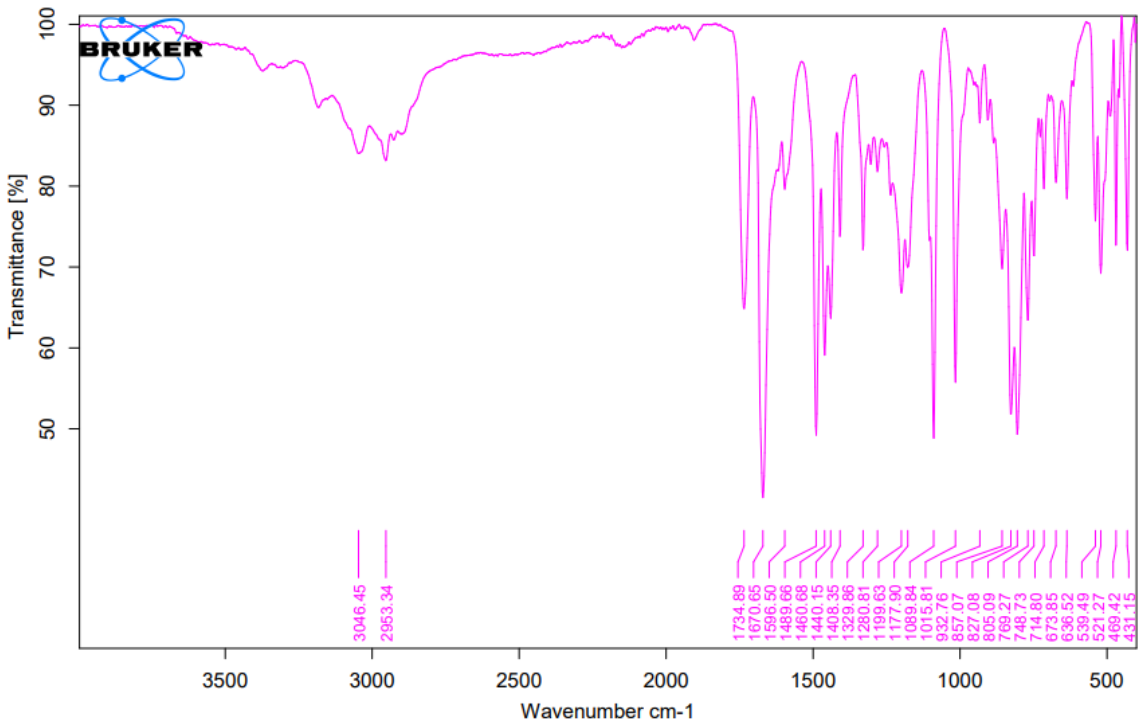

Methyl (*S*)-2-amino-2-(4-chlorophenyl)acetate (3.24)

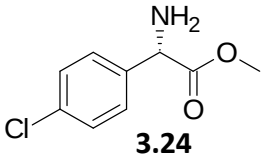

3.24

^{1}H NMR spectrum

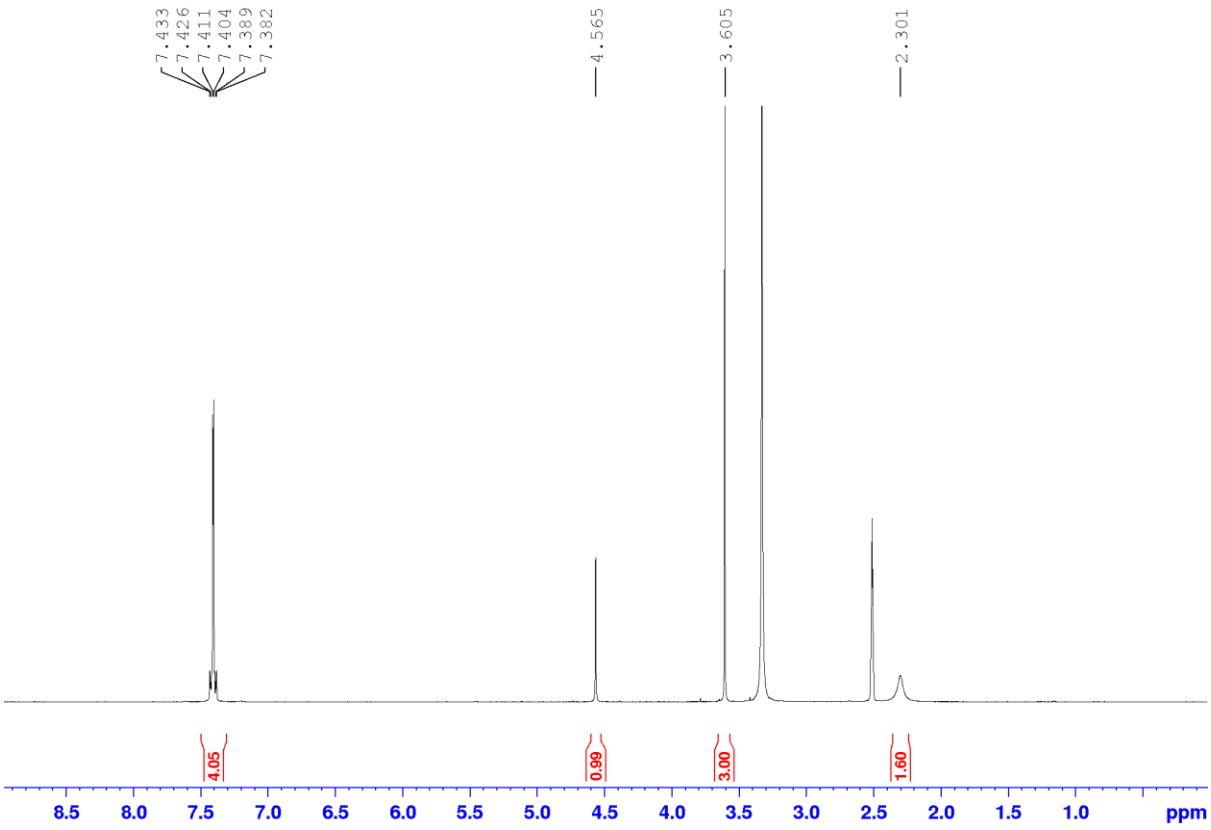

^{13}C NMR spectrum

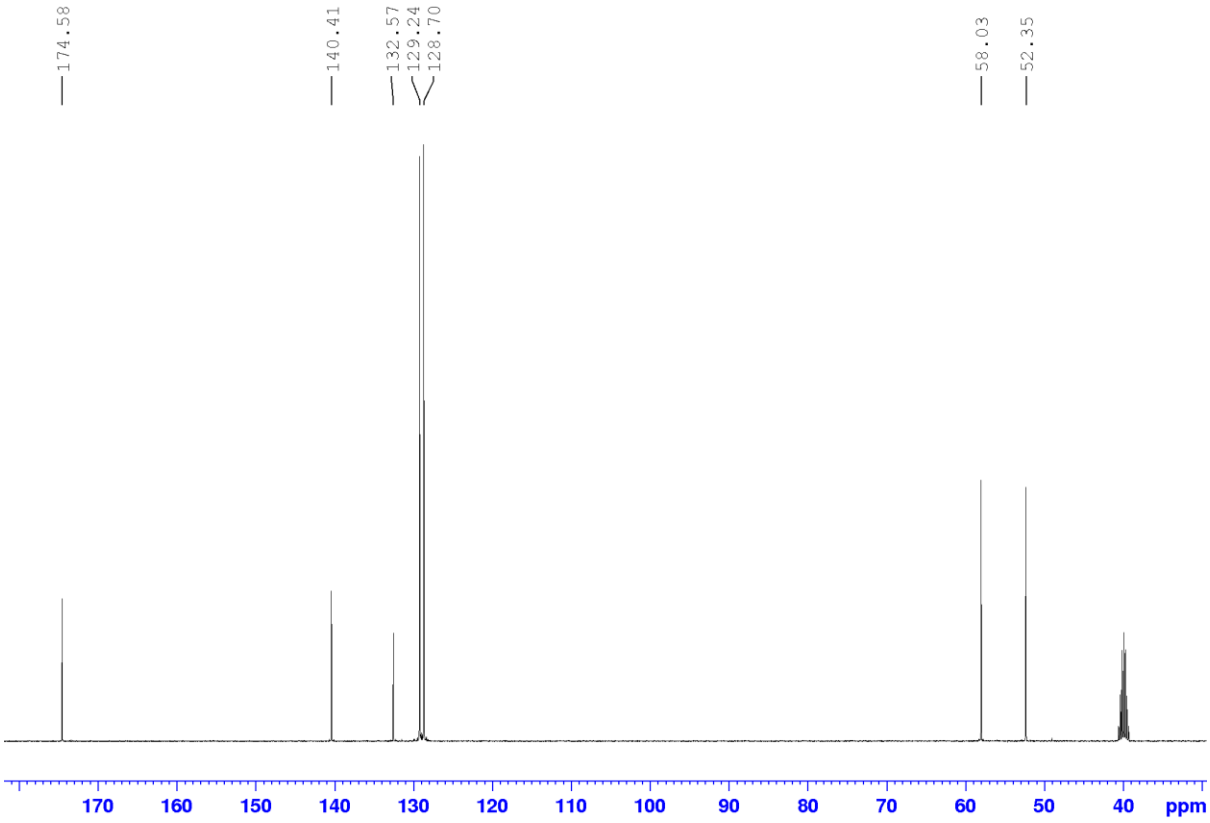

HRMS (ESI) spectrum

Elemental Composition Report **Page 1**

Single Mass Analysis
Tolerance = 5.0 PPM / DBE: min = -1.5, max = 500.0
Element prediction: Off
Number of isotope peaks used for i-FIT = 3

Monoisotopic Mass, Even Electron Ions
36 formula(e) evaluated with 1 results within limits (all results (up to 1000) for each mass)
Elements Used:
C: 5-10 H: 10-15 N: 0-5 O: 0-5 Na: 1-1 Cl: 0-1
sd_01_158 58 (1.921) Cm (1:61)

TOF MS ES+
1.56e+005

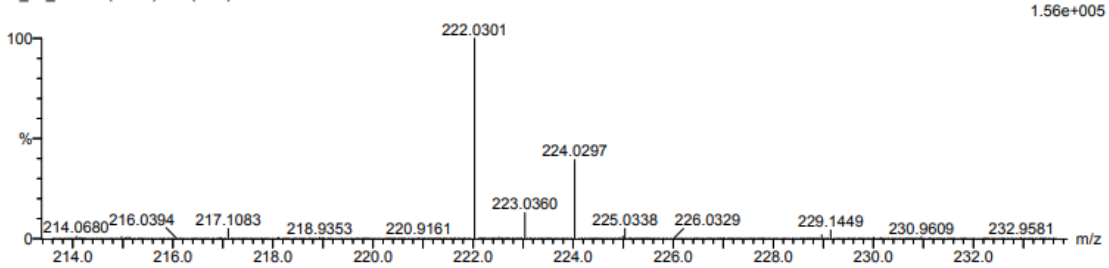

Minimum:				-1.5			
Maximum:		5.0	5.0	500.0			
Mass	Calc. Mass	mDa	PPM	DBE	i-FIT	i-FIT (Norm)	Formula
222.0301	222.0298	0.3	1.4	4.5	618.3	0.0	C9 H10 N O2 Na Cl

FTIR spectrum

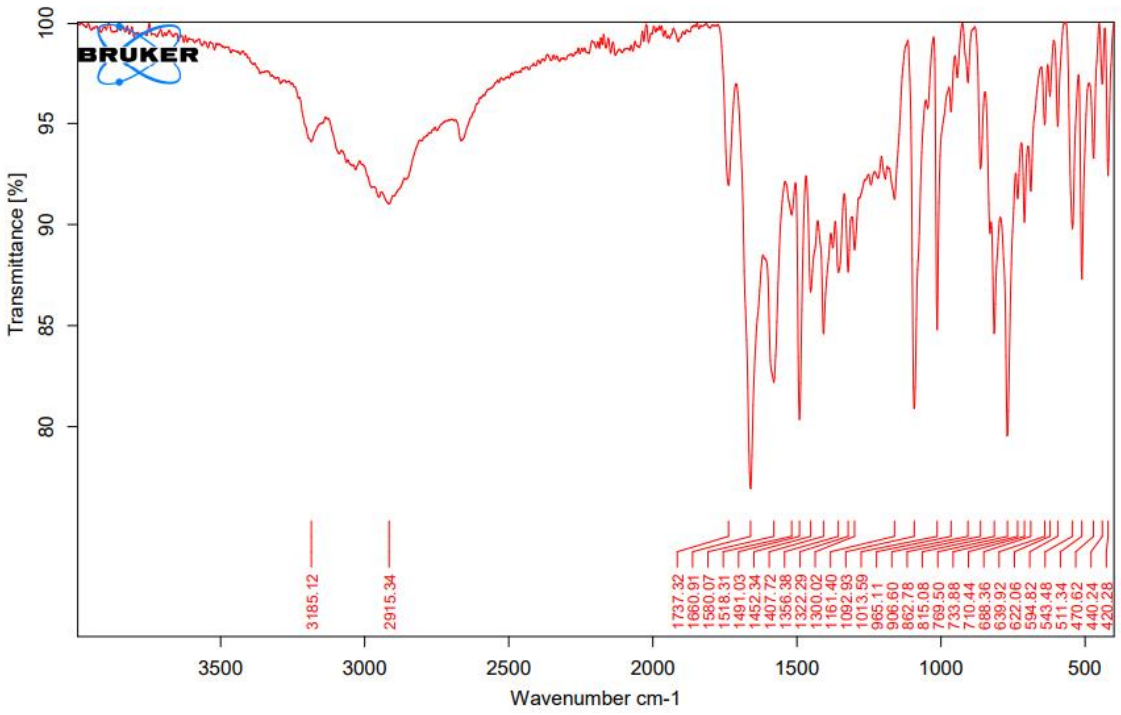

Methyl (*S*)-2-amino-3-(4-fluorophenyl)propanoate (3.28)

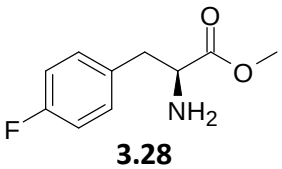

3.28

^{1}H NMR spectrum

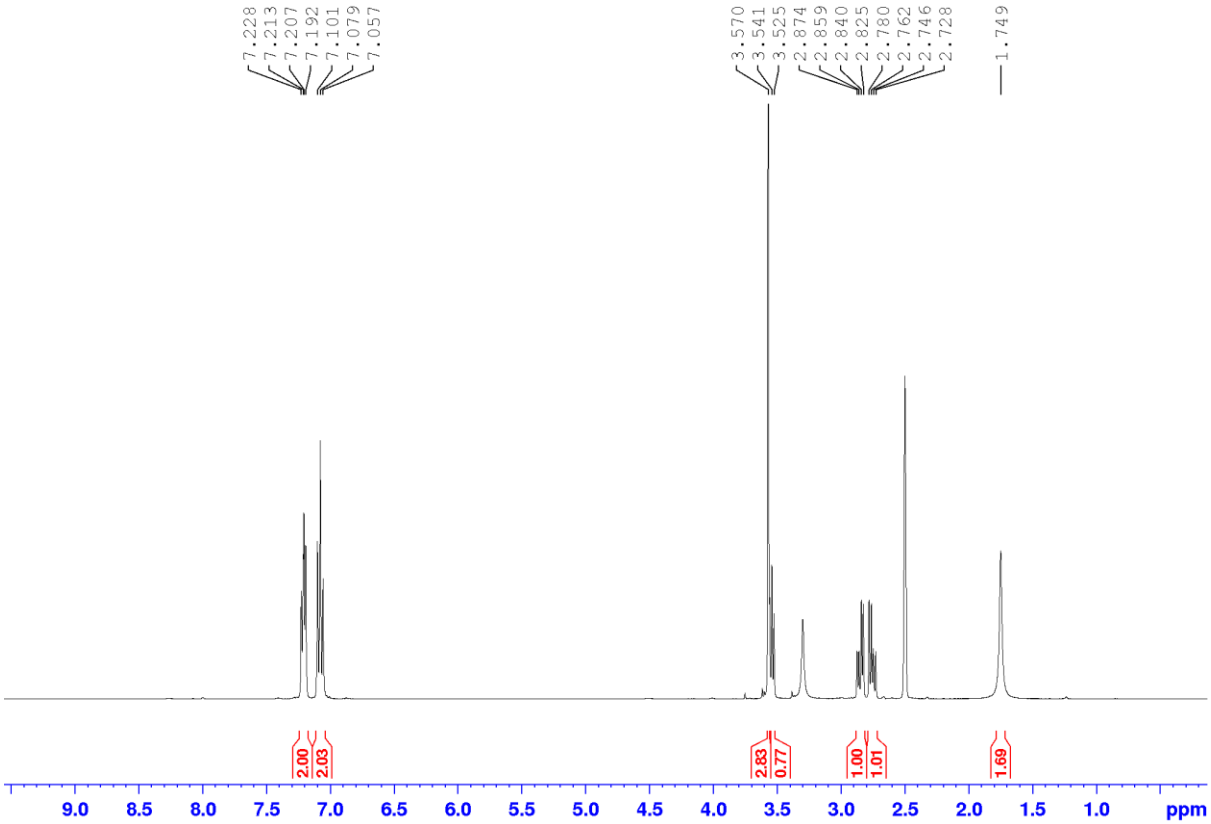

^{13}C NMR spectrum

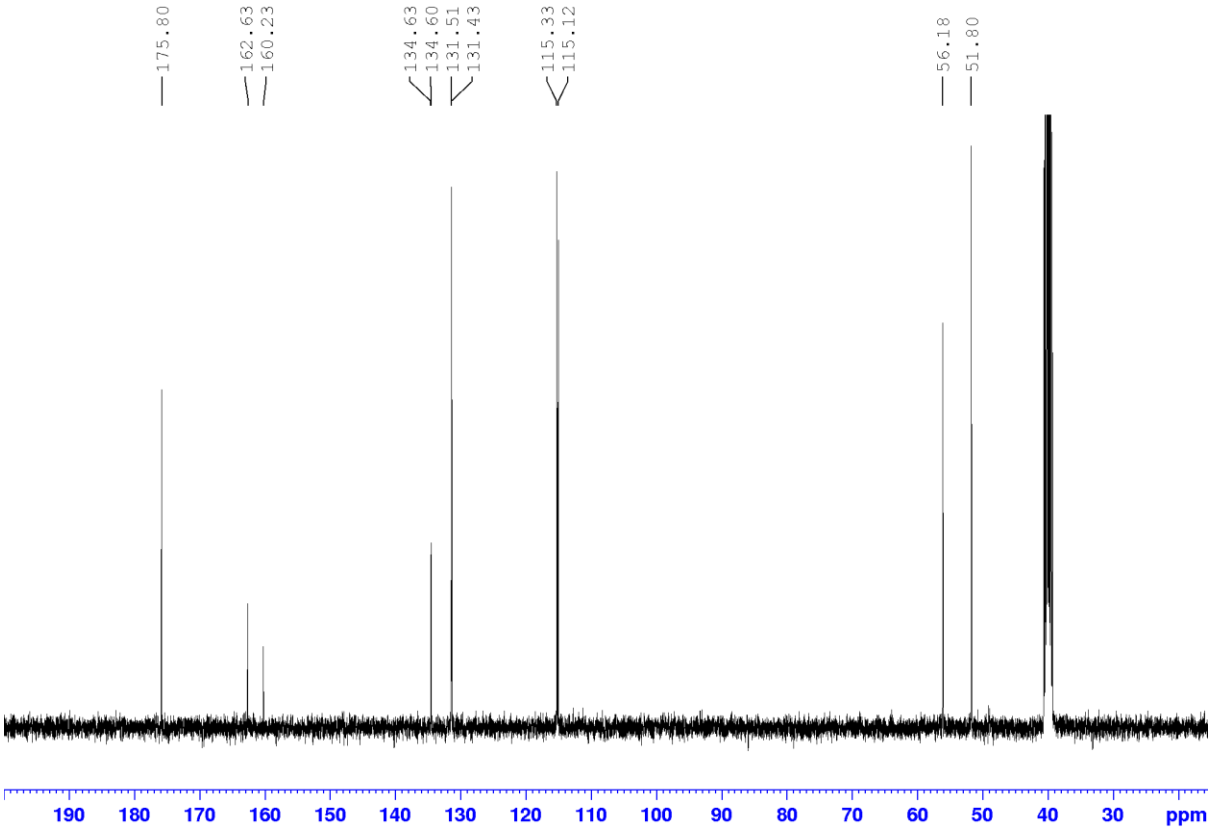

HRMS (ESI) spectrum

Elemental Composition Report **Page 1**

Single Mass Analysis
Tolerance = 5.0 PPM / DBE: min = -1.5, max = 500.0
Element prediction: Off
Number of isotope peaks used for i-FIT = 3

Monoisotopic Mass, Even Electron Ions
48 formula(e) evaluated with 1 results within limits (all results (up to 1000) for each mass)
Elements Used:
C: 10-15 H: 10-15 N: 0-5 O: 0-5 F: 0-1 Na: 1-1

sd_01_121 19 (0.607) Cm (1:61) TOF MS ES+ 1.26e+006

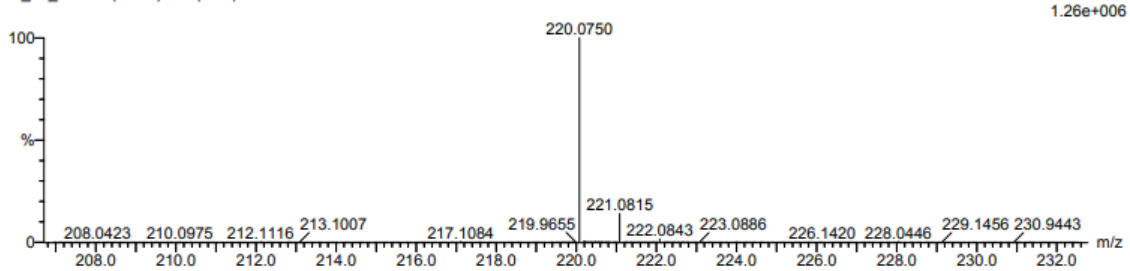

Minimum:				-1.5			
Maximum:		5.0	5.0	500.0			
Mass	Calc. Mass	mDa	PPM	DBE	i-FIT	i-FIT (Norm)	Formula
220.0750	220.0750	0.0	0.0	4.5	843.0	0.0	C10 H12 N O2 F Na

FTIR Spectrum

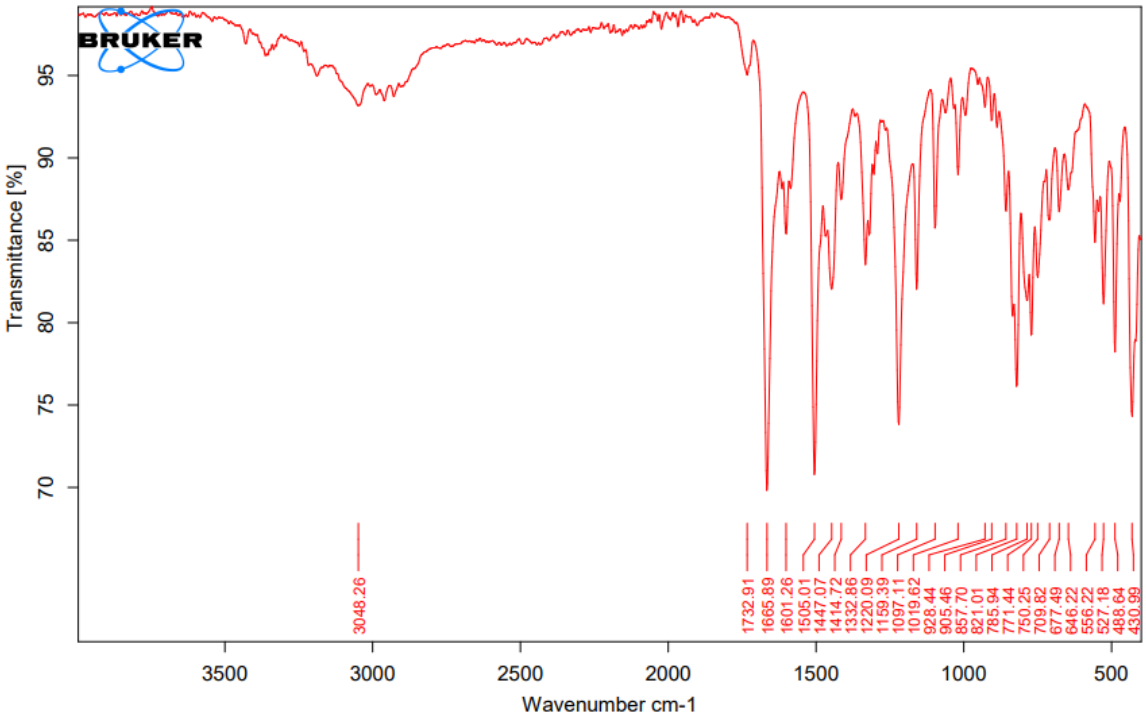

Methyl (*S*)-2-amino-3-(4-iodophenyl)propanoate (3.33)

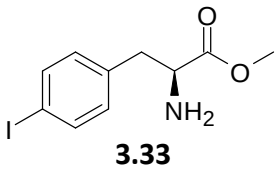

3.33

^{1}H NMR spectrum

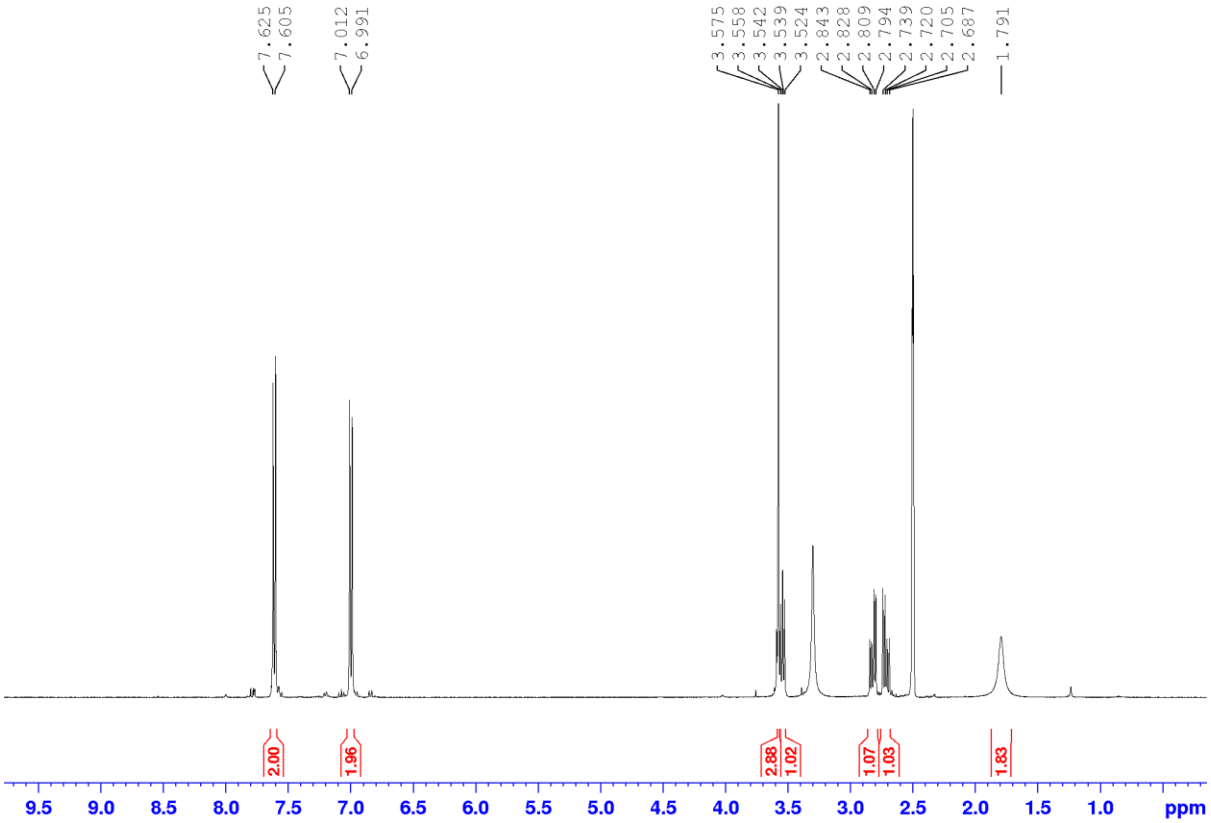

^{13}C NMR spectrum

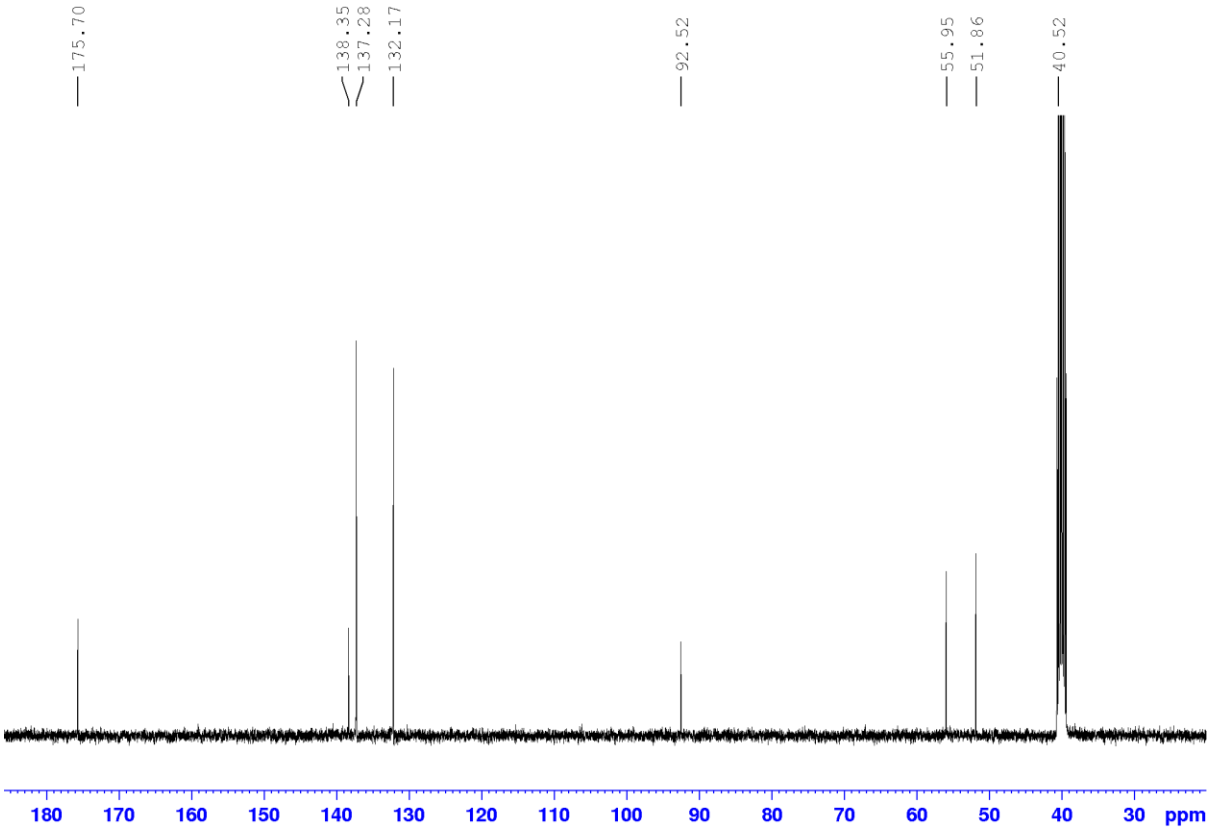

HRMS (ESI) spectrum

Elemental Composition Report **Page 1**

Single Mass Analysis
Tolerance = 50.0 PPM / DBE: min = -1.5, max = 500.0
Element prediction: Off
Number of isotope peaks used for i-FIT = 3

Monoisotopic Mass, Even Electron Ions
48 formula(e) evaluated with 1 results within limits (all results (up to 1000) for each mass)
Elements Used:
C: 10-15 H: 10-15 N: 0-5 O: 0-5 I: 0-1

sd_01_120 2 (0.034) Cm (1:61) TOF MS ES+ 2.48e+006

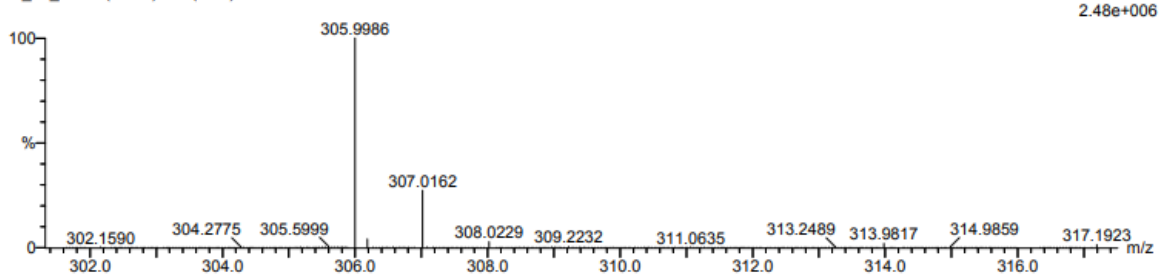

Minimum:				-1.5			
Maximum:		5.0	50.0	500.0			
Mass	Calc. Mass	mDa	PPM	DBE	i-FIT	i-FIT (Norm)	Formula
305.9986	305.9991	-0.5	-1.6	4.5	650.1	0.0	C10 H13 N O2 I

FTIR Spectrum

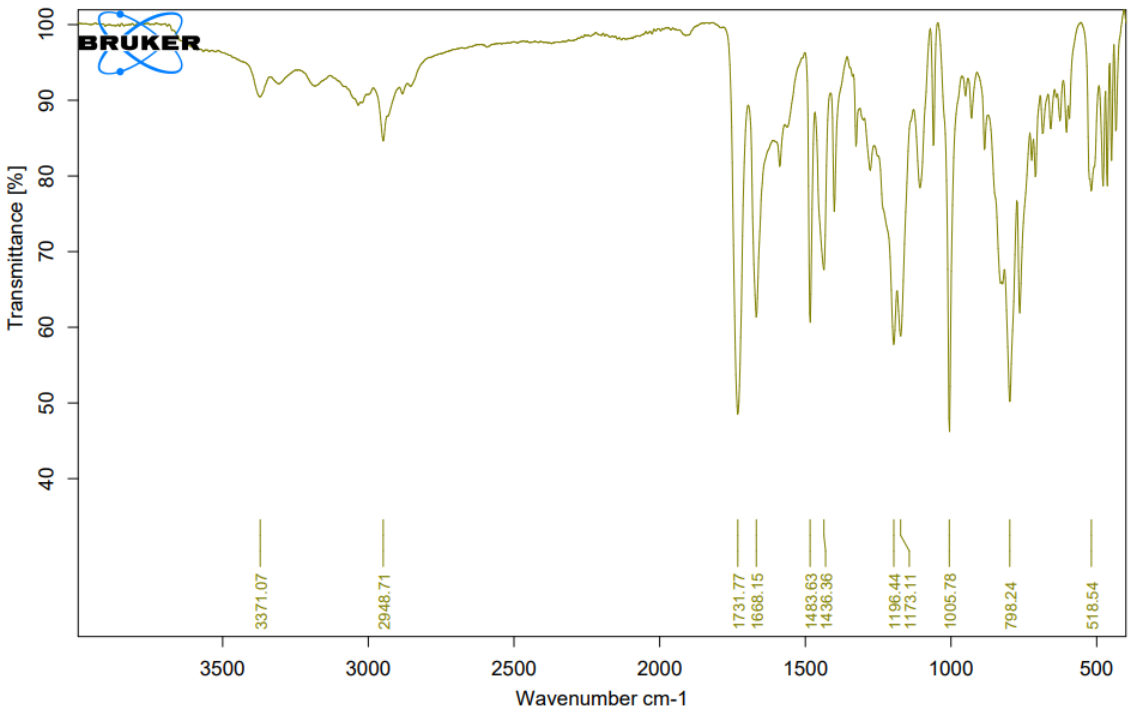

Methyl (*tert*-butoxycarbonyl)-*L*-tyrosinate (3.4)

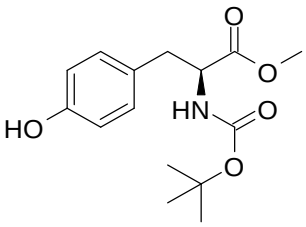

3.4

^{1}H NMR spectrum

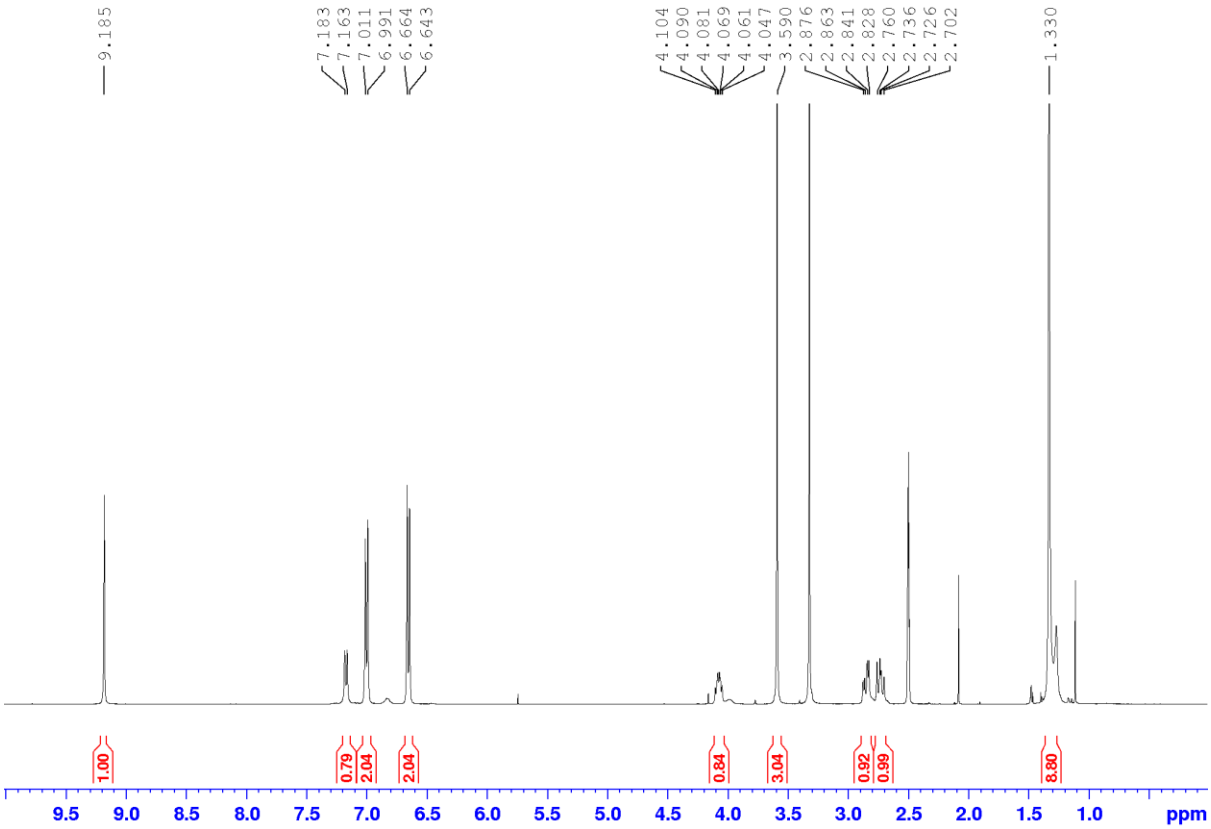

^{13}C NMR spectrum

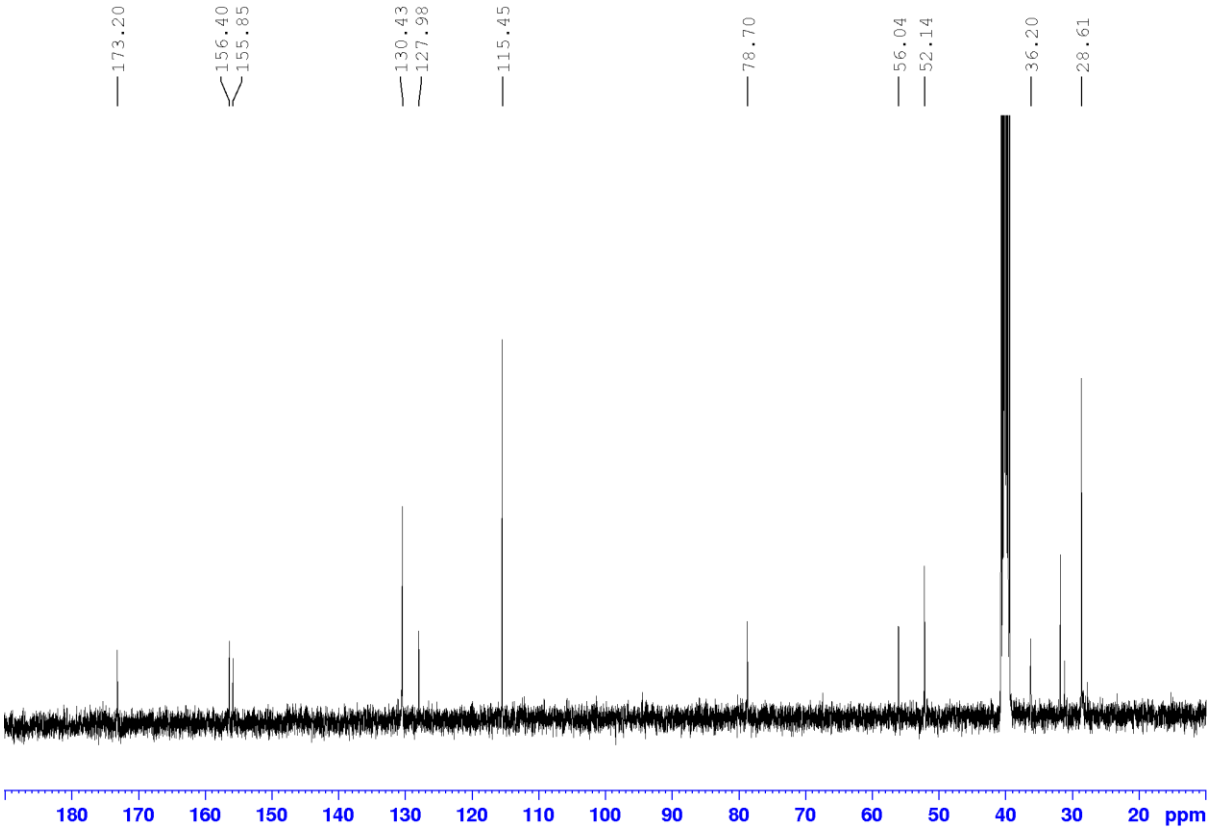

HRMS (ESI) spectrum

Elemental Composition Report **Page 1**

Single Mass Analysis
Tolerance = 5.0 PPM / DBE: min = -1.5, max = 500.0
Element prediction: Off
Number of isotope peaks used for i-FIT = 3

Monoisotopic Mass, Even Electron Ions
19 formula(e) evaluated with 1 results within limits (all results (up to 1000) for each mass)
Elements Used:
C: 10-15 H: 20-25 N: 0-5 O: 0-5
sd-071 61 (2.023) Cm (1:61)

TOF MS ES-
1.31e+005

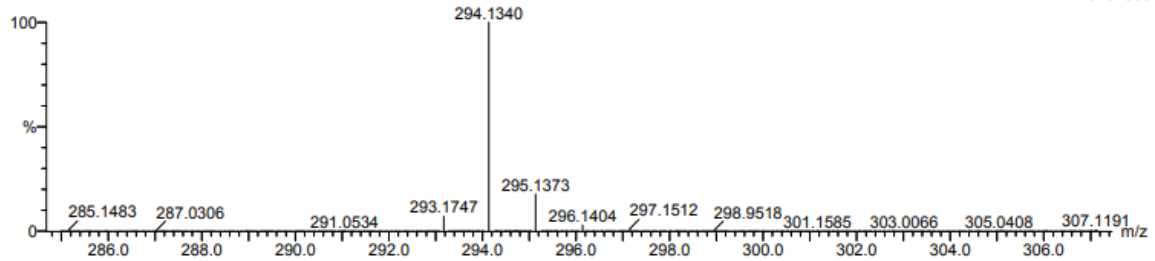

Minimum:				-1.5			
Maximum:		5.0	5.0	500.0			
Mass	Calc. Mass	mDa	PPM	DBE	i-FIT	i-FIT (Norm)	Formula
294.1340	294.1341	-0.1	-0.3	6.5	445.8	0.0	C15 H20 N O5

FTIR spectrum

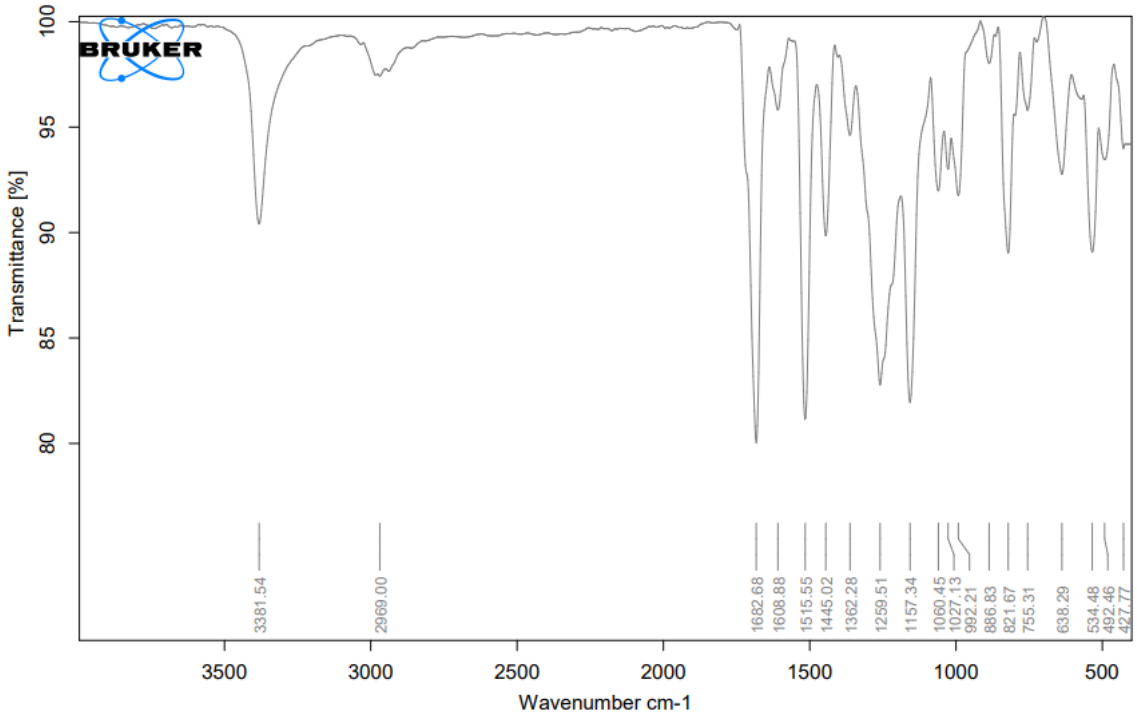

Methyl (*S*)-2-((*tert*-butoxycarbonyl)amino)-2-(4-hydroxyphenyl)aceatate (3.8)

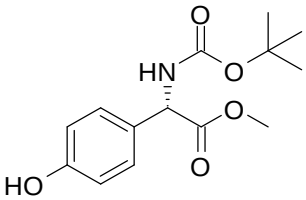

3.8

^{1}H NMR spectrum

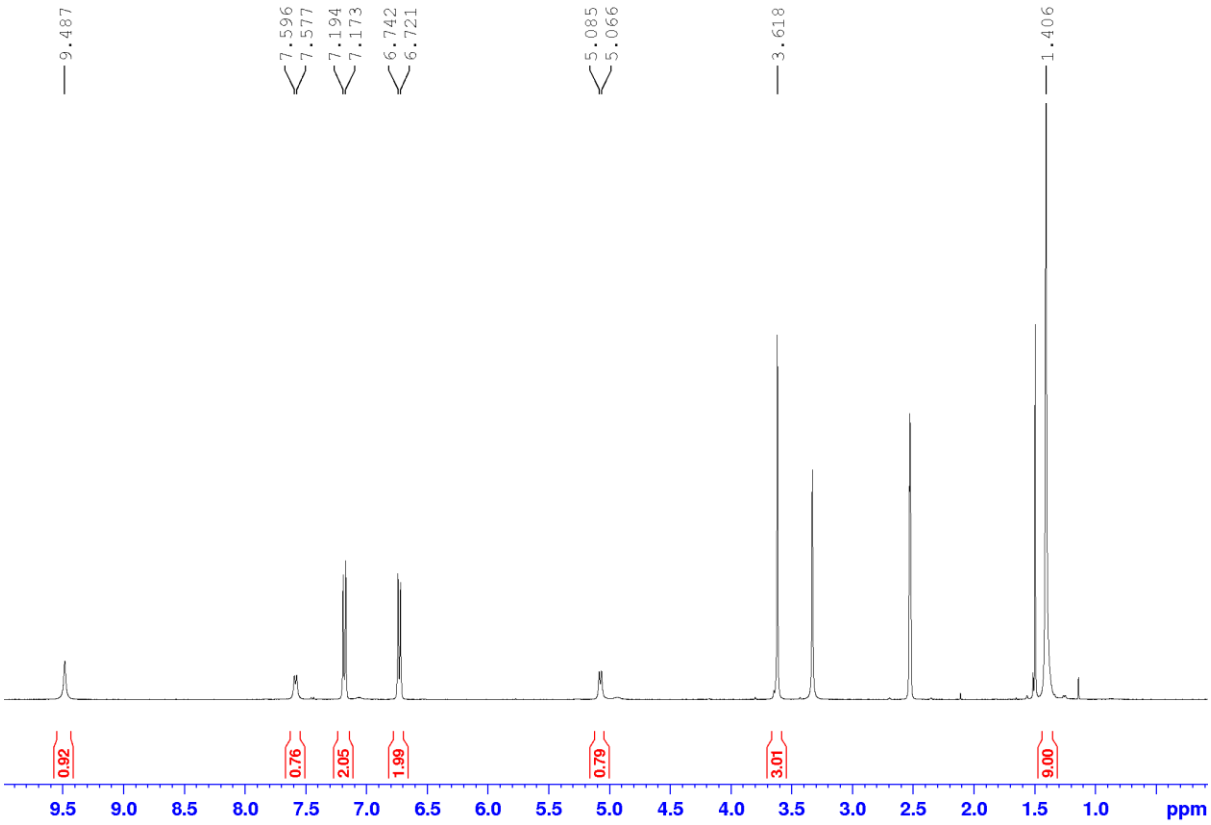

^{13}C NMR spectrum

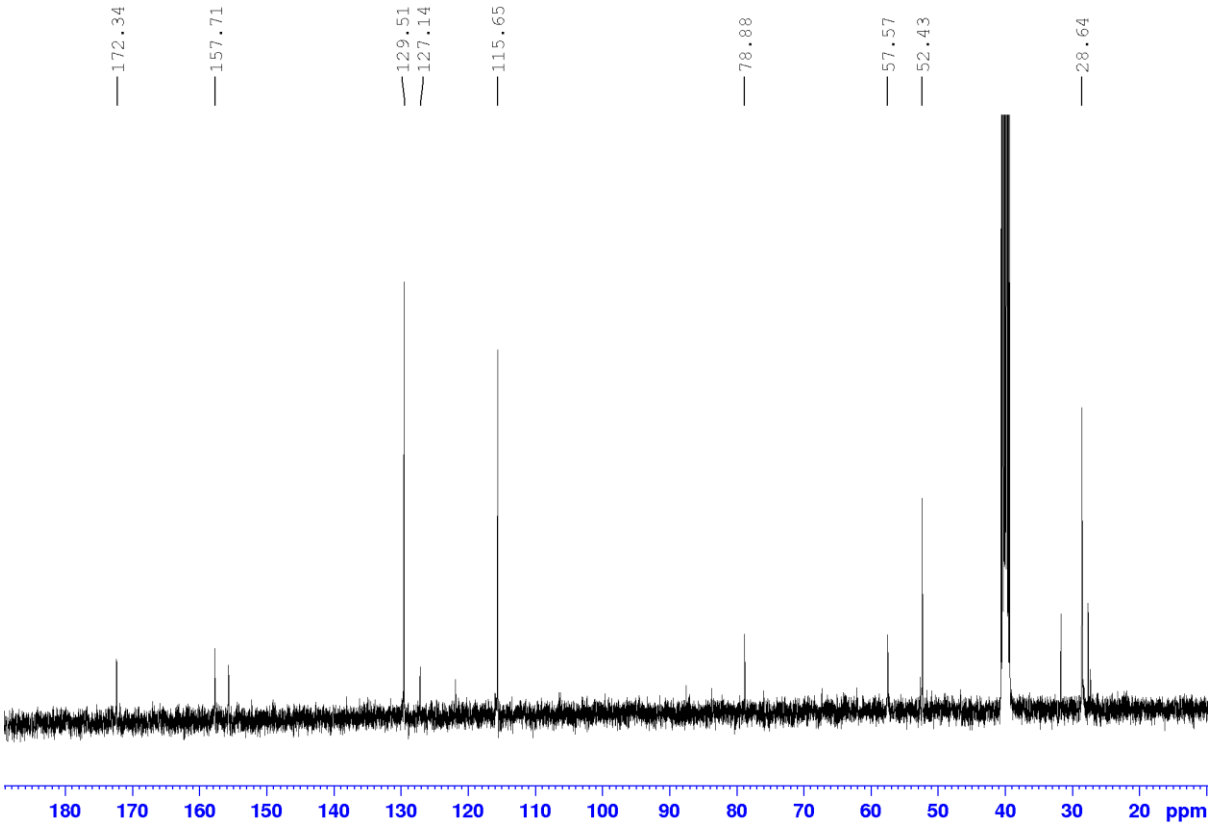

HRMS (ESI) spectrum

Elemental Composition Report **Page 1**

Single Mass Analysis
Tolerance = 5.0 PPM / DBE: min = -1.5, max = 500.0
Element prediction: Off
Number of isotope peaks used for i-FIT = 3

Monoisotopic Mass, Even Electron Ions
18 formula(e) evaluated with 1 results within limits (all results (up to 1000) for each mass)
Elements Used:
C: 10-15 H: 15-20 N: 0-5 O: 0-5 Na: 1-1
sd_01_114 54 (1.787) Cm (1:61)

TOF MS ES+
5.46e+005

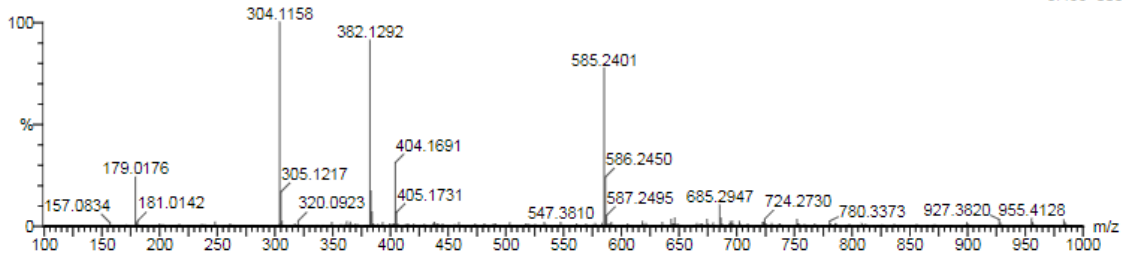

Minimum:				-1.5			
Maximum:		5.0	5.0	500.0			
Mass	Calc. Mass	mDa	PPM	DBE	i-FIT	i-FIT (Norm)	Formula
304.1158	304.1161	-0.3	-1.0	5.5	539.2	0.0	C14 H19 N O5 Na

FTIR spectrum

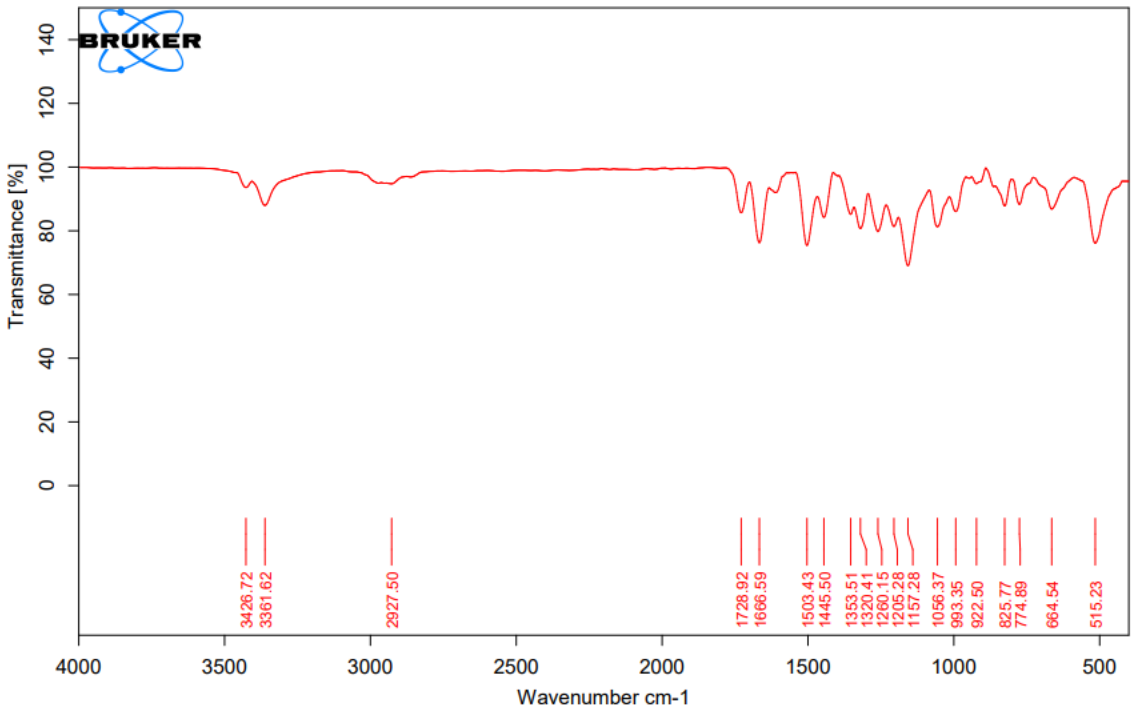

(*Tert*-butoxycarbonyl)-*L*-serine (3.12)

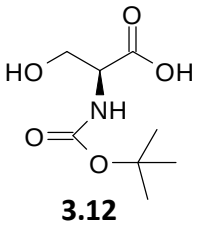

3.12

^{1}H NMR spectrum

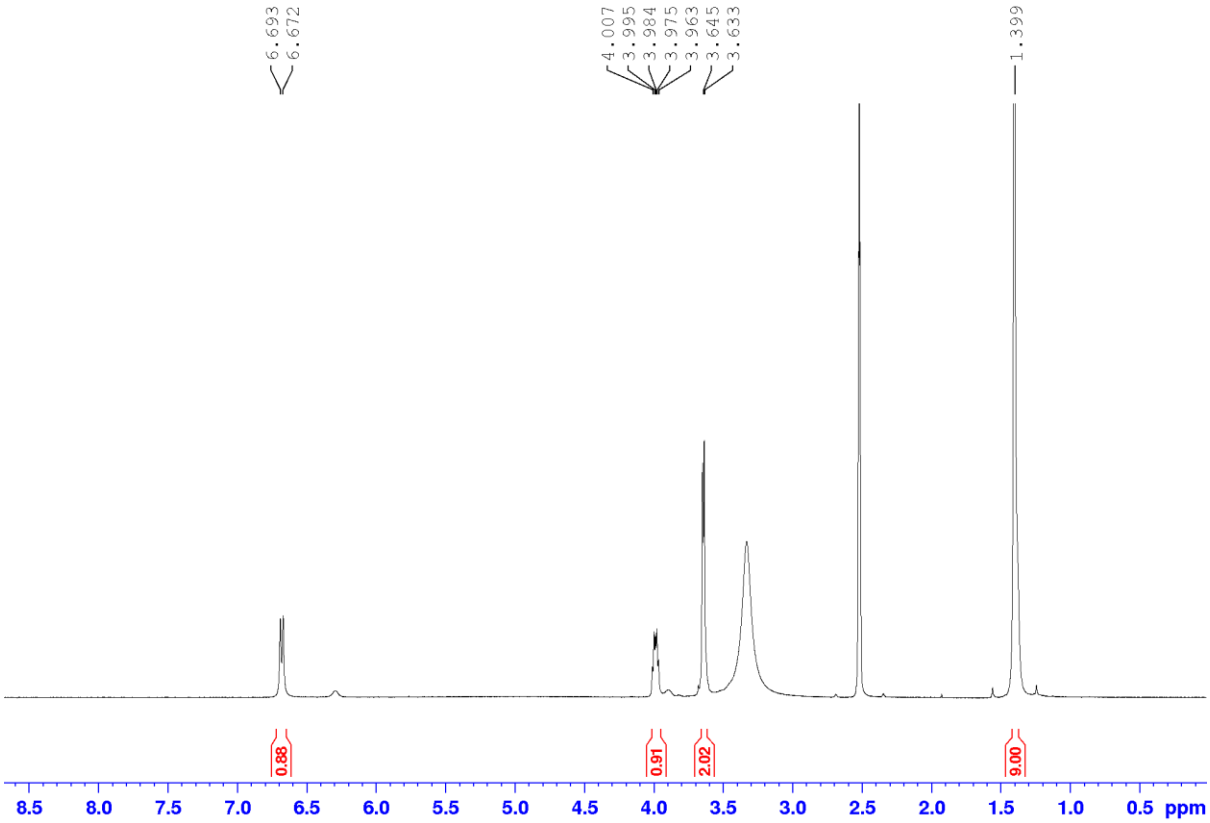

^{13}C NMR spectrum

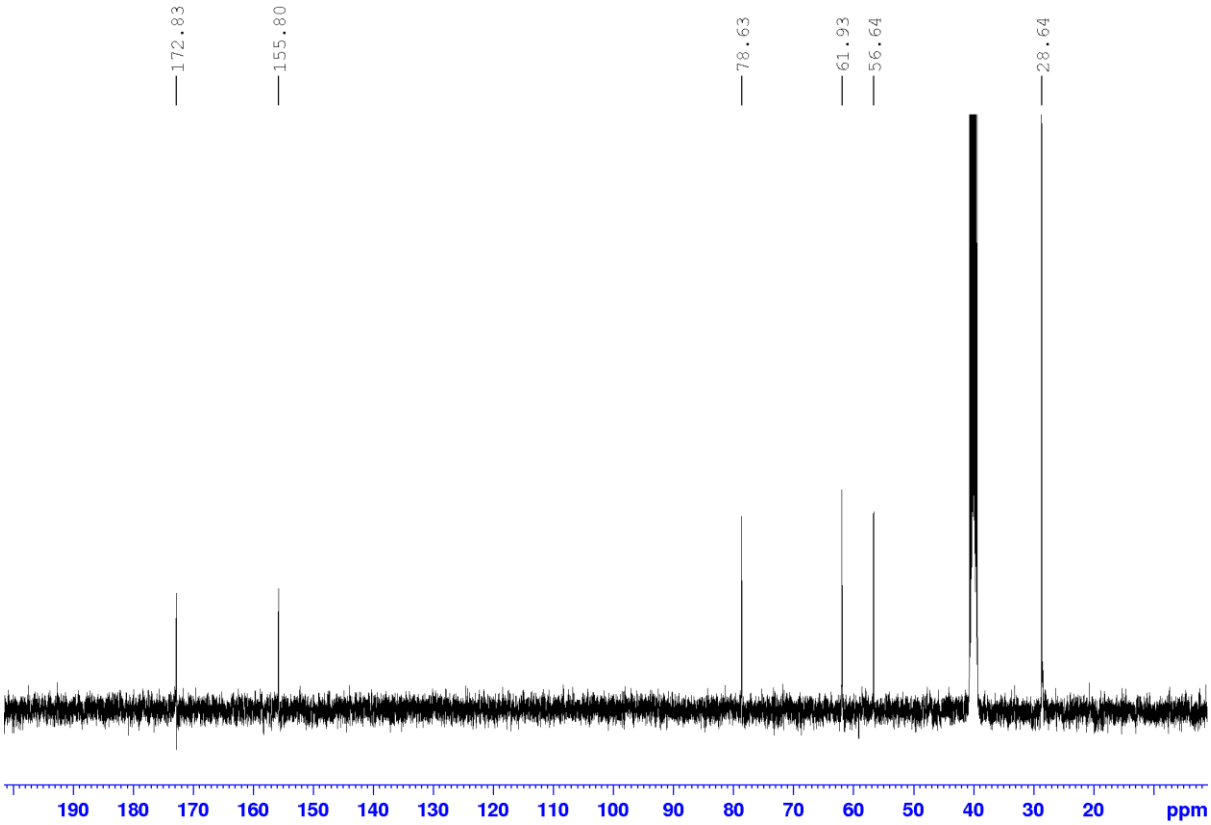

HRMS (ESI) spectrum

Elemental Composition Report **Page 1**

Single Mass Analysis
Tolerance = 5.0 PPM / DBE: min = -1.5, max = 500.0
Element prediction: Off
Number of isotope peaks used for i-FIT = 3

Monoisotopic Mass, Even Electron Ions
17 formula(e) evaluated with 1 results within limits (all results (up to 1000) for each mass)
Elements Used:
C: 5-10 H: 15-20 N: 0-5 O: 0-5 Na: 1-1

boc serine 2 (0.034) Cm (1:61) TOF MS ES+ 4.28e+005

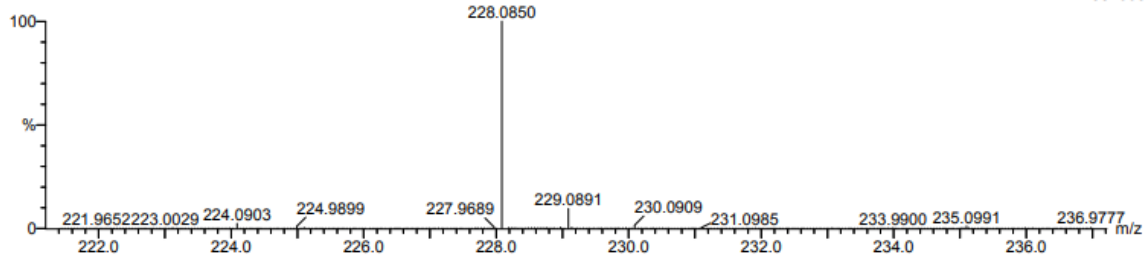

Minimum:				-1.5			
Maximum:		5.0	5.0	500.0			
Mass	Calc. Mass	mDa	PPM	DBE	i-FIT	i-FIT (Norm)	Formula
228.0850	228.0848	0.2	0.9	1.5	661.6	0.0	C8 H15 N O5 Na

FTIR spectrum

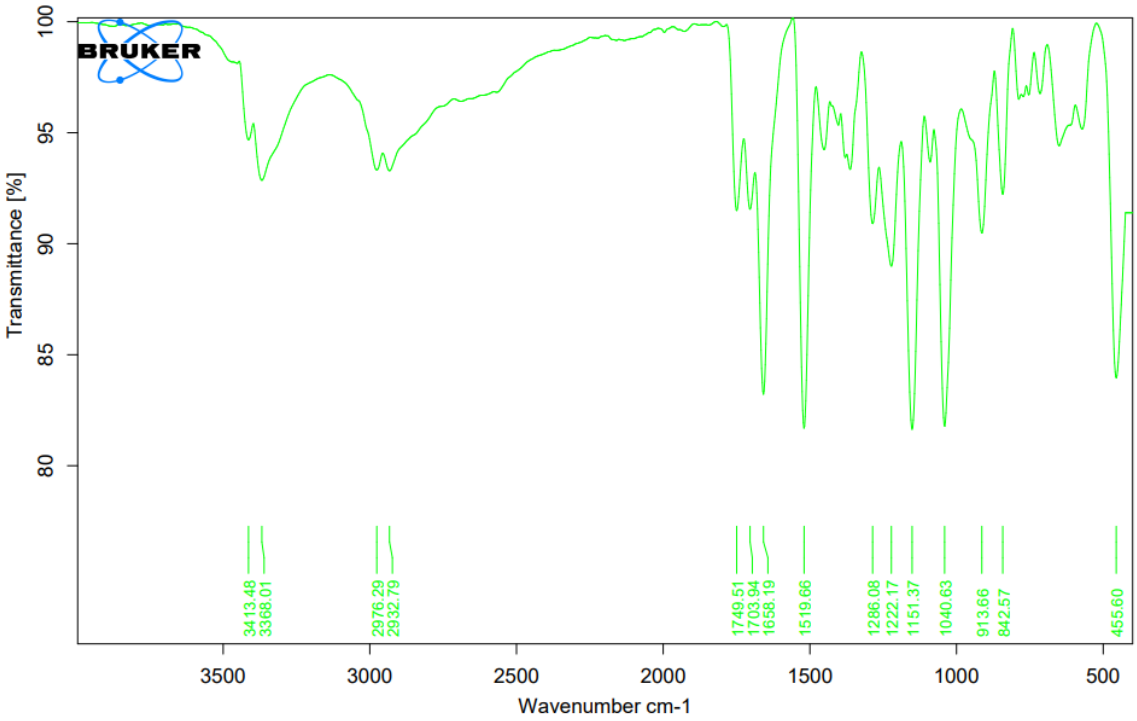

(*Tert*-butoxycarbonyl)-*L*-homoserine (3.16)

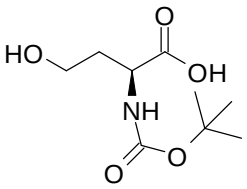

3.16

^{1}H NMR spectrum

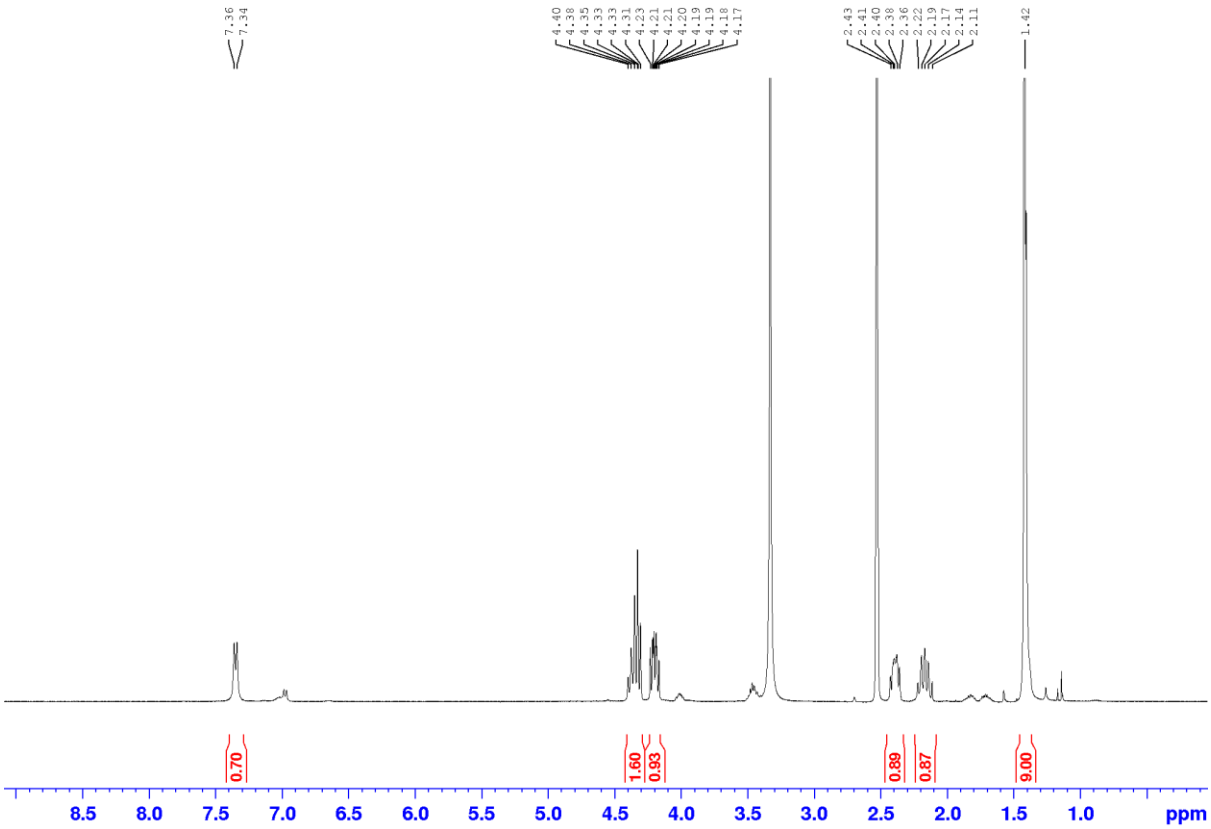

^{13}C NMR spectrum

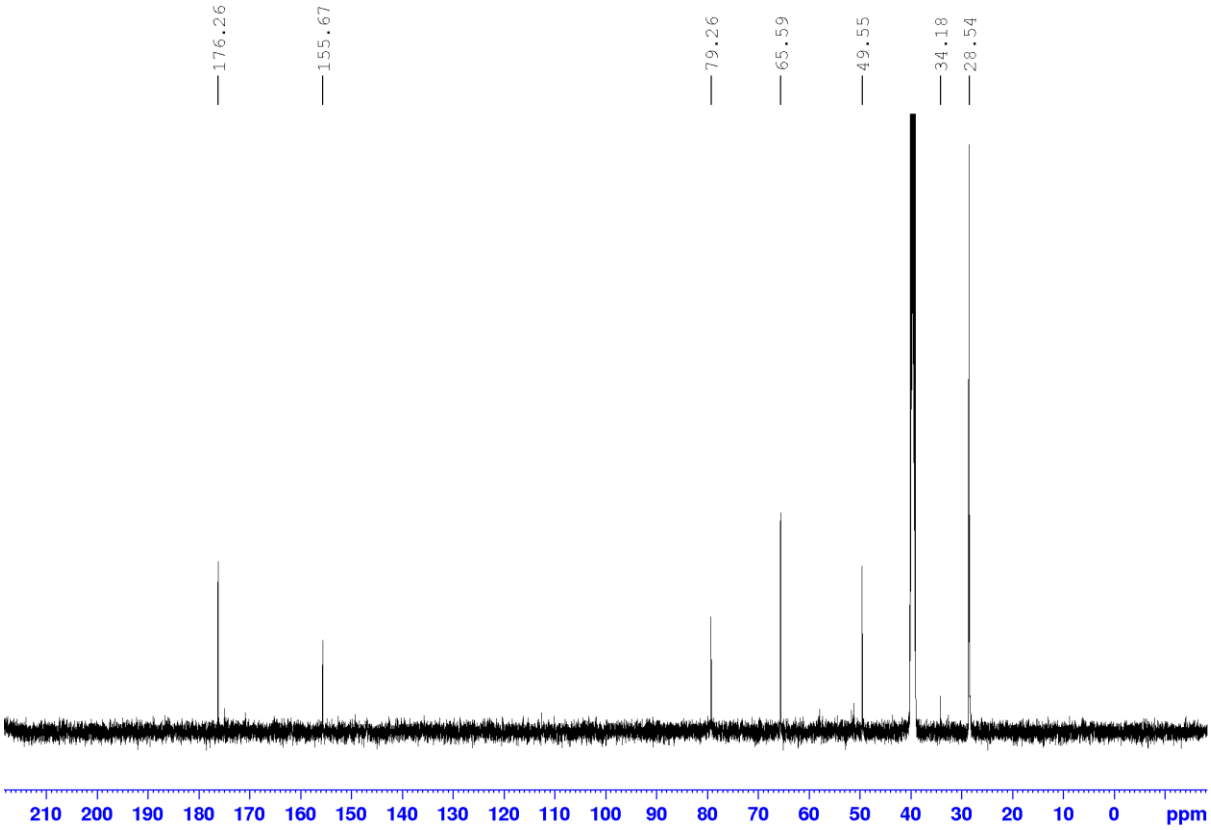

HRMS (ESI) spectrum

Elemental Composition Report **Page 1**

Single Mass Analysis
Tolerance = 5.0 PPM / DBE: min = -1.5, max = 500.0
Element prediction: Off
Number of isotope peaks used for i-FIT = 3

Monoisotopic Mass, Even Electron Ions
19 formula(e) evaluated with 1 results within limits (all results (up to 1000) for each mass)
Elements Used:
C: 5-10 H: 15-20 N: 0-5 O: 0-5
sd_01_155 49 (1.619) Cm (1:61)

TOF MS ES-
4.06e+004

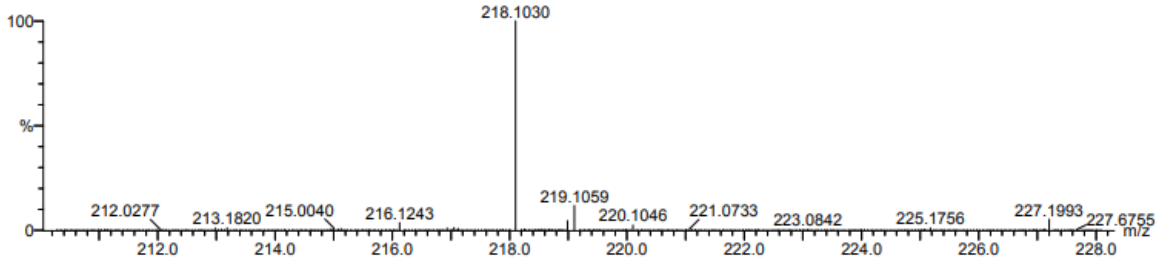

Minimum:				-1.5			
Maximum:		5.0	5.0	500.0			
Mass	Calc. Mass	mDa	PPM	DBE	i-FIT	i-FIT (Norm)	Formula
218.1030	218.1028	0.2	0.9	2.5	486.8	0.0	C9 H16 N O5

FTIR spectrum

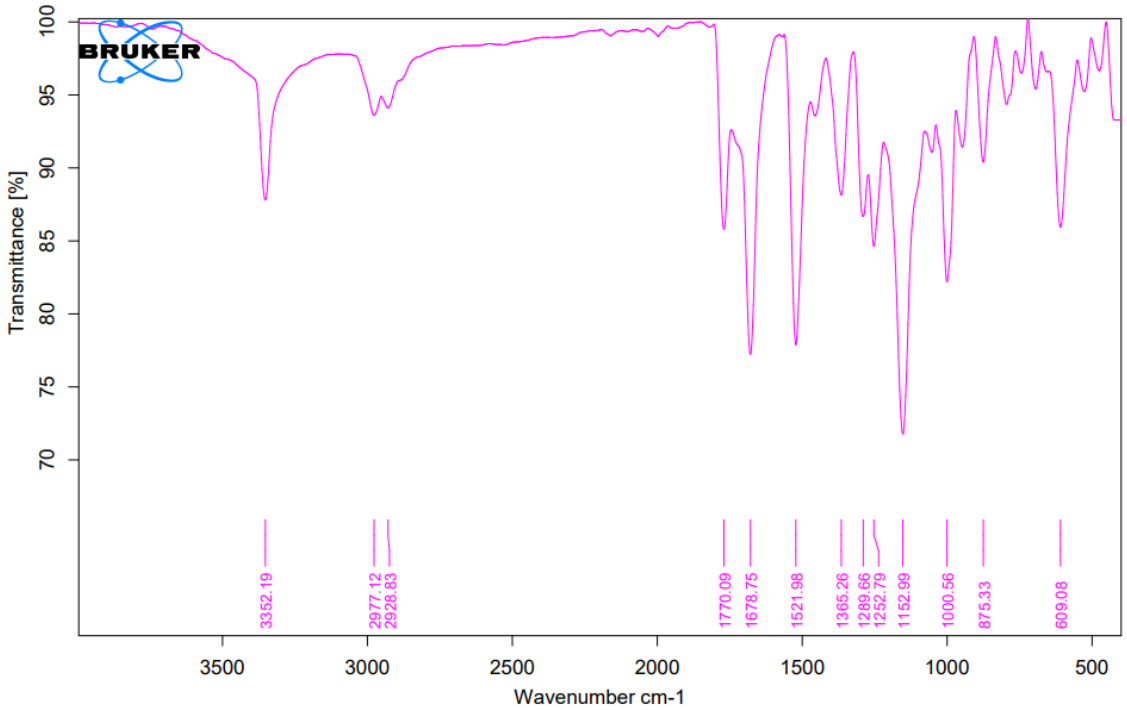

Methyl (*S*)-2-((tert-butoxycarbonyl)amino)-3-(4-chlorophenyl)propanoate (3.21)

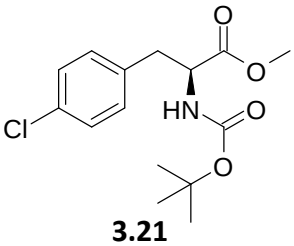

3.21

^{1}H NMR spectrum

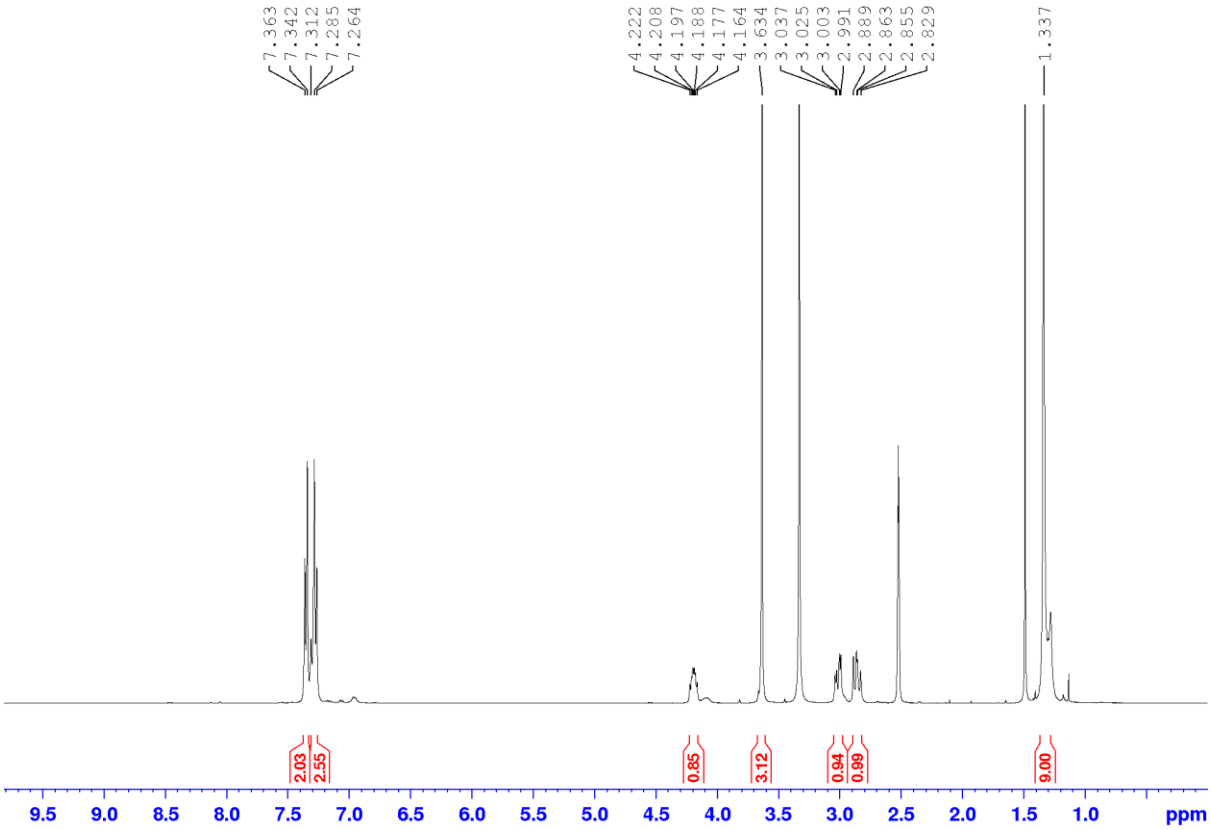

^{13}C NMR spectrum

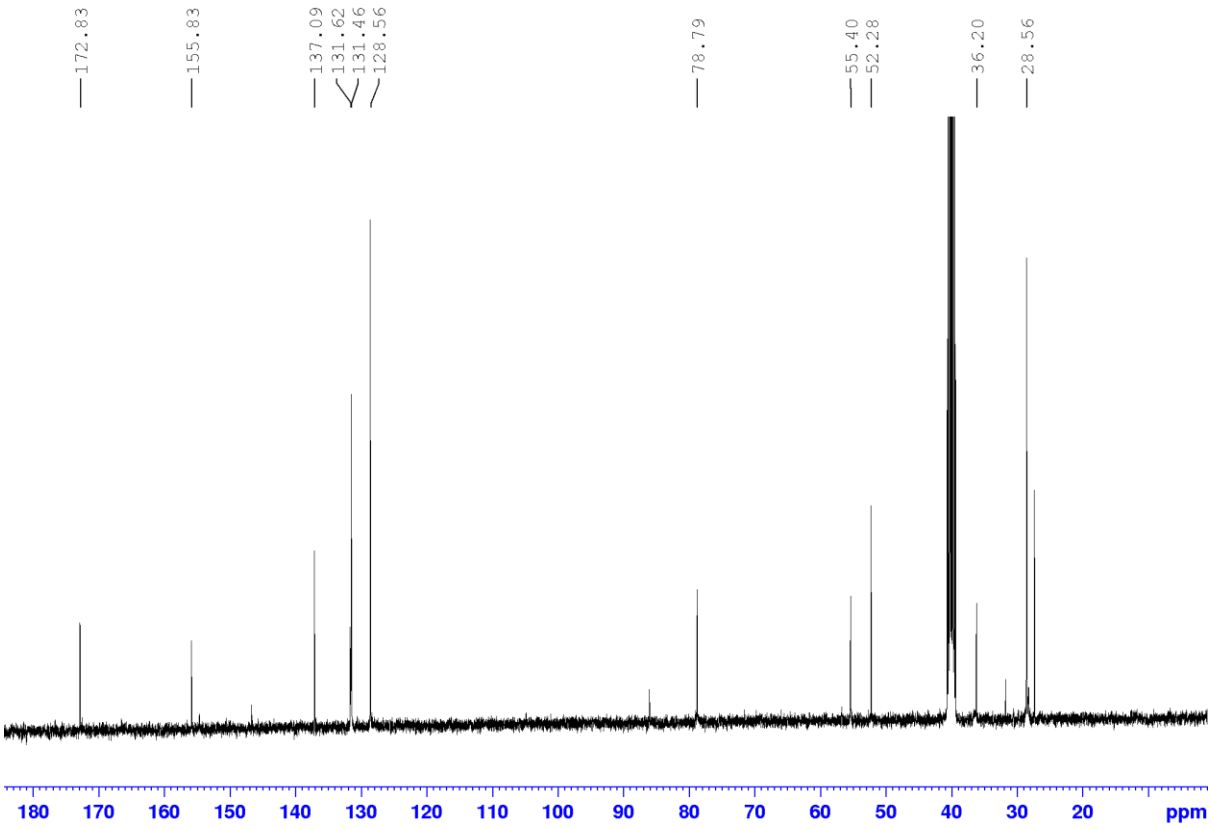

HRMS (ESI) spectrum

Elemental Composition Report **Page 1**

Single Mass Analysis
Tolerance = 5.0 PPM / DBE: min = -1.5, max = 500.0
Element prediction: Off
Number of isotope peaks used for i-FIT = 3

Monoisotopic Mass, Even Electron Ions
40 formula(e) evaluated with 1 results within limits (all results (up to 1000) for each mass)
Elements Used:
C: 10-15 H: 15-20 N: 0-5 O: 0-5 Na: 1-1 Cl: 0-1
sd_01_085 59 (1.958) Cm (1:61)

TOF MS ES+
1.83e+006

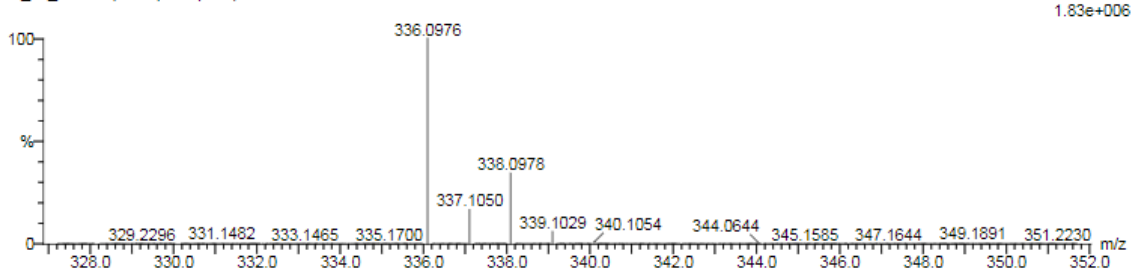

Minimum:				-1.5			
Maximum:		5.0	5.0	500.0			
Mass	Calc. Mass	mDa	PPM	DBE	i-FIT	i-FIT (Norm)	Formula
336.0976	336.0979	-0.3	-0.9	5.5	552.4	0.0	C15 H20 N O4 Na Cl

FTIR spectrum

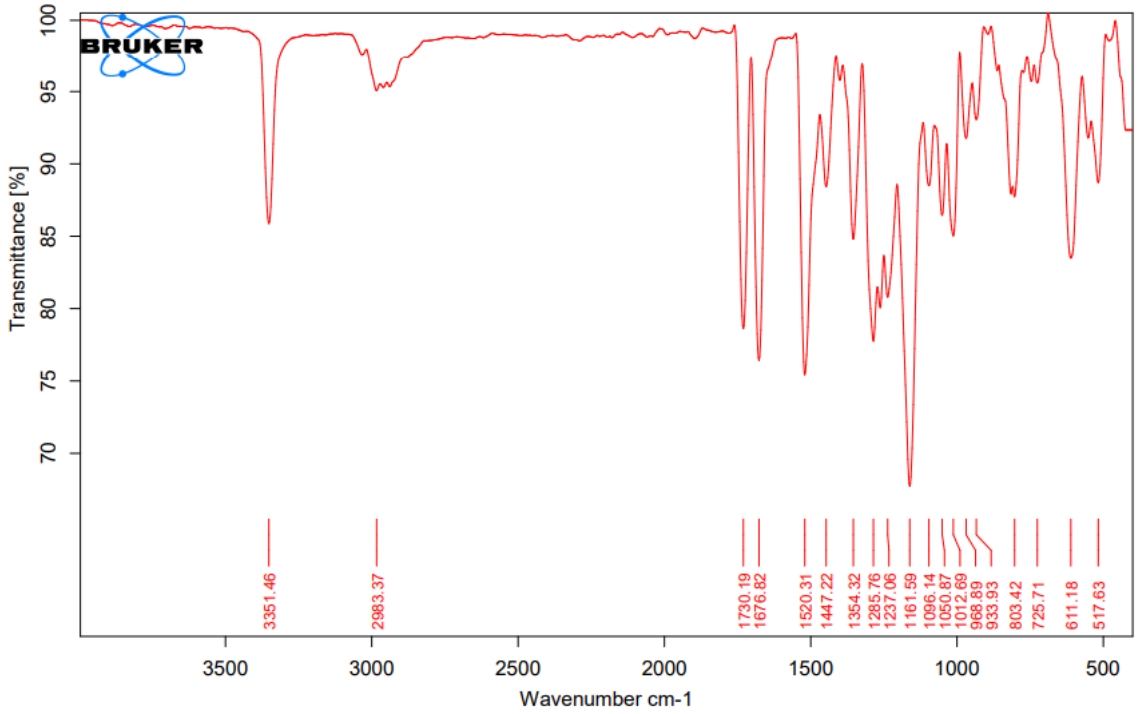

Methyl (*S*)-2-((*tert*-butoxycarbonyl)amino)-2-(4-chlorophenyl)acetate (3.25)

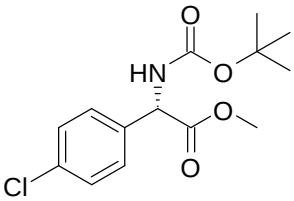

3.25

^{1}H NMR spectrum

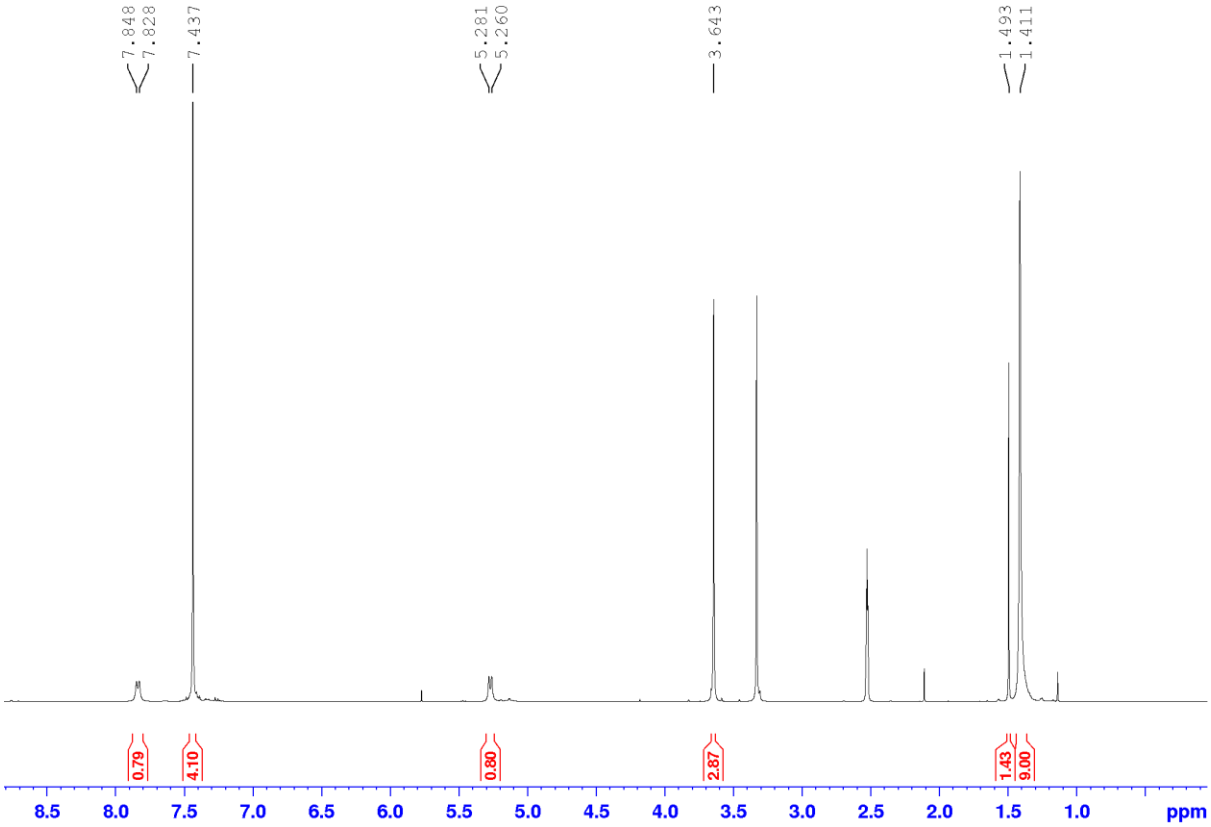

^{13}C NMR spectrum

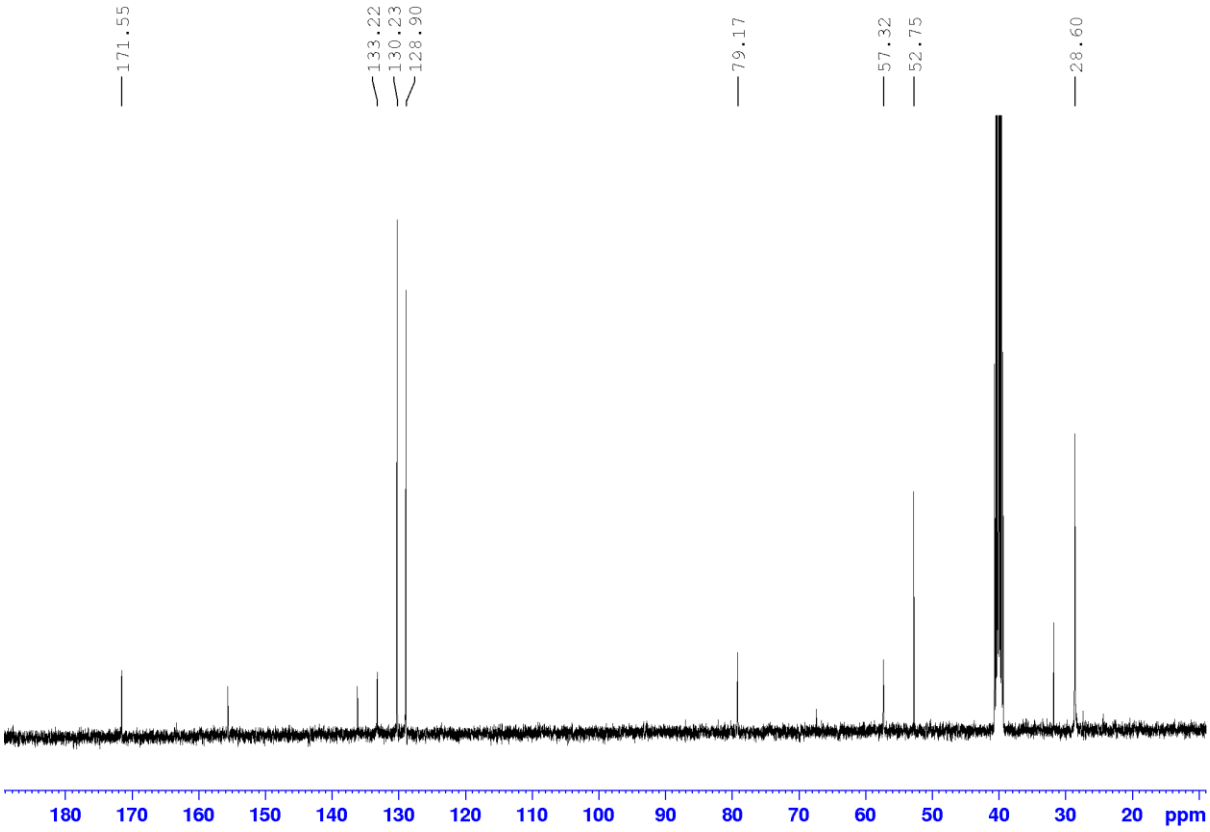

HRMS (ESI) spectrum

Elemental Composition Report **Page 1**

Single Mass Analysis
Tolerance = 5.0 PPM / DBE: min = -1.5, max = 500.0
Element prediction: Off
Number of isotope peaks used for i-FIT = 3

Monoisotopic Mass, Even Electron Ions
15 formula(e) evaluated with 1 results within limits (all results (up to 1000) for each mass)
Elements Used:
C: 10-15 H: 15-20 N: 0-5 O: 0-5 Cl: 1-1
sd-087 59 (1.956) Cm (1:61)

TOF MS ES-
5.34e+004

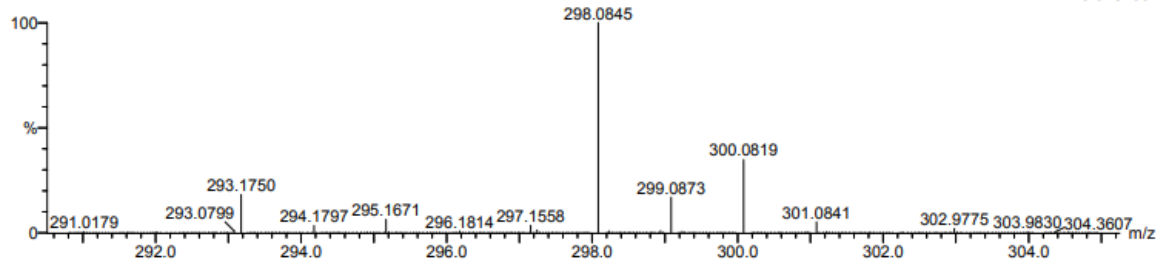

Minimum:				-1.5			
Maximum:		5.0	5.0	500.0			
Mass	Calc. Mass	mDa	PPM	DBE	i-FIT	i-FIT (Norm)	Formula
298.0845	298.0846	-0.1	-0.3	6.5	415.4	0.0	C14 H17 N O4 Cl

FTIR spectrum

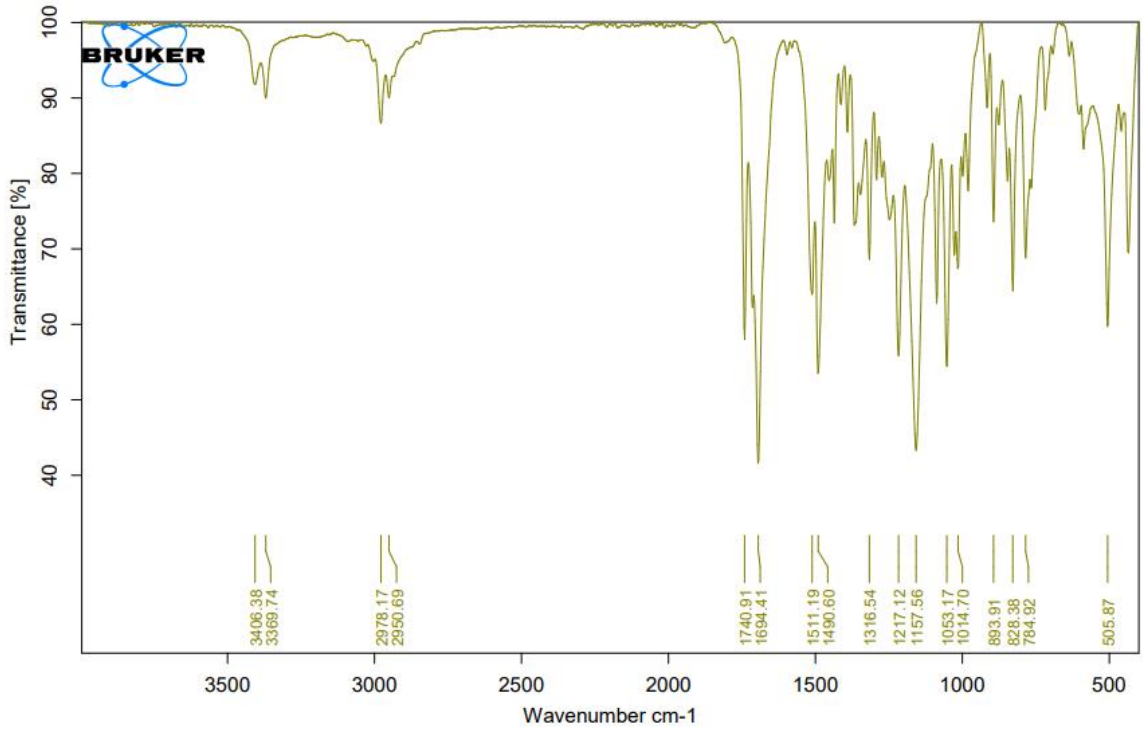

Methyl (*S*)-2-((*tert*-butoxycarbonyl)amino)-3-(4-fluorophenyl)propanoate (3.29)

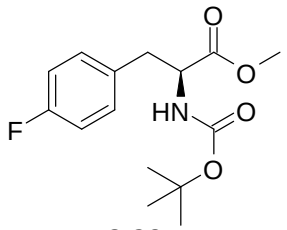

3.29

^{1}H NMR spectrum

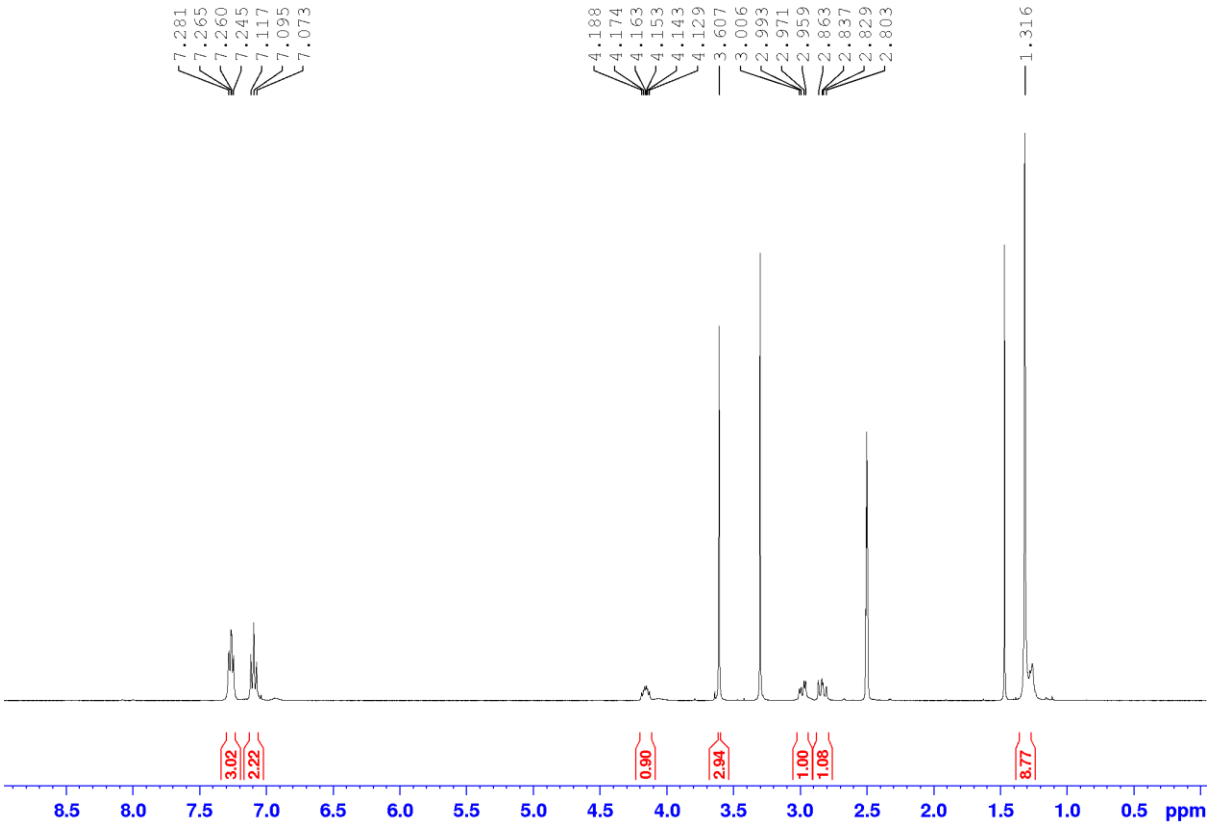

^{13}C NMR spectrum

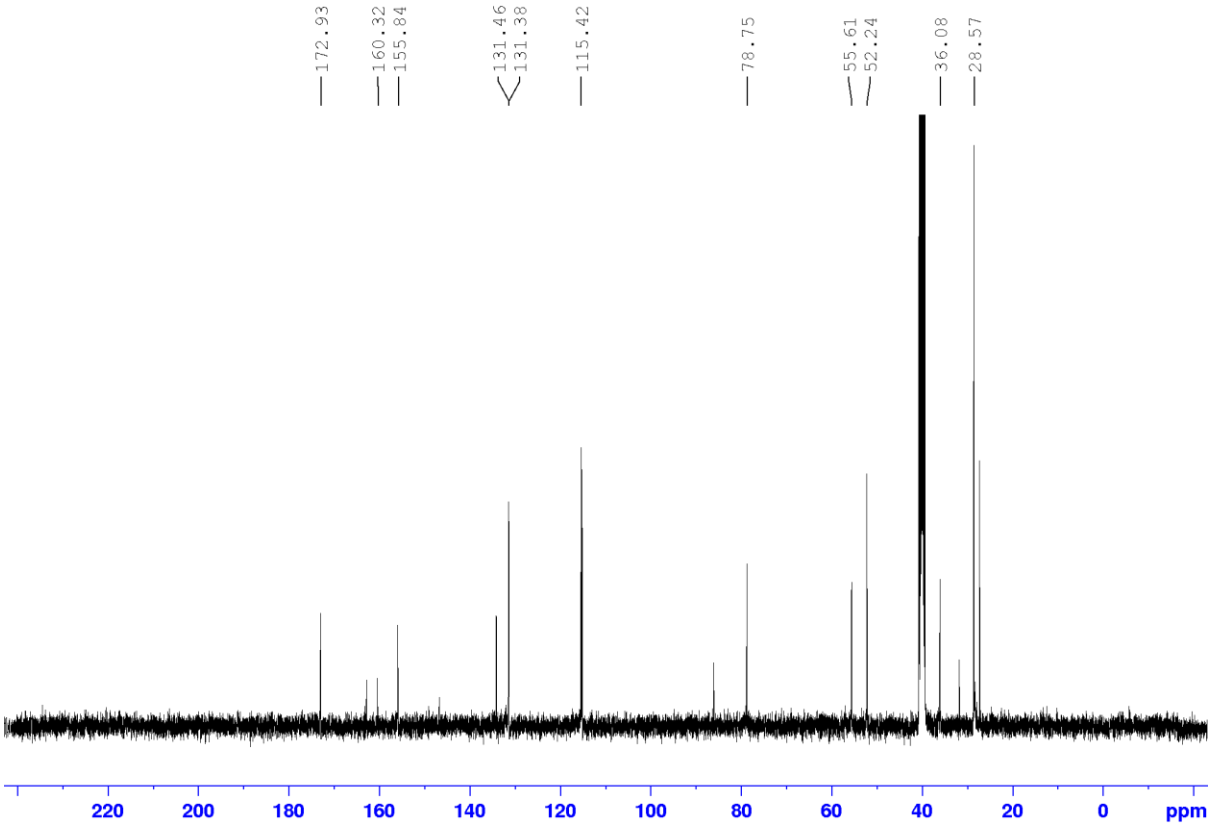

HRMS (ESI) spectrum

Elemental Composition Report **Page 1**

Single Mass Analysis
Tolerance = 5.0 PPM / DBE: min = -1.5, max = 500.0
Element prediction: Off
Number of isotope peaks used for i-FIT = 3

Monoisotopic Mass, Even Electron Ions
37 formula(e) evaluated with 1 results within limits (all results (up to 1000) for each mass)
Elements Used:
C: 10-15 H: 15-20 N: 0-5 O: 0-5 F: 0-1 Na: 1-1
sd_01_124 61 (2.023) Cm (1:61)

TOF MS ES+
1.08e+006

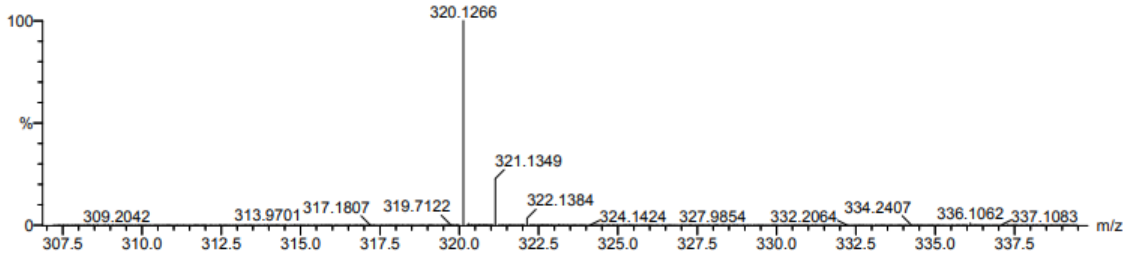

Minimum:				-1.5			
Maximum:		5.0	5.0	500.0			
Mass	Calc. Mass	mDa	PPM	DBE	i-FIT	i-FIT (Norm)	Formula
320.1266	320.1274	-0.8	-2.5	5.5	764.7	0.0	C15 H20 N O4 F Na

FTIR spectrum

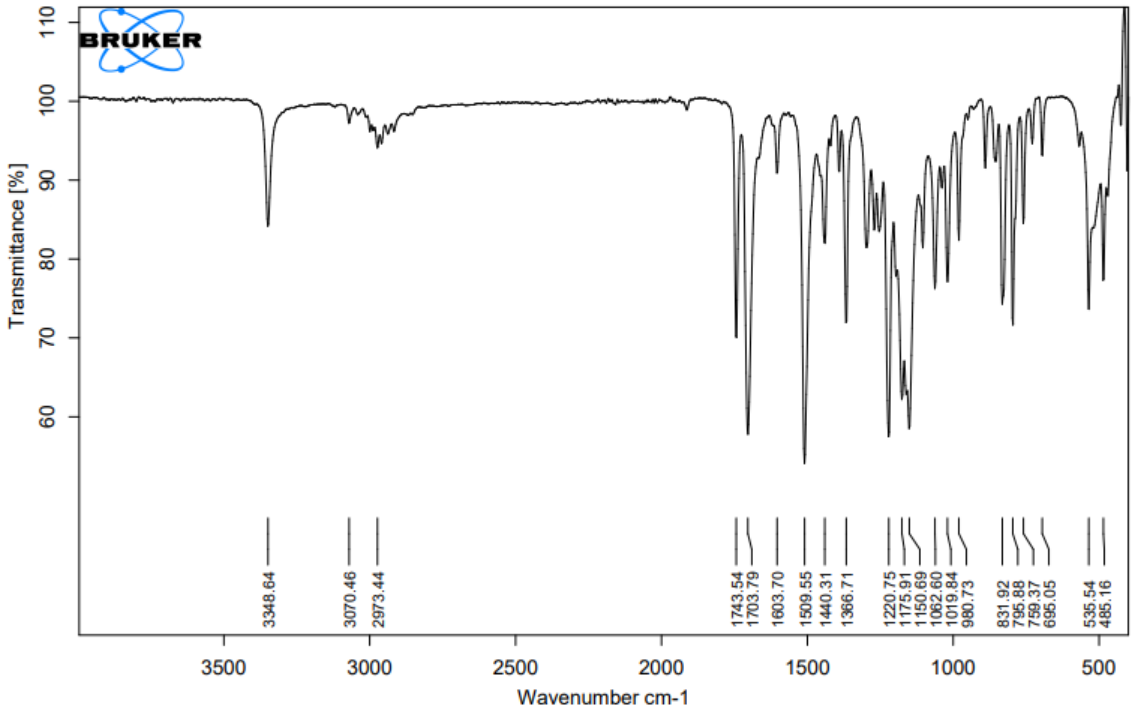

Methyl (*S*)-2-((*tert*-butoxycarbonyl)amino)-3-(4-iodophenyl)propanoate (3.34)

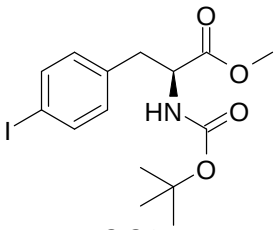

3.34

^{1}H NMR spectrum

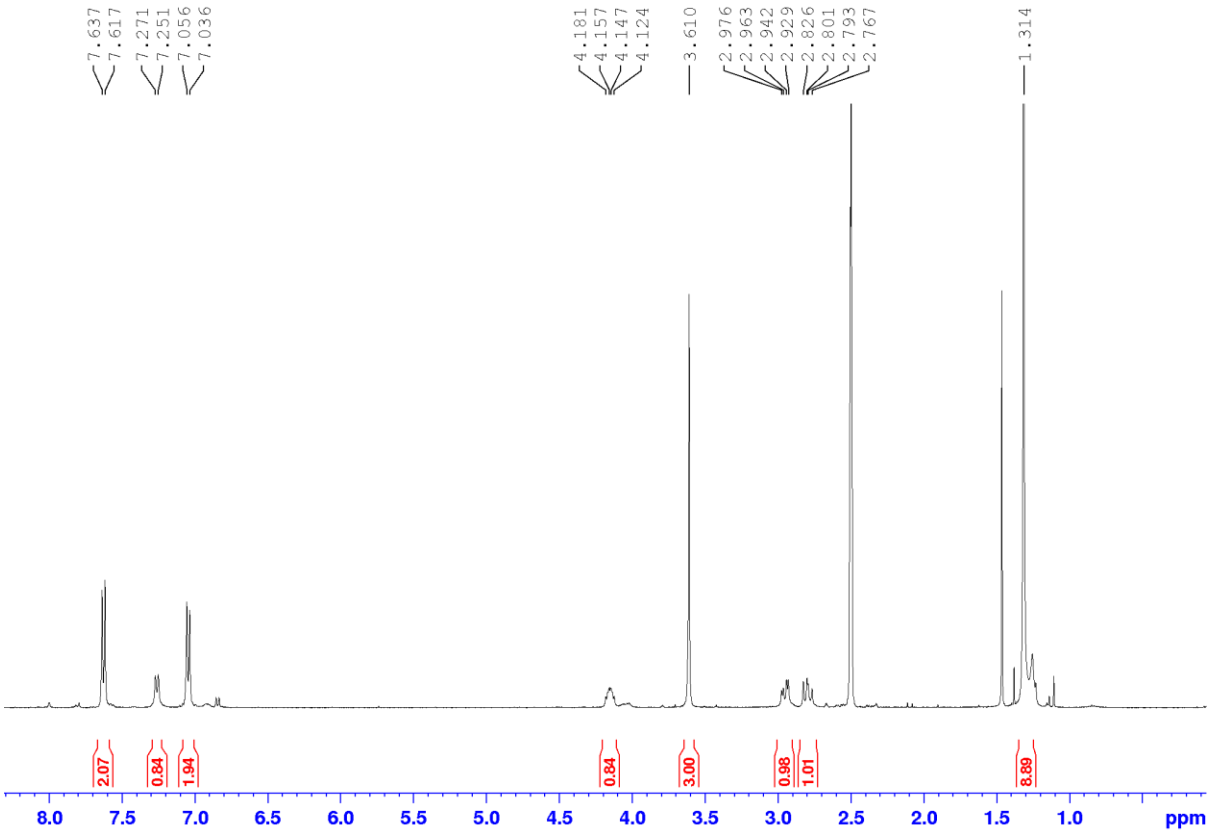

^{13}C NMR spectrum

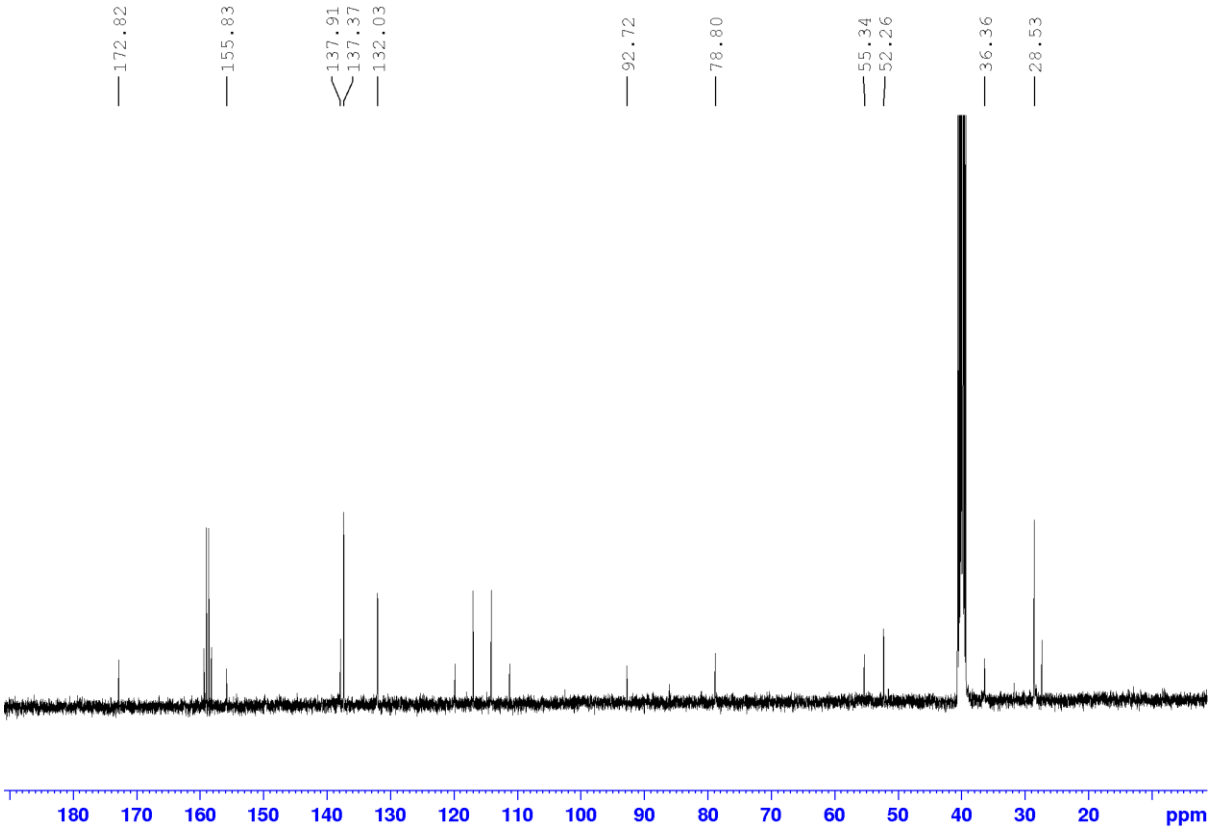

HRMS (ESI) spectrum

Elemental Composition Report **Page 1**

Single Mass Analysis
Tolerance = 5.0 PPM / DBE: min = -1.5, max = 500.0
Element prediction: Off
Number of isotope peaks used for i-FIT = 3

Monoisotopic Mass, Even Electron Ions
53 formula(e) evaluated with 1 results within limits (all results (up to 1000) for each mass)
Elements Used:
C: 10-15 H: 15-20 N: 0-5 O: 0-5 Na: 1-1 I: 0-1

sd_01_130 3 (0.068) Cm (1:61) TOF MS ES+ 3.39e+005

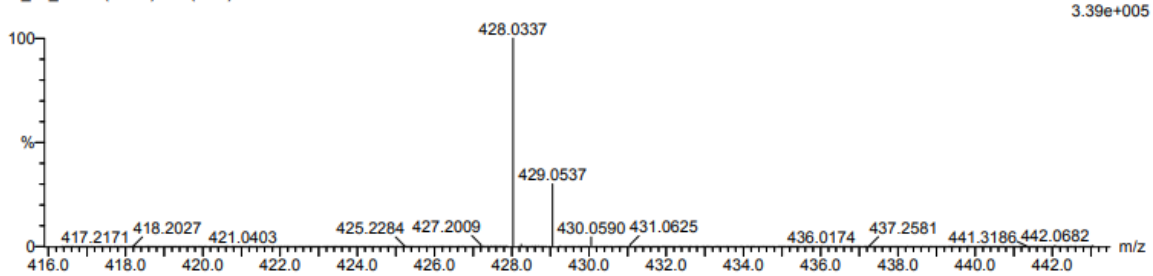

Minimum:				-1.5			
Maximum:		5.0	5.0	500.0			
Mass	Calc. Mass	mDa	PPM	DBE	i-FIT	i-FIT (Norm)	Formula
428.0337	428.0335	0.2	0.5	5.5	455.8	0.0	C15 H20 N O4 Na I

FTIR spectrum

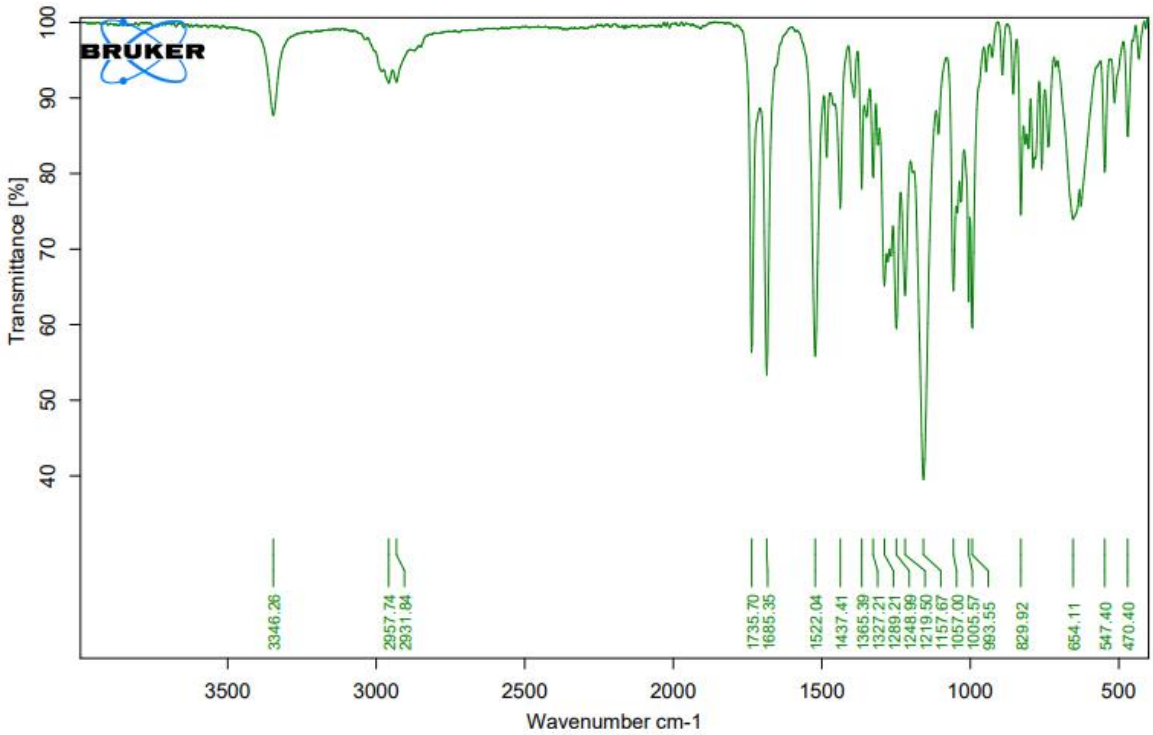

Ethyl (*tert*-butoxycarbonyl)-*L*-serinate (3.13)

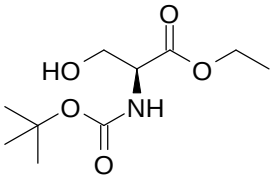

3.13

^{1}H NMR Spectrum

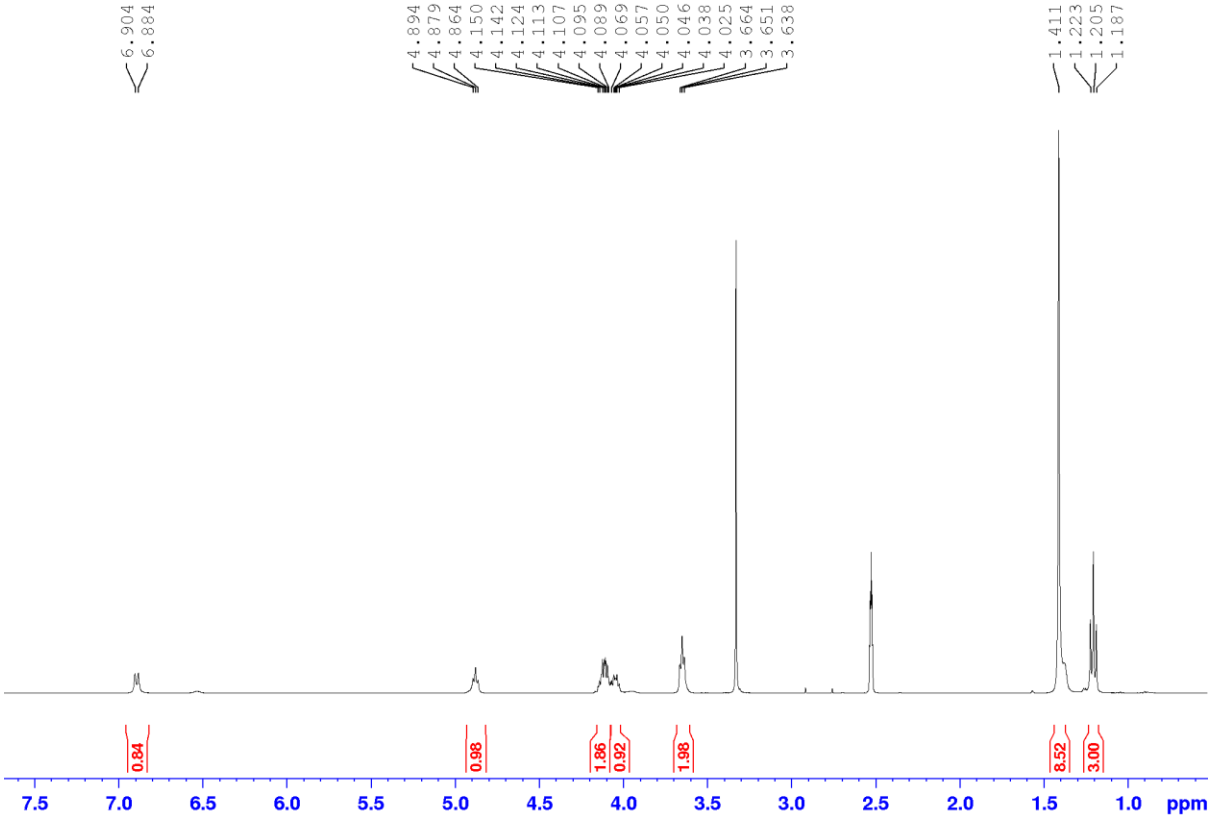

^{13}C NMR Spectrum

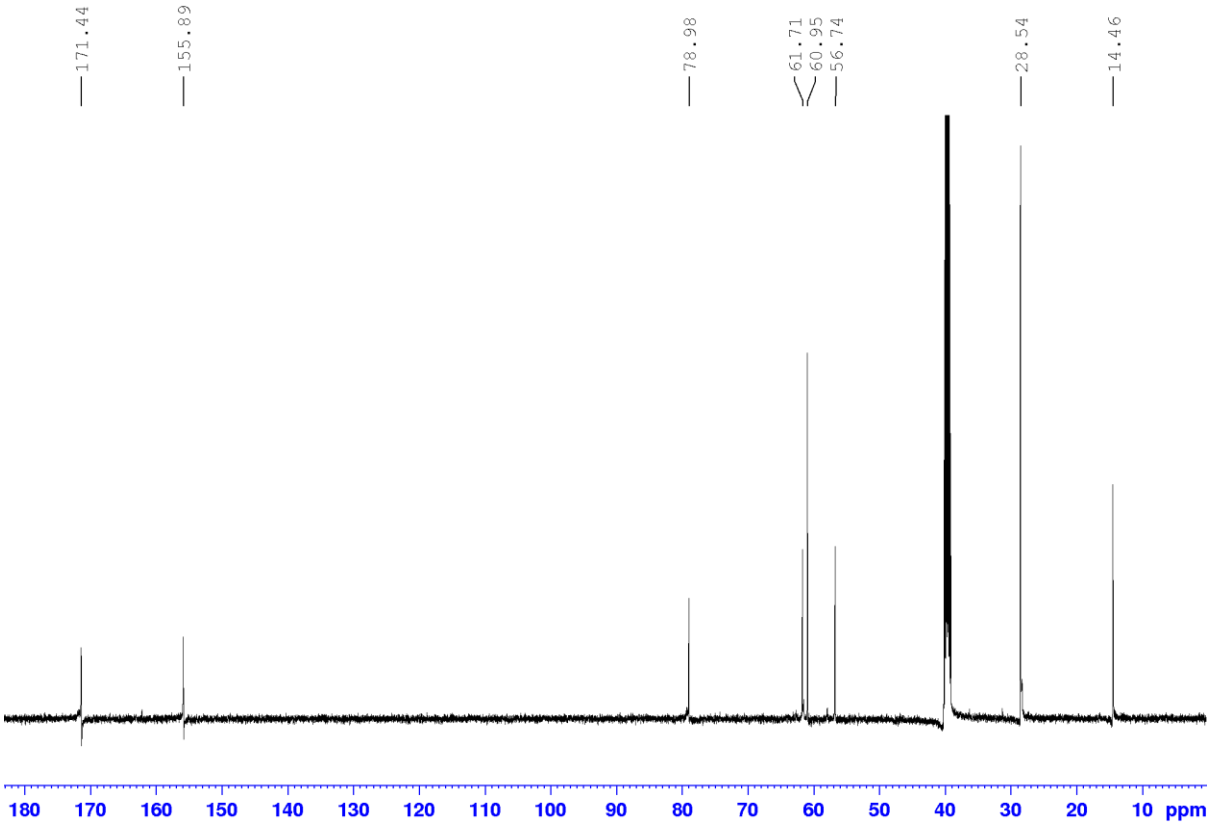

FTIR Spectrum

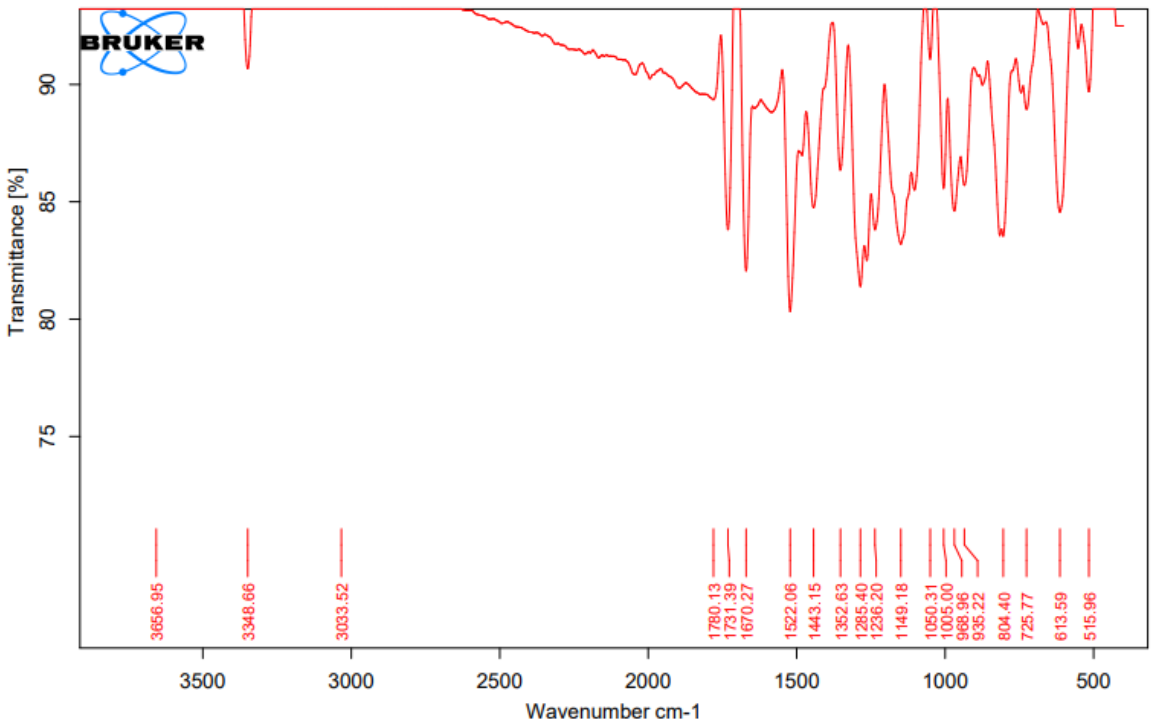

Ethyl (tert-butoxycarbonyl)-*L*-homoserinate (3.17)

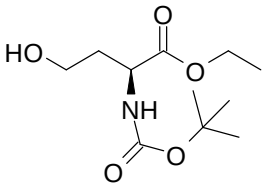

3.17

^{1}H NMR Spectrum

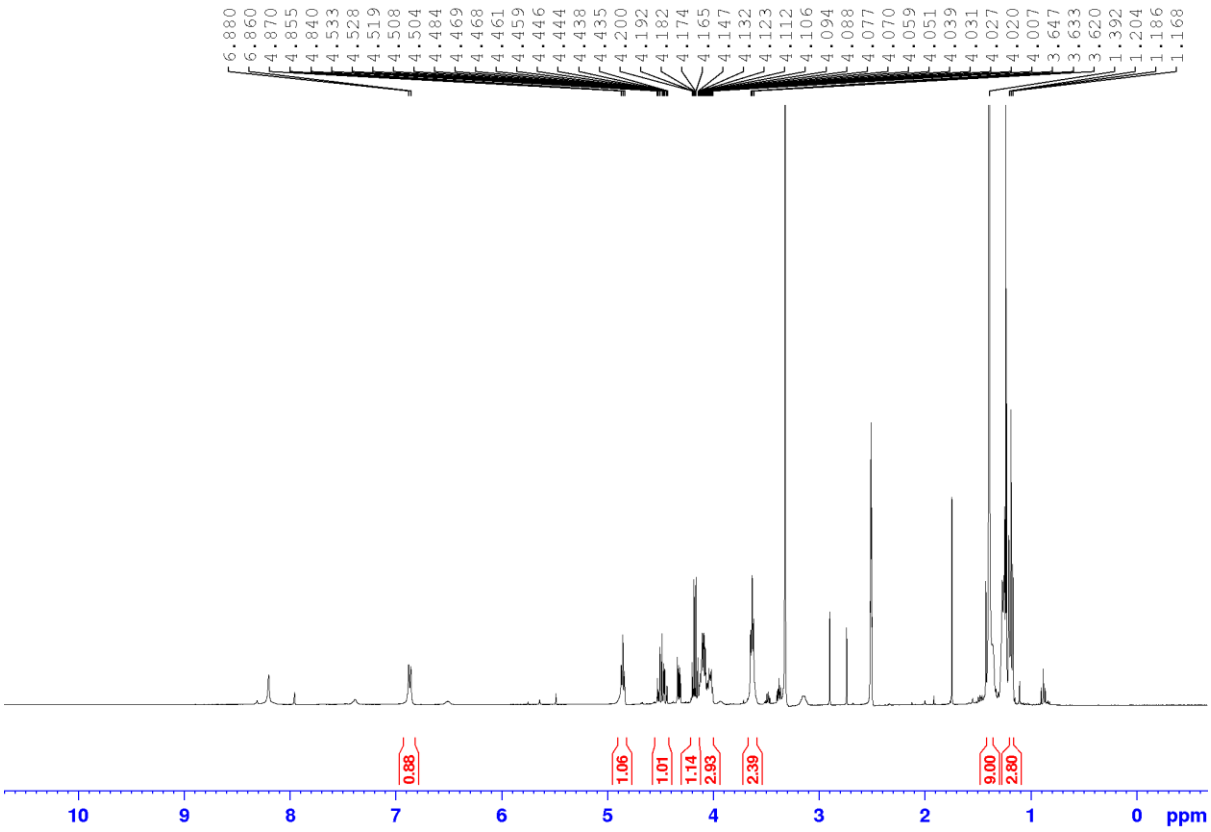

^{13}C NMR Spectrum

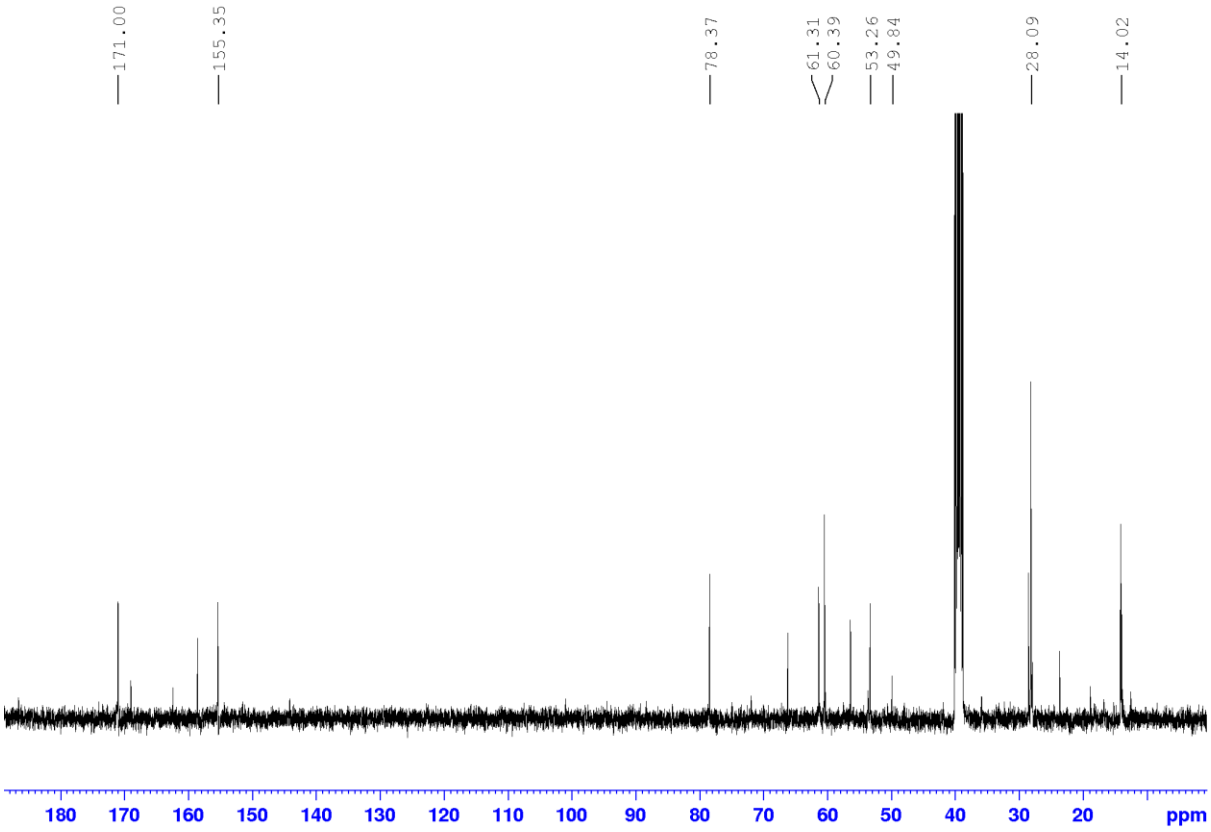

FTIR Spectrum

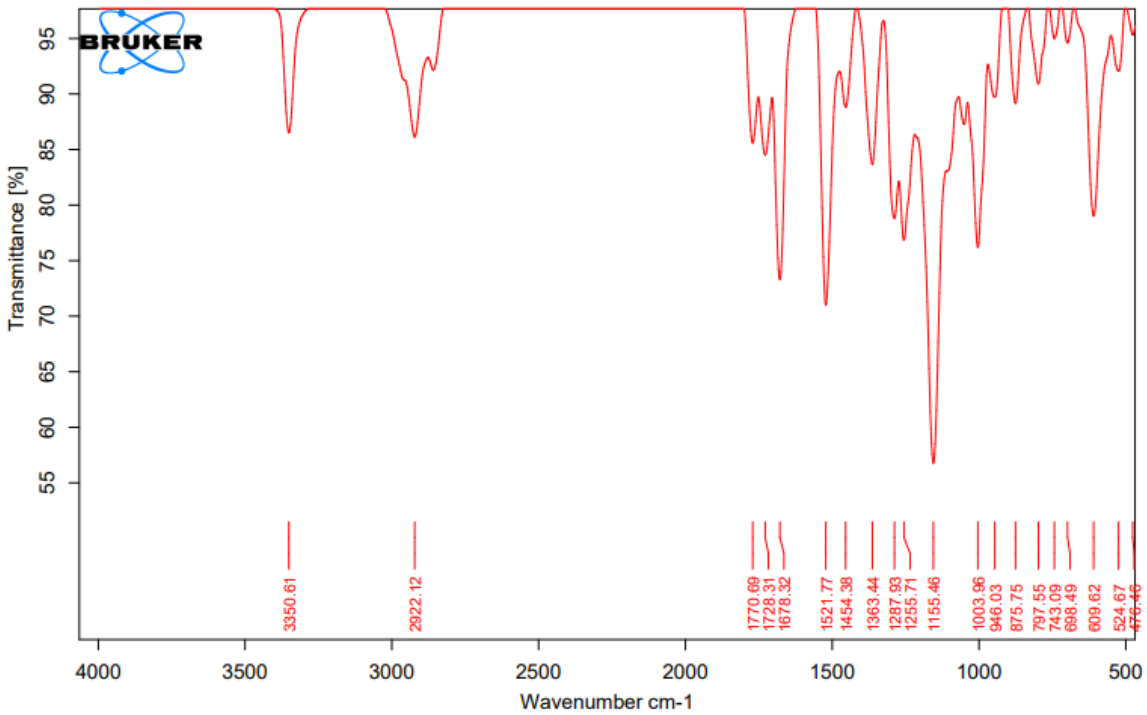

Methyl (*S*)-2-((*tert*-butoxycarbonyl)amino)-3-(4-((fluorosulfonyl)oxy)phenyl)propanoate (3.5)

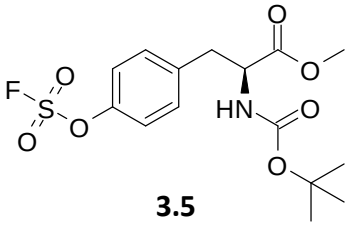

3.5

^{1}H NMR spectrum

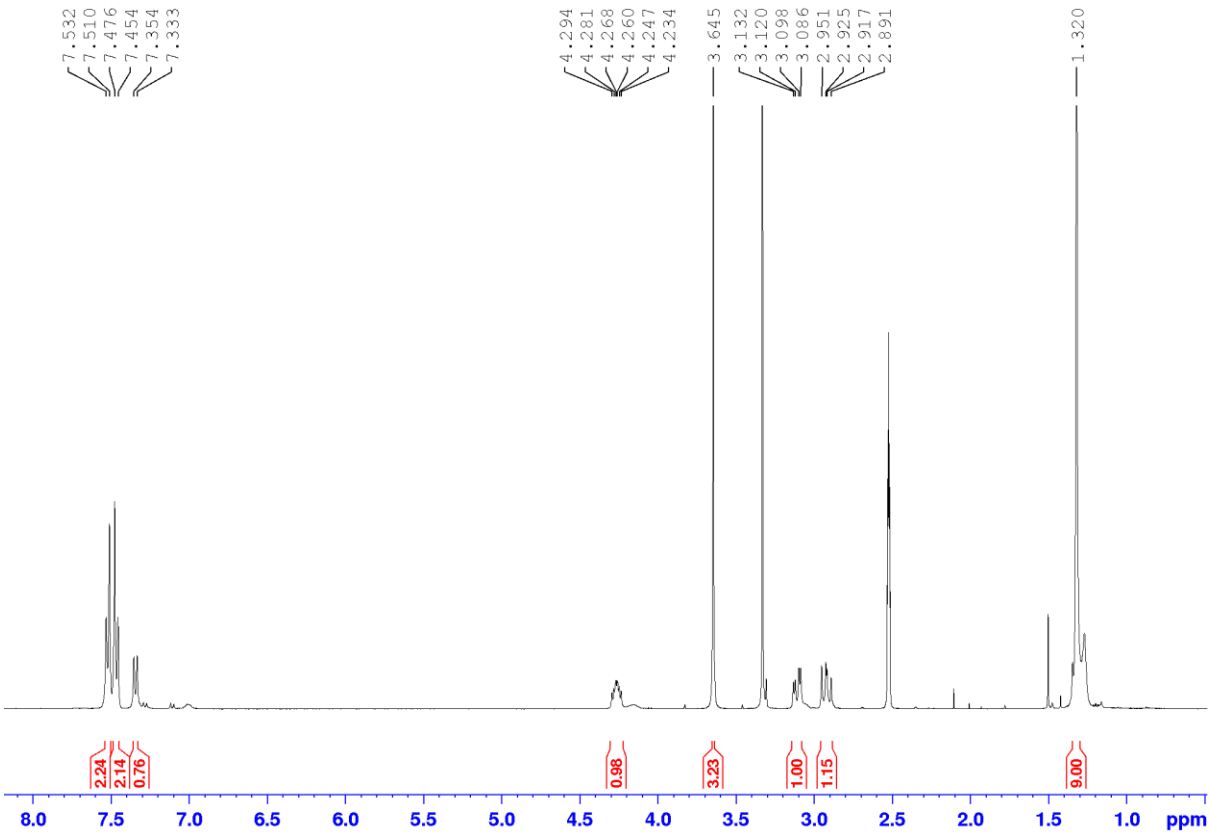

^{13}C NMR spectrum

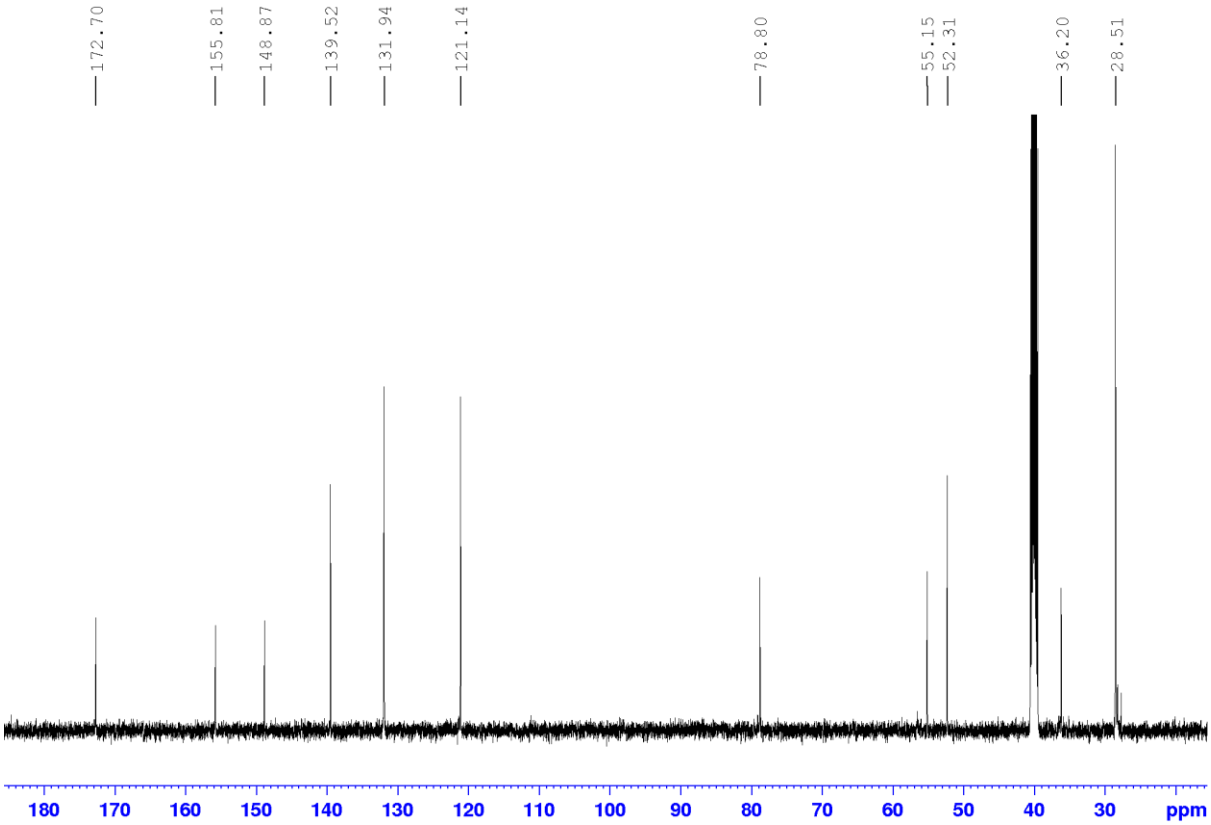

^{19}F NMR spectrum

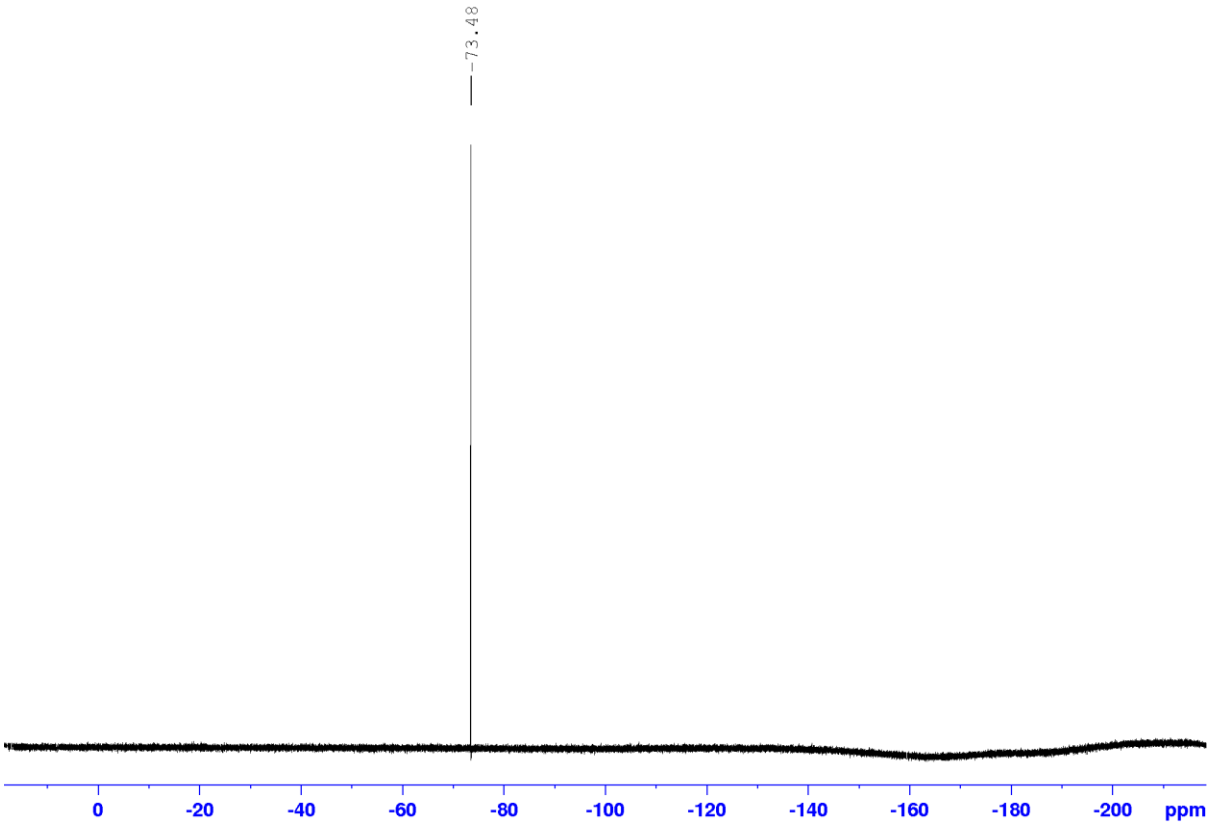

HRMS spectrum

Elemental Composition Report **Page 1**

Single Mass Analysis
Tolerance = 5.0 PPM / DBE: min = -1.5, max = 500.0
Element prediction: Off
Number of isotope peaks used for i-FIT = 3

Monoisotopic Mass, Even Electron Ions
138 formula(e) evaluated with 1 results within limits (all results (up to 1000) for each mass)
Elements Used:
C: 15-20 H: 20-25 N: 0-5 O: 5-10 S: 0-1 F: 0-1 Na: 0-1

sd_01_088 52 (1.791) Cm (1:58)

TOF MS ES+
5.43e+005

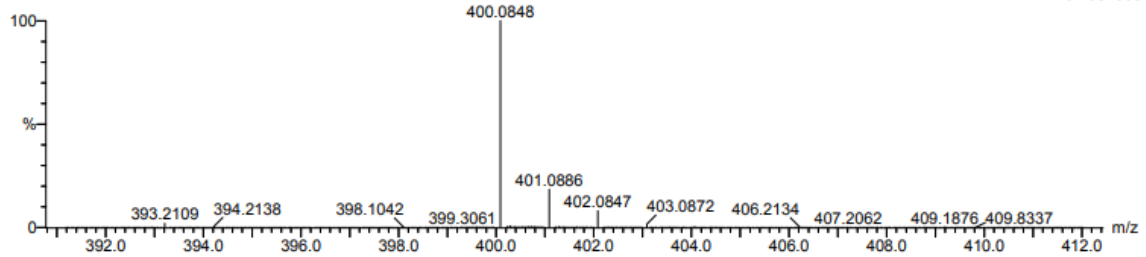

Minimum:				-1.5			
Maximum:		5.0	5.0	500.0			
Mass	Calc. Mass	mDa	PPM	DBE	i-FIT	i-FIT (Norm)	Formula
400.0848	400.0842	0.6	1.5	5.5	703.4	0.0	C15 H20 N O7 S F Na

FTIR spectrum

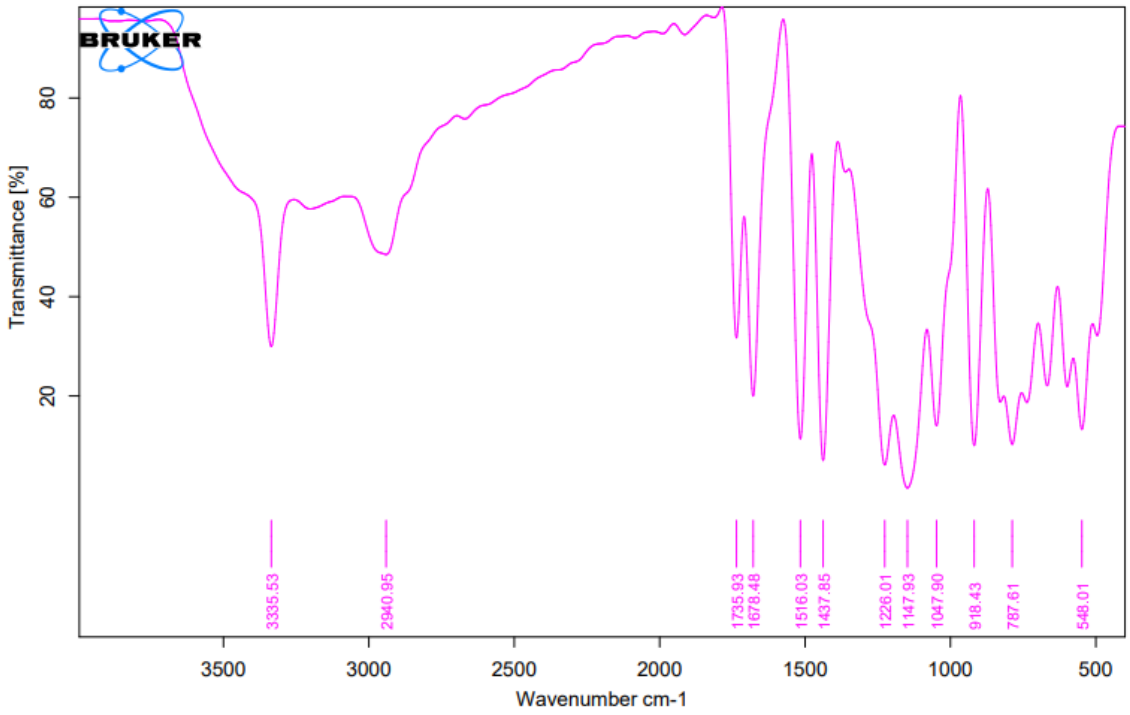

Methyl (*S*)-2-((tert-butoxycarbonyl)amino)-2-(4-((fluorosulfonyl)oxy)phenyl)acetate (3.9)

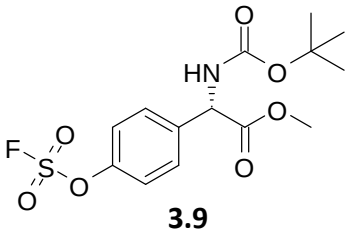

3.9

^{1}H NMR spectrum

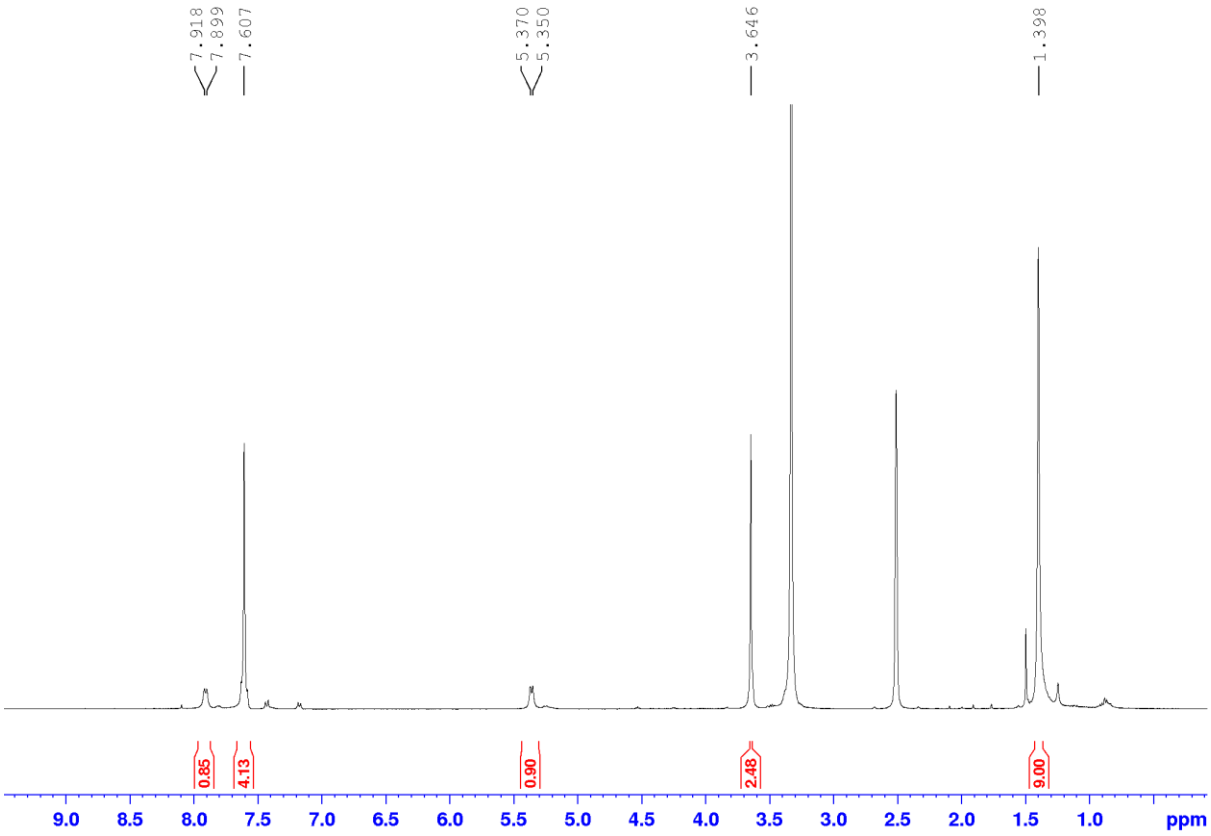

^{13}C NMR spectrum

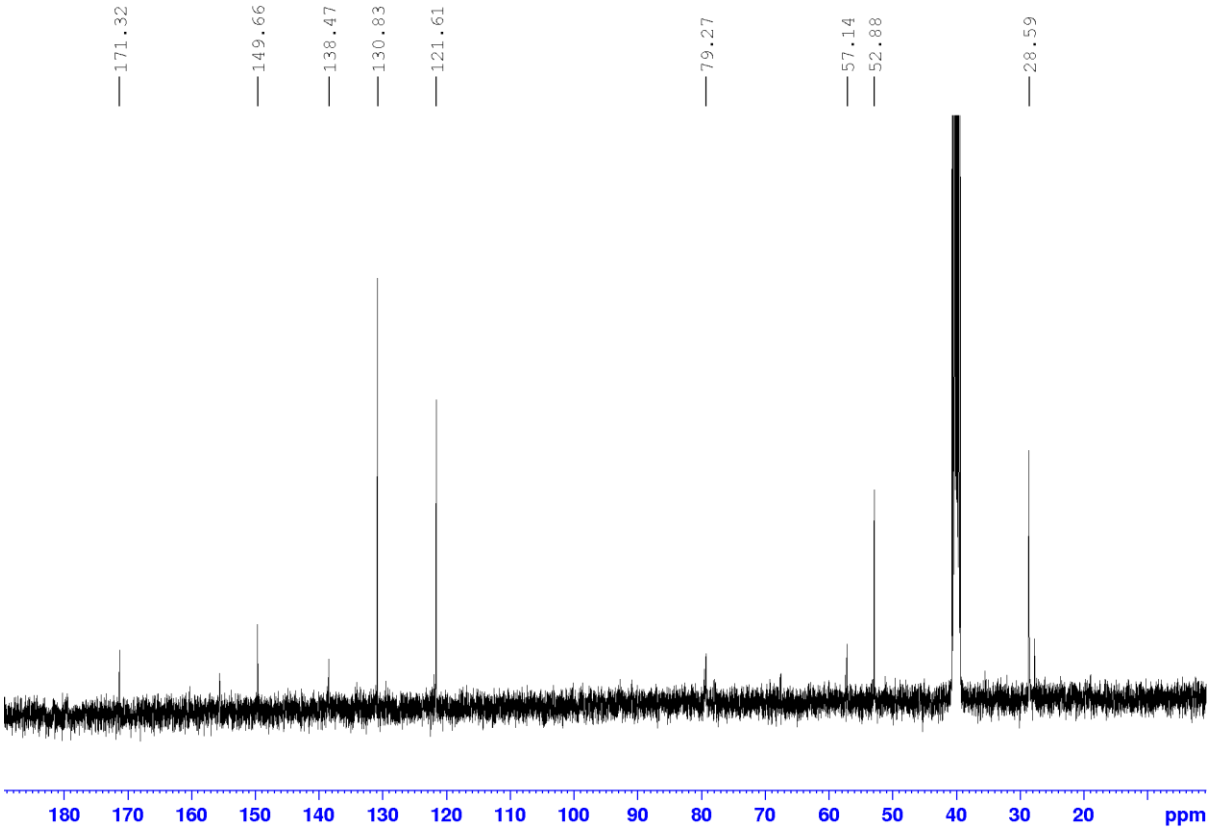

^{19}F NMR spectrum

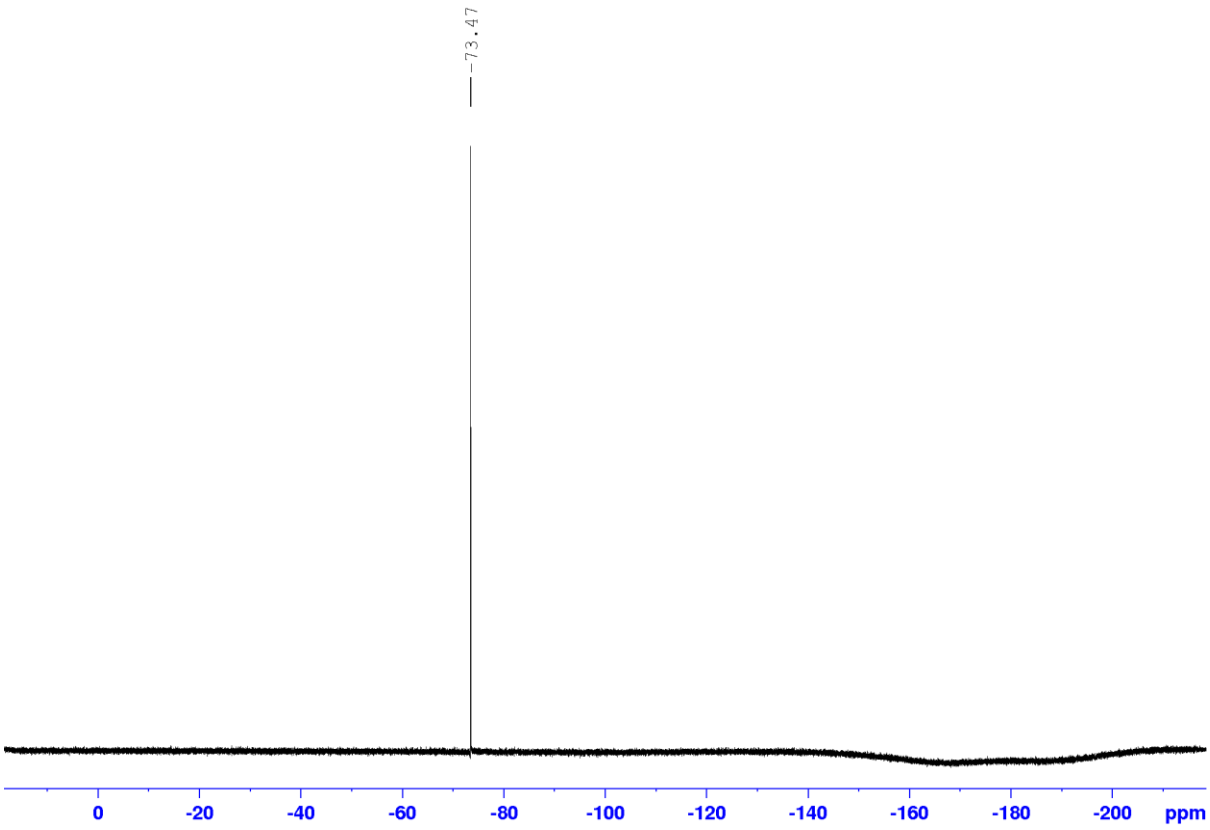

HRMS (ESI) spectrum

Elemental Composition Report **Page 1**

Single Mass Analysis
Tolerance = 5.0 PPM / DBE: min = -1.5, max = 500.0
Element prediction: Off
Number of isotope peaks used for i-FIT = 3

Monoisotopic Mass, Even Electron Ions
62 formula(e) evaluated with 1 results within limits (all results (up to 1000) for each mass)
Elements Used:
C: 10-15 H: 15-20 N: 0-5 O: 5-10 S: 0-1 F: 0-1 Na: 1-1

sd_01_065 89 (1.500) Cm (1:118)
TOF MS ES+

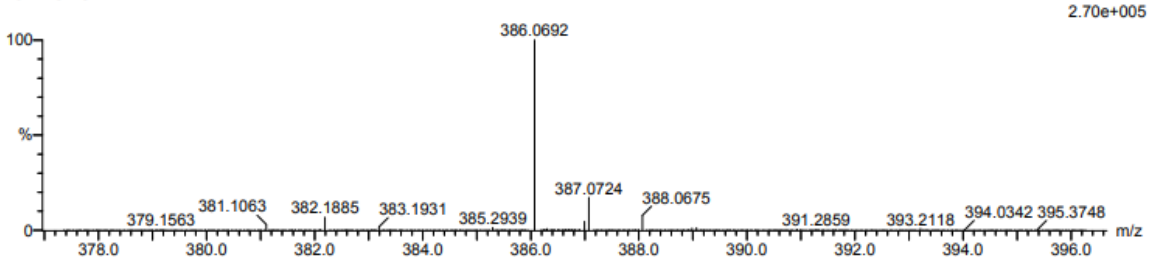

Minimum:				-1.5			
Maximum:		5.0	5.0	500.0			
Mass	Calc. Mass	mDa	PPM	DBE	i-FIT	i-FIT (Norm)	Formula
386.0692	386.0686	0.6	1.6	5.5	639.8	0.0	C14 H18 N O7 S F Na

FTIR spectrum

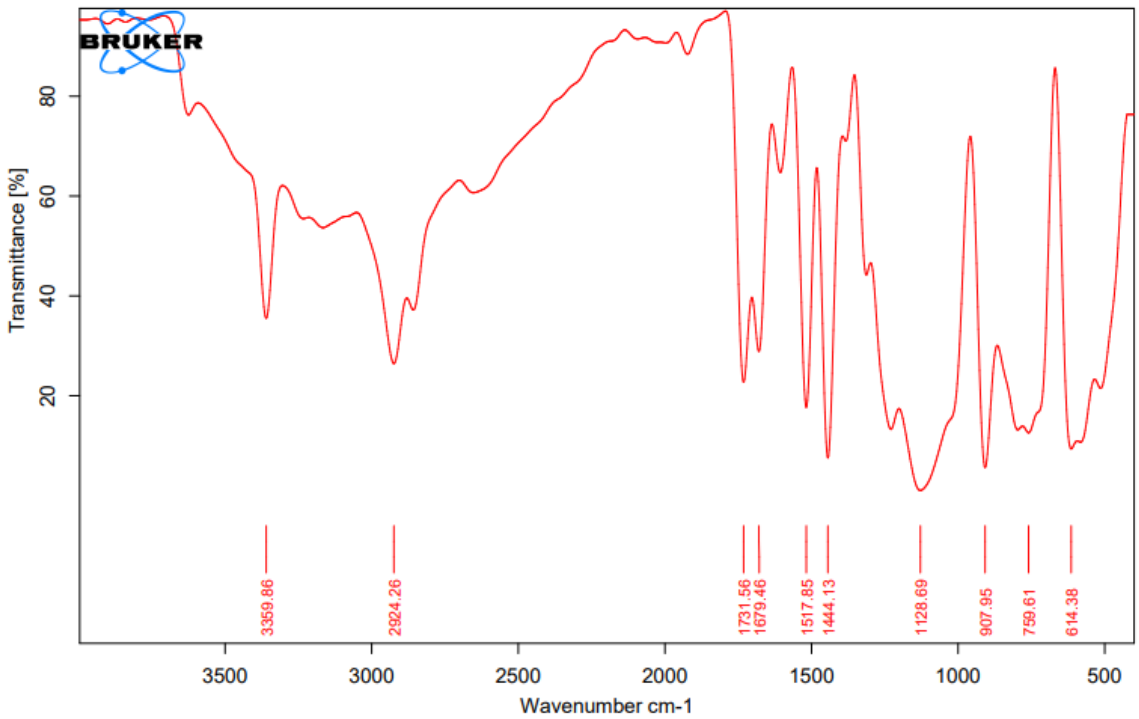

Methyl (*S*)-2-((*tert*-butoxycarbonyl)amino)-3-(4-(fluorosulfonyl)phenyl)propanoate (3.35)

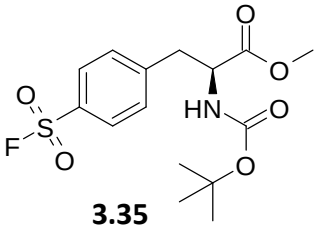

3.35

^{1}H NMR spectrum

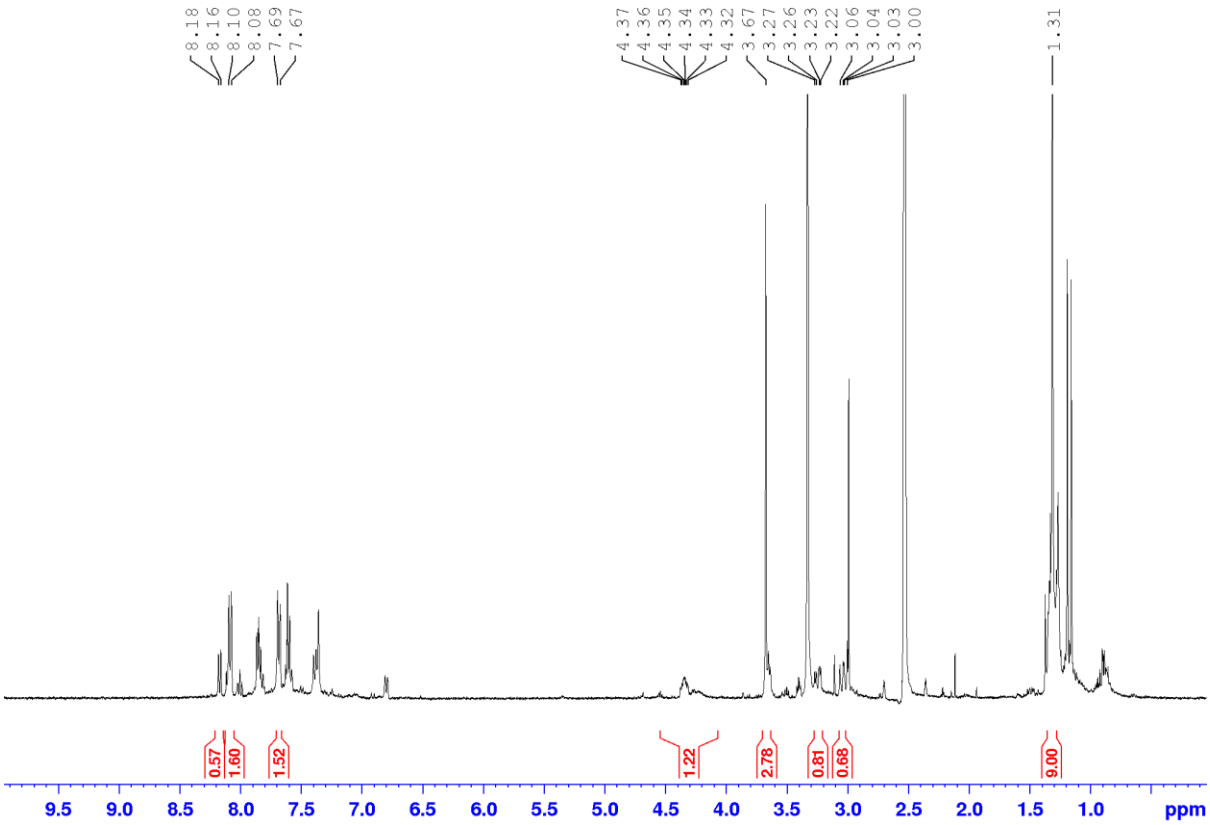

^{13}C NMR spectrum

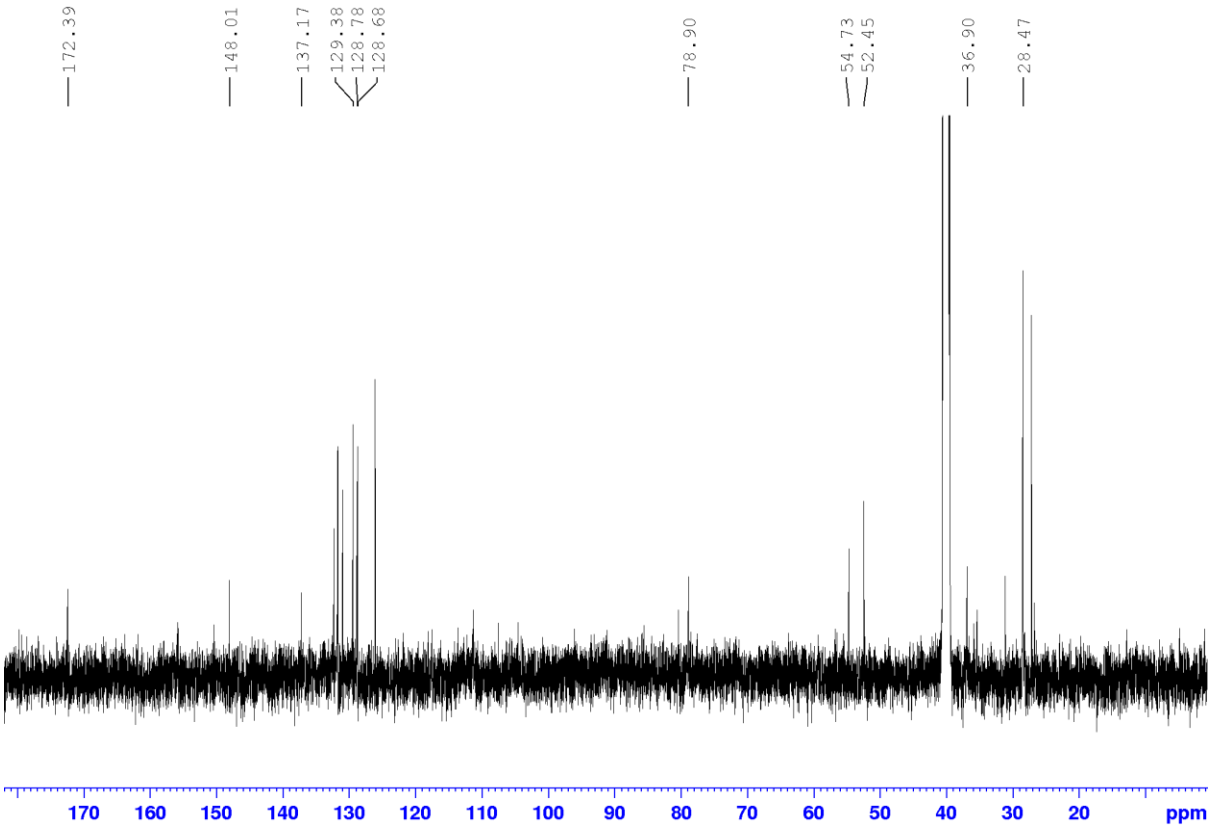

^{19}F NMR spectrum

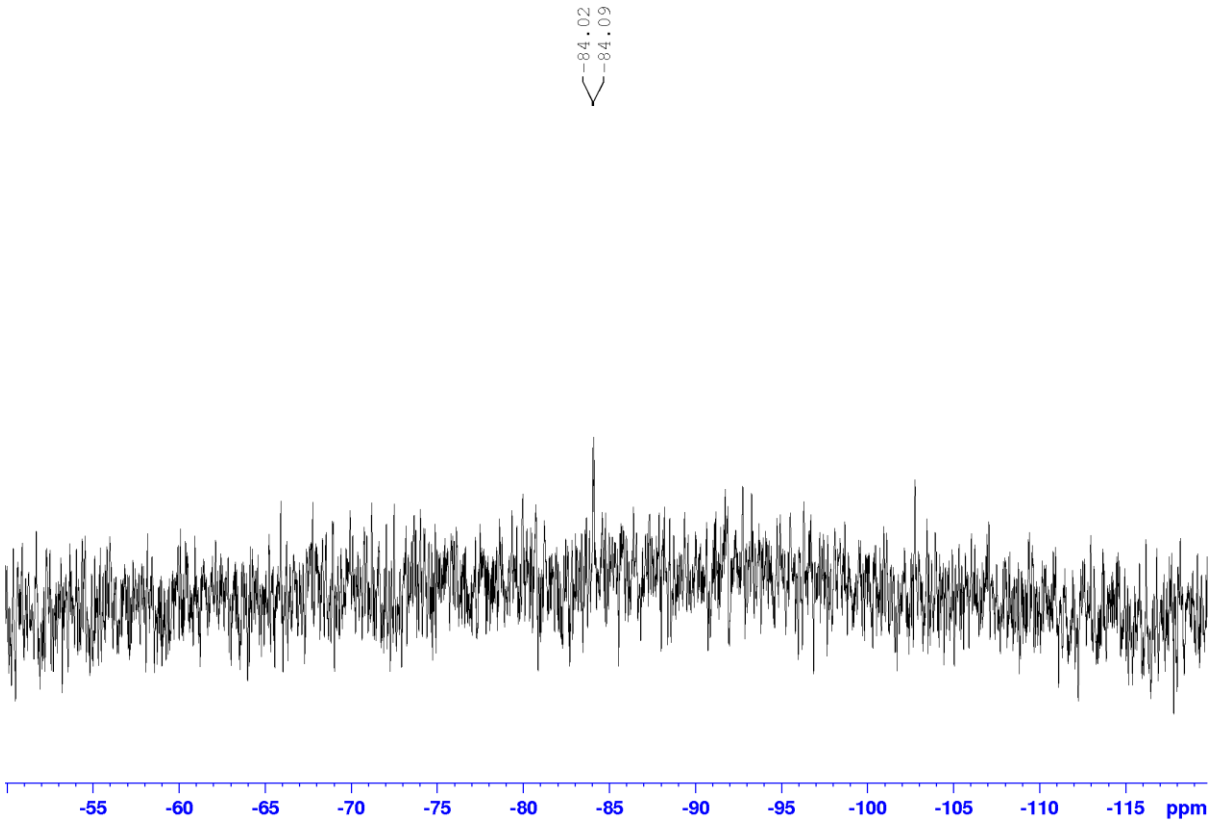

HRMS (ESI) spectrum

Elemental Composition Report **Page 1**

Single Mass Analysis
Tolerance = 5.0 PPM / DBE: min = -1.5, max = 500.0
Element prediction: Off
Number of isotope peaks used for i-FIT = 3

Monoisotopic Mass, Even Electron Ions
121 formula(e) evaluated with 1 results within limits (all results (up to 1000) for each mass)
Elements Used:
C: 10-15 H: 15-20 N: 0-5 O: 5-9 S: 0-1 Cl: 0-1 F: 0-1

sd_01_152 59 (1.989) Cm (1:60) TOF MS ES- 3.47e+005

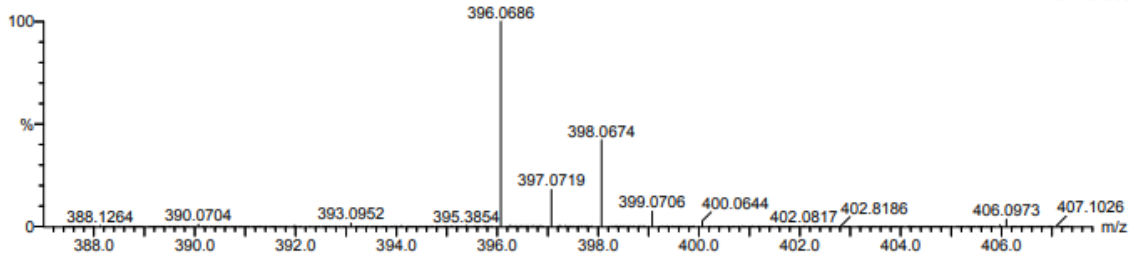

Minimum:				-1.5			
Maximum:		5.0	5.0	500.0			
Mass	Calc. Mass	mDa	PPM	DBE	i-FIT	i-FIT (Norm)	Formula
396.0686	396.0684	0.2	0.5	5.5	498.8	0.0	C15 H20 N O6 S Cl F

FTIR spectrum

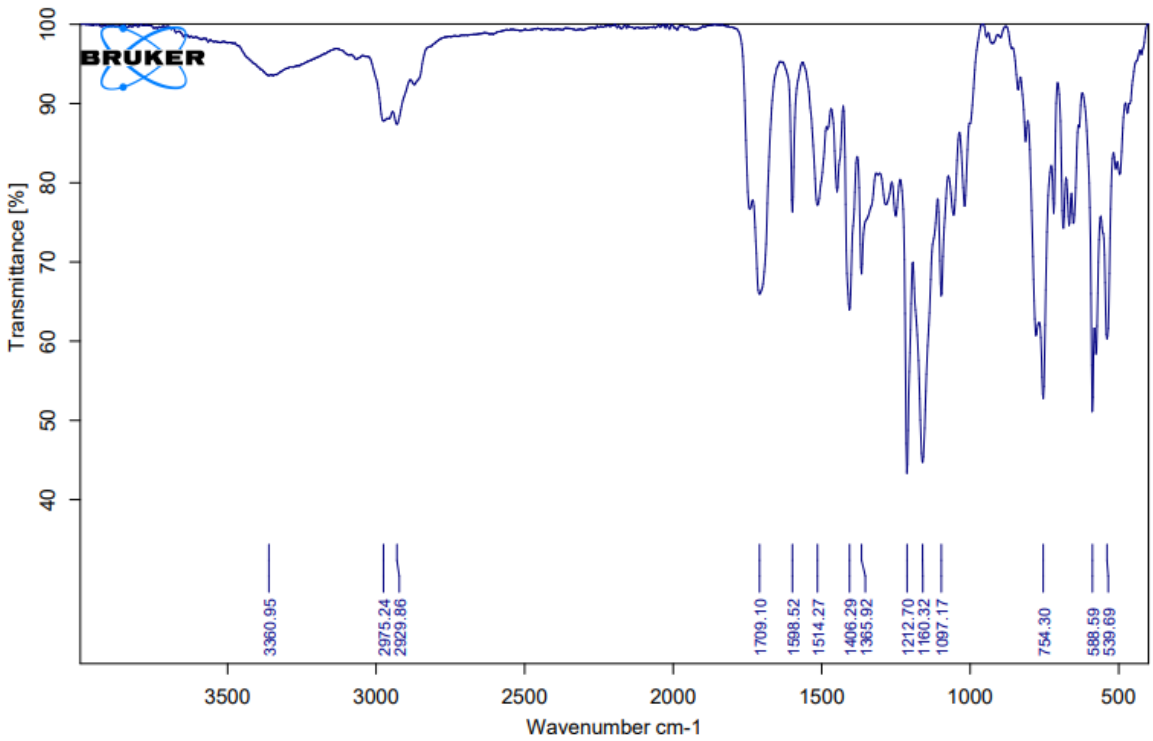

The LCMS Assay Spectra

(*Tert*-butoxycarbonyl)-*L*-lysine

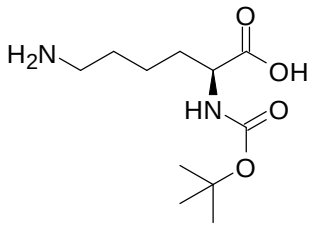

Chemical Formula: $C_{11}H_{22}N_2O_4$

Molecular Weight: 246,31

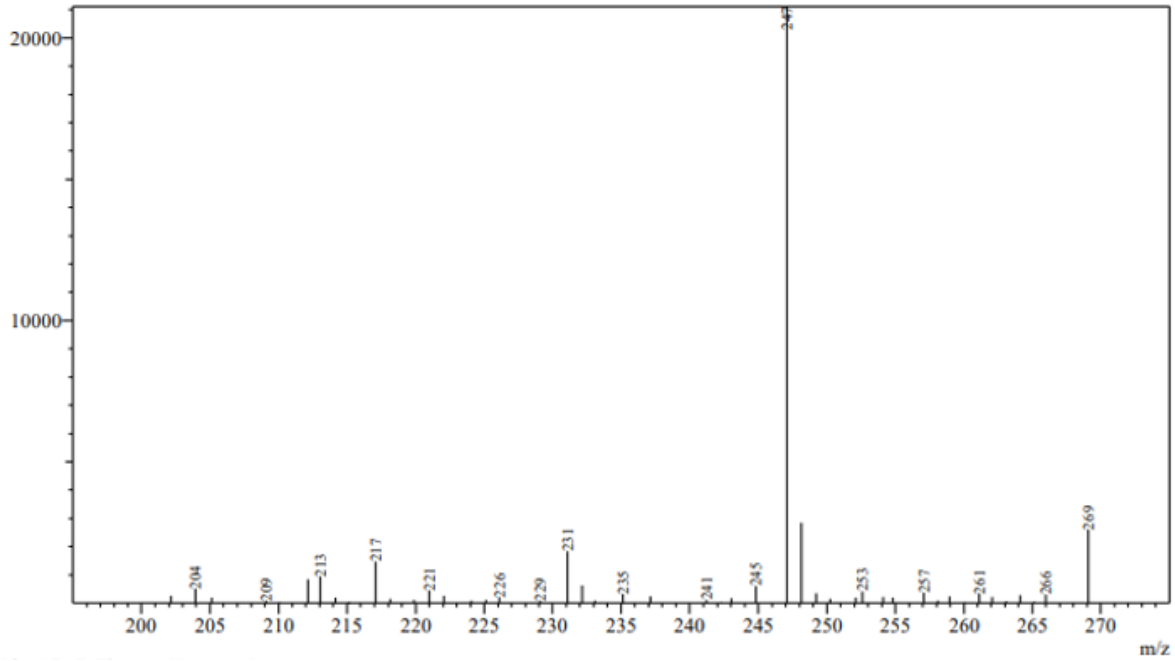

Methyl (*S*)-2-((*tert*-butoxycarbonyl)amino)-3-(4-((fluorosulfonyl)oxy)phenyl)propanoate (3.5)

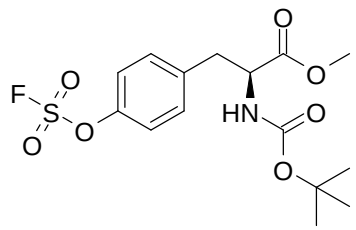

Chemical Formula: $C_{15}H_{20}FNO_7S$

Molecular Weight: 377,38

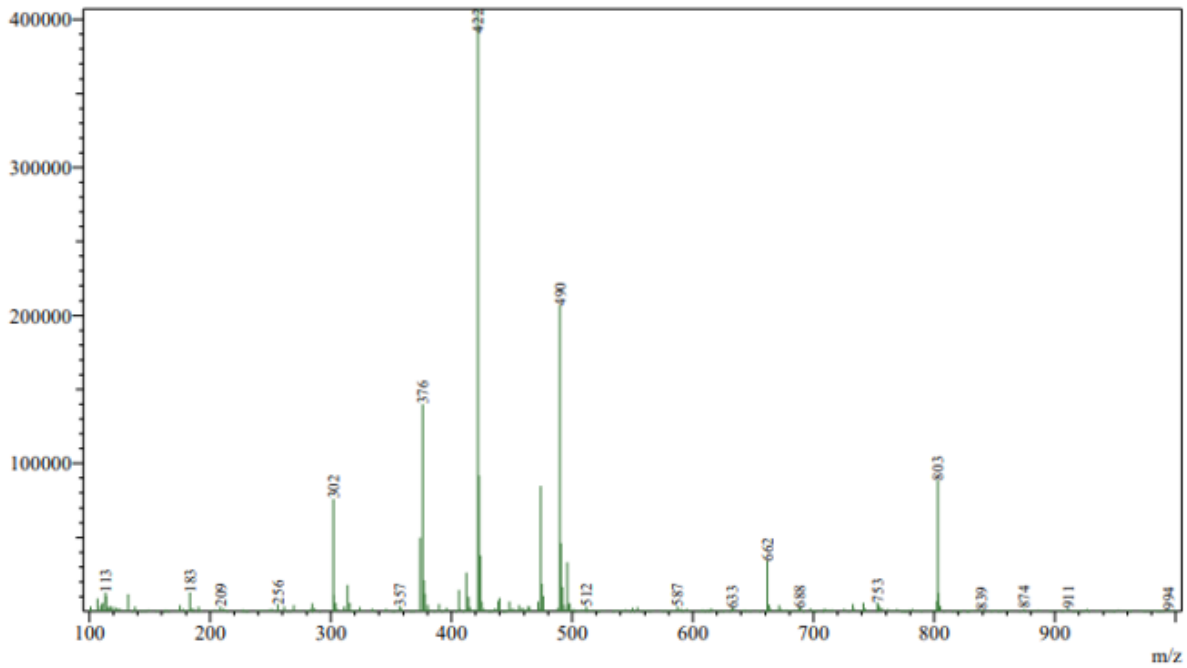

N^2-(*tert*-butoxycarbonyl)-N^6-((4-((*S*)-2-((*tert*-butoxycarbonyl)amino)-3-methoxy-3-oxopropyl)phenoxy)sulfonyl)-*L*-lysine (3.5a)

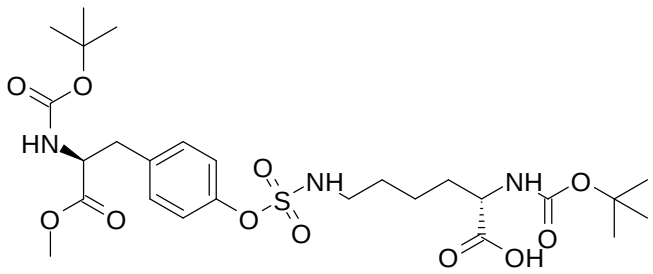

Chemical Formula: $C_{26}H_{41}N_3O_{11}S$

Molecular Weight: 603,68

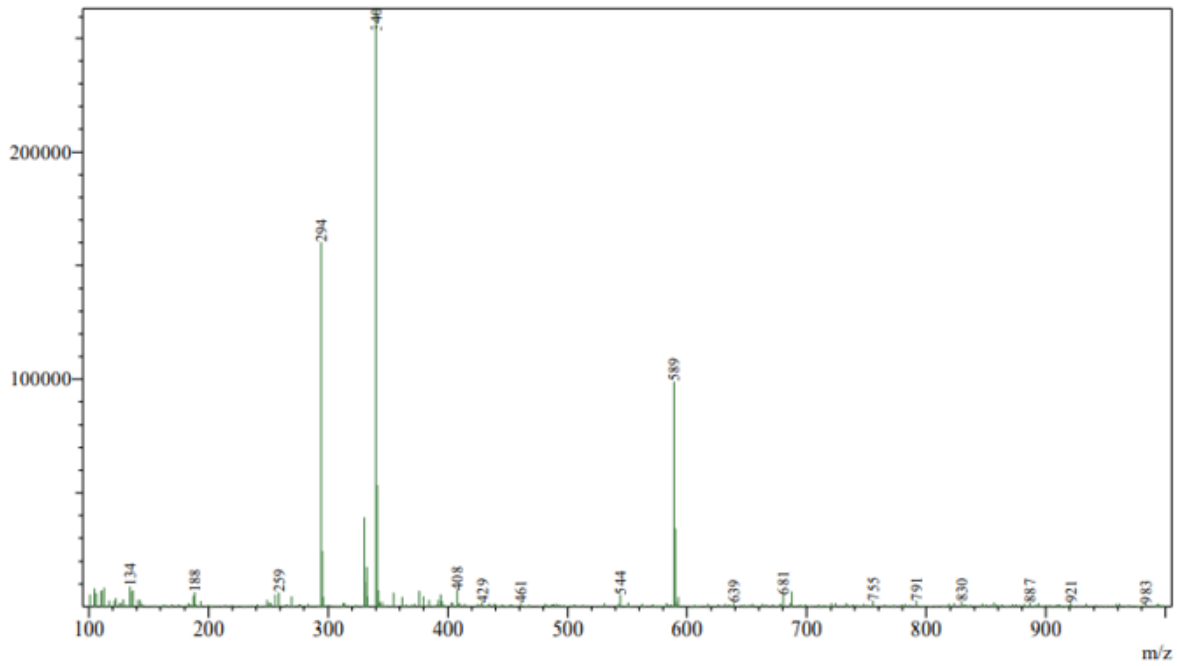

The NMR Assay Spectra

(*Tert*-butoxycarbonyl)-*L*-lysine

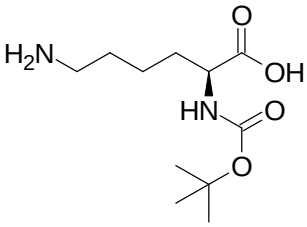

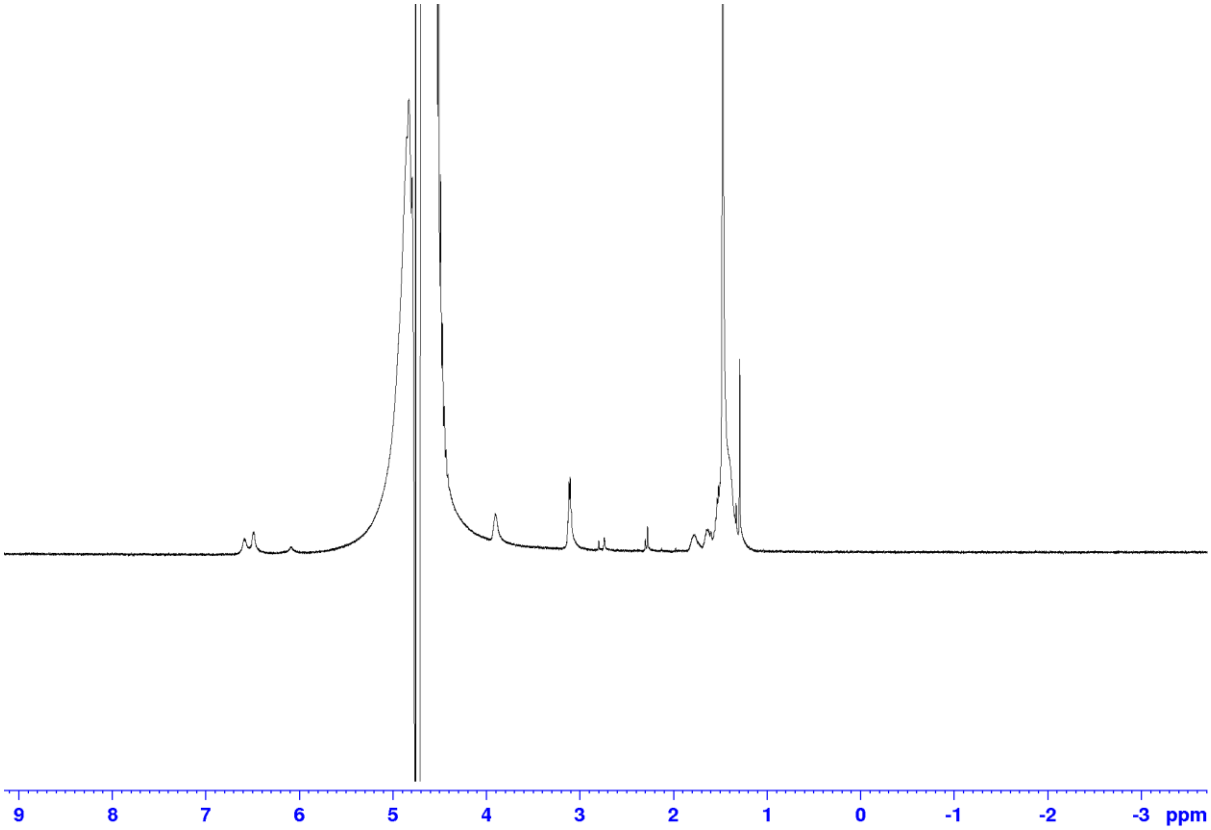

N^2-(*tert*-butoxycarbonyl)-N^6-((4-((*S*)-2-((*tert*-butoxycarbonyl)amino)-3-methoxy-3-oxopropyl)phenoxy)sulfonyl)-*L*-lysine (3.5a)

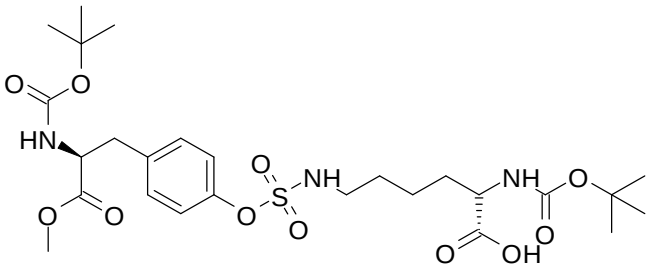

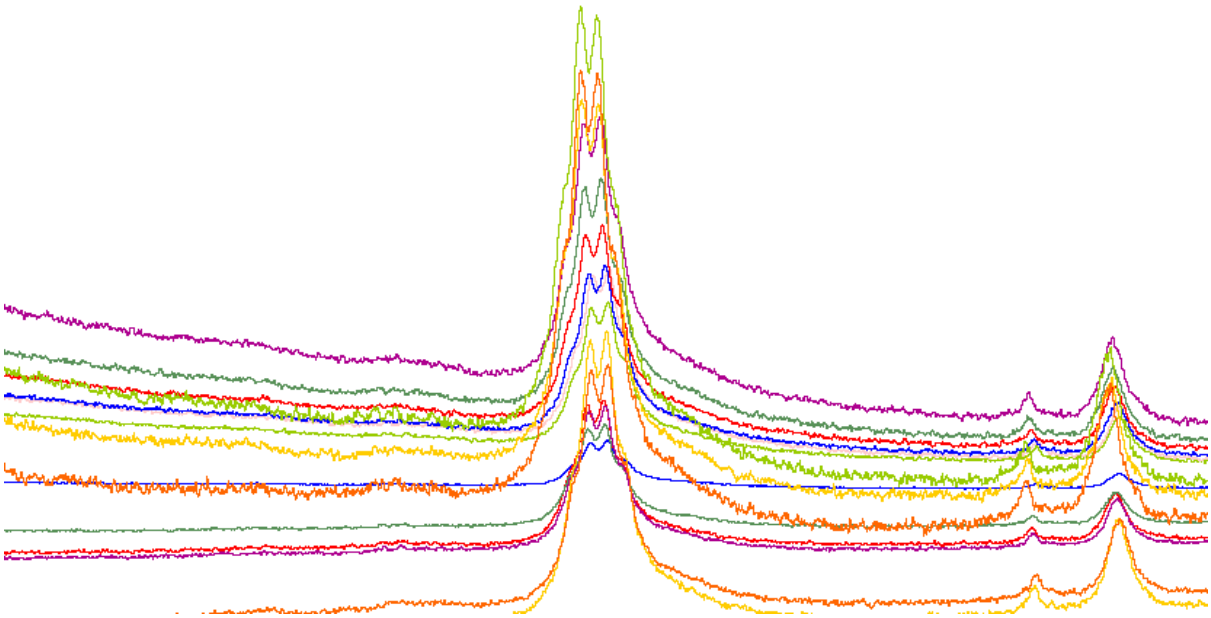

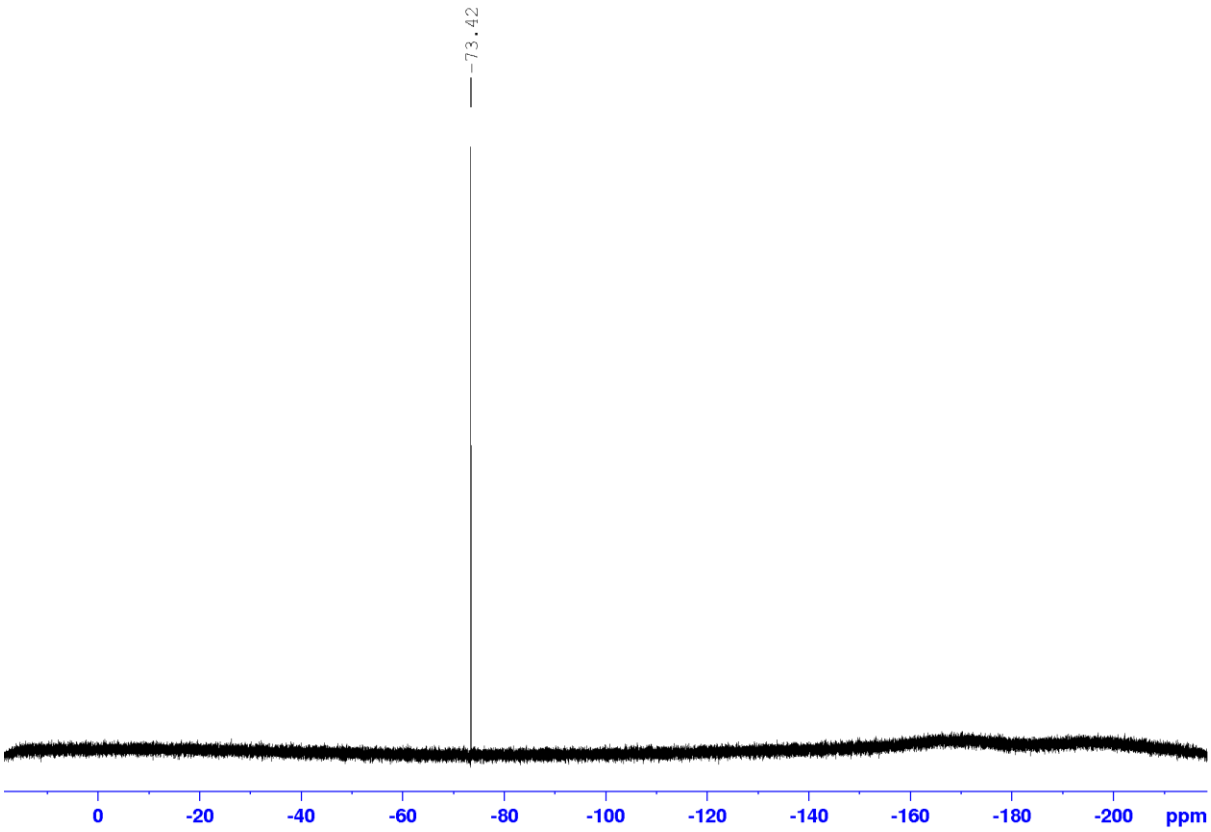
-73.42
0
-20
-40
-60
-80
-100
-120
-140
-160
-180
-200
ppm

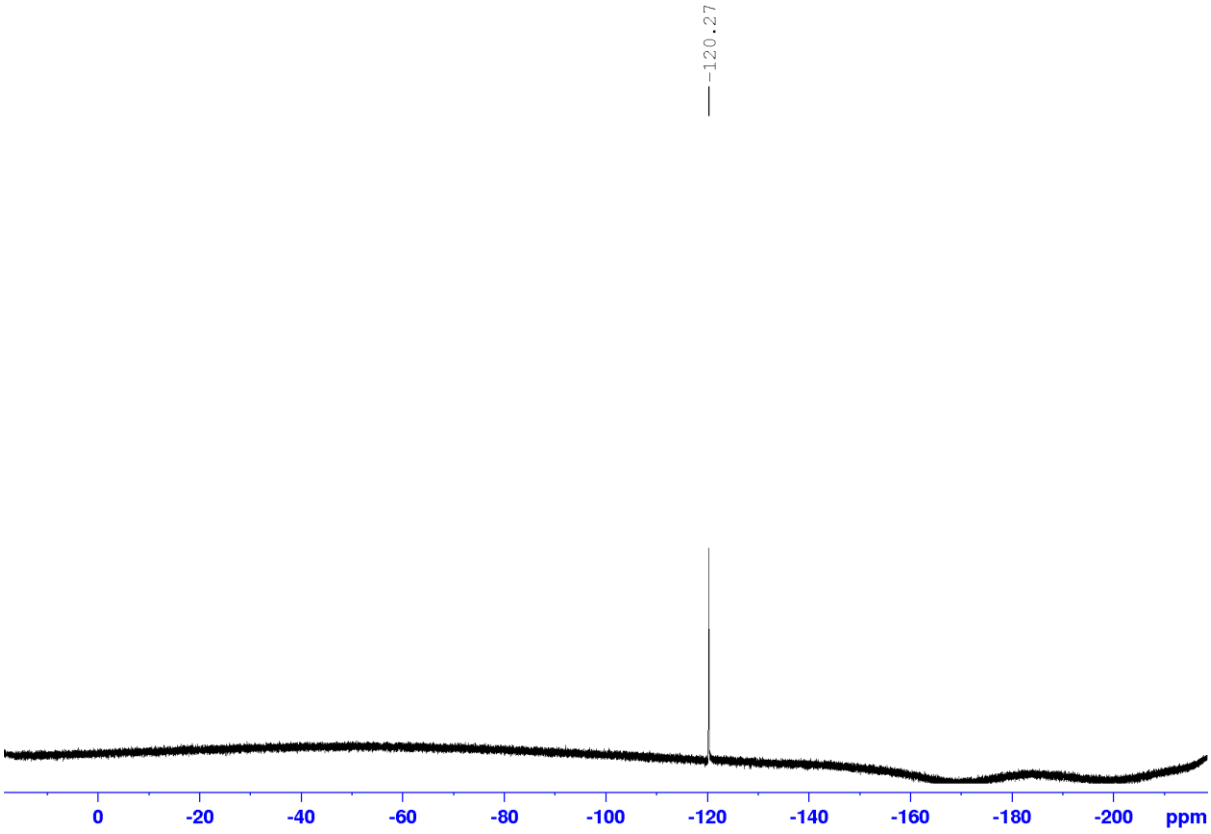
-120.27
0
-20
-40
-60
-80
-100
-120
-140
-160
-180
-200
ppm